BCEE2

Conference Proceedings

The Second International Conference on Buildings, Construction & Enviromental Engineering

BCEE2

October 17-18, 2015 - Beirut, Lebanon

Vol. IV, Transportations & Geomatics Engineering

The 2nd International Conference of Buildings, Construction and Environmental Engineering (BCEE2-2015)

SUPREME COMMITTEE

1. **Prof. Amin D. Thamir, UOT, Iraq/ Chair**
2. **Prof. Ryiad H. Hadi, UOT, Iraq**
3. **Prof. Makram Suidan, AUB, Lebanon**
4. **Prof. Mohamed Harajli, AUB, Lebanon**
5. **Eng. Estabraq I. El-Showq, MOCH, Iraq**
6. **Eng. Ibrahem Mustafa, Mayoralty of Baghdad, Iraq**
7. **Eng. Raad A. Abdulamir, MOWR, Iraq**
8. **Eng. Fouad A. Hamid, NIC, Iraq**

INTERNATIONAL ADVISORY COMMITTEE

1. **Prof. Riadh S. Al-Mahaidi, Swinburne University, Australia/Chair**
2. **Prof. Muthana H. Al-Dahan, University of Missouri, USA**
3. **Prof. Husham Al-Mansour, National Research Council, Canada**
4. **Prof. Tom Schanz, Ruhr University Bochum, Germany**
5. **Prof. Siamak Yazdani, North Dakota State University, USA**
6. **Prof. Andrzej M. Brandt, Polish Academy of Sciences, Poland**
7. **Prof. Caijun Shi, Hunan University, China**
8. **Prof. Namir K. Al-Saoudi, Australia**
9. **Prof. Hanaa A. Yousif, University of Akron, USA**
10. **Prof. Mohamed N. Hadi, University of Wollongong, Australia**

ORGANIZING COMMITTEE

1. **Prof. Ryiad H. Hadi, UOT, Iraq / Chair**
2. **Assoc. Prof. Ghassan Chehab, AUB, Lebanon/Co-Chair**
3. **Prof. Tareq S. Hadi, UOT, Iraq/ Co-Chair**
4. **Assist. Prof. Issam Srour, AUB, Lebanon**
5. **Assist. Prof. George Saad, AUB, Lebanon**
6. **Assist. Prof. Faris H. Mohammed, UOT, Iraq**
7. **Assist. Prof. Hasan H. Joni, UOT, Iraq**
8. **Assist. Prof. Mohammed A. Mahmoud, UOT, Iraq**
9. **Ms. Zakeya Deeb, AUB, Lebanon/ Exec Admin Assist**
10. **Mr. Helmi EL Khatib, AUB, Lebanon**

LOCAL SCIENTIFIC COMMITTEE

1. **Prof. Shakir A. Salih, UOT, Iraq / Chair**
2. **Prof. Emu. Kaiss F. Sarsam, UOT, Iraq**
3. **Prof. Hussain H. Karim, UOT, Iraq**
4. **Prof. Nabeel A. Jadoo'a, UOT, Iraq**
5. **Prof. Aqeel Al-Adili, UOT, Iraq**
6. **Prof. Hisham K. Ahmed, UOT, Iraq**
7. **Prof. Abdulrazzaq T. Ziboon, UOT, Iraq**
8. **Prof. Mohammed Y. Fattah, UOT, Iraq**
9. **Prof. Abdulhameed M. Jawad, UOT, Iraq**
10. **Assoc. Prof. Shadi Najjar, AUB, Lebanon**
11. **Assist. Prof. Abbas K. Zidan, UOT, Iraq**
12. **Assist. Prof. Waleed A. Abbas, UOT, Iraq**
13. **Assist. Prof. Hasan A. Omran, UOT, Iraq**
14. **Assist. Prof. Falah H. Rahil, UOT, Iraq**
15. **Assist. Prof. Mahmoud S. Mahdi, UOT, Iraq**
16. **Assist. Prof. Maan S. Hassan, UOT, Iraq**
17. **Dr. Hussain L. Zamil, MOWR, Iraq**
18. **Dr. Suhair K. Al-Habbobi, MOCH, Iraq**
19. **Eng. Ammar M. Abdulrassol, NIC, Iraq**
20. **Assist. Prof. Nisreen S. Mohammed, UOT, Iraq / Rapporteur and Secretary**
21. **Dr. Wael Shawky Abdulsahib, UOT, Iraq / Rapporteur and Secretary**

SPONSORS OF THE CONFERENCE

Our thanks and appreciation to the supporting points of the Conference

Ministry of Higher Education and Scientific Researches, Iraq

Hanwha Engineering and Construction Bismayah Project, Iraq

Veolia For Water Technology CO. France

Fugro - Maps, Lebanon

Al-Tariq Engineering Bureau for Pile Testing Iraq

PREPARATION COMMITTEE OF THIS BOOK

1. **Prof. Dr. Aqeel Al-Adili**
2. **Dr. Wael Shawky Abdulsahib**
3. **Dr. Bassman R. Muhammad**
4. **Eng. Luay Yaly**

REVIEWERS OF THIS TOPIC

1. **Prof. Dr. Hamid Al-Ani**
2. **Prof. Dr. Hussein H. Karim**
3. **Prof. Dr. Abd Al-Razzak Tarish**
4. **Prof. Dr. Aqeel Al-Adili**
5. **Dr. Hassan Hamodi Joni**
6. **Dr. Namir G. Ahmed**
7. **Dr. Imzahim A. Alwan**
8. **Dr. Mahmood Salih**
9. **Dr.Ammar Abbas Shubbar**
10. **Dr. Abbas Yass Al -Ethawi**
11. **Dr. Abbas Z. Khalaf**
12. **Dr. Mustafa Abd Jalil Ibrahim**
13. **Dr. Abbas Talib Al-Haddabi**
14. **Dr. Oday Z. Jasim**
15. **Dr. Zaynab I. Qassim**
16. **Dr. Firas Hassan Alwan**
17. **Dr. Ameen Ibrahim**
18. **Dr. Fanar Mansour**
19. **Dr. Khalid Ibrahim Hassan**
20. **Dr. Zainab Abdul-Sattar**
21. **Dr. Rasha M. Abd Al-Ameer**
22. **Dr. Mohammed Abbas Hassan**
23. **Dr. Ahlam Khudaier Razzak**
24. **Dr. Hamid Athab Al-Jameel**
25. **Dr. Miami M. Hilal**

Table of Contents

Consequences of Freight Vehicles on Transport Corridors in Kogi State, Nigeria

Adetunji Musilimu Adeyinka
Department of Geography, Faculty of Arts & Social Sciences
Federal University Lokoja, Lokoja, Kogi State
musilimuadetunji@yahoo.com, musilimu.adetunji@fulokoja.edu.ng

***Abstract*- Studies of the characteristics of freight transport are robust in the literature. However, research on the negative impacts of freight transport on Nigerian roads is not well documented in the literature. It is on this background that this study examines the consequences of freight vehicles on transport routes in Kogi state, Nigeria. Both primary and secondary data were used for this research. An average of one hundred set of questionnaires was administered randomly to public transport operators and other road users. Similarly, another one hundred set of questionnaires was administered to freight transport operators about the challenges encountered on their transit. Data on the road traffic crashes between 2006 and 2012 were obtained from the Federal Road Safety Corps in Lokoja. Descriptive statistics were used. The finding reveals that approximately 22% of road traffic crashes result in injuries and death of innocent citizens in the state, caused by freight vehicles. Okene- Lokoja route recorded the highest number of traffic crashes by freight vehicles in the state. The behaviour of freight transport operators requires much to be desired as they harass other road users and intimidate them through indiscriminate use of horns. More than 50% of other road users claimed that the size, weight and the speed of freight vehicles are the principal factors threatening them on the road, despite the fact that only 3.72% of freight vehicles ply the study area. The study recommends that the operations of heavy duty vehicles should be restricted mainly to inter-city highway as these may likely reduce traffic congestions and accidents on urban routes.**

KEYWORDS: Freight, transport Routes, Transport Externality, Safety and Planning,

1. Introduction

Studies of freight transport in Nigeria are overwhelming in the literature {7}; {12}; {13}; {14}. Some of the researches carried out have extensively discussed the types of freight, intermodal split in freight movement, and zonal distribution of goods. However, research on the negative external effects of freight transport on Nigerian roads is very scanty in the literature. This apparent gap in the field of knowledge is unwarranted because the negative external effect of freight transport is enormous. These includes road traffic crashes resulting in injuries and death of innocent people, emission of toxic substances into the atmosphere, intimidation of other road users and many others.

It is on this background that this study was designed to examine in details the problems of freight transportation in Kogi state, north central Nigeria, which serves as a focal point between northern and southern parts of the federation.

In a report on issues in freight transport in India, overloading of vehicles, poor infrastructure, barriers to free movement, highly competitive and low cost are major impediments to India's freight industry {2}. Also, the report shows that trucks are involved in over 50% of fatalities. The volume of freight transport has grown tremendously over the past few decades, which invariably puts pressure on transport infrastructure {6}; {14}. The resultant effect of this is that billions of Naira is expended on road infrastructure annually to maintain the transport routes in the country {9}.

The report of an evaluation of the impact of India's diesel price reforms on the trucking industries revealed that the India trucks usually go overloaded in one direction and return with an empty haul {10}. Apart from overloading, which has adverse effect on the vehicle condition and results in frequent break down of vehicles extortions by law enforcement agencies at every stage, starting from vehicle registration to the point of delivery of goods often leads to unnecessary delays and impediments to the efficiency of operators. Also, trucking industry in India is totally in the private domain and is dominated by small road transport operators; many of the customers who hire the truck are less accessible to the truck owners to book for transportation of their goods. The freight charges are usually decided by cargo operators who tend control and decide on the freight rates at the expense of the customers who hire their services {10}.

Also, in another report by the Federal Highway Administration in 2008, bottlenecks for trucks on America's highways caused 226 million hours of delay and cost 7.3 billion US dollars in 2006{5}. The freight contribute 27.9% of the US Green House Gas emissions from transportation, or 7.8 percent of the Green House Gas (GHG) emissions in 2007.This share has grown from 23 percent of transportation GHG

emission in 1990 due to the increase in emissions from trucking{16};{17}. An overview of literature on the operational characteristics of freight transport at any geographical space shed more light on the impacts of freight movement on natural environment such as air pollution, global climate concerns, noise, water pollution, accidents, land use and habitat fragmentation {19}. It is on this premise that this study was designed to examine in details the negative impacts of freight vehicles on transport routes and other road users in Kogi State so that appropriate freight transport policy could be recommended for other states in Nigeria.

2. Study Area

Kogi State is located on Latitudes 70 30'N and 80 10'N and Longitudes 60 01'E and 7º 50'E of the Greenwich meridian particularly in the north central part of Nigeria {1};{3}. A large movement of freight transport to and from different parts of the country flows through Kogi State daily. The resultant effect of this is high traffic congestion on road transport networks, which results in traffic crashes, emission of toxic substances into the atmosphere and many others. Also, the Dangote Cement Industry at Obajana in Kogi State, distributes cement to all parts of the country for construction purposes. Furthermore, the State is an agrarian society where large quantities of arable crops are produced for human consumption.

The distribution of farm produce as well as industrial products in the State has generated

a considerable pattern of movement of freight transport within and outside the state. A large movement of freight transport on transport corridors in the State has put pressure on natural environment particularly on traffic congestion, emission, road damage and many others. The problems of freight movement on transport routes in the state is so enormous that it has drawn the attention of people, government and all stake holders in the State and the country in general. It is on this background that this study was thereby designed to examine the problems of freight movement on transport routes in Kogi State in Nigeria.

3. Materials and Methods

The study utilized both primary and secondary sources of data. Two sets of questionnaires were designed to elicit information on the problems of freight movement on transport routes in the state. The first one hundred set of a questionnaires was administered to the public transport operators who ply different categories of routes in the State in four major terminals in Lokoja. The questionnaires were designed to elicit information on the challenges they encountered with freight transport during different journey particularly on non-consideration of other road users by freight transport operators, accident rate, harassment and many others. The second one hundred set of questionnaires were administered to the freight transport operators in the State. An average of one hundred questionnaires was randomly distributed to freight transport

operators at Kaba junction in Okene Township and at Lokoja at the International Market during the market day (The market alternates at intervals of four days), where freight transport coming from different parts of the state and other parts of the country convey goods of different types.

In each of park selected, where the number of freight transport operators is less than 20, all the operators were selected for questionnaire administration. Also, in a park, where the number of freight transport operators is more than fifty (50), an average of 50% of the freight transport operators were selected for questionnaire administration, which accounted for an average of one hundred (100) questionnaires administered. The volume of traffic flow in the study area is approximately 74,972 vehicles, while only **2**, 787 freight vehicles which accounted for only 3.72% of vehicles ply the road. The questionnaire was designed to gather information from freight transport operators on their mode of operation and challenges faced during their transit,

especially the average weight of the load usually carried, and problems normally encounter during transit. Secondary data was obtained from documentary sources particularly information about the effect of freight transport with reference to traffic crashes. This data was obtained from the seven unit command of the Federal Road Safety Corps in Lokoja between 2006 and 2012. Descriptive statistics were employed to analyze the data.

4. Results

Table 1 and 2 highlight loading capacity of freight vehicles and the effects of overloading on freight transport in the study area. The finding reveals that over loading is one of the major characteristics of freight transport in Nigeria. Table 1 reveals that 61.7% of freight transport operators affirm that they do carry more than the capacity of the vehicles, while the remaining 39.3% of the respondents claim that they carry the required specification of the load their vehicles is designed for. The result of this analysis is similar to the reports of the assessment of the impact of an India's diesel price reform, where India's truck usually overloaded on their journey and return with empty haulage {10}.

Table 1: Loading Capacity of your Freight Vehicle

Overloading	Percentage Total (%)
Yes	61.7%
No	39.3%
Total	**100.0%**

Source: Author's Field Survey, 2015

It is obvious that overloading of vehicles has adverse effects on the transport infrastructure most especially on the condition of the freight vehicles, roads and traffic crashes. It is disheartening to observe that 60.2% of the freight transport operators claim that overloading is responsible for the breakdown of their vehicles within the last six months.

Another 15.5% of the freight transport operators indicate that overloading is responsible for the damage of roads in the study area, while the remaining 24.3% of the respondents acknowledge that transportation of freight on transport routes were largely responsible for the emission of toxic substances in the atmosphere which is harmful to human beings in their natural environment.

Table 2: **Effects of Overloading of Freight Transport**

Effect of Overloading	Percentage Total
Breakdown of Vehicles	60.2%
Damage of Road	15.5%
Emission of Toxic Substances	24.3%
Total	**100.0%**

Source: *Author's Field Survey, 2015*

Many of the freight transport operators expressed their feelings about series of problems encountered during their transit. Generally, road blocks by law enforcement agents and task forces' are very rampant on transport routes demanding for bribe or payment for load carried. Table 3 indicates that 20% of freight transport operators claim that they were being extorted by law enforcement agents; highway robbers accounted for about 26.7% of the problems encountered on their transit, while 36.6% and 16.7% accounted for poor maintenance of

transport routes and breakdown of vehicles respectively.

Table 3: Problems Encountered by Freight Transport Operators during Transit

Problems encountered on transport routes	Total Percentage
Extortion by law enforcement agents	20.0 %
Breakdown of vehicles	16.7%
Highway robbers	26.7%
Problems of roads maintenance	36.6%
Total	**100.0%**

Source: *Author's Field Survey, 2015*

Generally, diesel is the major fuel used by freight transport, especially the heavy duty vehicles. The emission of toxic substances such as sulphur dioxide, lead compounds, and oxides of nitrogen, carbon monoxide, hydrocarbons, particulate matters, noise, smoke, odors and others are very high in diesel than petrol. The effects of these toxic substances are harmful to human health and reduction of Green House Gases {4} ;{ 11}. Table 4 indicates that 61.1% of freight vehicles in the state rely on diesel fuel, while 38.9% depend on petrol.

Table 4: Types of Fuel Used by Freight Vehicles in the State

Fuel Used	Percentage Total (%)
Petrol	38.9%
Diesel	61.1%
Total	**100.0%**

Source: *Author's Field Survey, 2015*

The attitude of freight transport operators to other road users is a major concern to all and sundry in the state as they terrorize both motorists and pedestrians during their transit through indiscriminate blaring of horns, wrongful overtaking and other forms of intimidation which sometimes result in traffic crashes on transport routes. Table 5 indicates that 46.1% of the public transport operators claim that they were being intimidated by wrongful overtaking by freight transport operators. Another 18.4% and 10.5% report of the public transport operators was that they were being threatened by indiscriminate blaring of horns and overspending of freight vehicles in the state. Further analysis shows that the size of the freight vehicles and their weight accounted for approximately 18.0% and 6.9% of the factors responsible for intimidating other road users in the state.

Table 5: Problems Faced by Public Transport Operators on transit

Types of Harassment or Intimidation experience	Percentage Total (%)
Wrongful overtaking	46.1
Indiscriminate blaring of horns	18.4
Over speeding	10.5
Size of the freight vehicles	18.0
Weight of the freight vehicle	6.9
Total	**100.0**

Source: *Author's Field Survey, 2015*

Many of the public transport operators also expressed their opinion about the problem of freight transportation in the state. Approximately 32.5% of the public transport operators claim that noise pollution is one of the major external effects of freight transport in the area. Traffic congestion on transport corridors which results in delay and late arrival of commuters to various destinations constituted 19.5% of the problems associated with the movement of freight vehicles in the study areas. The result of this analysis is tangential to the report of the American Federal Highway Administration in 2008, which emphasized that bottlenecks for trucks on American's highways caused 226 million hours of delay and cost 7.3 billion US dollars in 2006 {5}. Table 6 reveals that road damage, traffic crashes and indiscriminate parking constituted about 16.9%,

13.0% and 3.9% of the problems associated with the movement of freight vehicles in the area.

Table 6: Problems of Freight Transportation

Problems of Freight Transport	Percentage (%)
Road Traffic Crashes	13.0%
Noise Pollution	32.5%
Air Pollution	14.3%
Road Damage	16.9%
Traffic Congestion	19.5%
Indiscriminating Packing	3.9%
Total	**100.0%**

Source: *Author's Field Survey, 2015*

A detail analysis of road traffic crashes in the state reveals that approximately 37.9% of private vehicles were involved in road traffic crashes in the state with the highest occurrence (50%) along Kabba- Okene route. Further analysis reveals that commercial transport of different categories accounted for 40.5% of road traffic crashes in the state within the period under study. The incidence of road traffic crashes by commercial motorcycles is highest along Isanlu – Kabba routes. The establishment of the cement industry at Obajana, a distance of less than 15kms from Lokoja and the Iron Steel rolling Mills at Itakpe along Okene- Lokoja route were largely responsible for high volume of traffic of heavy duty trucks which may have increased traffic crashes in the state. Table 7 reveals that 21.6% of freight vehicles were involved in road traffic crashes along different routes in the state. The Zariagi - Okene road recorded the highest

volume of road traffic crashes involving heavy duty vehicles. The traffic crashes in this road account for approximately 26.8% of total road crashes in the state. It is pertinent to note that only 3.72% of freight vehicles ply the roads in the study area. Table 8 represents the percentage of freight vehicles in the study area.

Table 7: Proportion of Freight Vehicles involved Road Traffic Crashes

Route	Private	Public Transport	Freight Vehicle (Heavy Duty)	Total (%)
Lokoja-Obajana Junction	32.4	42.6	25	100
Ankpa-Ajaokuta-Okene	32.4	50	17.6	100
Kabba-Okene	50	44.6	5.4	100
koton karfe – Abaji	39.7	39.4	20.9	100
Zariagi-Okene	36.8	36.4	26.8	100
Isanlu-kabba	37.5	62.5	0.0	100
Ogori-Obehira Junction	42.4	40.0	17.6	100
Total average	37.91	40.52	21.56	

Source: *Federal Road Safety Corps (FRSC) in Lokoja RS 8.3, 2013*

Table 8: Composition of Vehicular Flow in the study area

Routes	Commercial	Private car	Freight	Total Traffic Flow
Muritala Muhammed way	4,249	2,910	93	7,252
Ganaja-Natako	9,837	4,192	821	14,850
Ganaja village-Barrack	1,884	998	139	3,021
Barrack road-Ganaja village	3,466	2,022	244	5,732
Natako-Ganaja village	8,912	4,616	680	14,208
Ganaja junction-Barrack	9,839	5,858	194	15, 891
Natako-Barrack	8786	4,616	616	14,018
Total	**46, 973**	**25,212**	**2787**	**74, 972**

Source: *Author's Field Survey, 2015*

Freight charge is another problem facing the freight industry in Nigeria. Many of the freight vehicles are owned by individuals or unorganized private domain and dominated by small road transport operators who tend to extort customers who hire their services. The results shows that 32.8% of the freight transport operators interviewed claim that the owners of their vehicles determine fixed daily return irrespective of the distance, weight and nature of the goods carried. Also, Table 9 indicates that 23.8% of the transport fare charged for conveying goods are controlled by freight transport operators. Further analysis shows that 44.2% of freight transport charges is controlled by union or the regulatory body.

Table 9: Agents Determining Freight Transport Charges in the Study Area.

Agents	Percentage (%)
Owner of the Freight Vehicle	32.8%
Freight Transport Operators	23.8%
Union / Regulatory body	44.2%
Total	**100.0%**

Source: *Author's Field Survey, 2015*

Conclusion and Planning Implications

This paper examined the negative effects of freight vehicles on other road users in Kogi State. The study collected both primary and secondary data for analysis. Information about the effect of freight transport with reference to traffic crashes were obtained from the seven unit command of the Federal Road Safety Corps in Lokoja between 2006 and 2012. Similarly, structured questionnaires were designed to elicit information from motorists and other road users on the effects of operation of freight vehicles on transport routes particularly on travel behavior of freight transport operators on the roads. Also, one hundred set of questionnaires were administered to freight transport operators to elicit information on challenges faced on transit and the mode of their operations on transport routes in the state. Descriptive statistics were used to analyze the data. The finding reveals that approximately 22% of road traffic crashes which result in injuries and death of innocent citizens in the state were caused by freight vehicles.

Okene- Lokoja route recorded the highest number of traffic crashes by freight vehicles in the state. The behavior of freight transport operators required much to be desired as they harass other road users and intimidate them through indiscriminate use of horns. More than 50% of other road users claimed that the size, weight and the speed of freight vehicles are the principal factors threatening them on their daily travels. The study therefore recommends that the operations of heavy duty vehicles should be restricted mainly to inter-city highways as these may likely reduce traffic congestions and accidents on urban routes.

References

1. Adeoye, N. O. : Spatio-Temporal Analysis of Land Use/Cover Change of Lokoja: A Confluence Town, Journal of Geography and Geology, 2012, Vol. 4, No. 4, pp. 40 ^51.
2. Alok, B,: Issues in Freight Transport-India, India Infrastructure Summit-FICCI, India, 2005
3. Babatimehin, O; Ayanlade, A; Babatimehin, M and Yusuf, J.O: Geo-Patterns of Health Care Facilities in Kogi State, Nigeria. The Open Geography Journal, 2011, pp. 141^ 147
4. Bourne, J..K, "Biofuels: Boon or Boondoggle?," *National Geographic*, Oct. 2007, pp. 38 ^ 59.
5. Cambridge Systematics, inc, Estimated Cost of Freight Involved in Highway Bottlenecks, 2008.
6. Eno Transportation Foundation: Transportation in America. Washington, C. 2002
7. Fatunde, O: Spatial Analysis of Multimodal Movement of Port-Oriented Freight within Nigeria. An unpublished Ph.D Thesis, Department of Geography, University of Ibadan, Ibadan, 1998
8. Federal Road Safety Corps in Lokoja RS 8.3, 2013: Unpublished Road Traffic Data for a Period of Seven Years RS8.3 between 2006-2012
9. FMWH: Survey of Road Constructions in Nigeria. Federal Ministry of Works and Housing Abuja, 1999 13 ^ 47
10. International Institute for Sustainable Development: The Impact of India's Diesel Price Reforms on the Trucking Industry, Published by the International Institute for Sustainable Development, New Delhi, India, 2013, Pp. 1 ^ 8.
11. Koplow, D, Government Support For Ethanol And Biodiesel In The United States Biofuels – At What Cost? Global Subsidies Initiative, International Institute for Sustainable Development, 2006 (www.globalsubsidies.org).
12. Ogunsanya, A. A.: Urban freight transport in a developing economy: The case of Lagos, Nigeria. Nigerian Geographical Journal, Nigeria, 1981,Volume 24, Issues 1& 2, pp. 147-165
13. Somuyiwa, O and Dosunmu, A : Logistics infrastructure and port development at Apapa Port, Nigeria, Pakistan Journal of Social Sciences, Pakistan, 2008, 5(9), pp. 953 ^ 959.
14. Ubogu, A : An Economic case for Intermodal; freight transport in Nigeria, Zaria Geographer, Zaria, Nigeria, 2005,Volume 16 Number 1, pp. 1 ^12
15. U.S. Department of Transportation; Federal Highway Administration: Freight Analysis Framework. (2002a)
16. U.S. Department of Transportation: Freight Facts and Figures 2009
17. U.S. Environmental Protection Agency, *Inventory of U.S. Greenhouse Gas Emissions and Sinks: 1990 – 2007*, 2009. United State Department of Transportation, National *Transportation* Statistics, 2009.
18. http://ops.fhwa.dot.gov/freight/freight_analysis/improve_econ/index.htm
19. http://www.oecd.org/trade/envtrade/2386636.pdf

Operational Analysis of Cross Section Intersection by using aaSIDRA Software for Traffic Flow

Dr Hasan Hamodi Joni, Ali Ahmed Mohammed *Member, IEEE*

Abstract— **Safety is a prime concern of transportation engineers. Traffic volumes have increased tremendously over the past years especially in Baghdad city. A computer simulation is more sophisticated for the analysis of freeways and urban street systems through simulation, transportation specialists can study the formation and dissipation of congestion on roadways. Intersection is one of the main reasons that have a significant effect on travel time. The aim of this paper is to analysis operational the traffic flow of the intersection to provide useful information for engineers to design the roads with the shortest travel time, The analyses Operational of existing in Al-jadryia intersection, near University of Baghdad by Utilization aaSIDRA and field measurements show that they can perform adequately despite relatively high traffic volumes in peak hours, The data required for the study were mainly collected through video filming technique also the calculation and evaluation are constructed with the aaSIDRA software. For general analyzing, this intersection is marked worst. This analyzing is indicated by "F" level which is meaning the lowest value for the quality and quantity of this intersection**.

***Index Terms*— aaSIDRA, analysis, Intersection, Traffic, simulation.**

I. Introduction

Traffic signals are a common form of traffic control used by State and local agencies to address roadway operations [1]. They allow the shared use of road space by separating conflicting movements in time and allocating delay. They can also be used to enhance the mobility of some movements as, for example, along a major arterial [2]. Traffic signals play a prominent role in achieving safer performance at intersections. Under the right circumstances, the installation of traffic signals will reduce the number and severity of crashes. But inappropriately designed and/or located signals can have an adverse effect on traffic safety, so care in their placement, design, and operation is essential [3], [4]. The dual objectives of mobility and safety conflict [5]. To meet increasing and changing demands, one element may need to be sacrificed to some degree to achieve improvements in another. In all cases, it is important to understand the degree to which traffic signals are providing mobility and safety for each of transportation[5].

This paper is to analysis operational the traffic flow of the intersection to provide useful information for engineers to design the roads with the shortest travel time, the analyses Operational of existing in Al-jadryia intersection, near University of Baghdad by Utilization aaSIDRA and field measurements show that they can perform adequately despite relatively high traffic volumes in peak hours. For general analyzing, this intersection is marked worst. This analyzing is indicated by "F" level which is meaning the lowest value for the quality and quantity of this intersection.

Dr Hasan Hamodi Joni Assistant prof in civil and structural Engineering, Department of Building and Construction, University of Technology, IRAQ phone: +964-790-1609533; e-mail: hassan_jony@yahoo.com).

Ali Ahmed Mohammed. Lecturer in Ministry of Higher Education and Scientific Research, Office Reconstruction and Projects / Follow up Department, IRAQ (e-mail: aliahmed@rpd-mohesr.edu.iq).

II. Literature Review

A. Review Stage

In various cities, chronic traffic jam happens and traffic congestions lose billions hours and money, In order to reduce these losses, it is required to create an efficient method to resolve traffic congestion and reduce the delay time [6]. Vehicle fuel consumption increases approximately 30% under heavily congestion [7] on the other hand the dynamic vehicular delay at intersections is a major current concern, because the standard static network equilibrium formulation fails to capture essential features of traffic congestion [8]. Build up excessively during peak periods on all approaches of the major intersections. The effects of such queues on motorists are severe at intersections controlled by roundabouts. In order to direct the traffic at roundabouts more smoothly, to give better chances for mass crossings of traffic, and to have better control on queue length it is necessary to have the traffic on such intersections controlled by police [9]. The software used for data analysis is aaSIDRA. The Australian Road Research Board (ARRB), Transport Research Limited, developed the aaSIDRA package as an aid for design and evaluation of intersections such as signalized intersections; roundabouts, two-way stop control, and yield-sign control intersections [9]. The main SIDRA is (Akcelik &Associates Signalized Intersection Design and Research Aid) software is for use as an aid for design and evaluation of the following Intersections

types , signalized intersections (fixed-time / pretimed and actuated), roundabouts, two-way stop sign control, all-way stop sign control, and Give-way (yield) sign-control[9].

In evaluating and computing the performance of intersection controls there are some advantages that the aaSIDRA model has over any other software model. The aaSIDRA method emphasizes the consistency of capacity and performance analysis methods for roundabouts, sign-controlled, and signalized intersections through the use of an integrated modeling framework. This software provides reliable estimates of geometric delays and related slowdown effects for the various intersection types. Strength of aaSIDRA is that it is based on the US Highway Capacity Manual (HCM) as well as Australian Road Research Board (ARRB) research results. Therefore aaSIDRA provides the same level of service (LOS) criteria for roundabouts and traffic signals under the assumption that the performance of roundabouts is expected to be close to that of traffic signals for a wide range of flow conditions[9].

It can be used aaSIDRA to obtain estimates of capacity and performance characteristics such as delay, queue length, stop rate as well as operating cost, fuel consumption and pollution emissions for all intersection types. Analyze many design alternatives to optimize the intersection design, signal phasing and timing specifying different strategies for optimization, Determine signal timing (fixed-time/pre timed and actuated) for any intersection geometry allowing for simple as complex phasing arrangements, Carry out a design life analysis to assess impact of traffic growth. Carry out a parameter sensitivity analysis for optimization, evaluation and geometric design purposes. Design intersection geometry including lane use arrangements taking advantage of the unique lane-by-lane analysis method of aaSIDRA,[10] Design short lane lengths (turn bays, lanes with parking upstream, and loss of a lane at the exit side),Analyze effects of heavy vehicles on intersection performance, Analyze complicated cases of shared lanes, opposed turns (e.g. permissive and protected phases, slip lanes, turn on red),Handel intersection with more than 4 legs, Analyze oversaturated condition making use of aaSIDRA`s time-dependent delay, queue length and stop rate formula [10]

III. Methodology

Level of service (LOS) aaSIDRA output includes results based on the concept described in the US Highway Capacity Manual (HCM) and various other publications. The HCM 97 uses the average control delay (overall delay with geometric delay) as the LOS measure for signalized and unsignalised intersections. aaSIDRA offers the following options for LOS determination: Delay (HCM method), Delay (RTA NSW method), Delay and degree of saturation using a method proposed (by Berry 1987), Degree of saturation only, and Degree of saturation (ICU method). The ICU (Intersection Capacity Utilization) method is used in the USA. Using the ICU method in aaSIDRA, the same degree of saturation criteria will apply for all types of intersection as seen in the table I below. Level-of-service definitions based on degree of saturation using the Intersection Capacity Utilization (ICU) method as shown Table I Queue length in aaSIDRA offers the following options for queue length estimation for all types of intersection: The cycle-average queue, the back of queue. The colour code used for movements in the Queues screen of GOSID is based on the queue storage ratio. The queue storage ratio is the ratio of the queue length (in meters or feet) to the available queue storage distance. The queue storage distance is set as the lane length (in meters or feet). For full-length lanes this equals the approach distance. For short lanes, the queue storage distance equals the short lane length [10].

TABLE I
USING THE ICU METHOD IN AASIDRA CRITERIA FOR ALL TYPES OF INTERSECTION [15]

Level of Service	Degree of saturation (x) All intersection types
A	x <= 0.60
B	0.60 < x <= 0.70
C	0.70 < x <= 0.80
D	0.80 < x <= 0.90
E	0.90 < x <= 1.00
F	1.00 < x

The colour code used in Graphical Output System for Intersection Design (GOSID) is based on the following values of the queue storage ratio irrespective of the (LOS) definition or the intersection type as shown table II, Performance Index (PI) is a measure which combines several other performance statistics, and therefore can be used as a basis for choosing between various designs options (the best design is the one which gives the smallest value of PI). The equation of the Performance Index is defined as [11]

PI might refer to Performance Index but *Tu* might refer to Total uninterrupted travel time (veh-h/h) while w_1 might refer to Delay weight. w_2 might refer to Stop weight, *K* might refer to Stop penalty. *H* might refer to Total number of stops (veh/h). but w_3 might refer to Queue weight , *N'* might refer to Sum of the average queue length values for all lanes of the movement. *qa* might refer to The arrival (demand) flow rate. and *tu* might refer to The uninterrupted travel time.

$$PI = Tu + w1\,D + w2\,KH/3600 + w3\,N' \quad (1)$$

$$Tu = qa\,tu \quad (2)$$

TABLE II
MOVEMENTS IN THE QUEUES SCREEN OF GOSID IS BASED ON THE QUEUE STORAGE RATIO. [16]

Colour code	Rating	Queue Storage Ratio
Green	Very Good	Up to 0.75
Blue	Good	0.75 to 0.90
Magenta	Acceptable	0.90 to 0.95
Red	Bad	Above 0.95

Degree of saturation (x) is defined as the ratio of demand flow to capacity, x = qa /Q (also known as volume/capacity, v/c, ratio). The movement degree of saturation is the largest degree of saturation for any lane of the movement. If there is no lane under-utilization, the degrees of saturation for all lanes and the movement (lane group). Movements in shared lanes will have the same degree of saturation except in the case of de facto exclusive lanes. The approach degree of saturation is the largest x value for any movement (or any lane) in the approach, and the intersection degree of saturation is the largest x value for any approach. That the colour code used for movements in the Degree of Saturation screen of GOSID (Graphical Output System for Intersection Design) is based on the following values irrespective of the LOS (level of service) definition or the intersection type [16] as shown table III. The colour code used for movements and approaches in the Delay & LOS screen of GOSID is based on the LOS values given in Table IV [11] as shown table IV

TABLE .III
MOVEMENTS IN THE DEGREE OF SATURATION SCREEN OF GOSID [4]

Colour code	Rating	Queue Storage Ratio
Green	Very Good	Up to 0.75
Blue	Good	0.75 to 0.90
Magenta	Acceptable	0.90 to 0.95
Red	Bad	Above 0.95

TABLE .IV
MOVEMENTS AND APPROACHES IN THE DELAY & LOS SCREEN OF GOSID [5]

Colour code	Rating	LOS
Green	Very Good	A or B
Blue	Good	C
Magenta	Acceptable	D
Red	Bad	E or F

IV. RESEARCH METHODOLOGY

A. Study Area

The study is usually carried out to collect traffic data for all directional flow at four intersections in the study area along (intersection). In this study, the survey was carried out on working days. The counts were carried out at 15 minutes in the morning peak hour from 7:15 am and in the afternoon, begin peak hour 3:00 pm in 10-12-2014. All computation is based on traffic flows in pcu/hr, figure 3 and has been converted from classified vehicles into passenger car equivalent. In this study the existing of cycle time each intersection also measured. The Intersection will be improved to reduce existing congestion and accommodate future growth .The intersection is a primarily located aljadryia. Shown Figure 1. The directions configuration has the following in the four legs Intersections' with signalized. The northbound peak-hour through movement demand volume exceeds the capacity of the one provided through lane. The peak hour demand volume exceeds the approach capacity, which results in queues that extend more than half the distance to the freeway mainline. The peak-hour demand volume for southbound through movement exceeds the approach capacity in the morning peak hour from 7:15 to 9:00 am and in the afternoon, begin peak hour 2:00 to 3:00 pm, which result in queues that extend to the drive intersection. To minimize southbound queues at this intersection from extending into the interchange, the green time for the eastbound approach is shortened, which results in long queues [12].An intersection will be congested because of the heavy traffic flow in every direction especially vehicle from (intersection) then exit to the highway. A long queue on north leg and east leg and lots of heavy vehicles especially busses going in the west leg (educational area) .While in intersection four legs intersections' The southbound peak-hour through movement demand volume exceeds the capacity of the one provided through lane. As shown Figure 1.

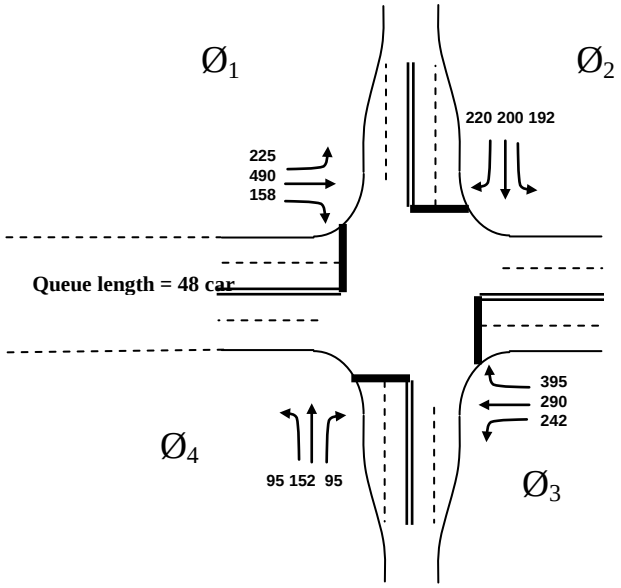

Figure.1 an illustration of signalized intersections

B. Data Collection (Traffic Surveys)

The study consists of eight main activities as shown in Figure 1. The main activities are data collection, determination of phasing sequences, determination of optimum cycle by

Webster a formula. In this phase the data was visually collected from the videotapes. All the videotapes were studied visually to extract the traffic volumes and turning movements for the analysis. Every vehicle coming from all the approaches for a period of 15 minutes was recorded on pre-prepared data collection sheets. The peak-hour demand volume for southbound through movement exceeds the approach capacity in the morning peak hour from 7:00 to 9:00 am and in the afternoon, begin peak hour 2:00 to 4:00 pm hourly counts were used as input data for analysis using aaSIDRA software.

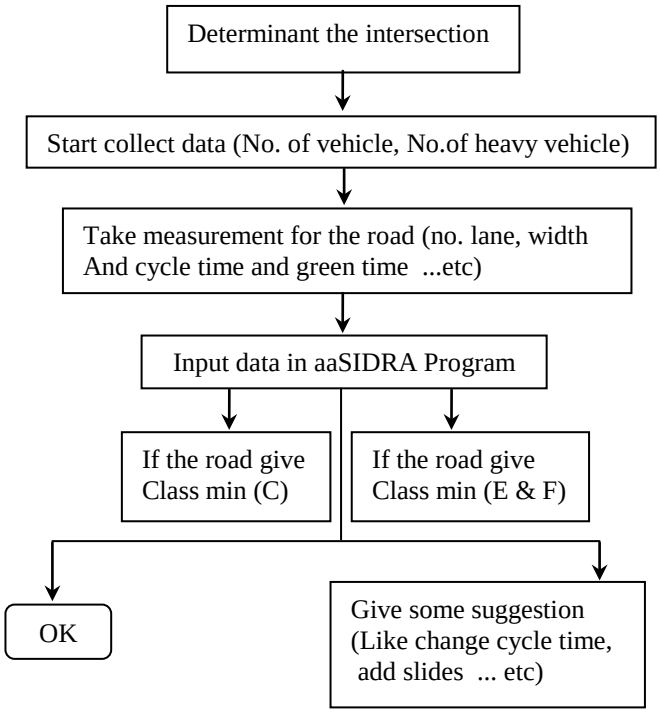

Figure. 2 Flow chart showing the Main Procedure analysis

V.EXPERMENTAL RESULTS FOR OPTIMUM CYCLE TIME

Calculation the optimum common cycle time ,green time split for each intersection and offset time by assume amber for all =3 sec ,all red time = 1 sec , speed =36 km/h ,h=2 sec ,loss=2 sec as shown table V

A. Optimum Cycle time

The maximum cycle time will be 120 seconds .The Webster a formula is given as follows [5].

$$C_o = \frac{1.5L + 5}{1 - \sum y} \quad (3)$$

Saturated Flow=1800*2=3600 pcu/h (4)

L= 4 directions (4 sec) = 16 $_{sec}$

C_0 = 1.5*16 +5/ (1- 0.667) = 87 $_{sec}$

Cycle time = effective green time + Amber time + All red (5)

Amber for all = 3*4 =12 sec

All red = 1*4 =4 sec

Effective green time = 87 - (4+12) =67

= 67 sec as shown table VI

TABLE .V

ESTIMATE THE EFFECTIVE GREEN TIME IN INTERSECTION

Phase	Left	Straight	Right	Total Actual Flow (a)	Saturated Flow pcu/h (v)	Y=a/v
Ø1	225	302	158	685	3600	0.190
Ø2	220	200	192	612	3600	0.17
Ø3	232	290	242	764	3600	0.212
Ø4	95	152	95	342	3600	0.095
						Y=0.667

TABLE .VI

CLASSIFICATION EFFECTIVE GREEN FOR EACH INTERSECTION

Phase	Y=a/v	Effective green time (sec)
Ø1	0.190	0.190/0.667*67= 19
Ø2	0.17	17
Ø3	0.212	21
Ø4	0.095	10
	Y=0.667	67 sec

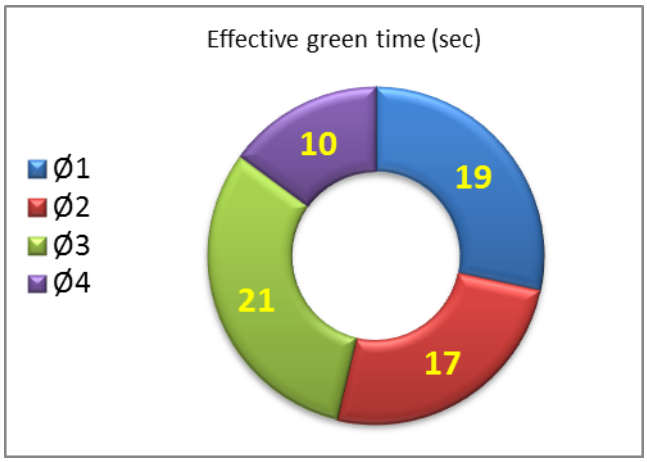

Figure 3. Signal Controller Setting

B. Offset Time)

Queue length is one the parameters required to determine the suitable offset time in a network of signalized intersections. As the queue becomes longer at the downstream intersection, the offset time becomes shorter as given in equation (6). The reduction in offset time is mainly to clear the queued vehicles before the platoon of vehicles from the upstream intersection arrive at the stop line [12],[13]

$$T_{ideal} = \frac{L}{S} - (Qh + Loss) \quad (6)$$

T_{ideal} =400/10-(48*2+2)

= 58 sec

Tideal =400/10-(48*2+2)
= 58sec

VI. RESULT

Analysis data collection for the traffic flow of the intersection in aljadrea. The data are collected from videotapes for the peak periods visually in 15-minute periods, and hourly data was then input to the aaSIDRA software for analysis. The data analysis was done separately for the AM and PM hourly volumes but the procedure followed was the same for both sets of data. This was done to see whether the results differed due to the differences in before and after traffic volumes for both AM and PM traffic counts, as there was more traffic during the PM period than during the AM period traffic counts, as there was more traffic during the PM period than during the AM period, peak hour from 7:00 to 9:00 am and in the afternoon, begin peak hour 1:00 to 4:00 pm.

There are several reasons that they are used for the intersection such as geometry, Delay and Loss, Queue, Stops, flow, movements and Degree of saturation. This paper tries to analysis the data the result with each other to find out what is the best choice for the roads.

Regarding to the table VII there are some items that are shown the impact of the intersection on the traffic such as intersection geometry, level of service, average intersection delay, degree of saturation, Practical Spare Capacity (lowest), Total vehicle capacity, all lanes (veh/h), Total vehicle delay (veh-h/h) and some more items. From the above tables it's obvious that having the intersection is worst because the Intersection Level of Service (LOS) is (F), regarding the effects of various types of movements on aaSIDRA results all movements except dummy and movements are considered when determining the intersection degree of saturation (largest degree of saturation for any movement), For the Delay and LOS rating is bad in the level (F) in three phases but in other phase is rating is acceptable in the level (D) shown Figure (V5).But at the Intersection Level For the Queues rating is Bad in the level (F) in three phases but in other phase is rating is very good in the level(A) shown Figure(VI6). While For the Level Stops rating is bad in the level (F) in four phases shown Figure (VII7). Finally for the Level degree of saturation rating is bad in the level (F) in three phases but in other phase is rating is good in the level (C) as shown Figure (VIII 8).

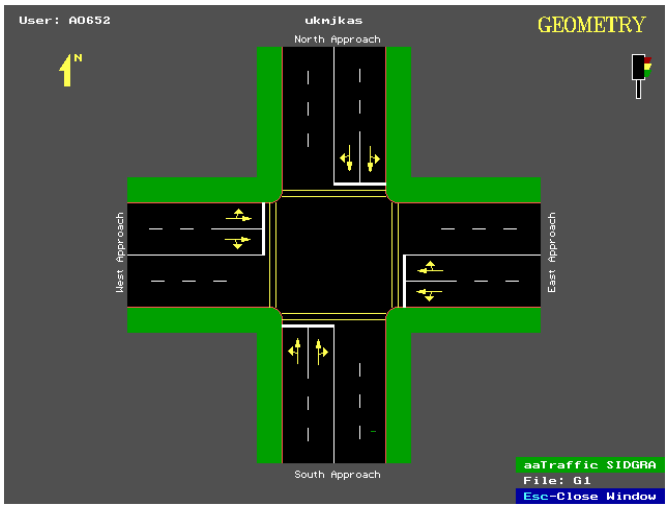

Figure 4. Intersection road (main road)

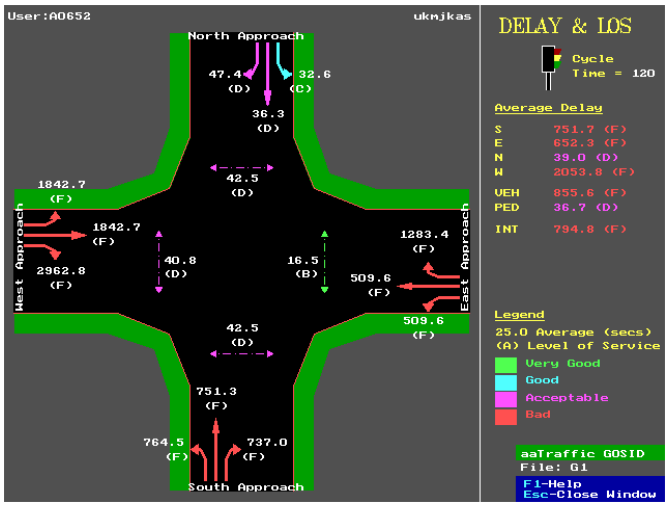

Figure V. Description delay and LOS

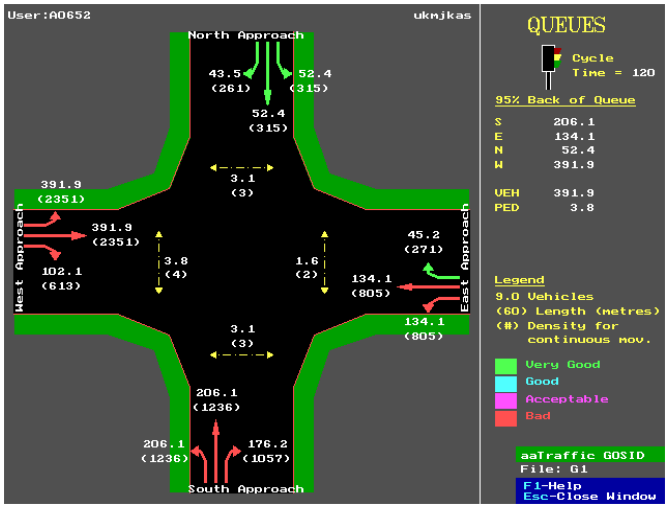

Figure VI.Description of Existing Queues at the intersection

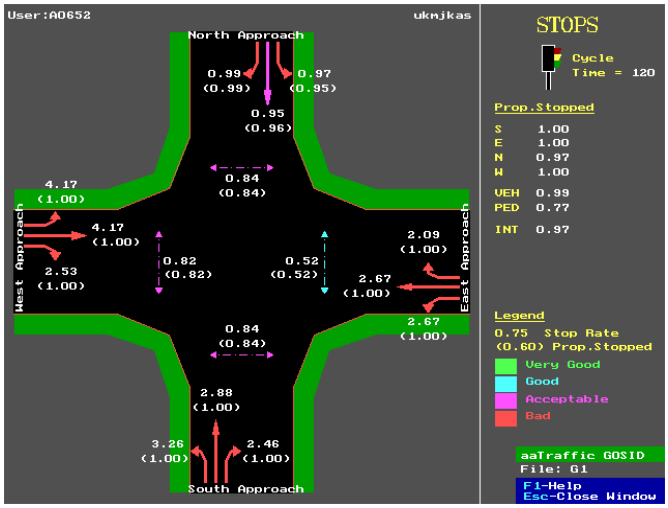

Figure VII. Description of Existing Condition Stops

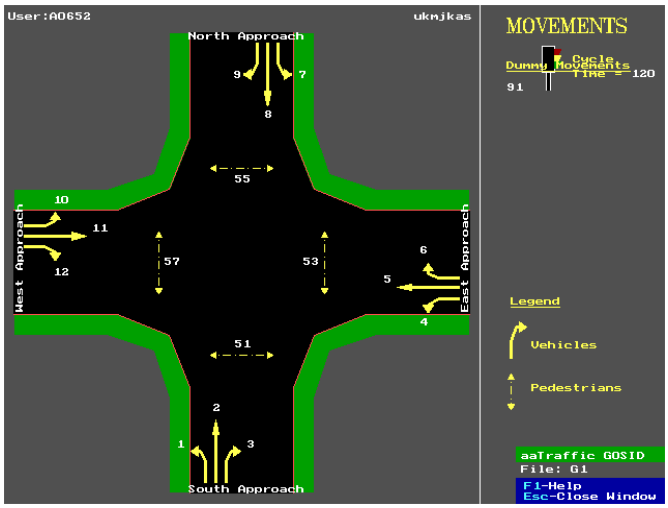

Figure X: Description of Existing Condition Movements

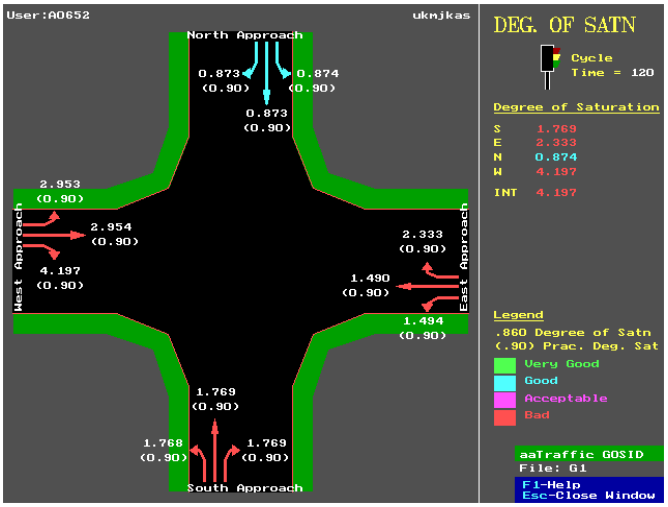

Figure VIII: Description of Existing Condition degree of saturation

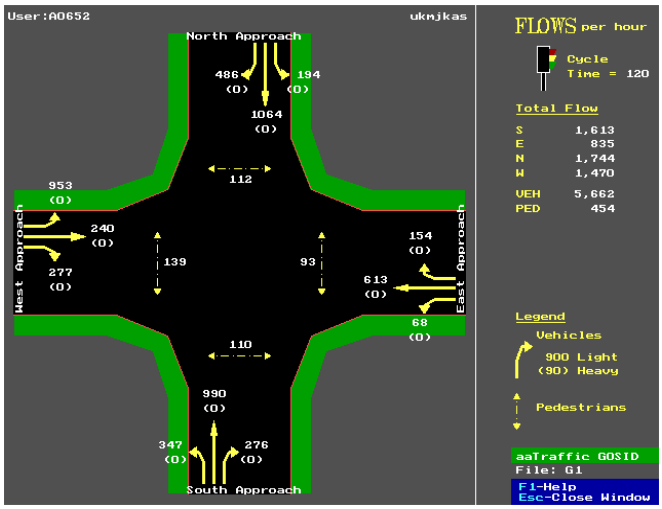

Figure XI: Description of Existing Condition Flows per hour

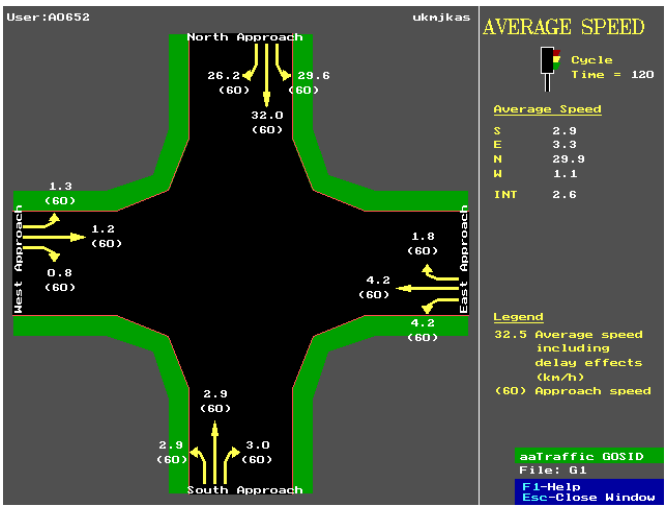

Figure IX: Description of Existing Condition Avarge Speed

TABLE .VII
RESULT FOR C STUDY (INTERSECTION)

INTERSECTION PARAMETERS	
Cycle Time:	= 87
Intersection Level of Service	= F
Worst movement Level of Service	= F
Average intersection delay (s)	= 36.5
Largest average movement delay (s)	= 74.2
Largest back of queue, 95% (m)	= 109
Performance Index	= 122.91
Degree of saturation (highest)	= 1.0
Practical Spare Capacity (lowest)	= 3 %
Total vehicle capacity, all lanes (veh/h)	= 8203
Total vehicle flow (veh/h)	= 3619
Total person flow (pers/h)	= 450
Total vehicle delay (veh-h/h)	= 36.75
Total person delay (pers-h/h)	= 50.52
Total effective vehicle stops (veh/h)	= 3299
Total effective person stops (pers/h)	= 4948
Total vehicle travel (veh-km/h)	= 2350.6
Total cost ($/h)	= 1845.87
Total fuel (L/h)	= 299.1
Total CO2 (kg/h)	= 747.66

VII. CONCLUSION

The aaSIDRA has a good result for analyzing the intersection starting delay, stops, queues, capacities, flows and also phase sequences. Based on the data analyzing from aaSIDRA, it is concluded generally that the direction. It might be caused by low queues value, which is mean the number of the vehicles that pass aljadriya site lower than another sites. And the other hands, the mobility of this site show the dynamic of changing vehicle movement. Besides, it also performs the good quality of air which is produced by the vehicles emission. For the Delay and LOS rating is bad in the level (F) in three phases but in other phase is rating is acceptable in the level (D) shown Figure (V).But at the Intersection Level For the Queues rating is Bad in the level (F) in three phases but in other phase is rating is very good in the level(A) shown Figure (VI). While For the Level Stops rating is bad in the level (F) in four phases shown Figure (VII). Finally for the Level degree of saturation rating is bad in the level (F), for general analyzing, this intersection is marked worst. This analyzing is demonstrated by “F” level of this intersection.

ACKNOWLEDGMENT

I expressions Special thanks to Assist. Prof. Dr.Hasan Hamodi Joni for guidance in the research.

REFERENCES

[1] R.Akceklik,and B.Besley, “Acceleration and deceleration models. Paper presented at the 23rd Conference of Australian Institutes of Transport Research”(CAITR 2001), Monash University, Melbourne, Australia, 2001 10-12 December.
[2] R.Akceklik, “New Features of aaSIDRA 2.1-summary,”Australia, Victoria,2004.
[3] R .Akcelik “aaSIDRA User Guide.Akcelik and Associates Pty Ltd,”Melbourne, Australia(2002).
[4] A. Ahmed, “ Intersection Analysis by aaSIDRA Software for Computer Simulation to Optimize the Traffic Flow,” in Eng. &Tech.journal, Vol. 31, No.4, 2013. pp.774-792.
[5] A. Ahmed, O. Ali, “Traffic Flow Analysis For Intersection Using Computer Simulation Aasidra Software: A Case Study In Bangi Malaysia,” in Tikrit Journal of Engineering Sciences, Vol. 20, No. 7,2013.pp. 10-25
[6] R .Akcelik," Traffic Signals: Capacity And Timing Analysis", Research Report ARR No. 123. ARRB Transport Research Ltd, Vermont South, Australia. (6th reprint: 1995).
[7] R .Akcelik, "Calibrating aaSIDRA. Australian Road Research Board", Research Report ARR No. 180 (2nd edition, 1st reprint 1993).
[8] R .Akcelik, "Alternative Delay Models for Actuated Signals", Discussion Note WD TO 95/013-B. ARRB Transport Research Ltd, Vermont South, Australia .
[9] R .Akcelik and E. Ching, "Traffic performance models for unsignalised intersections and fixed-time signals", Proceedings of the Second International Symposium on Highway Capacity, Sydney, ARRB Transport Research Ltd, Vermont South, Australia, Volume 1,1994.pp. 21-50.
[10] McShane W. R., Roess R. P. and Prassas E. S. (1990). Traffic Engineering. Prentice Hall, New Jersey, Pp. 599-623.
[11] P.Sisiopiku,O. Heung-Un Oh," Evaluation of Roundabout Performance Using aaSIDRA", Journal of Transportation Engineering, ,2001
[12] R. Vincent, A. Mitchell, D. Robertson, " User Guide to TRANSYT Version 8", Transp. Road Res. Lab. (U.K.), TRRL Lab. Report LR 888, 2001.
[13] D. Greenwood and C.Bennett , “The Effects of Traffic Congestion on Fuel Consumption,” in Road & Transport Research, Vol. 5, No. 2, , pp. 18-31, June 1996.

Assist. Prof. Dr.Hasan Hamodi Joni Head of Highways & Bridges Engineering branch in Building Construction Eng. Dept. University of Technology. Graduated BSc. In Civil Engineering, 1988, form Al-Rasheed Engineering College/ University of Technology. The M.Sc. degree in Civil Engineering (Highway Engineering),1995, from Al-Rasheed Engineering college/University of Technology. The Degree of Doctor of Philosophy in Civil Engineering (Highway Engineering) from University of Technology (2006) and Assist. Prof. Degree in (2011). Worked as a Director Manager of Scientific & Engineering Consulting Bureau/University of Technology, Baghdad-Iraq from 2006 until 2010. Supervisor for a number of M.Sc. theses in Transportation and Geotechnical Engineering. Lecturer of Postgraduate courses for higher Diploma and M.Sc. students in Transportation Engineering. Consultant for civil Engineering Works in many agencies especially in transportation and highway Engineering.

Runway orientation problems – A case study of Middle Euphrates International Airport MEIA

S. I. Sarsam

***Abstract*—It has been planned to design and construct a major international airport at the middle Euphrates region of Iraq to support the commercial development plan and serve the pilgrim's occasional visit to the holly shrine at Holly Karbala and Najaf provinces. The airport site is 30 km west of Karbala at the edge of the great western desert. The design includes construction of two parallel runways of 4500 m length, and 2300 m center to center apart. Metrological data regarding the wind intensity, duration, direction and speed have been obtained for the site, and the wind rose diagram has been drawn. The selected project area practices a calm wind speed throughout the past 25 years. The runway orientation of maximum coverage was designed to be NW-SE (315 – 135). The site was adjacent to power station plant and problems arise with the interference of the 35 m height chimney of the plant with the air field. Four alternatives have been considered to solve such problem based on a comparative analysis. The first one was to move the location of the runways system to the North West in order to reduce the portion of OLS approach surface above the power plant. The second alternative was to increase the center to center distance between the runways to 3000 m in order to have the power plant out of the OLS approach surface. The third alternative was to increase the spacing between runways to 3000 meters and shift the second Runway to the extreme north. The fourth alternative was to change the orientation by 15 ° clockwise to a new one of (330 – 150) with minimal effect of 3% on wind coverage. The paper presents the details of such alternatives and finalizes the decision on runway orientation based on economic justification and site condition.**

***Index Terms*— comparative analysis; metrological data; orientation; runway; wind coverage.**

I. Introduction

It was decided to establish an international airport at Holly Karbala governorate, two major issues are required to be considered; the first issue is that the airport should be located at 30 km west of the city center, while the second issue is that the airport should be located within the administrative boundaries of the Holly Karbala province. Based on those issues, the final site selected was located west of Euphrates River as shown in plate 1. The airport site is located within the gypsoferious desert land, and midway between Najaf and Karbala.

Manuscript received June 28, 2015.

S. I. Sarsam, is with the department of Civil Engineering, College of Engineering, University of Baghdad, Baghdad, IRAQ (corresponding author phone: 00964-7901878167; e-mail: saadisasarsam@coeng.uobaghdad.edu.iq.

II. Collection of Metrological Data

The Metrological organization was in charge of measuring and supplying of data from 24 stations across the country; these stations have daily records on climatic conditions for the regions on which they exist. Such data covers the past 20 year's period for the whole country. The wind data which includes wind direction, speed and percentage intensity (duration) have been collected, from Holly Karbala, Najaf and Hilla metrological stations. Such data were fed to the database of the developed software [1] and to the FAA software.

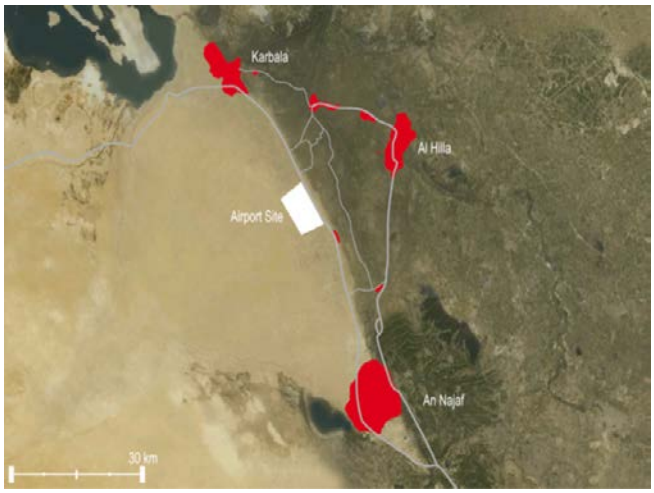

Plate 1. Site location of MEIA Airport

a. Design of runway orientation

Wind coverage was calculated using a wind rose, which graphically depicts wind data. The wind rose is essentially a compass rose with graduated concentric circles representing wind speed. Each box in the wind rose represents a compass direction and, when filled, indicates the percentage of time wind travels in that direction at that speed, [2].

The wind rose template has a polar coordinate system that is made of circles and radial lines, Circles on the template represent the wind speed, while the radial lines illustrate the angles or the wind blowing directions. Each cell bounded by two circle segments and two radial lines, which stores the percentage of time, that the winds correspond to a given direction and velocity range. The circle with label represents the speed of crosswinds the runway will experience during its operations, and it is less than that of the allowed crosswinds. A transparent runway template is placed on the wind rose to

represent the proposed runway that accommodates the size and operating characteristics of aircraft, [3]. The template is rotated around the center of the wind rose in order to search for an optimal runway orientation. At each rotating angle, the total percentage of allowable crosswinds in the wind rose that are covered by the template is calculated, and a best angle that can give the maximum percentage of coverage is determined. Fig.1. shows the work sheet of the method, while Fig.2 Illustrates the wind rose diagram.

The optimized runway orientation obtained was (SE - NW; 135/315) orientation. The wind coverages for various crosswind component are illustrated in Table 1. The metrological data of the three governorates were fed to the software, it was noticed that data of holly Karbala was similar to those of Hilla and Najaf, and the variation was not significant. It was considered to use the data of holly Karbala for the wind rose analysis.

Table 1.
Wind coverage analysis

Crosswind component	Wind coverage results, (135/315) orientation
37 km/h (20kt)	99.51%
24 km/h (13kt)	97.27%
19.5 km/h (10.5kt)	94.86%

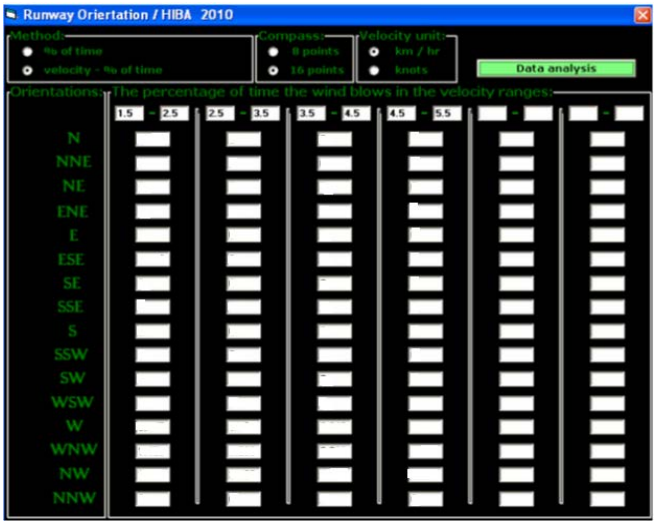

Fig.1 Work sheet for wind rose

b.Site Problems with Runway Orientation

Problems arise when checking the designed orientation with the airport site, at the 315 side, an oil refinery exists with a chimney of 50 meters height. This chimney will interfere with the obstacle limitation approach surface (OLS). As per ICAO [4], the location of OLS above the power plant chimney was not recommended. The proximity of the refinery to the airport can be managed regarding the obstacles created by the refinery facilities. The risks associated with the refinery smokes also appear manageable in terms of visibility since opaque smokes are not expected during normal operations. However, with the height of chimney, the refinery obstacles are a deviation from ICAO recommendations based on a specific safety case analysis, (ICAO, Annex 14) as per ICAO recommendation, and commissioned by the Civil Aviation Authority.

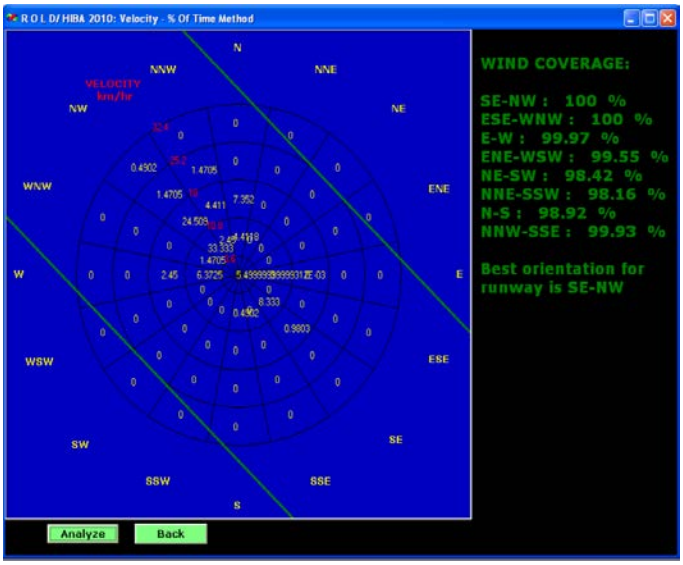

Fig.2 The wind rose diagram

On the other hand, the Iraqi Environmental Regulation provided by MOT states that refinery projects should be located 15 km from the "main infrastructures" or "basic designs" in the wind direction and 10 km in the other direction. If this regulation apply to the airport, a change of the airport site or of the refinery would be required. It has to be noted that the benchmark of existing major international airports located within distances of refineries similar to the MEIA case tend to show such locations are be acceptable. Fig.3 illustrates a schematic longitudinal section of the Approach Obstacle Limitation Surface from the northern threshold (sketch for illustration, not drawn to scale but figures are exact). The longitudinal distance between the second stage runway northern threshold and the power plant further corner, which is the most remote location where the chimney can be, is 7400m. Fig.3 shows that the top of the chimney is located only 100m below the Approach Surface, whereas FAA recommendation is to avoid overflight of such chimney by less than 300m from the top of the chimney. Fig.4 shows the chimney location and the designed orientation.

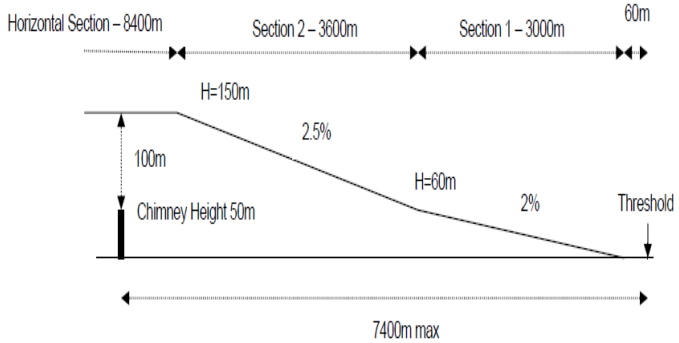

Fig.3 Typical section of the OLS above the runway

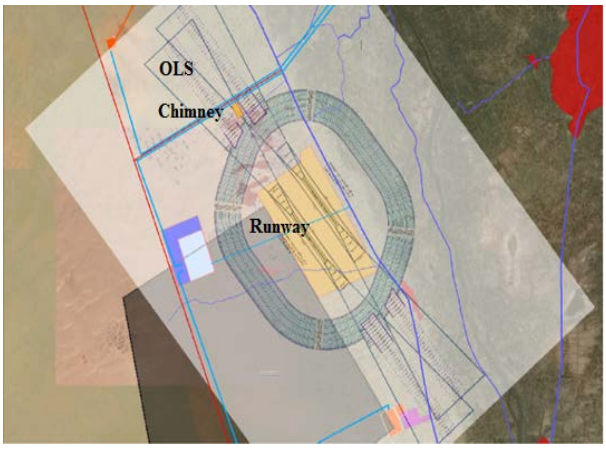

Fig.4 Chimney location and the designed orientation

Different alternatives have been considered. The first alternative (Option 1) consists of moving the runway system to the North West in order to reduce the portion of OLS approach surface above the power plant. Fig.5 illustrates the runway orientation and the chimney location for this option. This option is not solving the problem.

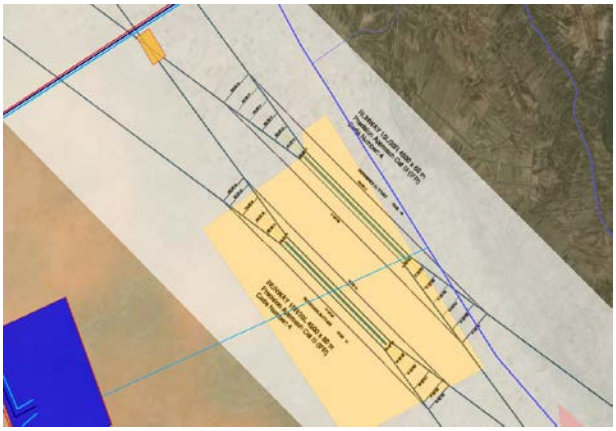
Fig. 5. Runway orientation 135/315 Shifted to North – West

The second alternative (Option 2) consists in increasing the distance between the two runways, in order to have the power plant out of the OLS approach surface. Fig.6 demonstrates such option.

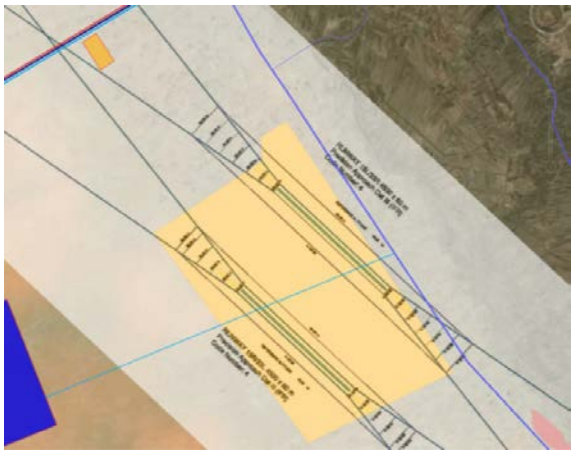
Fig. 6. Runway orientation 135/315 with 3000m centerline spacing

This alternative is not recommended since the chimney still lies under the approach surface and implies conflicts with the land-use, so this option does not work safely.

The third option was increasing the spacing between runways to 3,000m and locating the second runway at the extreme north, the ILS approach lighting ramps for runway threshold 31R and 13L are outside the Airport Site boundary, the power plant chimney would still be located under the approach surface as shown in Fig.7.

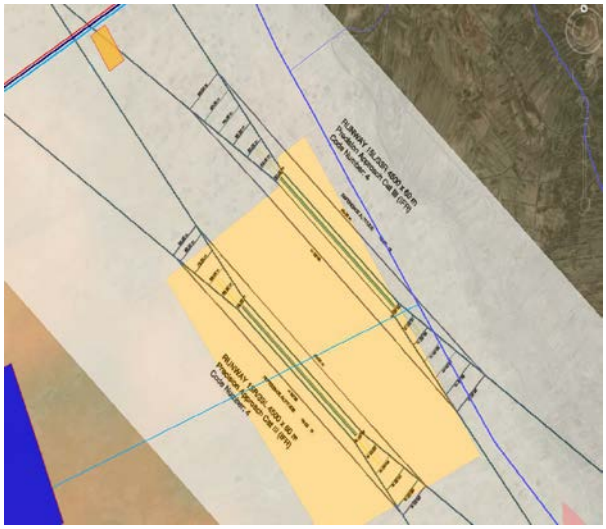
Fig.7. Runway orientation 135/315, second Runway shifted to North and keeping 3000m centerline spacing

In addition, with a centerline spacing of 3,000m the spacing between the runways needs to be increased by 700 m. This has many impacts such as increase in cross-taxiway length by 700 m, corresponding to an additional cost of Code F taxiways, excluding shoulders, increase in road system length, apron, taxiing times and airline fuel costs to compensate the increased spacing.

However, in this case it is not possible to avoid a situation in which the Power Plant would still be located under the approach surface of both runways and the power plant chimney under the approach surface of either runway 1 or runway 2. ILS approach lighting ramp of runway 15L and airport fence would lie outside of Site boundary, and within the 5km perimeter around the power plant, which does not comply with the environmental regulation considered in the site selection. The first runway OLS would not represent an issue. However, in this approach, the constraints result from the second airport runway. With a 135/315 orientation it is not possible to find a suitable location inside the Airport site for runways and associated ILS approach systems so that the Karbala gas power plant is outside the OLS approach surface of the second runway.

The fourth option is to change the orientation by 15 ° clockwise to a new one of (330 – 150) and check the impact of wind coverage. Fig.8 shows the fourth option. The new orientation data were fed to FAA software, the metrological data of the three governorates were fed to the software, and the

new wind rose was obtained as demonstrated in Fig. 9.

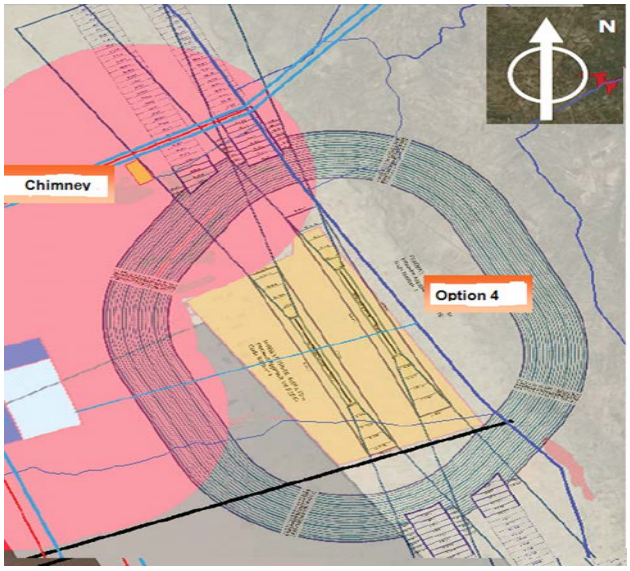

Fig.8 Runway orientation 150/330

The above three alternatives are not recommended, since its negative impacts in terms of costs, operations and flexibility by far outweigh the very slight benefit in term of wind coverage. Furthermore, it is not possible to avoid having the power plant inside the approach surface of runway 2 in any of the layouts considering a 135-315 runway orientation. Then alternative four was assessed as possible alternative to overcome the problem of orientation.

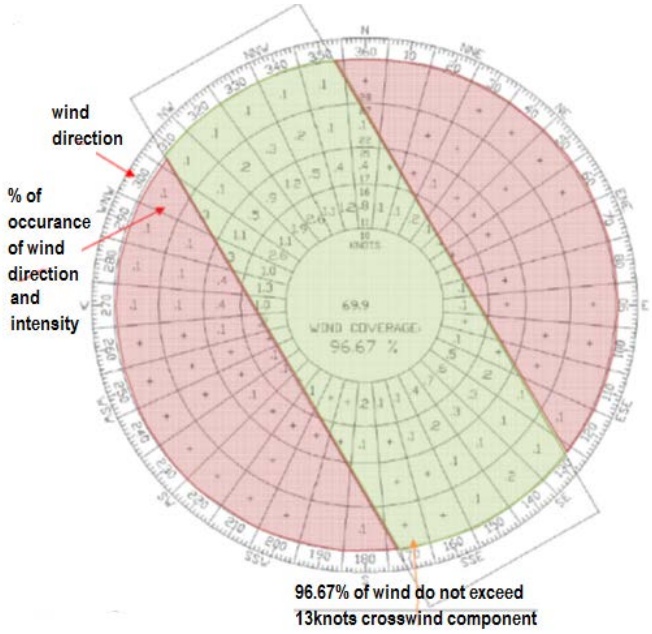

Fig. 9. FAA Wind rose diagram for the 150/330 orientation

c. Wind coverage analysis

Table 2 illustrates the wind coverage analysis for the metrological data obtained from Holly Karbala station, the analysis was based on both runway orientations, and three different crosswind component. As shown on the tables, the coverage difference between the two orientations is only 1.11% for aircraft with reference field length under 1,200m (light general aviation piston or turboprop aircraft) when considering the wind data from Karbala station. This represents only 4 days of runway unavailability over a year for small aircraft for the 150/330 orientation compared to the 135/315 orientation. Fig.10 shows typical output of FAA software for 20 knots of cross wind component.

Table 2.
Wind Coverage Analysis –Data for Karbala Station

Crosswind component	Aero plane Reference Field Length	Wind Coverage Results – Runway Orientation 330/150	Wind Coverage Results – Runway Orientation 315/135	Difference
37 km/h (20kt)	1500m or over	99,44%	99.51%	0.07%
24 km/h (13kt)	1200m or up to but not including 1500m	96.67%	97.27%	0.60%
19.5 km/h (10.5kt)	Under 1200m	93.75%	94.86%	1.11%

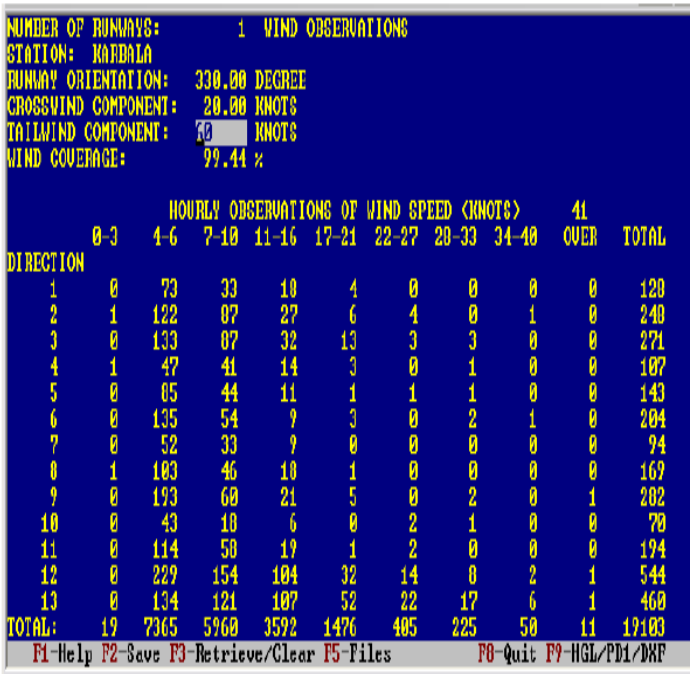

NUMBER OF RUNWAYS: 1 WIND OBSERVATIONS
STATION: KARBALA
RUNWAY ORIENTATION: 330.00 DEGREE
CROSSWIND COMPONENT: 20.00 KNOTS
TAILWIND COMPONENT: 10 KNOTS
WIND COVERAGE: 99.44 %

HOURLY OBSERVATIONS OF WIND SPEED (KNOTS)

DIRECTION	0-3	4-6	7-10	11-16	17-21	22-27	28-33	34-40	41 OVER	TOTAL
1	0	73	33	10	4	0	0	0	0	120
2	1	122	87	27	6	4	0	1	0	248
3	0	133	87	32	13	3	3	0	0	271
4	1	47	41	14	3	0	1	0	0	107
5	0	65	44	11	1	1	1	0	0	143
6	0	135	54	9	3	0	2	1	0	204
7	0	52	33	9	0	0	0	0	0	94
8	1	103	46	10	1	0	0	0	0	169
9	0	193	60	21	5	0	2	0	1	282
10	0	43	18	6	0	2	1	0	0	70
11	0	114	50	17	1	2	0	0	0	194
12	0	229	154	104	32	14	0	2	1	544
13	0	134	121	107	52	22	17	6	1	460
TOTAL:	19	7365	5960	3592	1476	485	225	50	11	19183

F1-Help F2-Save F3-Retrieve/Clear F5-Files F8-Quit F9-HGL/PDI/DXF

Fig.10. Typical output of FAA software for 20 knots of cross wind component

III. CONCLUSION

Based on the analysis conducted, the following conclusions may be drawn:

1- In the site selection for a new airport, it is essential to conduct an intensive investigation on the existence of industrial properties nearby the site, which could restrict or interfere the development and operation of the airport, and its possible future expansion.

2- An intensive wind coverage study should be conducted

using new metrological data based on more than one metrological station; the (climate-change) issue should be taken into consideration.

3- The impact of changing the runway orientation slightly on the wind coverage could be assessed by back calculation process as explained in this work.

REFERENCES

[1] S. I. Sarsam and H. A. Ateia " Development of a computer program for Airport runway location, Orientation, and length design in Iraq" Proceedings, T & DI Congress, March 13–16, 2011, in Chicago, Illinois, USA © ASCE, 2011, pp 291-300.

[2] L.W. Falls and S. C. Brown "Optimum runway orientation relative to crosswind", NASA Technical note TND-6930, National aeronautics and space administration, Washington DC, September- 1972.

[3] R. Mousa and S. Mumayiz " Optimization of Runway Orientation", Journal of Transportation Engineering, Volume 126, Issue 3, May/June 2000 pp. 228-236.

[4] ICAO International Civil Aviation Organization: Annex 14, "Aerodrome Design and Operations". 2004.

Terrestrial Laser Scanning to Preserve Cultural Heritage in Iraq Using Monitoring Techniques

Fanar M. Abed, Omar A. Ibrahim, Luma K. Jasim, Yousif H. Khalaf, Hassan M. Hameed, Zahraa A. Hussain

***Abstract*— In the last two decades Terrestrial Laser scanning (TLS) was found to be the best digital technology to provide an effective solution to preserve and sustain heritage buildings. This can be achieved by monitoring and identifying any differential movements, deflection, cracks in such structures and deliver an applicable scientific solution and avoid extinction to this valuable heritage. The data delivered from this technique are required to study and further analyze the behavior of these structures from construction and geomatics point of view in order to assess its stability by allowing to detect a very huge number of information with relatively short time and high accuracy. This research is aiming to preserve al-Kadhimiya Holy Shrine in Baghdad/IRQ by monitoring the deflection in constructed Minarets and cracks holds due to engineering works followed building expansion project, ground water and time factor effects. The project was hold for 12 months with monthly observation monitoring using Stonex X300 TLS device and traditional field surveying techniques. The scan was made using fine resolution and camera close-rage coverage. The data have been processed using 3D Reconstructor software/ Survey 2014 Module resulting three-dimensional model represents what often is of concern. The geometry of the structure was described through the analyses of the captured point clouds along the monitoring period of time. The Minarets' deflection and available cracks were the main focus of this study. The observations were run alongside traditional surveying techniques and photogrammetric modelling. The validation process were accomplished with the aid of traditional measuring instrument whereas the photogrammetric work and their accompany results will be presented in a separate paper work in near future with comparison study of the three used techniques. The overall motivation of this research is to preserve the cultural heritage in IRAQ using new laser techniques for the first time for such important applications by aiming to deliver high accurate results and saving both time and efforts as compared with available traditional process.**

***Index Terms*—Cultural heritage, 3D reconstructing, Deformation, Monitoring, Terrestrial laser scanning.**

I. INTRODUCTION

CULTURE Heritage objects with various shapes, sizes, and complexity, are representing nations treasures from small artefacts and heritage items to large landscapes and ancient historical buildings including archaeological sites [1].

Documenting all these important cultural information has been of great interest in the last decade through the International Society of Photogrammetry and Remote Sensing (ISPRS) to preserve civilizations and the historical legacy of nations. This has been well demonstrated through the developments of the Terrestrial 3D laser scanners which brought these massive landscapes to the recording, preservation, and study following digital technology [2]. Due to the rapid data that 3D scanners can capture, laser scanners has become the most practical and effective tool to use alongside image based documentary to preserve cultural heritage and reconstruct the 3D models from these data [3]. 3D laser scanners can record three-dimensional information of massive object points with a relative short period of time and accurate results. In order to deliver these information, the laser transmitter sent a laser beam to scan the object surface with certain specification to fulfil the scan need and the range accuracy [4]. The scanning effect is achieved using mirrors to allow the required scan pattern. This allow changes in the incidence angles in small increments when the beam spotted the objects with a specific footprint size [5].

In the last few years, many 3D scanners have appeared in the market for downstream applications such as surveying, modelling, environmental, etc. To deliver effective outputs, the 3D scanner should be close ranged to the object and has the ability to rotate with a certain range both horizontally and vertically to accomplish the mission with a suitable field of a view and deliver 3D coverage [6]. This powerful technology is also able to provide promising solutions to several problems which need to be overcome when applying a successful and reliable survey. Such kind of problems can be identifying differential movements, deflection, cracks in heavy and historical structures and delivering a practical solution to avoid extinction of this valuable heritage. This technology is considered important especially when these deformations are difficult to be accessed due to complex scenarios such as towers (i.e. limited accessibility and visual obstructions). Unaware of art and history that surrounds them, citizens can be "awakened" by the 3D reconstructions of high accuracy and range resolution those obtained from massive point clouds detected by 3D laser scanners [7].

Many researches have been presented in this aspect for cultural heritage applications. One of these studies was the accurate 3D site recording of the treasury (Al-Kasneh) in Petra, Jordan by [8]. Mensi GS100 3D laser scanner was used

Manuscript received March 4, 2015 and accepted August 30, 2015. Date of publication September 1, 2015.

The authors are with the Department of Surveying Engineering, College of Engineering, University of Baghdad, Baghdad, IRQ. (e-mail: fanar_mansour@yahoo.com, eng.omarali@gmail.com, j.lumakhalid@yahoo.com, husain_yousif@yahoo.com, zahraaazeldeen@yahoo.com).

in this project with 360° and 60° field of view angles in horizontal and vertical directions respectively. The distance measurement is obtained using time of flight principals based on 532 nm laser allowing distance between 2 and 100m. The system can capture up to 5000 point per second. For texturing purposes, photogrammetric data was integrated using Fuji S1Pro camera. The point clouds have been processed using Innovmetric's Poly-Works™ software. The produced 3D model have an average resolution of 5 cm from millions of captured point clouds. A textured 3D model of the A-Kasneh site was produced demonstrating the possible and the successful integration of laser scanning data with photogrammetry to historical site documentary.

In 2004, the pyramids archaeological site at Giza, Egypt was scanned for topographic long-distance modelling [9]. The main purpose of scan was documentary and monitoring standing monuments. Riegl LMS Z420i long-range scanner was used to scan the site in this project. The scanner was combined with a built-in high resolution digital camera for texture information. The purpose of the scan was to document and model the Cheops Pyramid, Sphinx and surroundings. In addition to extract high resolution 3D elevation model of the Giza plateau. The data have been processed automatically with some manual steps to generate the textured triangulated surfaces of the scanned monuments.

Another archaeological investigations were conducted with terrestrial laser scanners between 2007 and 2008 in a mining landscape in the lower Inn Vally, Northern Tyrol, Austria. The scan was conducted to search for numerous traces of underground mining, mineral processing and ore smelting those have been located in the mentioned site. The data have delivered using Trimble GX laser scanner with at least four stations for a single field with an average density of point cloud reaches to 5 mm at a distance of 4 m. The post-processing was conducted using Trimble Realworks™ software to deliver the 3D texture models [10-12].

Similar project was obtained to the Abby of Niedermunster, Alsace, France for archaeological applications also. It is a Roman-style Abby which has been devastated during the War of the Peasants in 1525, and by two fires in 1542 and 1572 respectively. The data have been captured using Trimble GX advanced 3D terrestrial laser scanner with a very high density of 1000 point per m^2. Fifteen different scan position were used to deliver 40 different scans and giving a total of approximately 30 million points for the entire site [13].

Terrestrial laser scanning techniques for cultural heritage applications is not only based on traditional approaches of preservation by aiming to deliver high resolution 3D models of the scanned sites or for documentary purposes. It also can be invested to apply accurate measurements and monitor deformation in cultural buildings to preserve these buildings from extinction due to time effect. Those information are of great interest to history specialists to restore artistic heritage. These techniques are based on measurements and analysis which are directly computed on the points cloud itself and it does not need always to go through hard processing and modeling, which takes long time. Such innovative approach, which is based on the engineering perspective, aims to provide useful information for structural analyses.

Based on this purpose, this paper presents a modified technique to monitor deflection and deformation in the al-Kadhimiya Holy Shrine Minarets located in Baghdad/IRQ holds due to engineering works following building expansion project, ground water and time factor effects. The methodology presented is applied using Stonex X300 close-range terrestrial laser scanner with built-in high resolution digital camera for texturing information. The results have processed, analyzed, and validated against data delivered from accurate field measurements from traditional techniques to demonstrate the validity of the applied routine as stated in the next sections.

II. AL-KADHIMIYA HOLY SHRINE

The Al-Kadhimiya Holy Shrine is a Mosque located in the Kadhimiya district to the west bank of the River Tigris in Baghdad, Iraq on Geographic coordinates 33°22′47.89″ to the North and 44°20′16.64″ to the East as shown in Figure 1. It contains the tombs of the seventh Twelver Shiah Imam Musa Ibn Jafaar (Al-Kadhim) and the ninth Twelver Shiah Imam Muhammad at-Taqī. These two tombs in additional to other tombs belong to two other famous scholars at that time (762 AD) are marked with four historical Minarets with approximate height reaches to 39m above ground, refer to Figure 2.

Terrestrial laser scanner Stonex X300 from Stonex Positioning Company was used to scan the site and monitor the deflection in the historical Minarets constructions and cracks holds due to engineering works followed site expansion project, ground water and time factor effects. Stonex X300 is a compact and lightweight 3D laser scanner. It works based on time of flight (TOF) laser range finder system. The laser range finder finds the distance to the Earth's object by timing the round-trip of the light pulse [6]. A laser is used to emit a beam of light and the travel time between the laser sensor and the object is measured by the system detector [5]. Since the speed of light c is known, the round-trip time determines the travel distance of the light, which is twice the distance between the scanner and the object. If t is the round-trip time, then the distance will equal to $c.t/2$. The accuracy of the registered time-of-flight in the 3D laser scanners depends on how precisely the time is measured based on the device components [14]. The main features and technical components of Stonex X300 can be found in Stonex X300 datasheet [15].

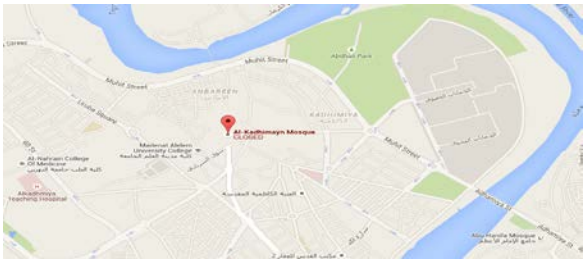

Figure 1: 2D map of Al- Kadhmiyia case study (Google ©).

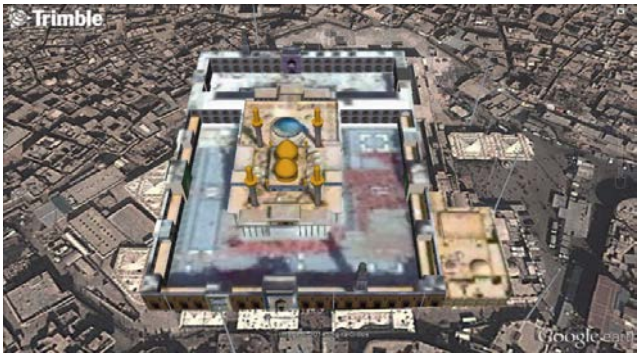

Figure 2: 3D map of Al- Kadhmiyia case study (Google ©).

III. METHODOLOGY

A. Preface

Today, Al-Kadhimia Holy Shrine requires a lot of maintenance as an important historical construction. The General Secretary of the Holy Shrine complete several engineering projects supervised by the Department of Engineering Affairs including the Imam Haram expansion with a completion of 80% of its first phase of Roofing work to the eastern side of the Haram. This includes the installation of the iron foundations and setting up the iron columns structure with a height reaches to 11.6 m in addition to setting the ceiling bridges and columns supporters. Project roofing works started in 2013, including digging the ground for setting the new foundations and downloading piles with depth reach to 24m in the ground alongside the original old foundations. These old foundations are very weak and damp as a result of the historical origins and groundwater available in the region.

During the final stages of roofing work, the Department of Engineering Affairs has noticed the increasing of the Minarets deflection and the occurrence of new cracks in the oldest Minaret body from inside and outside. This confirms the disruption in the Minarets foundations and underground soil of the Haram and the surrounded buildings due to Haram expansion work as well as the impact of the groundwater that withdrawal across many wells available in the region and close several meters from the Haram used for blessing purposes.

This research aims to monitor the deflection and cracks acquired in Holy Shrine Minarets due to Haram expansion project works. This includes a comprehensive study to address the problem and recommend a valid engineering solution to avoid the problems facing old foundations and soil as a result of the penetration of groundwater. This includes the use of rigorous digital techniques to measure this deflection accurately to be ready for the next phase of problem solution regarding soil injection to strength the soil materials and thus the building foundations.

The first technique includes traditional field work measurements using electronic devices such as Total Stations alongside the second new digital technique of 3D laser scanning within the same time frame, technical and artistic conditions in order to check validity and compare of results. The second technique is a new technology which never used before in Iraq in such projects. It can deliver 3D models and very accurate 3D measurements in a very rapid and manner. A third technique of digital photogrammetry have been applied alongside the other mentioned ones. However, Photogrammetric data processing and analysis are not the main focus in this research.

B. Devices and Softwares

In order to achieve accurate and reliable results, several electronic Surveying devices have been utilized in the field. Further, multiple softwares and in-house automatic tools to process the delivered datasets have been used in the laboratory. Table 1 is referring to all devices and softwares used in this research alongside their purpose of use.

TABLE 1: TOOLS UTILIZED FOR MONITORING

	TOOL	ITEM	PURPOSE
1.	Trimble M3 Total Station	1	1st set GCPs target measure
2.	Topcon GTS Total Station	2-3	2nd set GCPs target measure
3.	Topcon GNSS GR5	1	Corrected GCPs measure
4.	Leica Disto	1	Measuring approximate distances
5.	Stonex X300 Terrestrial Laser Scanner	1	Scan site objects
6.	Trimble Business Center Software	1	Processing field work data
7.	Stonex Reconstructor Software	1	Processing laser point clouds
8.	Quick Terrain Modeler Software	1	Visualizing laser point clouds
9.	Matlab Software	1	Adjustment computations

C. Monitoring Approach

The main workflow of the monitoring work implemented in this research is illustrated in Figure 3 and Figure 4 respectively. As demonstrated in these figures, the monitoring work was divided into two separate phases to maintain the results with the required accuracy level and validate the results delivered from laser scanning survey. The work starts in September 2014 on monthly bases by monitoring the Minarets deflection using traditional field surveying with total station and GPS whereas laser scanning monitoring was started later due to some technical issues. The ground stations was selected and measured accurately in a distribution that make a closed traverse in order to monitor all targets on the body of the Minarets and assess the results accuracy. A specific strategy was developed to ensure accurate outputs of target measurements during the period of monitoring in order to meet the project requirements. The targets were selected to be on several rings on each Minaret body that meet a circle circumference.

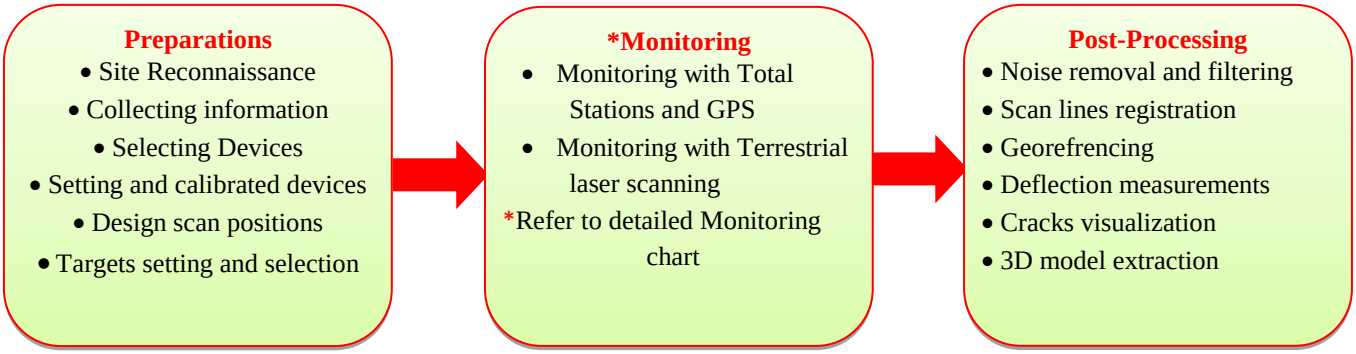

Figure 3: Methodology workflow

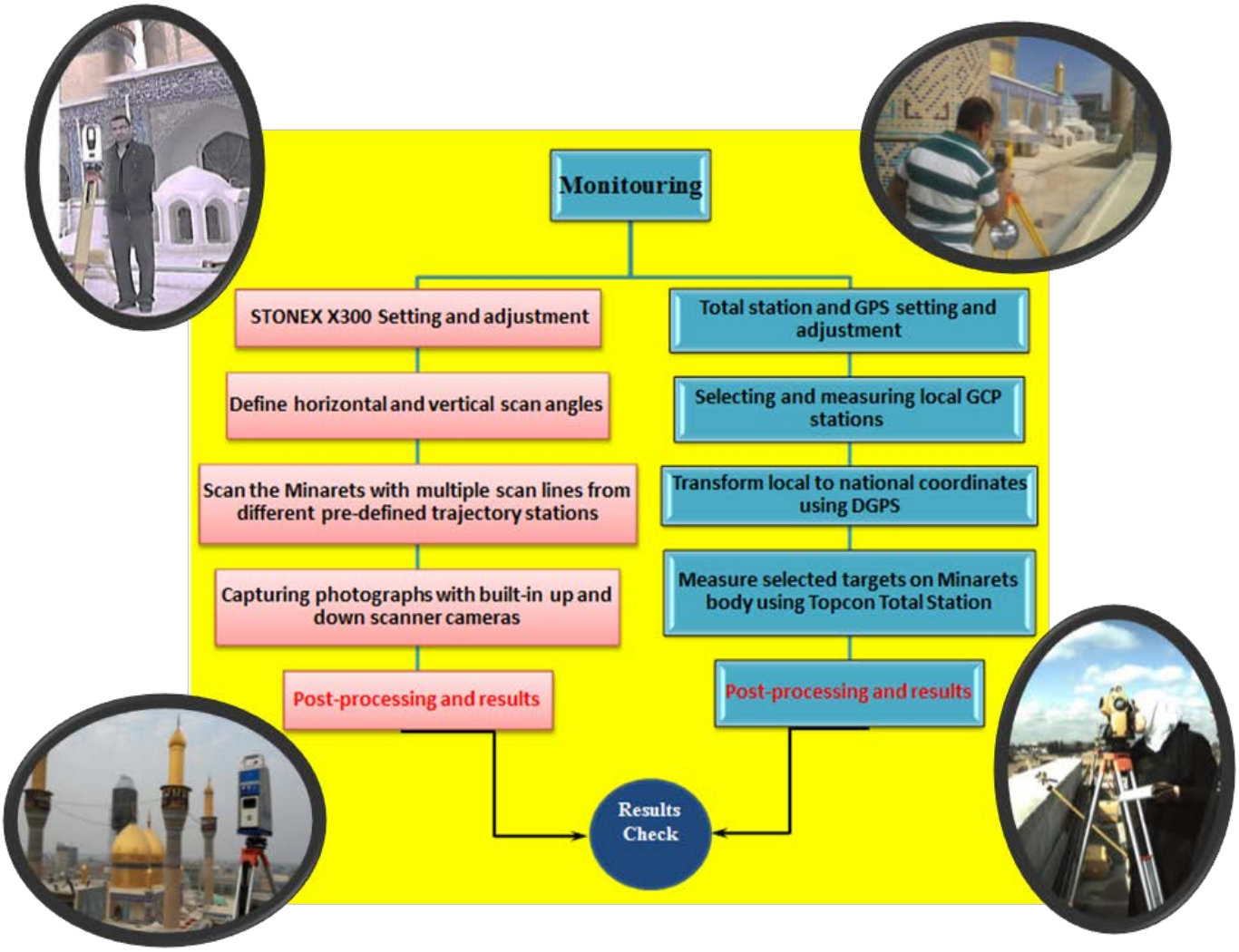

Figure 4: Detailed monitoring process

This methodology was proposed to compute the central line coordinated in 3D of each Minaret following least squared fitting based on center point and radius parameters as follow [16]:

$$(x - x_c^o)^2 + (y - y_c^o)^2 - r^{o^2} = 0 \quad (1)$$

Where, *x* &*y* are referring to measured targets, and x_c, y_c, and *r*, are referring to central point coordinates and the circle radius respectively. Bear in mind that the measurements here are in 3D, thus the elevation of each point (*z* value) is added to the general model.

Following least squares, the general adjustment formula used is as following [16,17]:

$$\left((x_i + vx_i) - (x_c^o)\right)^2 + \left((y_i + vy_i) - (y_c^o)\right)^2 + \left((z_i + vz_i) - (z_c^o)\right)^2 - r^{o^2} = 0 \quad (2)$$

The general observation equation is [16,17]:

$$Av + B\Delta = f \quad (3)$$

Where, *A* is the matrix of partial derivatives with respect to observations, *v* is the matrix of residuals, *B* is the matrix of partial derivatives with respect to unknowns, Δ is the matrix of unknowns, and *f* if the matrix of closure.

During the survey, it was noticed that each Minaret body is not constantly deflect from the center line in a certain direction from the bottom up to the top. Therefore the measurements was divided into three sections for individual Minarets as shown in Figure 5.

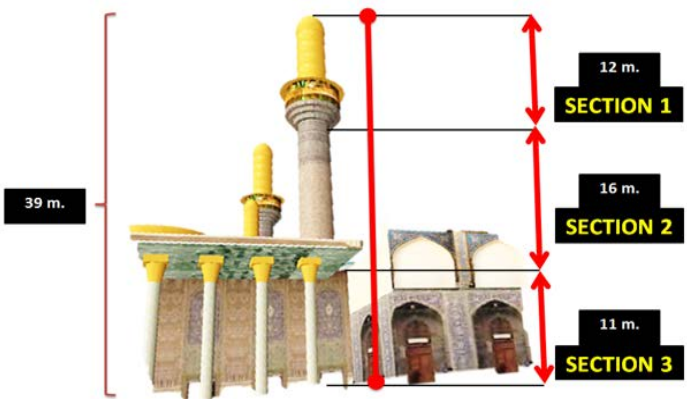

Figure 5: Minarets' measurements sections

All the mathematical computations and adjustment to the observations delivered from individual monthly survey was applied using in-house matlab tool for least squares fitting and adjustment which have been designed and written particularly for this research. However, all site plans and 3D models have been applied with the supplementary of Trimble Business Center, Reconstructor, and QT Modeler softwares.

The laser scanning survey was first due on December 2014. This survey was run on monthly basis alongside the traditional survey. The scan was applied from fixed stations with known positions as trajectory stations to scan the Minarets and deliver very dense 3D point clouds in individual strips with more than 400 pt/m^2 based on the distance between the scanner and the Minaret. In order to deliver a complete facets coverage for all Minarets, a multiple strips was captured with a reasonable overlap areas for later registration process and 3D models extraction. Following georeferencing manipulation, real 3D point clouds of all minarets have been delivered in UTM system. This has been followed by central line computations as explained earlier to compute the magnitudes and the directions of the deflection acquired in the Minarets' structure. Extra measurements were made to compute the cracks available in the body of the older Minaret (A) based on laser ability to penetrate between the holes available and reflected from the background wall. These scans were made from outside and inside the Minaret building to assure accurate results and define whether the cracks were penetrated alongside the whole body thickness or not. The 3D Models of the Minarets have been extracted using 3D reconstructor software. The QT Modeler was also utilized for additional visual interface as presented in results section.

IV. RESULTS AND DISCUSSION

The Minarets have been named from south-west direction of the old Minarets towards the left as A, B, C, and D to demonstrate differences in the measurements applied to individual buildings. Due to difficulties to measure the deflection in the Minarets' bodies along section 3 as shown in Figure 5, this section was excluded from the survey measurements during the monitoring work. These difficulties were come from the impossible measure of the cylinder body of the Minarets in this ground section as it was built-in and included within the entire building structure and thus cannot make measurements from outside to shape the circumference of the circle cross-section of the Minaret body. Thus Measurements in this research was made to section 1 and 2 only based on multiple trajectory stations those set on the Haram roof and as presented in the following sections.

A. Traditional Survey Results

The first survey measurements was due in May 2014 which show a significant deflection in the four Minarets bodies. The magnitude of the deflection alongside its direction was computed based on the measurements made to the targets selected on the Minarets bodies for individual structure rings alongside section 1 and section 2 as shown in Figure 6 and Figure 7 respectively.

It was found that there was an increasing in the deflection magnitude between May 2014 and January 2015. These values have turned to be constant after January 2015 and keep steady to date for all Minarets. The minimum and the maximum deflection values of the measurements delivered was listed in Table 2. It is important to mention that due to Minarets maintenance work run by a private company under General Secretary of the Holy Shrine supervision, no rigorous measurements have been delivered to D Minaret. The perspective 2D and 3D site maps of the computed central line of the four Minarets are shown in Figure 8 and Figure 9 respectively. The small white marks in both figures show the deflected path of the central lines of the four Minarets.

B. Laser Scanning Results

In this research, Stonex X300 terrestrial laser scanner device was used to capture the data from multiple fixed ground stations. At first stage, a fast scan with 360° horizontal angle was captured to the entire site to compute the optimal ranges needed to set trajectory stations that deliver the required field of view (FOV) which allows a complete coverage of the Minarets with the maximum spatial resolution, refer to Figure (10). Two points were located on the eastern side of the site on a highest point at the roof of the main hall of the campus. These stations allow a complete view to the entire site including the four targeted Minarets. Two other points were selected on the opposite side upper the balcony of the main south clock building in the campus. These points were selected to deliver 3D coverage to the entire site for pre-scanning process. Figure 11 show a fly-through 3D point cloud of the Al-Kadhimyia site.

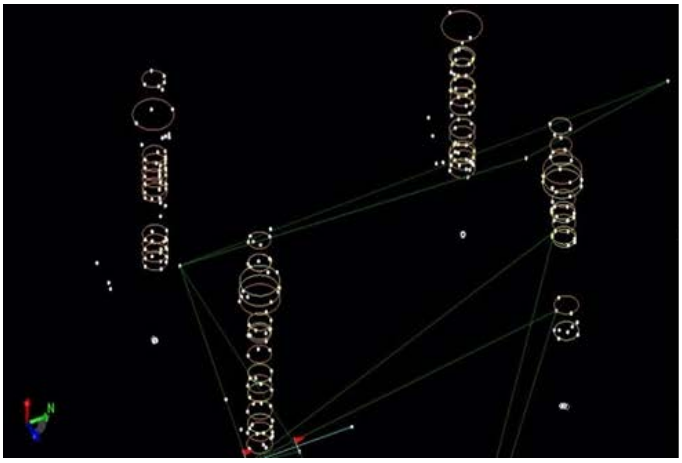

Figure 6: Targets point clouds on Minarets body.

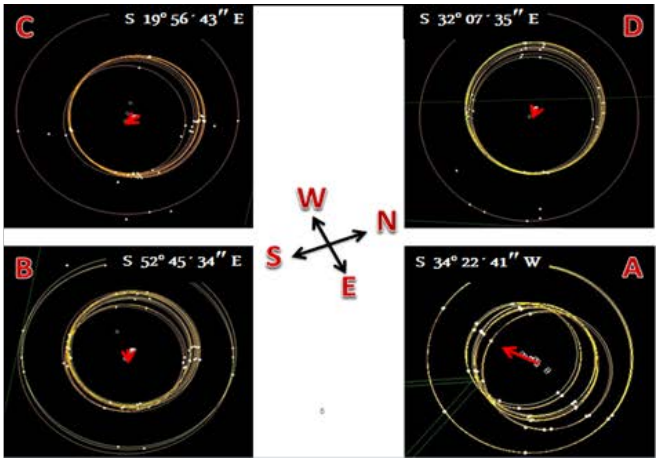

Figure 7: Deflection directions.

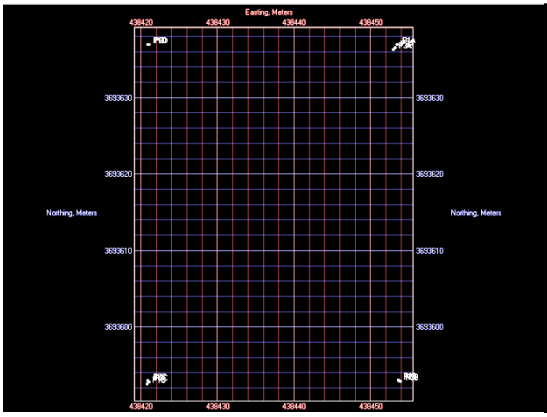

Figure 8: 2D site map of the Minarets center lines.

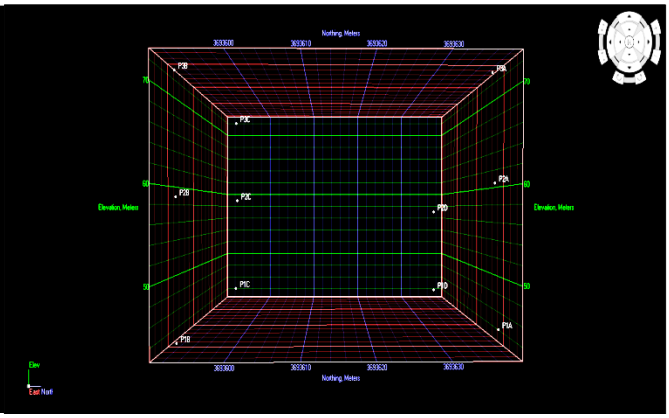

Figure 9: 3D site map of the Minarets deflected center lines.

Table 2: Deflection values.

DEFLECTION (CM)				
MINARET	MINUMUM	DATE	MAXIMUM	DATE
A	77.60	May 2014	80.66	January 2015
B	26.50	May 2014	29.72	January 2015
C	33.20	May 2014	36.80	December 2014
D	3.50	May 2014	-	-

Later, close trajectory stations were selected and set on the ground around every Minarets. GPS static was used later to deliver the 3D coordinates of these stations after adjustment to prepare the dataset for post-processing. Ten strips have been captured of ~13m range for each Minaret with a reasonable overlap to make sure that registration process can run smoothly and delivering a highly 3D registered un-gridded point clouds. Every point cloud display three-dimensional (X, Y, Z) coordinates and therefore can easily choose points from the base of each Minaret and their corresponding points at the top. According to what has been adopted in the traditional field survey method the differences in the coordinates can be computed and thus calculate the amount of the deflection in each Minaret. These measurements were run on monthly basis to monitor the deflection. The results of the deflection from laser scanning technique was constant for all surveying measurements with differences from 2 to 5 millimeters only. The mean deflection results from this technique are listed in Table 3.

These results prove the superiority outputs of this new technique in close-range monitoring applications. They also showed close output and obvious convergence to those delivered from the traditional field survey results within the accepted level of accuracy. The differences delivered are expected to be acquired due to systematic errors delivered from errors in user measurements. The only significant difference that can be noticed in Table 3 in comparison with those listed in Table 2 is the D Minaret deflection value. This can be logically expected due to maintenance work in this Minaret as explained earlier.

Following filtering and noise removal processing, registration and georeferencing process have been applied with 0.8mm RMS accuracy by integrating all strips for individual Minarets using Stonex X300 Reconstructor software as demonstrated in Figure 12 and Figure 13 respectively. Later, the 3D models of individual Minarets were extracted successfully from dense accurate point clouds. By integrating the color information from the build-in Stonex cameras, the 3D model of the campus has been generated as shown in Figure 14 and Figure 15 respectively.

Fig 10: 2D laser image showing the FOV of Stonex X300.

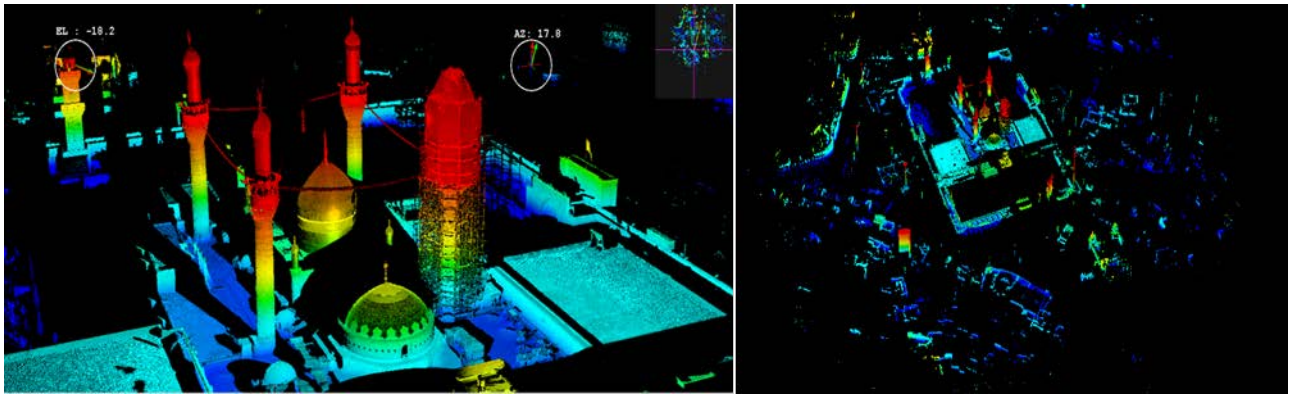

Figure 11: Fly- through view of 3D laser scanning point clouds.

Table 3:Laser scanning deflection measurements.

MINARET	DEFLECTION (CM)
A	81.12
B	32.76
C	33.40
D	17.65

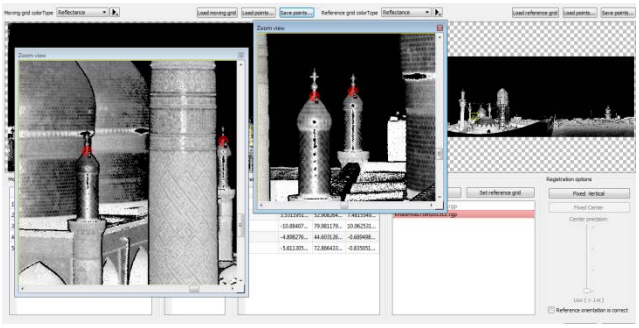

Figure 12: Laser scanning registration process.

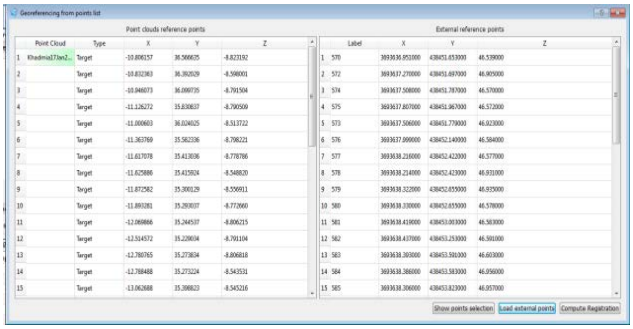

Figure 13: Laser scanning georeferencing process.

Figure 14: 3D laser scanning color model.

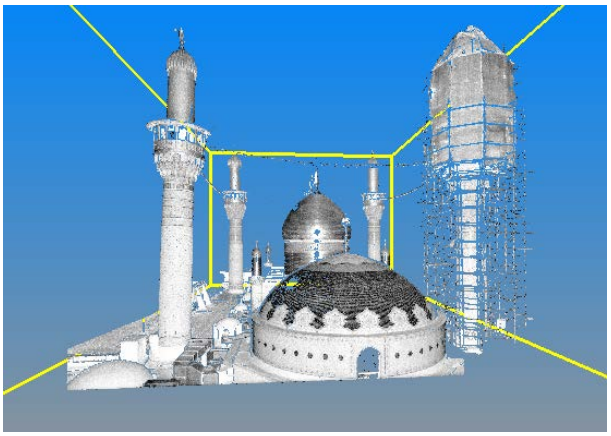

Figure 15: 3D laser scanning B/W model.

As for cracks measurements, the experiments did not delivered any significant results. This is acquired due to limitations in the range resolution of the scanner device in addition to difficulties to scan the cracks from inside the Minaret following small distance which is less than the minimum range distance (2.5 m) of the Stonex X300 Device. This particular issue need further investigations and experiments in future works.

V. CONCLUSIONS

In this research, a practical and accurate monitoring routine was presented and applied for the first time in IRAQ to preserver cultural heritage in Al- Khadimia site using laser scanning technique. The described approach proposes a new and innovative use of laser scanning technique for cultural heritage applications: attention is not paid to artistic and architectonic elements in the presented case study. The aim is not only to return the 3D surface model of the investigated structure for qualitative assessments.

The basic idea aims to deliver an accurate measure to the deflection acquired in the investigated structure through the computation of its central line based on circumferences target measurements. The research was aiming to monitor these deflection measurements and cracks in the main body building acquired due to different variables. The data delivered was processed and analyzed accurately following accurate post-processing approaches.

The results proved superior relative and absolute results in compression with traditional techniques. Cracking investigations were challenging due to this critical issue for the effective stability of the structure. However, this particular issue of cracking measure need further work due to invalid results. It was demonstrated that three dimensional point clouds can be valuable sources of information for extracting measurements and parameters which are helpful to foresee the structural behavior, for highlighting whether

differential displacements and deformations occur or not and for making hypothesis about any additional load that increases imposed stresses. This confirms the usefulness of laser scanning as a diagnostic tool for structural analysis.

As a consequence, the research may conclude by asserting that laser scanning is a sufficiently complete and accurate technique to be considered as the basis for geometric investigations. The above discussion confirms that the analysis allowed to extract lots of information about the structure as well as its status. The presented project is still in progress and further steps will focus on multidisciplinary approach in order to provide a comprehensive methodology for studying cultural heritage.

ACKNOWLEDGMENTS

The authors would like to thank the General Secretary of Al-Kadhimyia Holy Shrine for funding this research.

REFERENCES

[1] Vosselman, G. and Maas, H.-G.: Airborne and terrestrial laser scanning, 2010, Scotland, UK: Whittles Publishing.

[2] Kadobayashi, R. et al: Comparison and evaluation of laser scanning and photogrammetry and their combined use for digital recording of cultural heritage, 2004, IAPRS&SIS, 35(5): 401-406, Istanbul, Turkey.

[3] Kraus, K.: Photogrammetry- Geometry from images and laser scans, 2000, Berlin, Germany: Walter de Gruyter.

[4] Abed, F. et al: Echo amplitude normalisation of fullwaveform airborne laser scanning data based on robust incidence angle estimation, 2012, IEEE Transactions on Geoscience and Remote Sensing, 50 (7), 9 p.

[5] Abed, F.: Calibration of full-waveform airborne laser scanning data for 3D object segmentation, 2012, PhD thesis, Newcastle University, UK.

[6] Shan, J. and Toth, C. K.:Topographic laser ranging and scanning - principles and processing, 2009, FL, USA: Taylor & Francis.

[7] Castagnetti, C. et al: Terrestrial laser scanning for preserving cultural heritage- Analysis of geometric anomalies for ancient structures, 2012, Proceedings of the FIG workshop week on knowing to manage the territory, Protect the environment, Evaluate the cultural heritage, Rome, Italy.

[8] Alshawabkeh, Y. and Haala N.: Laser scanning and photogrammetry- a hybrid approach for heritage documentation, 2004, 3rd International conference on science and technology in archaeology and conservation, Amman, Jordan.

[9] Neubauer W. et al.: Combined high resolution laser scanning and photogrammetrical documentation of the pyramids at Giza, 2005, XXth CIPA International Symposium, Torino, Italy.

[10] Doneus, M. and Briese, C.: Digital terrain modelling for archaeological interpretation within forested areas using full-waveform laser scanning, 2006a, The 7th International Symposium on vertical reality, Archaeology and cultural heritage VAST, Nicosia, Cyprus.

[11] Doneus, M. and Briese, C.: Full-waveform airborne laser scanning as a tool for archaeological reconnaissance, 2006b, Proceedings of the 2nd International conference on remote sensing in archaeology, Rome, Italy.

[12] Doneus, M. et al.: Archaeological prospection of forested areas using full-waveform airborne laser scanning, 2008, Journal of Archaeology Science, 35, 882-893.

[13] Koehl, M. and Grussenmeyer, P.: 3D model for historic reconstruction and archaeological knowledge dissemination, The Niedermunster abbey's project, 2008, International archives of photogrammetry, remote sensing and spatial information sciences, 37 (Part B5), 325-330.

[14] Balsavias, E. P.: Airborne laser scanning- basic relations and formulas, 1999, International journal of photogrammetry and remote sensing, 54(2-3), 199-214.

[15] Stonex X300 dataseheet: http://www.stonexpositioning.com/images/Brochure_ridotte/x300.pdf.

[16] Wolf, P. R. and Ghilani C.: Adjustment Computations-Statistics and least squares in surveying and GIS, 1997, New York, John Wiley and Sons.

[17] Mikhail E. M. and Ackermann F.: Observations and least squares, 1976, Thomas Y. Crowell Inc., New York, Donnelly Publisher.

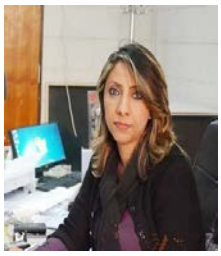

Fanar M. Abed received the B.Sc. degree in Surveying Engineering and the M.Sc. degree in Photogrammetry from Baghdad University, IRQ in 1999 and 2002 respectively. She specialized in Laser Scanning after receiving her PhD degree from the School of Civil Engineering and Geosciences, Newcastle University, Newcastle upon Tyne, U.K, in 2012. She is currently a staff member in Surveying Engineering Department, College of Engineering, University of Baghdad, Baghdad, IRQ. Her main research interests span the field of Photogrammetry and Laser Scanning for different Engineering applications.

Omar A. Ibrahim received the B.Sc. degree in Surveying Engineering and the M.Sc. degree in Geodesy from Baghdad University, IRQ in 2001 and 2005 respectively. He is currently assistant lecturer in Surveying Engineering Department, College of Engineering, University of Baghdad, Baghdad, IRQ. His research interests the G.N.S.S. and related applications.

Luma K. Jasim received the B.Sc. degree in Surveying Engineering and the M.Sc. degree in Photogrammetry from Baghdad University, IRQ in 2004 and 2011 respectively. She is currently assistant lecturer in Surveying Engineering Department, College of Engineering, University of Baghdad, Baghdad, IRQ. Her research interests the field of Photogrammetry and related applications.

Yousif H. Khalaf received the B.Sc. degree and the M.Sc. degree in Surveying Engineering from Baghdad University, IRQ in 2000 and 2009 respectively. He is currently assistant lecturer in Surveying Engineering Department, College of Engineering, University of Baghdad, Baghdad, IRQ.

Hassan M. Hameed received the B.Sc. degree in Agriculture from Baghdad University, IRQ in 2003. He involved in different Surveying projects in IRQ after 2003. He is specialized in Surveying field work and related sectors.

Zahraa A. Hussain received the B.Sc. degree in Surveying Engineering and the M.Sc. degree in Geodesy from Baghdad University, IRQ in 2005 and 2014 respectively. She is currently assistant lecturer in Surveying Engineering Department, College of Engineering, University of Baghdad, Baghdad, IRQ. Her main research interests are in designing geodetic networks and G.N.S.S. applications.

Evaluate the Energy Required to cause Yielding of Modified Asphalt Binders

Assistant Prof Dr. Abdulhaq H. Abedli Al-Haddad

Abstract--The yield energy (the energy required to fracture covalent molecules) can be used to describe the relative performance of bituminous materials, and the stress-strain curve can be useful in identifying the presence of polymer modifiers in the material.
The complex shear stress and complex shear strain of pure and modified local asphalt binders were measured at temperatures between 25 ^{o}C and 50 ^{o}C by Dynamic Shear Rheometer. The stress-strain graph of each sample was used to analyse the experimental data and calculate the yielding energy required to starting fracture of the asphalt binders. Yield energy required to failure ranged from $2.98*10^{5}$ Pa to $1.1*10^{6}$ Pa for DAB and $2.67*10^{6}$ Pa to $4.43*10^{6}$ Pa for NAB. The values of toughness energy are $9.67*10^{5}$ Pa to $2.53*10^{6}$ Pa for DAB and $1.06*10^{6}$ Pa to $1.04*10^{7}$ Pa for NAB. The effects of test temperature, asphalt type, polymer content, and type on the yield energy for failure were studied. The results indicate that the yield energy for failure can be used as a good design parameter of a flexible pavement. The yield energy increases with complex shear strain rate and decreases with increased temperature.

Keywords: Yielding energy, elastic energy, toughness energy, fracture energy, modified asphalt, DSR.

1. Introduction

Flexible pavement can be defined as a combination of aggregates, bitumen and filler, mixed in a specified percentage and sometimes, in order to improve the performance of a pavement, additives are used.
The flexible pavement is constructed to serve different purposes (able to resist deformation, cracking and moisture damage – resist effect of water); and be durable over time (resist effect of weather and ageing); these purposes depend on the traffic level, climate and subgrade layer characteristics (layer underneath and support the pavement system).
The primary use of asphalt is in pavement construction, where the asphalt binder is used as the glue for aggregate particles. Asphalt is a heavy, dark brown to black mineral substance, one of several mixtures of hydrocarbons called bitumen. Asphalt is a strong, versatile, weather and chemical-resistant binding material which adapts itself to a variety of uses. Asphalt binds crushed stone and gravel (commonly known as aggregate) into firm, tough surfaces for roads, streets, and airport runways (AASHTO, 2009).
One of the most clear but at the same time most difficult problems in dealing with failure criteria is that of defining the yield stress and the stress at failure. These properties are needed to calibrate failure criteria parameters like elastic modulus, yield stress, and stiffness of asphalt binder.
The terms yield point, proportional limit, yield strength, yield energy; toughness energy, stress and strain at failure have been used for the first property to represent failure stages during the test. For partially ductile or very ductile materials there is uncertainty and confusion about how to determine the yield stress and then strength (Christensen, 2013). Yield strength is defined as the stress at which a material changes from elastic deformation to plastic deformation. Once the point known as the yield point is exceeded, the material will no longer return to its original dimensions after the removal of the stress (Hetnarski, and Ignaczak, 2006). Yield strength can be explained, in engineering application and science of materials, as the stress at which a material begins to plastically deform. Prior to the yield point, the material will deform elastically and will return to its original shape when the applied stress is removed. Once the yield point is passed, some fraction of the deformation will be permanent and non-reversible. (Christensen, 2013; http://www.failurecriteria.com , accessed date 12/03/2015)
Determining the yield strength is very important in the asphalt mixture designing process, since it usually represents the maximum applied load. Yield strength is very important to be controlled in many material production techniques, such as forging, rolling or pressing.
The value of yield energy is a very important parameter in the construction of flexible pavement; the flexible pavements are able to perform in the elastic region under normal servicing conditions. However, when pavement structures are faced with heavy loads, the plastic region of the material becomes crucial, as a large amount of the energy being absorbed by the asphalt mixture materials under such circumstances is mainly contributed by the plastic region. As such, having a higher toughness energy means that the materials are able to withstand such heavy loading for a longer period of time so as to allow more time for safety measures to be carried out (Christensen, 2013).
In design applications, the yield strength is often used as an upper limit for the allowable stress that can be applied. It is especially important in material applications that require precise dimensional tolerances to be maintained in the presence of high stresses and loads. By altering dislocation

Manuscript received March 2, 2015; this paper has been reviewed for publication in the conference July 25, 2015 and final accepted is Augest 20, 2015.

Visitor Researcher, School of Engineering, University of Liverpool, Liverpool, United Kingdom .The University of Mustansiriyah; Engineering College, Highway and Transportation Dept., Baghdad, Iraq (Abdulhaq@liverpool.ac.uk, abdulhaq1969@gmail.com)

density, impurity levels and grain size (in crystalline materials), the yield strength of the material can be fine-tuned. For materials without a clear distinct yield point, yield strength is usually stated as the stress at which a permanent deformation of 0.2% of the original dimension will result, which is known as the 0.2% yield stress.

The fracture energy or toughness energy has proven to be a good design parameter that can be used in fracture mechanics to analyse the crack propagation of a pavement (Shen et. al., 2007; Kim and Buttlar, 2009; Denneman, 2010).

2. Data Calculation and Analysis

The experimental results obtained from DSR are used to calculate the binder yield energy and other parameters as follows:

1) Draw the relationship between complex shear stress and complex shear strain as shown in Figure 1,
2) Determine the maximum complex shear stress (Pa) at yielding point,
3) Determine the complex shear strain (%) at yielding point,
4) Calculate the amount of energy required to cause yielding of asphalt binder as follows:
   a) Microsoft Excel has been used to calculate the area under the curve of graph of complex shear stress (Pa) versus the complex shear strain (%). However, for curves produced from data, analytical integration may not be possible. In these cases, the most common way to find the answer is to perform the integration "numerically". The trapezoidal rule is one way to calculate this integral that is (1) easy to implement; (2) quite accurate; and (3) quite robust. The idea is to break the function up into a number of trapezoids and calculate their areas. The area under the graph is therefore the sum of the trapezoid slides.
   b) The area of the first slide can be calculated as a triangular shape:

$$A_{i-1} = \frac{\tau_{i-1} * \varepsilon_{i-1}}{2} \quad \ldots 1$$

   c) The incremental energy between second and first steps can be presented by area under trapezoidal between each data point until maximum complex shear stress, as shown in the following equation:

$$A_i = \frac{(\tau_i - \tau_{i-1})}{2} * (\varepsilon_i - \epsilon_{i-1}) \quad \ldots 2$$

   d) The total area recorded as yield energy can be calculated as:

$$\text{Yield Energy} = A_{i-1} + \sum_{i=1}^{N} (\tau_i - \tau_{i-1})/2 * (\varepsilon_i - \varepsilon_{i-1}) \quad \ldots 3$$

   e) The toughness energy can be calculated using the same idea and extended to failure point (total area under the curve until failure).
   f) A plot of complex shear stress versus complex shear strain before yield point gives a straight line (preoperational limit within the elastic region) with a slope of *E* (Elastic Modulus). The elastic energy can be calculated as area under linear region curve *Ee*.

Dynamic Shear Rheometer (DSR) is used for determining rheological properties of the asphalt binder complex shear stress (τ) and complex shear strain (%), at test temperatures between 25 and 50 ^{o}C under constant shear rate mode equal to 1%.

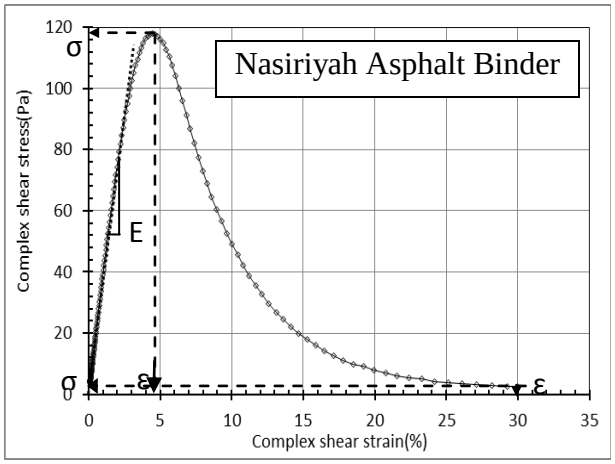

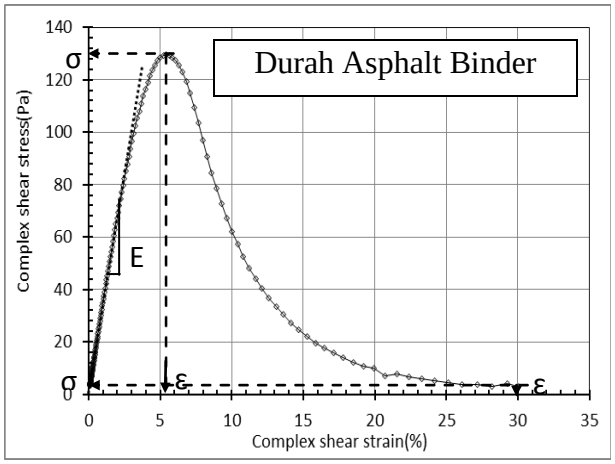

Figure 1. Example of complex shear stress-stain curve and calculation of energy parameters for modified asphalt binders (9% GG) by using DSR at 25 ^{o}C test temperature.

3. Objectives of this study

The main objectives of this paper are to:

a. Calculate binder elastic, plastic and toughness energies (binder energy properties) of different modified bitumen,
b. Evaluate the amount of energy required to cause yielding and fracture of asphalt binder based on the results obtained from DSR, and
c. Predict required E_y to failure in order to use in asphalt mixture design process.

4. Materials and Experimental Procedures

4.1 Materials

4.1.1 Pure Asphalt

Two local asphalt binders from Durah and Nasiriyah refineries (middle and southern regions of Iraq) were tested to evaluate locally available paving materials.

To prepare a sample for the DSR test, an oven was preheated to (softening point + 90 or 160-170 °C (340 °F)), at which point the samples were placed in the oven and allowed to melt. The average melting time of the samples was approximately 30 minutes. A small amount of the melt was poured into three small circular moulds. All samples were cooled for an additional hour prior to the test (BS EN 14770:2012), as shown in Table 1.

Table 1. Properties of the asphalt binder.

Property	Nasiriyah	Durah
Penetration (0.1 mm, 100 g and 5	41	43
Softening point (°C) – ASTM D36	52	53
Penetration Index (PI)	-1.0	-0.35
Viscosity (cP, 135 °C) ASTM D	500	481.3

It can be seen that the Nasiriyah asphalt binder viscosity is better than Durah asphalt binder and more sensitive to temperature.

4.1.2 Asphalt Modification

a) Styrene-Butadiene-Styrene (SBS)

In this work, two types of Styrene-Butadiene-Styrene (SBS) were used to modify base asphalt binder, as shown in Table 2.

Table 2. Summary properties of elastomer used (Kraton Polymers, 2006).

Property	D 1101 K SBS	D 1184 K SBS
Tensile strength, ASTM D412, psi.	4,600	4,000
Elongation, ISO37, %.	880	820
Specific gravity,ISO2781	0.94	0.94
Brookfield viscosity. ASTM D4402, cps at 77 °F	4,000	20,000
Diblock,%.	16%	16%
300% modulus, ISO37, psi.	400	800
Molecular structure	Linear	Radial

b) Micro-silica (Elkem Micro-silica G940-U)

Elkem Micro-silica consists of sub-micron, amorphous, non-porous spheres of silicon dioxide (silica, SiO_2) and small agglomerates of these. The average particle size of the spheres is about 0.15 μm. Although some of the spheres exist as single entities, most of them form primary agglomerates with typical particle range 0.1-1μm. The test results according to ASTM C989/C989M-13 and BSEN15167-1, 2- 2006 are shown in the following table.

Table 3. Properties of Elkem Microsilica Grade 940*.

Chemical and Physical Requirements	Specification (characteristic values)
SiO_2 (%)	> 90
H_2O (moisture content when packed, %)	> 90
Loss on Ignition, LOI (%)	< 3.0
Retained on 45 micron sieve (tested on	< 1.5
Bulk Density - Undensified (when packed,	200 - 350
Bulk Density - Densified (when packed,	500 - 700
* The above Elkem specification refers to analysis performed using	

c) Ground Granulated Blast furnace Slag (GGBS)

Ground Granulated Blast furnace Slag (GGBS or GG) is a by-product from the blast furnaces used to make iron. These operate at a temperature of about 1,500 degrees centigrade and are fed with a carefully controlled mixture of iron ore, coke and limestone. The iron ore is reduced to iron and the remaining materials form a slag that floats on top of the iron. This slag is periodically tapped off as a molten liquid and, if it is to be used for the manufacture of GGBS, it has to be rapidly quenched in large volumes of water. The quenching optimises the cementation properties and produces granules similar to coarse sand. This 'granulated' slag is then dried and ground to a fine powder. The chemical properties of GG are shown in the following table.

Table 4. Chemical Properties of GG.

	Principal Oxides (%)				
	CaO	SiO_2	Al_2O_3	MgO	Fe_2O_3
Regen Company*	40	35	12	10	0.2
Portland Cement	65	20	5	1	2

* Regen Ground Granulated Blast furnace Slag (GGBS) is a cement substitute, manufactured from a by-product of the iron-making industry. The use of Regen in concrete reduces embodied CO_2 emissions by over 900 kg per tonne of cement, and also increases its durability. http://www.heidelbergcement.com/uk/en/hanson/products/cements/ggbs_and_related_products/regen_ggbs.htm

4.2 Experimental Procedures

The samples were heated in the oven for approximately 1 hour at (160 °C±5 °C) for the unmodified binders and (160 °C±5 °C) for the modified binders in order for them to be fluid enough to easily pour; after heating, the samples were poured into prepared silicon moulds.

The modified asphalt binders were prepared using the Silverson Shear mixer under controlled temperature, time and shear rate conditions. It has been reported and recommended that SBS polymers and other types of modifier do not require a high shear rate for asphalt mixing; therefore, the shear rates and mixing time were 1200 rpm and 10 minutes, respectively, as adopted by some researchers (ASTM D7175 2008). In addition, the mixing temperature was 160 ℃± 5 ℃. The asphalt binder was preheated in an oven to the selected mixing temperature while, during mixing, the mixing temperature was maintained using a heater container to keep a uniform temperature to achieve consistent mixing; and the container was also covered with an insulation mantel which was preheated to the required temperature.

A Kinexus Pro$^+$ rheometer from the Malvern Company was used to determine their viscoelastic properties. It is a rotational rheometer system that applies controlled shear deformation to a sample under test, to enable measurement of flow properties (such as dynamic shear viscosity from flow tests) and dynamic material properties (such as viscoelastic modulus and phase angle from oscillation tests). The rSpace software ver.1.6 developed by the Malvern Company was used to determine the complex shear stress (τ) and complex shear strain (ε). For the tests presented within this work, the parameters were set as outlined in Table 5.

Table 5. Test parameters.

Test parameter	Test value
Total test time	30 min
Soak period at each temperature	10 min
Measurement period	10 sec
Temperatures	25 and 50 ^{o}C
Test frequency	10 Hz (10 cycle/sec)
Shear strain	1.0% within the LVER
Control mode	Shear strain mode

In this study, two testing geometries are used with the DSR: 8 mm diameter plate with a 2 mm testing gap and a 25 mm diameter plate with a 1 mm testing gap. The selection of the testing geometry is based on the operational conditions, with the 8 mm plate geometry generally being used at an intermediate temperature of 25 ^{o}C and the 25 mm geometry at a high temperature of 50 ^{o}C, according to BS EN 14770:2012 and ASTM D7175:2008. Details of this test are described as follows:

1. The dynamic data (complex shear stress and complex shear strain) were collected over a range of temperatures and frequencies (i.e. 25-50 ^{o}C and 10 Hz). This combination produced 62 data sets for each trial.
2. At each binder sample, five readings generated at 15-minute intervals were averaged and used in the analysis.

5. Results and Discussion

5.1 Energy Evaluation of Different Asphalt Binders

According to point 2 above, the experimental results (dynamic shear stress and strain) obtained from DSR are drawn and processed to calculated all required parameters for each asphalt type, as shown in Figure 2.

The experimental results obtained from DSR with different types and amount of modifier at test temperature 25 ^{o}C are simulated in Tables 6 and 7.

In order to understand the effect of adding modifier materials on the required five parameters, calculated change ratio (CR) can be defined as a ratio between the new value of the parameter after adding the modifier and the previous value before adding it.

The results of the change ratio with standard division of each required parameter are as tabulated in the tables 8 and 9 and as shown in the Figures 3.

The following can be concluded from the figures and tables:

1) Yield Energy Analysis

a) Effect of adding Micro-silica

1) Adding 2% to DAB will increase Ey by 6 times but Ey will decrease when increasing the proportion of added silica.
2) Adding 2% to NAB will increase Ey by 1.6 times but Ey will decrease when increasing the proportion of added silica.

b) Effect of adding GG

1) The Ey increases with the increasing proportion of GG added to DAB.
2) The Ey decreases with the increasing proportion of GG added to NAB.

c) Effect of adding SBS 1101

1) The Ey increases with the increasing proportion of SBS 1101 added to DAB up to 1.15 when adding 9%.
2) The Ey decreases with the increasing proportion of SBS 1101 added to NAB.

d) Effect of adding SBS 1184

1) There is an inverse relationship when adding SBS 1184 and the best improvement can be obtained when adding 3%.
2) There is a direct correlation when adding SBS 1184, which means Ey is enhanced by increasing the added percentage.

2) Elastic Modulus Analysis

a) Effect of adding Micro-silica

1) The E decreases by about 13-60% with the increasing proportion of the Micro-silica added to DAB.
2) The E decreases by about 14-91% with the increasing proportion of the Micro-silica added to NAB.

b) Effect of adding GG

1) The E decreases by about 58-64% with the increasing proportion of the GG added to DAB.
2) The E decreases by about 53-63% with the increasing proportion of the GG added to NAB.

c) Effect of adding SBS 1101

1) The E decreases by about 12-21% with the increasing proportion of the SBS 1101 added to DAB.
2) The E decreases by about 0.03-0.08% with the increasing proportion of the SBS 1101 added to NAB.

d) Effect of adding SBS 1184

1) The E decreases by about 12-20% with the increasing proportion of the SBS 1184 added to DAB.
2) The E decreases by about 0.04-0.17% with the increasing proportion of the SBS 1184 added to NAB.

3) Elastic Energy Analysis

a) Effect of adding Micro-silica

1) The Ee decreases with the increasing proportion of the Micro-silica added to DAB and the best result is obtained at 2%.
2) The Ee increases by about 6 times when the Micro-silica is added to NAB and decreases with the increasing proportion of the modifier.

b) Effect of adding GG

1) The Ee decreases by about 30-55% with the increasing proportion of the GG added to DAB.
2) The Ee increases by about 1.8 times with the increasing proportion of GG added to NAB.

c) Effect of adding SBS 1101
1) The Ee increases by about 2.4 times when 2% SBS 1101 is added and decreases with the increasing proportion of its addition to DAB.
2) The Ee decreases by about 0.004-0.9% with the increasing proportion of its addition to NAB.

d) Effect of adding SBS 1184
1) The Ee increases by about 1.9 times when 6% of SBS 1184 is added to DAB.
2) The Ee increases by about 1.8 times when 9% of SBS 1184 is added to NAB.

4) Toughness Energy Analysis

a) Effect of adding Micro-silica
1) Adding 2% to DAB will increase E_t by 6.5 times but it decreases when increasing the proportion of added silica.
2) Adding 2% to NAB will increase E_t by 15 times but it decreases when increasing the proportion of added silica.

b) Effect of adding GG
1) The E_t increases by about 1.1-1.26 times with the increasing proportion of the GG added to DAB.
2) The E_t increases by about 1-1.07 times with the increasing proportion of GG added to NAB.

c) Effect of adding SBS 1101
1) The E_t increases with the increasing proportion of the SBS 1101 added to DAB up to 7 times when adding 9%.
2) The E_t decreases with the increasing proportion of SBS 1101 added to NAB and the best improvement can be obtained when adding 3%, about 3.7 times.

d) Effect of adding SBS 1184
1) There is an inverse relationship when adding SBS 1184 and the best improvement can be obtained when adding 3%, about 8.2 times.
2) The E_t increases about 10 times with the increasing proportion of added 9% of SBS 1184 to NAB.

5) Yield Stress Analysis

a) Effect of adding Micro-silica
1) Adding 6% to DAB will increase σ_y by 5.2 times but it decreases when increasing the proportion of added silica.
2) Adding 2% to NAB will increase σ_y by 1.6 times but it decreases when increasing the proportion of added silica.

b) Effect of adding GG
1) The σ_y increases with the increasing proportion of GG added to DAB.
2) The σ_y decreases with the increasing proportion of GG added to NAB.

c) Effect of adding SBS 1101
1) The σ_y increases with the increasing proportion of SBS 1101 added to DAB up to 1.15 when adding 9%.
2) The σ_y decreases with the increasing proportion of SBS 1101 added to NAB.

d) Effect of adding SBS 1184
1) There is an inverse relationship when adding SBS 1184 and the best improvement can be obtained when adding 3%.
2) There is a direct correlation when adding SBS 1184, which means σ_y is enhanced by increasing the added percentage.

6) Yield Strain Analysis

a) Effect of adding Micro-silica
1) Adding 2% to DAB will increase εy by 7.6 times but it decreases when increasing the proportion of added silica.
2) Adding 2% to NAB will increase ε_y by 10.3 times but it decreases when increasing the proportion of added silica.

b) Effect of adding GG
1) The ε_y increases with the increasing proportion of GG added to DAB.
2) The ε_y increases by about 1.5 times with the increasing proportion of GG added to NAB.

c) Effect of adding SBS 1101
1) The ε_y increases with the increasing proportion of SBS 1101 added to DAB up to 6 times when adding 3%.
2) The ε_y decreases with the increasing proportion of SBS 1101 added to NAB and the best improvement was when adding 3%, about 6.5 times.

d) Effect of adding SBS 1184
1) There is an inverse relationship when adding SBS 1184 and the best improvement can be obtained when adding 6% to obtain increases of about 9.6 times.
2) Adding 6% SBS 1184 enhanced ε_y by about 10.4 times and then it reduced when increasing the added percentage.

7) Stress at Failure

a) Effect of adding Micro-silica
1) Adding 2% to DAB will increase σ_f by 1.2 times but it decreases when increasing the proportion of added silica.
2) Adding 2% to NAB will increase σ_f by 8.8 times but it decreases when increasing the proportion of added silica.

b) Effect of adding GG

1) The σ_f increases with the increasing proportion of GG added to DAB.
2) The σ_f increases with the increasing proportion of GG added to NAB.

c) Effect of adding SBS 1101
1) The σ_f increases with the increasing proportion of SBS 1101 added to DAB up to 3.3 when adding 9%.
2) The σ_f increases with the increasing proportion of SBS 1101 added to NAB.

d) Effect of adding SBS 1184
1) There is an inverse relationship when adding SBS 1184 and the best improvement can be obtained when adding 6%.
2) Adding 6% SBS 1184 enhanced σ_f by about 3.3 times.

8) Strain at Failure

a) Effect of adding Micro-silica
1) Adding 2% to DAB will increase ε_f by 3.3 times but it decreases when increasing the proportion of added silica.
2) Adding 2% to NAB will increase ε_f by 3.3 times but it decreases when increasing the proportion of added silica.

b) Effect of adding GG
1) The ε_f increases with the increasing proportion of GG added to DAB.
2) The ε_f decreases with the increasing proportion of GG added to NAB.

c) Effect of adding SBS 1101
1) The ε_f increases with the increasing proportion of SBS 1101 added to DAB.
2) The ε_f decreases with the increasing proportion of SBS 1101 added to NAB.

d) Effect of adding SBS 1184
1) The best improvement can be obtained when adding 3%.
2) There is a direct correlation when adding SBS 1184, which means ε_f is enhanced by increasing the added percentage.

5.2 Effect of Test Temperature

Figure 4 provides an example of calculated energy parameters for different pure and modified asphalt binder at 25 ^{o}C and 50 ^{o}C temperatures based on the experimental results obtained from the DSR:

1) The yield, elastic and toughness (fracture) energies decreased with increased test temperature due to reduced viscosity of asphalt.
2) The yield and failure (fracture) stresses decreased with increased test temperature due to increased reduction in complex shear strain and reduced stiffness and viscosity of the asphalt binder.
3) The yield and failure (fracture) strains increased with increased test temperature due to reduced viscosity of asphalt binder and broke the molecular composition of the asphalt and thus will decrease the amount of stress necessary for the failure to occur.
4) The asphalt binder production in Nasiriyah refinery required more yielding energy than production in Durah refinery.
5) The elastic properties of asphalt binder production in Durah refinery are greater than production in Nasiriyah refinery.

It can be noticed from figure 5; change ratio of energy parameter;

1) At test temp. 25 ^{O}C ; the CR for yield energy, elastic modulus, toughness energy , yield stress, yield strain , stress at failure , strain at failure and elastic energy for asphalt binder production in Nasiriyah refinery is greater than another type.
2) At test temp. 50 ^{O}C; the CR for elastic modulus, toughness energy, yield strain and stress at failure for asphalt binder production in Durah refinery is greater than another type.
3) At test temp. 50 ^{O}C ; the CR for yield energy, yield stress, strain at failure and elastic energy for asphalt binder production in Nasiriyah refinery is greater than another type

6. Conclusions

Analysis of the experimental results of complex shear stress and strain obtained from DSR for two asphalts from different sources with different types of modifier showed:

1) Adding 2% Micro-silica to asphalt binder increased yield, elastic and toughness energies, stress and strain at failure, and yield stress for both types of asphalt binder.
2) Adding 9% GG slag to DAB enhanced yield and toughness energies, yield strain and strain at failure, and reduced elastic modulus and energy, yield stress and stress at failure.
3) Adding 6% GG slag to NAB improved yield, elastic and toughness energies, and yield stress and strain at failure but decreased the elastic modulus stress and strain at failure.
4) Adding 9% SBS 1101 to DAB increased yield and toughness energies, yield stress and strain, and strain at failure but reduced elastic modulus, elastic energy and stresses at failure.
5) Adding 3% SBS 1101 to NAB reduced elastic modulus and energy and so yield stresses but improved yield and toughness energy, stress and strain at failure and yield strain.
6) Adding 3% SBS 1184 to DAB improved yield and toughness energies, yield stresses and strain and so stress and strain at failure but reduced elastic modulus and energy.
7) Adding 9% SBS 1184 to NAB reduced the amount of elastic modulus and at the same time increased yield,

elastic and toughness energies, yield stresses and strain, and stress and strain at failure.

8) The yield, elastic and toughness (fracture) energies decreased with increased test temperature.
9) The yield and failure (fracture) stresses decreased with increased test temperature.
10) The yield and failure (fracture) strains increased with increased test temperature.

7. Acknowledgements

The writer sincerely thanks Dr Hussain A Khalid at the University of Liverpool for allowing the use of DSR to evaluate the local asphalt binders.

8. References

[1] AASHTO, D. (2009),"*Standard Method of Test for Yield Energy of Asphalt Binders Using the Dynamic Shear Rheometer*"; Draft, AASHTO Designation: T XXX-09.

[2] Barnes, H. A. (1999),"*The Yield Stress—A Review or 'παντα ρει'—everything flows? "Journal* of Non-Newtonian Fluid Mechanics Vol. 81(1): pp. 133-178.

[3] Braham, A. and C. Mudford (2012),*"Development of Fracture Resistance Curves for Asphalt Concrete"*, Journal of Materials in Civil Engineering, Vol. 25(11): pp.1631-1637.

[4] Christensen, R. M. (2013),"*Failure Theory for Materials Science and Engineering*", Oxford University Press, [http://www.failurecriteria.com,Accessed date24/03/2015]

[5] Christensen, R. M. (2013),"*The Theory of Materials Failure*", Oxford University Press.

[6] Collins, J. H., Bouldin, M. G., Gelles, R., & Berker, A. (1991),"*Improved Performance of Paving Asphalts by Polymer Modification (with discussion)*", Journal of the Association of Asphalt Paving Technologists Vol.60.

[7] D7175 (2008),"*Determining the Rheological Properties of Asphalt Binder Using a Dynamic Shear Rheometer (DSR)*", ASTM Standards.

[8] Denneman, E. (2010),"*Method to Determine Full Work of Fracture from Disk Shaped Compact Tension Tests on Hot-Mix Asphalt*", Proceedings of the 29th Southem African Transport Conference (SATC 2010), Pretoria, South Africa. ISBN: 978-1-920017-47-7.

[9] Herh, P. K., Colo, S. M., Hedman, K., & Rudolph, B. K. (1999),"*Dynamic Shear Rheometers Pave the Way for Quality Asphalt Binders*", American laboratory Vol.31: pp.16-21.

[10] Hetnarski, R. B. and J. Ignaczak (2006),"*Mathematical Theory of Elasticity*", Journal of Thermal Stresses Vol. 29(5): pp.505-506.

[11] Hill, R. (1998),"*The Mathematical Theory of Plasticity*", Oxford Classical Texts in the Physical Sciences.

[12] Johnson, C., Bahia, H., & Wen, H. (2009),"*Practical Application of Viscoelastic Continuum Damage Theory to Asphalt Binder Fatigue Characterization*", Asphalt Paving Technology-Proceedings Vol. 28: pp. 597.

[13] Johnson, C. M. (2010), *"Estimating Asphalt Binder Fatigue Resistance using an Accelerated Test Method*",PhD thesis,Civil & Environmental Engineering, UNIVERSITY OF WISCONSIN–MADISON.

[14] Kim, H. and W. G. Buttlar (2009),"*Discrete Fracture Modelling of Asphalt Concrete*",International Journal of Solids and Structures Vol. 46(13): p.p. 2593-2604.

[15] Noguera, A. H. and R. Miró (2011),*"Efecto de la tenacidad del asfalto en la resistencia a fatiga de las mezclas asfálticas*", Revista ingeniería de construcción Vol.26(2): pp. 224-239.

[16] Pellinen, T. and M. Witczak (2002),"*Stress Dependent Master Curve Construction for Dynamic (Complex) Modulus (with discussion)*", Journal of the Association of Asphalt Paving Technologists Vol. 71.

[17] Roque, R., Niu, T., Lopp, G., & Zou, J. (2012),*"Development of a Binder Fracture Test to Determine Fracture Energy*", PhD thesis University of Florida, Department of Civil and Coastal Engineering.

[18] Rosales, A. (2011),"*Fracture Energy Method for Determining Stiffness in Polymer Modified Asphalt Binders Using the Single Edge Notched Beam*", McNair Scholars Research Journal Vol. 7(1): pp. 15.

[19] Shen, S. y. and S. Carpenter (2007),"*Development of an Asphalt Fatigue Model Based on Energy Principles*", Journal of the Association of Asphalt Paving Technologists Vol. 76: p.p. 525-574.

[20] Sokolnikoff, I. S. and R. D. Specht (1956),*"Mathematical Theory of Elasticity*", McGraw-Hill New York.

[21] Timoshenko, S. P. and J. Goodier (2014), *"Theory of Elasticity"*, International Journal of Bulk Solids Storage in Silos Vol. 1(4).

Post-Dr Researcher Dr.Abdulhaq Hadi Abed Ali ; Assistant Professor in Highway and Transportation Dept.; Engineering College Al-Mustansiriyh University; Baghdad; Iraq.
Visitor Staff - School of Engineering - Liverpool University - UK

e-mail abdulhaq_alhaddad@yahoo.com ; abdulhaq1969@gmail.com; abdulhaq@liverpool.ac.uk

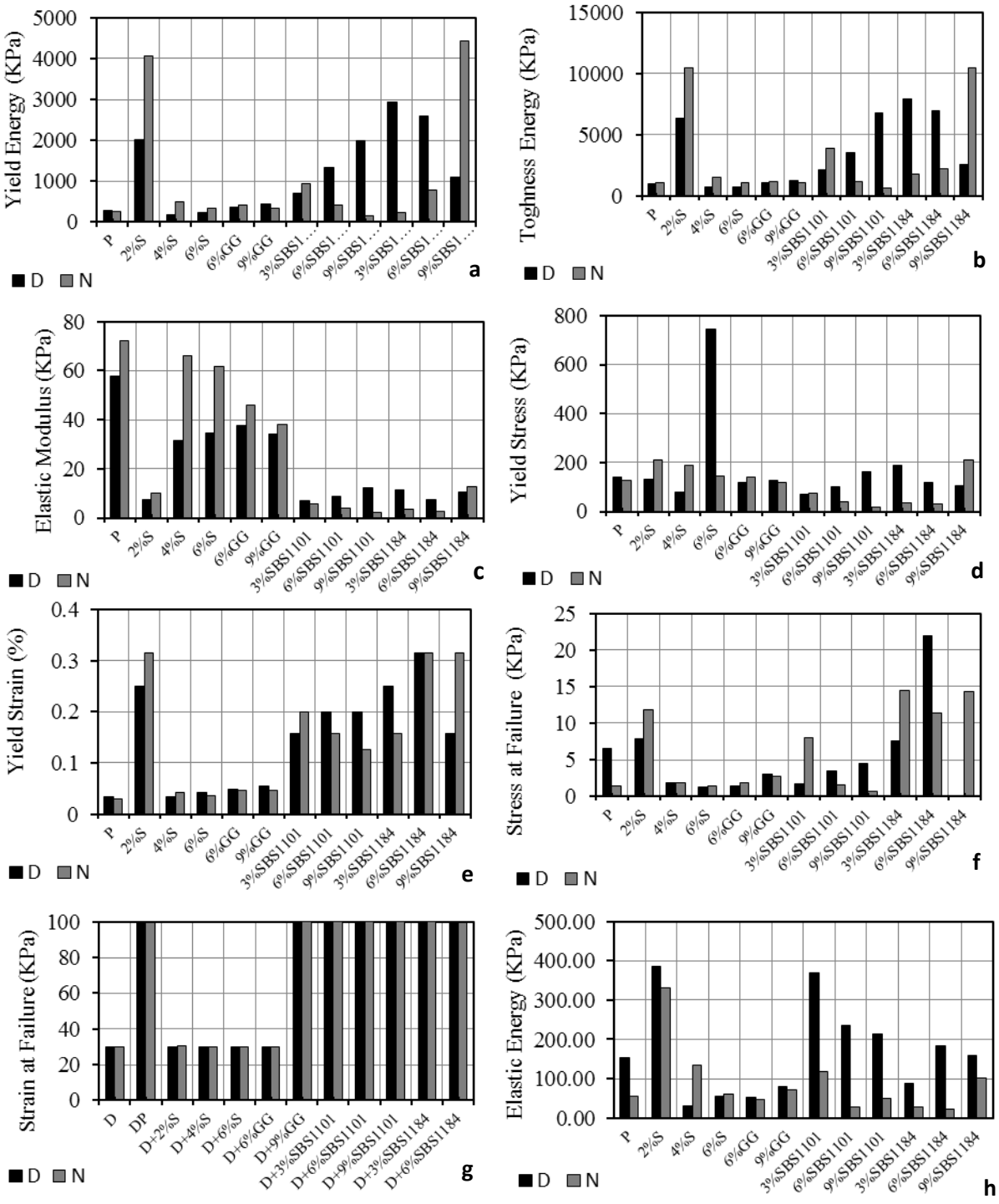

Figure 2. Characteristics of energies for local asphalt binders.

Table 6. Average value of energy characteristic of Durah Asphalt.

Parameters	Yield Energy	Elastic Modulus	Elastic Energy	Toughness Energy	Yield stress	Yield strain	Stress at failure	Strain at failure
	E_y (Pa)	E (Pa)	E_e (Pa)	E_t (Pa)	σ_y (Pa)	ε_y (%)	σ_f (Pa)	ε_f (%)
DP	297905.7	58007	153738.2	966926.2	142200	3.28829	6489	30.0126
D+2%S	2017891	7545.1	386231.2	6341144	130000	25.0182	7850	99.9477
D+4%S	172151.5	34736	29483.91	685262.7	80030	3.41712	1793	30.0139
D+6%S	236819.7	34736	54647.07	743635.9	743635.9	4.1402	1260	30.0115
D+6%GG	369365.3	37484	51035.90	1069481	120600	4.82605	1357	30.005
D+9%GG	434488.8	33977	79548.61	1219723	129600	5.41484	2949	30.0157
D+3%SBS1101	697281.5	6928.6	368193.9	2152473	68800	15.7787	1720	99.9821
D+6%SBS1101	1344388	8956.2	235424.0	3570084	100000	19.8519	3430	99.9849
D+9%SBS1101	1995883	12412	214544.4	6815932	164000	19.918	4440	99.9491
D+3%SBS1184	2928372	11426	88362.36	7928535	187200	25.042	7617	99.9389
D+6%SBS1184	2592586	7320.7	182865.6	6953712	118500	31.4893	21900	99.8073
D+9%SBS1184	1095546	10536	158002.6	2533891	107300	15.7602	52.4	100.002

Table 7. Average value of energy characteristic of Nasiriyah Asphalt.

Parameters	Yield Energy	Elastic Modulus	Elastic Energy	Toughness Energy	Yield stress	Yield strain	Failure stress	Failure strain
	E_y (Pa)	E (Pa)	E_e (Pa)	E_t (Pa)	σ_y (Pa)	ε_y (%)	σ_f (Pa)	ε_f (%)
NP	266845.762	72111	53823.87	1057465.106	126900	3.045	1437	30.001
N+2%S	4075835.07	10268	330051.31	10473153.26	210400	31.511	11760	99.911
N+4%S	496780.466	66239	133701.25	1490882.524	189200	4.141	1847	30.442
N+6%S	346932.455	61578	61783.63	1086167.459	144800	3.689	1439	29.984
N+6%GG	414293.487	45986	46321.03	1140376.096	139500	4.646	1850	30.005
N+9%GG	351784.837	38246	70872.19	1064704.280	117800	4.645	2691	30.004
N+3%SBS110	938404.199	5876.1	119208.06	3896507.140	74210	19.884	7994	99.967
N+6%SBS110	408369.245	4169.5	26310.87	1162791.594	40950	15.811	1568	99.993
N+9%SBS110	164220.929	2414.6	49351.21	679324.325	20280	12.566	687.8	99.994
N+3%SBS118	236631.114	3438.5	27447.90	1791761.478	34640	15.818	14520	99.976
N+6%SBS118	776349.741	2888	23009.15	2213300.543	32530	31.587	11340	99.970
N+9%SBS118	4430266.92	12582	100279.56	10434944.95	208800	31.430	14380	99.882

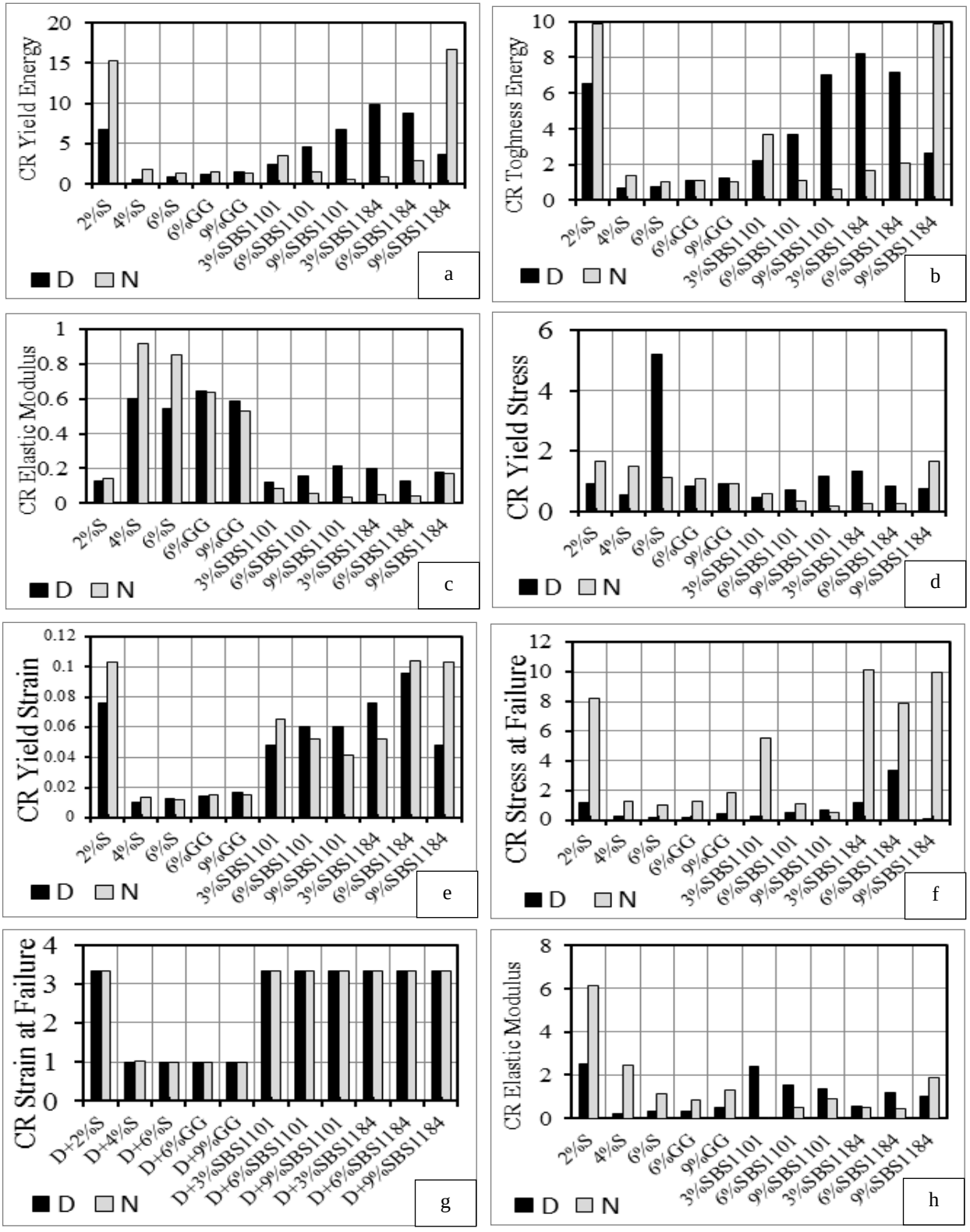

Figure 3. Change ratio calculation for local asphalt binder at 25 ^{o}C test temperature.

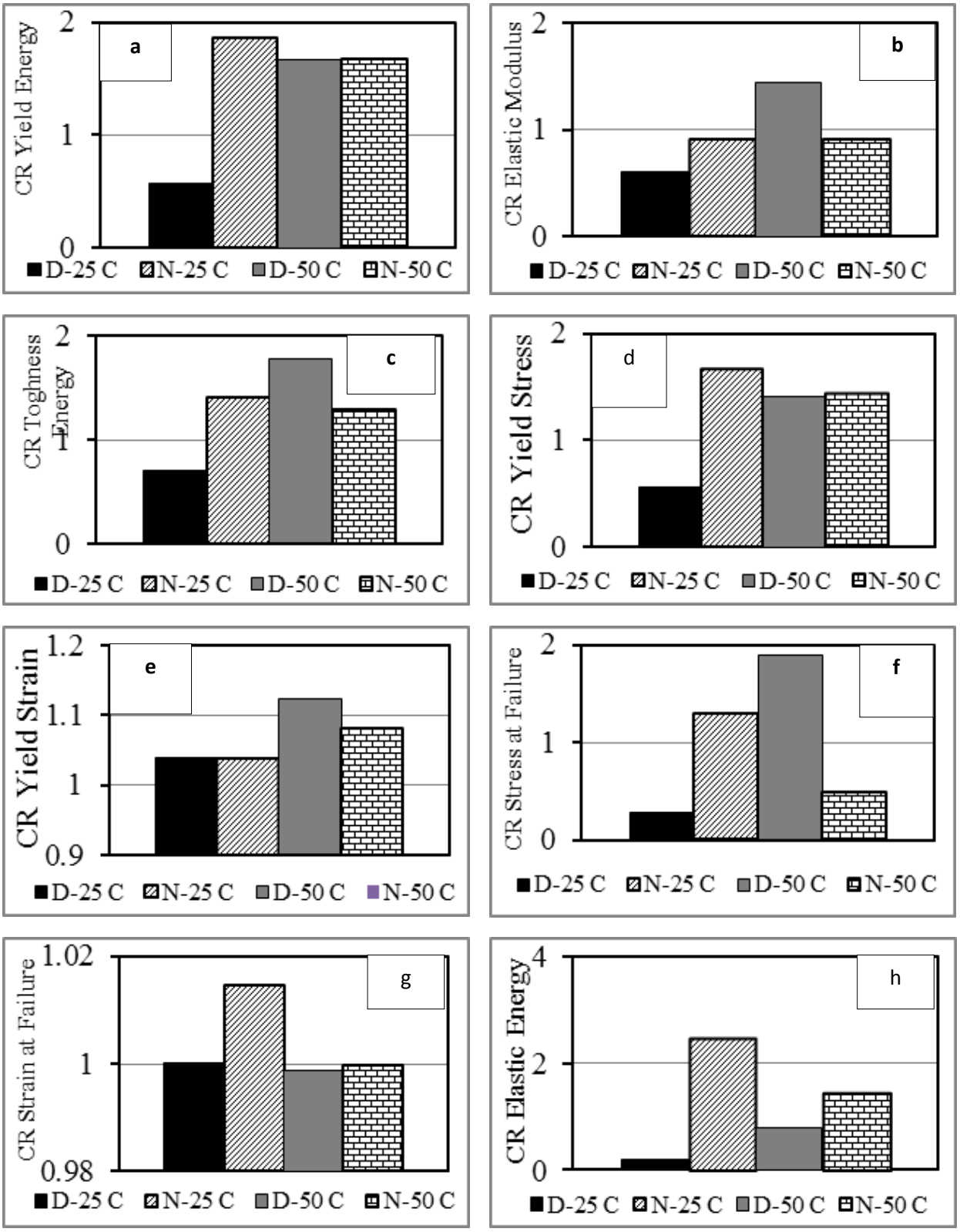

Figure 4. Example of calculation of energy parameters for local asphalt binder modified by using 4% Micro-silica at different test temperatures

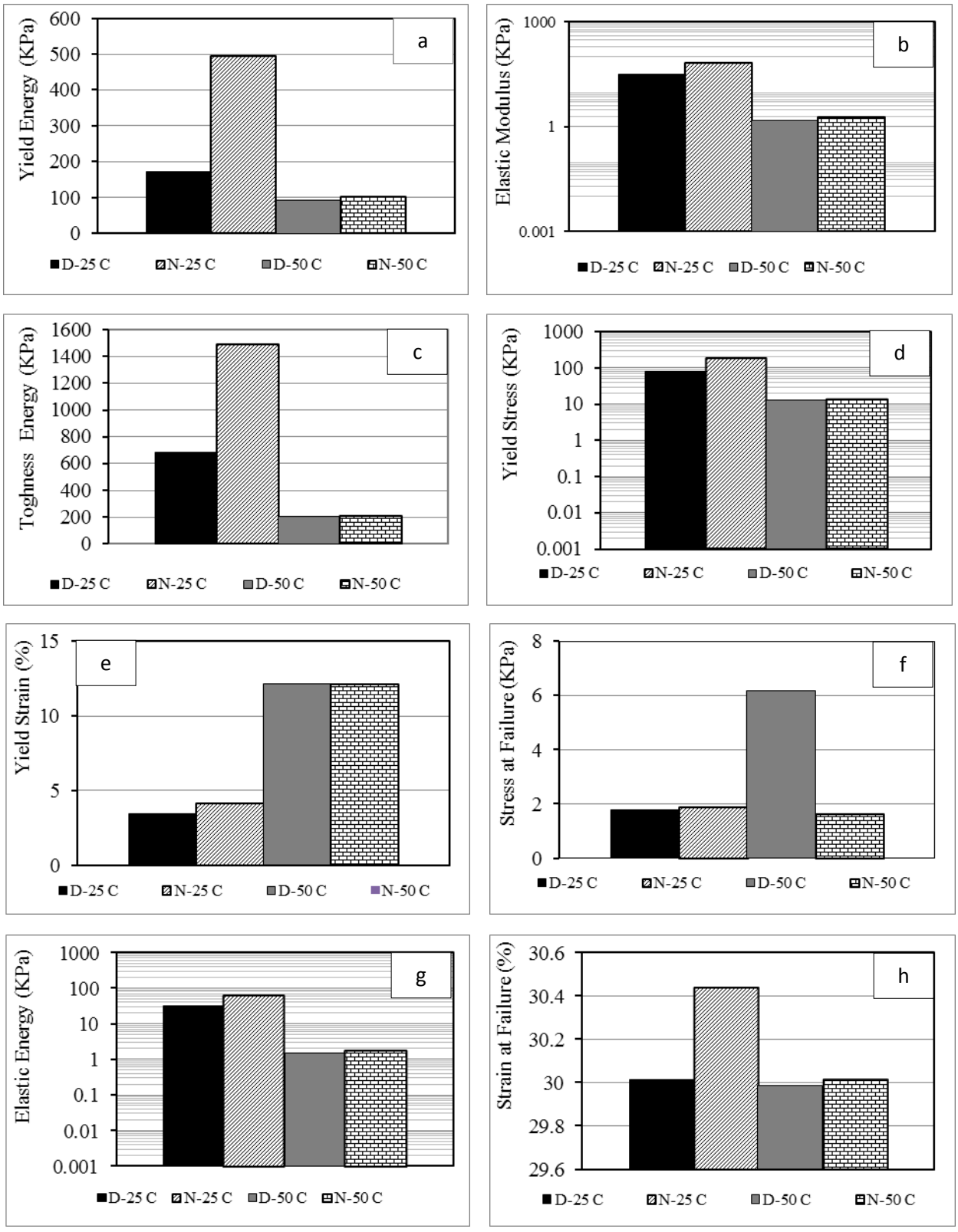

Figure 5. Change ratio of energy parameters for local asphalt binder modified by using 4% Micro-silica at different test

Table 8. Change Ratio with standard division for energy parameters of Durah Asphalt Binder (DAB)

Parameters	Yield Energy		Elastic Modulus		Elastic Energy		Toughness Energy		Yield stress		Yield strain		Failure stress		Failure strain	
	E_y -Pa	σ	E_e -Pa	σ	E_e -Pa	σ	E_t-Pa	σ	σ_y-Pa	σ	ε_y -%	σ	σ_f-Pa	σ	ε_f -%	σ
D+2%S	6.774	2.013	0.130	1.815	153738.2	2.27	6.558	2.403	0.914	1.357	7.608	2.575	1.210	2.252	3.330	1.909
D+4%S	0.578	1.145	0.599	1.032	386231.2	1.29	0.709	1.367	0.563	0.772	1.039	1.465	0.276	1.281	1.000	1.086
D+6%S	0.795	3.664	0.599	3.303	29483.91	4.14	0.769	4.374	5.230	2.470	1.259	4.440	0.194	3.883	1.000	3.292
D+6%GG	1.240	2.361	0.646	2.128	54647.07	2.67	1.106	2.819	0.848	1.592	1.468	3.020	0.209	2.641	1.000	2.239
D+9%GG	1.458	1.364	0.586	1.230	51035.90	1.54	1.261	1.628	0.911	0.920	1.647	1.745	0.454	1.526	1.000	1.294
D+3%SBS1101	2.341	2.314	0.119	2.086	79548.61	2.61	2.226	2.763	0.484	1.560	4.798	2.960	0.265	2.589	3.331	2.195
D+6%SBS1101	4.513	3.142	0.154	2.832	368193.9	3.55	3.692	3.751	0.703	2.118	6.037	4.019	0.529	3.515	3.331	2.980
D+9%SBS1101	6.700	2.214	0.214	1.996	235424.0	2.50	7.049	2.643	1.153	1.493	6.057	2.832	0.684	2.477	3.330	2.100
D+3%SBS1184	9.830	1.012	0.197	0.912	214544.4	1.14	8.200	1.208	1.316	0.682	7.616	1.295	1.174	1.132	3.330	0.960
D+6%SBS1184	8.703	0.987	0.126	0.890	88362.36	1.11	7.192	1.178	0.833	0.665	9.576	1.263	3.375	1.104	3.326	0.936
D+9%SBS1184	3.677	1.231	0.182	1.110	182865.6	1.39	2.621	1.470	0.755	0.830	4.793	1.575	0.008	1.377	3.332	1.168

Table 9. Change Ratio with standard division for energy parameters of Nasiriyah Asphalt Binder (NAB)

Parameters	Yield Energy		Elastic Modulus		Elastic Energy		Toughness Energy		Yield stress		Yield strain		Failure stress		Failure strain	
	E_y -Pa	σ	E_e -Pa	σ	E_e -Pa	σ	E_t-Pa	σ	E_y -Pa	σ	E_e -Pa	σ	E_e -Pa	σ	E_t-Pa	σ
N+2%S	15.274	2.104	0.142	2.412	53823.87	1.899	9.904	1.658	1.658	2.563	10.348	2.251	8.184	2.168	3.330	1.079
N+4%S	1.862	1.197	0.919	1.372	330051.3	1.080	1.410	0.943	1.491	1.458	1.360	1.280	1.285	1.233	1.015	0.614
N+6%S	1.300	3.829	0.854	4.390	133701.2	3.456	1.027	3.018	1.141	4.666	1.211	4.097	1.001	3.947	0.999	1.963
N+6%GG	1.553	2.467	0.638	2.829	61783.63	2.227	1.078	1.945	1.099	3.007	1.526	2.640	1.287	2.543	1.000	1.265
N+9%GG	1.318	1.425	0.530	1.634	46321.03	1.287	1.007	1.124	0.928	1.737	1.525	1.525	1.873	1.469	1.000	0.731
N+3%SBS1	3.517	2.418	0.081	2.772	70872.19	2.183	3.685	1.906	0.585	2.947	6.530	2.587	5.563	2.493	3.332	1.240
N+6%SBS1	1.530	3.283	0.058	3.764	25.13	2.964	1.100	2.588	0.323	4.001	5.192	3.513	1.091	3.384	3.333	1.684
N+9%SBS1	0.615	2.314	0.033	2.653	26310.87	2.088	0.642	1.824	0.160	2.819	4.127	2.475	0.479	2.385	3.333	1.186
N+3%SBS1	0.887	1.058	0.048	1.212	49351.21	0.955	1.694	0.834	0.273	1.289	5.195	1.131	10.104	1.090	3.332	0.542
N+6%SBS1	2.909	1.031	0.040	1.183	27447.90	0.931	2.093	0.813	0.256	1.257	10.373	1.104	7.891	1.063	3.332	0.529
N+9%SBS1	16.602	1.286	0.174	1.475	23009.15	1.161	9.868	1.014	1.645	1.568	10.321	1.376	10.007	1.326	3.329	0.660

Delineation Landfill Depth using 2D Electrical Resistivity Imaging (ERI) Technique in Kut City, Eastern Iraq

Hussein H. Karim[1], Imzahim A. Alwan[2], and Fatima A. Tayeb[3]

Abstract—Electrical resistivity surveys were carried out at a site of project construction in Kut City, Wassit Governorate, Eastern Iraq. The aim of this work is to identify the landfill depth in the site for engineering purposes. The resistivity survey was carried out by using 1D and 2D imaging techniques. For 1D survey, 14 VES points with spread length 50-100 m were applied using Schlumberger array. While for 2D electrical resistivity imaging (ERI) technique, Wenner-Schlumberger array was applied with total surveyed lengths was 3304 m. The length of these spreads was varied from 40 to 200 m using different electrode spacings (0.5 to 2.5 m). The data collected from 2D ERI by Terrameter SAS 4000, generated sections of the acquired data helped to map the landfill depth, which was delineated as an area of high resistivities. These obtained sections from 2D inversions have been processed by RES2DINV software. The maximum depth of investigation was about 34 m with resistivity values range from <1 to >1000 Ω.m. The landfill layer was recognized as the upper layer consists of domestic wastes and broken fragments with high resistivity ranging from 30 Ω.m to more than 1000 Ω.m. This layer appears at different depths starting from ground surface and sometimes from 2 m to a depth of 8 m and sometimes deeper. The sections also show a layer with medium resistivity (5-30 Ω.m) represents the clayey sand layer at depth ranging from 8-10 m overlapping with a layer of very low resistivity (<5 Ω.m at depth >18 m) that represents the silty clay. Some sections show deeper high anomalies reaching a depth around 23 m. The outputs interpretation is in agreement with borehole logs available in the site of the study.

***Index Terms*—2D Resistivity Imaging Technique, Landfill, RES2DINV, Kut City-Iraq**

I. INTRODUCTION

SURFACE-geophysical methods afford quick, inexpensive and non - invasive means to help in characterization the subsurface geophysical formation. They provide information on subsurface properties, such as soil and landfill thickness, depth to bedrock, location and distribution of conductive fluids, and fracture zones and faults. However, there are numerous limitations to the information obtained by the geophysical techniques and they shall not be expected to provide reliable results under all circumstances. All geophysical information should be crossed-checked by borings and/or other direct methods of exploration.

Electrical resistivity of the soil is considered as an indicator for the variation of soil properties [1]. Electrical Resistivity Survey is carried out to determine the resistivity distribution of earth layers. Electrical current is injected to the ground and then potential difference is measured. This measured potential difference pattern provides information on the subsurface condition and electrical properties of the soil [2]. The main objective of the present study is applying detailed 2D resistivity surveying in the site of investigation to delineate the depth of landfill by correlating resistivity data with geotechnical data taken from boring.

II. BASIC PRINCIPLES OF ELECTRICAL RESISTIVITY

The purpose of electrical surveys is to define the subsurface resistivity distribution with outward measurements. The basic principles of Resistivity Imaging (RI) depend on the linear relationship between electric current (I) and potential difference (V) which is given by the Ohm's law in the following equation [3] [4]:

$$V = IR \quad (1)$$

Here, V is the potential difference measure in volt and I is the current which is typically measured in ampere, and R is the electrical resistance inohm or simply Ω.

For a given material (conductor), the resistance is proportional to its length (L *in* m) and inversely proportional to its cross-sectional area (A *in* m^2). Thus in general, the resistivity ρ (Ω.m) is determined as:

$$R = \frac{\rho L}{A} \quad (2)$$

The proportionality constant (ρ) is the resistivity of the conductor. It is a physical property of the conductor which expresses its ability to resist the flow of electric current. The expression reciprocal of resistivity is conductivity (σ), where,

$$\sigma = \frac{1}{\rho} \quad (3)$$

In a homogeneous and isotropic half space, electrical equipotential is hemispherical as shown in Fig. 1. For a

Manuscript received July 6, 2015; accepted August 16, 2015.

[1] Professor, Building and Construction Engineering Department, University of Technology, Baghdad, Iraq. (corresponding author: e-mail: husn_irq@yahoo.com).

[2] Asst. Professor, Building and Construction Engineering Department, University of Technology, Baghdad, Iraq. (e-mail: mzahim74@yahoo.com).

[3] M.Sc. in Geomatics Engineering. (e-mail: fm.alkobaisi@gmail.com).

homogeneous ground with single electrode, the potential will separate radially outward the current source, where area (A) will be a half sphere ($2\pi r^2$) with radius (r). Thus, "(1) is rewritten as" [5]:

$$\rho = RK \quad (4)$$

where K=2πr for the half sphere. "Equation (4) consists of two parts: the first is the resistance (R) and the second is called the geometric factor (K) which describes the geometry of the electrode configuration" [4] [6].

For a homogeneous ground with four electrodes, the geometric factor in "(4)" will be varied according to the type of electrodes configuration as shown in Fig. 1. The most common electrode arrays used in Electrical Resistivity Imaging (ERI) are Wenner, Wenner-Schlumberger and dipole-dipole arrays [7].

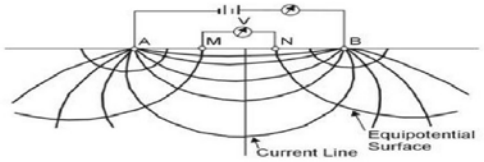

Fig. 1. Equipotential and current lines for a pair of current electrodes A and B on a homogeneous half-space [8].

III. SITE LOCATION AND GEOLOGY OF THE STUDY SITE

Kut area is part of the Mesopotamia Plain which occupies the central and the southern parts of Iraq (Fig. 2). The Mesopotamia Plain is covered by different Quaternary sediments ranging in age from Pleistocene to Holocene, and in thickness from few meters to 180 m, they are represented by fluvial sediments of the Tigris and Euphrates Rivers. It is a potential region of subsidence in the Neogene, and a significant basin of alluvial sediment accumulation in the Quaternary. It is a very mobile basin and contains several evidences pointing to its recent tectonic activity [9] [10].

Soil Site Stratification

Ground conditions encountered in the exploratory holes showed that soil profile consists of three main layers (Fig. 3). The uppermost layer consists of fill materials to a depth of 2.0-4.5 m. The second layer consists of cohesive soil of silty clay to clayey silt of low plasticity and sometimes from clayey soil with silt. This layer extended from the fill materials layer to a depth ranging from 6.5 to 12 m. The third layer consists of cohesion less soil of silty sand to sandy silt and sometimes sand with silt. This layer extends from the second layer to a depth of 19.5 m. The range of measured N values is between 12 at depth 2.5 m and 24 at 8 m (medium–stiff soil) to >30 (stiff –hard soil) to the end of boring. Groundwater levels have been recorded from 1.50 and 1.63 m below natural ground level [13].

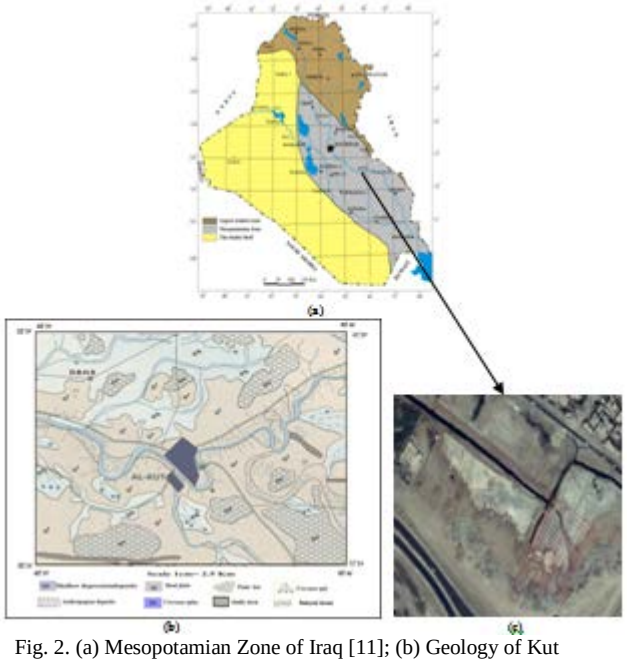

Fig. 2. (a) Mesopotamian Zone of Iraq [11]; (b) Geology of Kut Quadrangle [12]. (c) Site location of the study area in Kut City.

BOREHOLE LOG

Borehole NO.: 1	Borehole Elevation:----- m.a.s.l.
Borehole Dia. : 150 mm	Date of Drilling: 17/11/2008
Depth of Borehole: 25 m	Method of Drilling: Rotary Auger Drilling

Depth (m) From	Depth (m) To	Layer Thickness (m)	Strata Symbol	Sample Type	S.P.T. 15 cm	15 cm	15 cm	N	Description of Strata
0.0	1.5	1.5		DS					Fill Materials
1.5	4.5	3.0		DS					Fill Materials
4.5	6.0	1.5		DS					Brown silty clay with sand
6.0	6.5	0.5		US					Soft to medium brown clayey silt
6.5	8.0	1.5		DS					Brown clayey sand
8.0	8.5	0.5		SPT	8	12	12	24	Brown clayey sand
8.5	10.5	2.0		DS					Brown clayey sand
10.5	11.5	1.0		DS					Brown clay with silt
11.5	12.0	0.5		SPT	38	40	20	>50	Brown clay with silt
12.0	13.5	1.5		DS					Brown clay with silt
13.5	15.0	1.5		DS					Brown clayey sand
15.0	16.0	1.0		DS					Green sand
16.0	16.5	0.5		SPT	18	23	22	45	Green sand
16.5	18.0	1.5		DS					Brown clayey sand
18.0	19.0	1.0		DS					Gray to brown clayey sand
19.0	19.5	0.5		SPT	12	13	18	31	Gray to brown clayey sand
19.5	22.5	3.0		DS					Dark brown silty clay to clayey silt
22.5	24.5	2.0		DS					Brown clayey silt with sand
24.5	25.0	0.5		SPT	20	21	25	46	Brown clayey silt with sand
End of Boring									

Ground Water Level (Final):1.63m

Fig. 3. Borehole log [13].

IV. FIELD WORK (1– AND 2-DIMENSIONAL SURVEYS)

The aim of this work is to identify the landfill depth in the site for engineering purposes. ABEM Terrameter SAS 4000 was used for data collection of ERI. The total area of the site under investigation is about 29000 m^2. Field work consists two parts, 1-D and 2-D surveys. For 1-D survey, 14 VES points shown in Figure 4 have been investigated along spreads of 50 to 100 m long by using Schlumberger array for sounding technique. For 2D imaging survey, 36 spreads with total length of 3304 m and different electrode spacing have been surveyed as follows: 2 (200 m long- 2.5 m spacing), 5 (120 m long; 1.5 m spacing), 25 (80 m long; 1 m spacing), 2 (100 m long; 1.25m spacing), 1(64 m long; 0.8 m spacing) and 1(40 m long; 0.5 m spacing) by using Wenner-Schlumberger array for

all spreads. The 2D inversion resistivity sections for Lines 1 to 7 and 14 to 34 are trending from SW to NE direction and Lines 8 to 13 and 24 to31 are trending from SE to NW, while Lines 35 and 36 are the diagonals of this grid (Fig. 4). The maximum depth of investigation of the surveyed site was about 34 m.

Fig. 4. Survey design layout for site location.

Data Processing

RES2DINV software is designed to interpolate and interpret field data of electrical resistivity (conductivity) and induced polarization. The inversion of the resistivity and IP data is conducted by least-square method involving finite-element and finite-difference methods. Remove bad data points is the first step of data processing. To use the results, a measurement of the difference is given by the root-mean squared (RMS) error which needs to be considered. However the model with the lowest possible RMS error can sometimes show large and unrealistic variations in the model resistivity values and might not always be the "best" model from a geological perspective. However for this analysis, the RMS error must not exceed 30%.

V. RESULTS AND DISCUSSION

A feasible study has been presented for an integrated investigation of landfill sites using modern techniques. In this study, we have attempted to demonstrate some of the advantages of integrating information from different data sets.

The VES curves can be classified into two groups; the first involves 5 VES points consists of four geoelectrical layers of QH, KQ, QQ and QH. The second group appears three geoelectrical layers involving 9 VES points of Q type. Fig. 5 shows resistivity curves for VES 29 and VES 31 as representative curves.

In general, VES curves reveal the following points: a decrease in apparent resistivity values with depth; low apparent resistivity values under the position of most VES points could be due to the water content and the presence of salts; high conductivity (which is due to clay content and saline groundwater) resulted in relatively low measured apparent resistivity; high resistivity values are caused by presence of sands or landfill material.

The apparent resistivity sections are obviously shown a decrease in apparent resistivity values with depth, and they give a primary picture about the distribution of deposits. Resistivity and thickness values from deep VES were confirmed by borehole and geotechnical information, where 3-4 main geoelectrical zones interpreted with decreasing resistivity with depth.

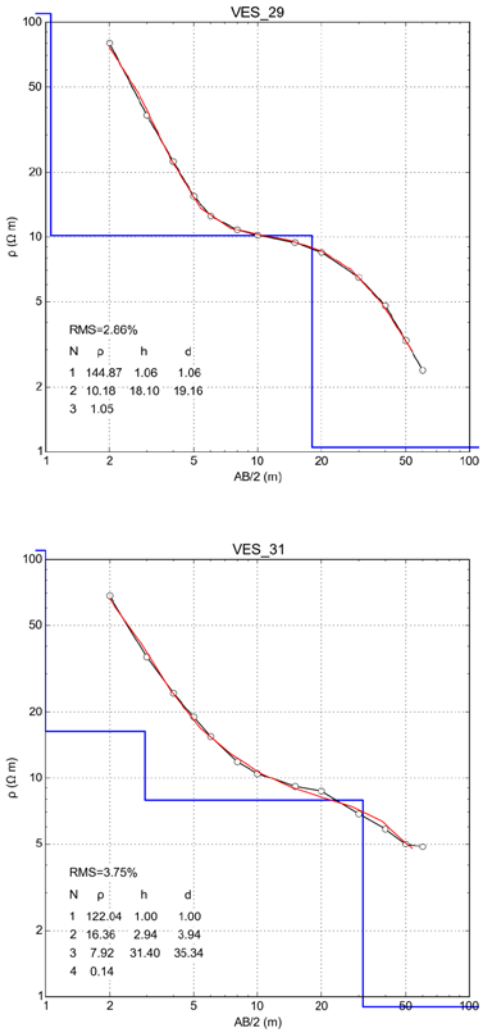

Fig. 5. 1-D resistivity curve for VES 29 and VES 31.

The results of this survey study are also used to create 2D images with RES2DINV software. From the analysis of all sections, the maximum depth of investigation was about 34 m and resistivity values are ranging from 1 to more than1000 Ω.m. The RMS of < 20% after different iterations. Fig. 6 shows the inverse models of 2D imaging for the parallel Lines 27 to 31as representative sections.

The landfill layer was recognized as the upper layer with high resistivity ranging from 30 Ω.m to more than 1000 Ω.m with higher values in middle and right parts, with depth ranging between 2- 8 m with higher vales to the right part. This layer mainly consists of domestic wastes and broken bricks and fragments. These findings are in confirmation with the geotechnical data obtained from available boreholes, where N values are between 12- 24 at depths 2.5- 8 m respectively reaching N>30 after the later depth to the end of

boring. In addition, these sections also show a layer with medium resistivity (5- 30 Ω.m) represents the clayey sand layer overlapping with layer by very low resistivity (<1-2.5 Ω.m) that represents the silty clay.

This study has shown the ability of electrical resistivity tomography to detect defects and heterogeneity in the cover material, indicating that it is a good means of monitoring the quality of landfill cover both when it is put in place and subsequently.

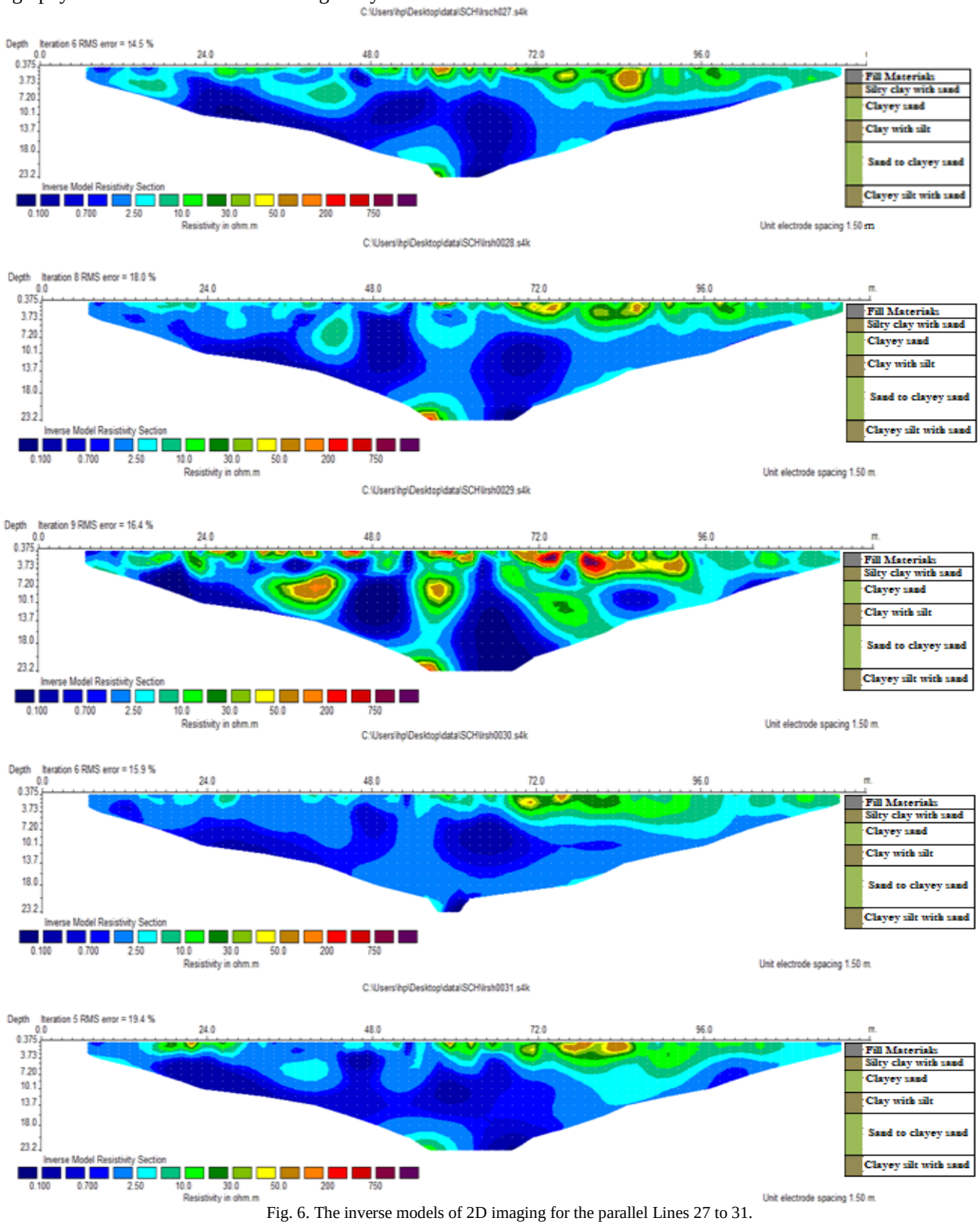

Fig. 6. The inverse models of 2D imaging for the parallel Lines 27 to 31.

Figs. 7 and 8 show the contour maps of isoresistivity and depth of the landfill layers. The resistivity and depth contour maps show that the resistivity values are ranging between 30 to more than 170 Ω.m (Ignoring the very high resistivity

values for drawing requirements) and the depth values are ranging between 2 to 15 m. The maximum values of resistivity are concentrated in the NW and NE parts of the area, while the minimum values are concentrated in SE of the area. The maximum values of landfill depth appear in NE and SW parts of the area and the minimum values are concentrated in the NW and SE parts of the study area.

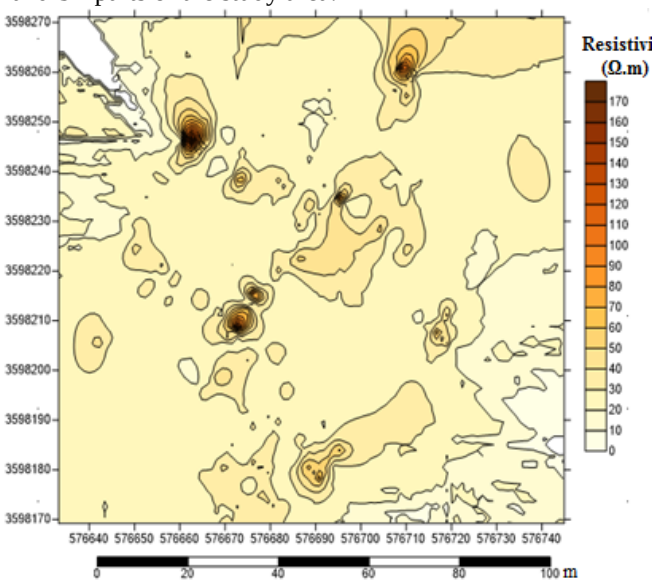

Fig. 7. Contour map for landfill resistivity.

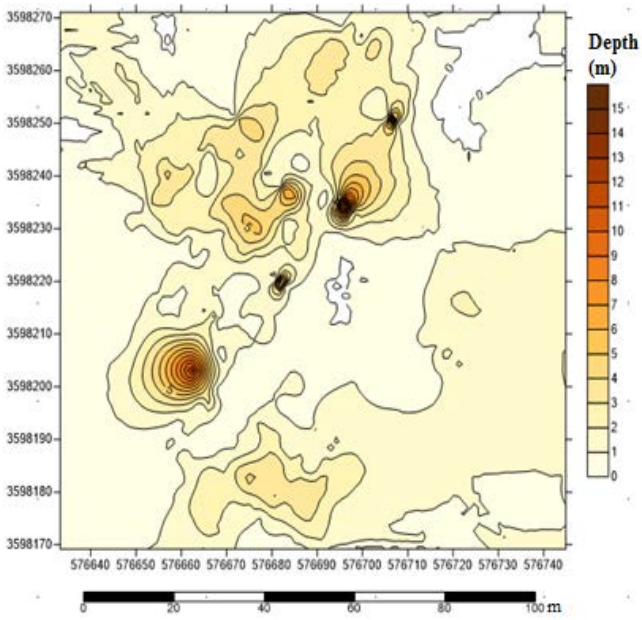

Fig. 8. Contour map for landfill depth.

VI. CONCLUSION

In the light of this study, the following conclusions can be drawn:

1. The landfill has been identified as the upper resistive feature (layer) consists of domestic wastes and broken fragments and is characterized by its low N-values**.**
2. The landfill layer appears at different depths from ground surface to a depth of 8 m and it was recognized with high resistivity ranging from 30 Ω.m to more than 1000 Ω.m.
3. The inversion sections also show a layer with medium resistivity (5-30 Ω.m) represents the clay and layer overlapping with layer by very low resistivity (< 5 Ω.m) that represents the silty clay.
4. The outputs interpretation is in agreement geotechnical data obtained from the borehole logs available in the site of the study.
5. The resistivity and depth contour maps show that the resistivity values are ranging between 30 to more than 170 Ω.m and the depth values are ranging between 2 to 15 m.

REFERENCES

[1] O. Banton, M. K. Seguin, and M. A. Cimon, "Mapping field-scale physical properties of soil with electrical resistivity," *Soil Sci. Soc. Am. J.*, vol. 61, No. 4, 1997, pp. 1010-1017.

[2] P. Kearey, M. Brooks, and I. Hill, *An introduction to geophysical exploration*, Wiley- Blackwell, 2002.

[3] *W. Lowrie*, *Fundamentals of geophysics*, 2nd ed., Cambridge University Press, 2007, 381 P.

[4] R. A. Serway, and J. W. Jewett, *Physics for scientists and engineers*, 6th ed., Thomson Brooks / Cole, 2007.

[5] A. Samouëlian, I. Cousin, A. Tabbagh, A. Bruand, and G. Richard, "Electrical Resistivity Survey in Soil Science: A Review," *Soil & Tillage Research*, vol. 83, no. 2, pp. 173-193, 2005.

[6] H. A. Al-Musawi, "The use of GIS and resistivity imaging techniques to determine landslide probability based on internal and external causal factors," PhD. thesis, University Sains Malaysia, 2010.

[7] J. M. Reynolds, *An introduction to applied and environmental geophysics*, John Wiley and Sons, Ltd, 1997.

[8] S. I. Ibeneme, K. K. Ibe, A. O. Selemo, J. O. Nwagbara, Y. E. Obioha, K. O. Echendu, and B. O. Ubechu, "Geoelectrical investigation of a proposed dam site in a sedimentary terrain: Case Study of Aba River at Amapu-Ideobia, Akanu Ngwa Southeastern Nigeria," vol.4, pp.1376-1381, 2013.

[9] S. F. A. Fouad, and V. K. Sissakian, "Tectonic and structural evolution of the Mesopotamian Plain," *Iraqi Bull. Geol. Min.*, Special Issue, No.4, 2011: Geology of the Mesopotamia Plain, pp. 33-46, 2011.

[10] T. Buday, and S. Z. Jassim, *The regional geology of Iraq*, vol. 2, Tectonism and magmatism and metamorphism (I.I. Kassab and M. J. Abbas: Eds.), Baghdad, 1987, 445 P.

[11] S. Z. Jassim, and J. C. Goff, *Geology of Iraq*, Dolin, Prague and Moravian Museum, Brno, 2006, 341 P.

[12] *CEB, Consulting Engineering Bureau*: College of Engineering, University of Baghdad, Report/ 2008.

Prof. Dr. Hussein Hameed Karim received the B.S. and M.S. degrees in Earth Science/ Geophysics from the University of Baghdad, in 1978 and 1982 respectively, and the Ph.D. degree in Engineering Geophysics from University of Baghdad in 1996, Iraq.

From 1983 to 1997 he was within the academic staff of University of Basrah and graduated from Asst. lecturer to Asst. Professor. Since 1997 he is within the academic staff of University of Technology. Since 2000, he has been a Professor with the Building & Construction Engineering Department/ University of Technology. He is the supervisor of more than 45 post graduate (M.Sc. and Ph.D) students, the author of 5 books, and one under preparation, more than 100 scientific researches, more than 100 scientific articles, and two patents. His research interests include Engineering Geophysics, Soil & Rock Mechanics, Site Investigation, and Geomatics Engineering.

Prof. Karim was chosen by the Committee of University of Technology as the 1st Professor in the University of Technology for the academic year (2010-2011). Prof. Karim's awards and honors include training session to Bordeaux University- France (4 months, 1984); Visiting Professor to University of Hodeidah University- Yemen (3 months, 2002); Visiting Professor (one month, 2010) to Malaya University- Kuala Lumpur, Malaysia; and 3 Professor Visits sponsored by DAAD (Germany), Bauhaus University- Weimar 2006, Rhur University – Bochum 2010 and 2014 (3-months for each).

Real-time Calibration of Close Range Digital Non-Metric Camera with Precise Portable Control System.

Dr. Abbas Z. Khlaf, Israa H. Mohammed, and Tariq N. Otaiwi

***Abstract*— Now a day, two type of cameras are used for data acquisition in analytical photogrammetry, metric and non-metric (digital) cameras.**

Metric cameras are designed and manufactured for photogrammetric data acquisition, they have very well defined, precise and stable Interior Orientation Parameters "IOP".

On the other hand non-metric (digital) cameras are designed and manufactured for commercial use, which are mainly interested in the image resolution inexpensive of lens distortion accordingly, non-metric digital cameras suffer from unstable and Interior Orientation Parameters "IOP" with significant lens distortion, consequently there is no "permanent" calibration of non-metric (digital) camera.

In this research a numerical approach with a portable control system will be used to determine the IOP for each photographing seasons with zoom [changeable focal length] digital camera.

***Index* Analytical Photogrammetry, Camera calibration, IOP.**

I. INTRODUCTION

Analytical Photogrammetry deals with the solution of photogrammetric problems by mathematical computations, using measurements made on the photographic as input data (photo coordinates). In general, a mathematical model is constructed to represent the relation between points in the object space and their corresponding images on the photographs. The principle of perspective and projective geometry is inherent in this(Ghosh, K.1979).

Analytical Photogrammetry is based fundamentally on the collinearity equations which are also called central projection equations these equations relate the photographic coordinates to the ground coordinates through several parameters, these parameters are classified into exterior and interior orientation parameters. The interior orientation parameters are usually determined through the process of calibration. The exterior orientation parameters are usually determined together with three dimensional coordinates of the object space points.

This research deals with analytical photogrammetric problem of determining the interior orientation parameters through different approaches for different focal lengths.

II. PROBLEM STATEMENT

The main objective of any analytical photogrammetric project is the reconstruction of the 3D model of the photographed object through the central projection theory represented by the collinearity condition or the coplanarity equation.

The parameters involved in the collinearity condition can be divided into three parts:

Part I: the interior orientation parameters IOP, represented by eight parameters, the principle distance c, the photo coordinates of the principle point xo,yo , radial lens distortion coefficients ko,k1,k2, and the tangential lens distortion coefficients p1,p2.

Part II: the Exterior orientation parameters EOP, represented by six parameters, the orientation angles ω, φ, κ and the ground coordinates of the perspective center X_o, Y_o, Z_o.

Part III: the 3D (X,Y,Z) ground coordinates of the object points.

Part II and part III parameters are determined through the application (use) of one of the analytical data processing approaches; sequential, bundle (simultaneous) or the relative absolute orientation.

Part I parameters are determined through the calibration of the camera; pre (lab)- calibration, on job calibration and the self calibration.

Metric cameras are mostly calibrated through the use of the pre (lab) calibration approach, simply because the IOP of the metric cameras are stable and used for infinity one focusing.

Non – metric "digital" cameras are calibrated through the use of on job calibration or the self calibration.

Several analytical approaches were developed for the calibration of non-metric digital cameras based on designing a specific target forms as shown in figure (1).

For the calibration of the camera, a number of photographs were taken to the target form from different camera stations with different orientation.

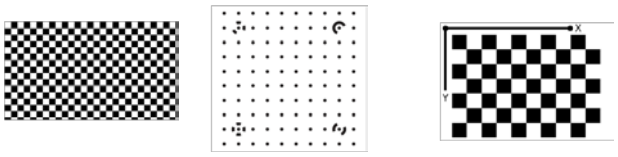

a- Lens calibration pattern

b- PhotoModeler

c- Matlab Checheboard

Fig. 1. calibration target

III. MATHEMATICAL MODELING

The colinearity equation consist of three set of parameters; IOP,EOP, and the 3D ground (X,Y,Z) coordinates of the photographed points.

The IOP includes:

The photo coordinates of the perspective center (xo,yo,c)

Radial and tangential Lens distortion coefficients (ko,k1,k2,p1,p2), which are generally termed "additional parameters" ($\delta x, \delta y$)

$$(x - x_o) + \delta x = -c\left[\frac{m_{11}(X - X_L) + m_{12}(Y - Y_L) + m_{13}(Z - Z_L)}{m_{31}(X - X_L) + m_{32}(Y - Y_L) + m_{33}(Z - Z_L)}\right]$$

$$(y - y_o) + \delta y = -c\left[\frac{m_{21}(X - X_L) + m_{22}(Y - Y_L) + m_{23}(Z - Z_L)}{m_{31}(X - X_L) + m_{32}(Y - Y_L) + m_{33}(Z - Z_L)}\right]$$

Where :

$$\delta x = x'(k_o + k_1 r^2 + k_2 r^4 + ...) + p_1(r^2 + 2x'^2) + 2p_2 x' y'$$

$$\delta y = y'(k_o + k_1 r^2 + k_2 r^4 + ...) + 2p_1 x' y' + p_2(r^2 + 2y'^2)$$

IV. CALIBRATION OF CAMERA WITH ZOOM LENS.

Most of close range photogrammetry projects requires large scale photographing, consequently the camera principle distance must be increased as the, photographing distance increased, furthermore higher precision required smaller object pixel size which can be obtained with higher principle distance.

In other words in close range photogrammetry its more practical (required) to use a camera having a variable (changeable) principle distance (zoom lens) varying from a small principle distance (such as 18mm) to cover most of the close range photogrammetric projects to a large principle distance (such as 200 mm).

For which it can be stated that there is no permanent calibration for zoom lens camera and the IOP must be the camera "lens" focusing to the photographed object.

Furthermore a single lens camera with a certain focal length can be calibrated using one of the approaches with the target form shown in figure (1).

However in this case a photograph must be taken to the required object "construction" from a minimum of two camera station without changing the "calibration" focusing at all, which the blurring of the image will increased as the as the different.

V. CASE STUDY

Non-metric digital camera with zoom lens (18-200) mm where use to perform the calibration with the different approaches stated above for different focal lengths.

For two cases:

A. *Case1: IOP = (xo,yo,c) only*

Target form:

For this case the grid form (a) was used to take different set of photo graphs with different focal lengths, the result were given in table (1).

Field control points

For this case a portable control system consist of (24) 3D control points were used to take different set of photo graphs with different focal lengths, the result were given in table (2).

TABLE I
TARGET FORM

Focal length	f(x)	f(y)	c(x)	c(y)
18	3642.19	3677.06	2410.77	1561.59
24	4710.33	4725.47	2410.28	1583.25
50	10710.5	10707.4	2481.07	1578.60
80	16103.8	16083.5	2563.67	1648.49
135	25112.3	25114.4	2964.36	1670.81
170	29240.6	29210.1	2980.44	1742.92

B. *Case I: IOP = (xo,yo,c) with the additional parameters*

TABLE 2
FIELD CONTROL POINTS

Focal length	Calibrated focal length	c(x)	c(y)
18	18.3897	11.6839	7.5495
24	24.5161	12.4062	7.3646
50	49.8412	11.9416	7.6278
80	70.2617	15.8103	6.6050
135	123.9596	11.6036	7.4906
170	141.1354	11.9539	7.4060

(ko,k1,k2,p1,p2).

Target form:

For this case the grid form (1) were used to take different set of photo graphs with different focal lengths, the result were given in table (3).

Furthermore the radial lens distortion curves as well as the tangential lens distortion curves for each focal length are shown in figure (2).

TABLE 3
TARGET FORM

Focal length	f(x)	f(y)	c(x)	c(y)	ko	k1	k2	p1	p2
18	3856	3855	2415	1554	-0.208	0.153	-0.041	-0.001	-0.000
24	4847	4848	2415	1534	-0.155	0.274	-0.158	-0.003	-0.000
50	10524	10533	2430	1446	0.168	1.75	-14.78	-0.010	-0.00
80	15833	15858	2435	1277	0.634	-2.09	42.74	-0.023	-0.00
135	24779	24821	2273	1194	1.398	-6.69	198.3	-0.033	-0.016
170	28906	2894	2281	1057	1.82	-13.1	-1.667	-0.04	-0.015

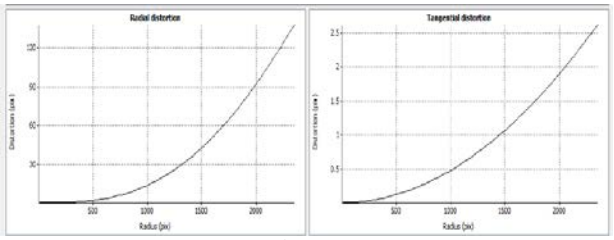
a- 18 focal length

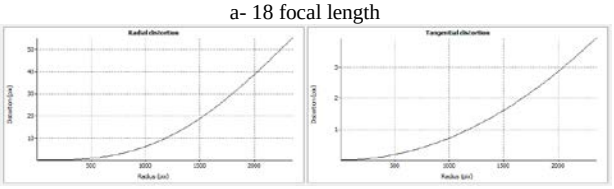
b- 24 focal length

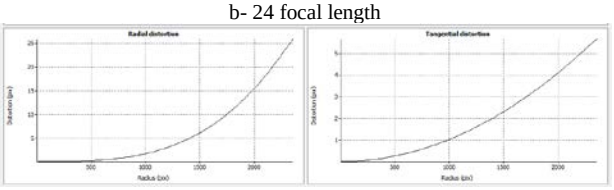
c- 50 focal length

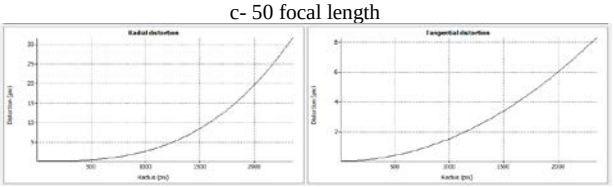
d- 80 focal length

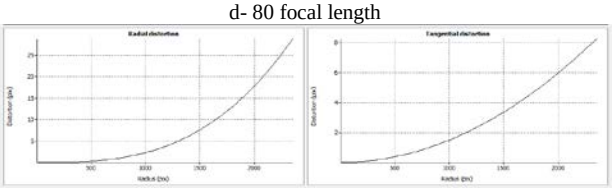
e- 135 focal length

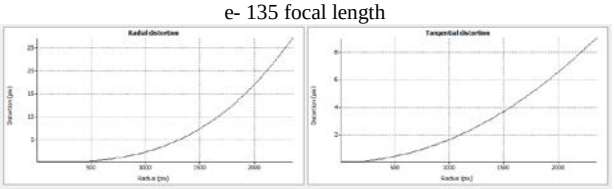
f- 170 focal length

Fig. 2. Radial lens distortion curves as well as the tangential lens distortion curves for each focal length

Field control points

For this case a portable control system consist of (24) 3D control points were used to take different set of photo graphs with different focal lengths, the result were given in table (4).

TABLE 4
FIELD CONTROL POINTS

Focal length	Calib. F.l.	c(x)	c(y)	ko	k1	k2	p1	p2
18	18.55	11.69	7.5620	-2.15	1.004	-1.074	-3.871	-5.030
24	24.69	12.40	7.3715	-1.382	5.10	-4.730	-6.573	4.553
50	49.84	11.94	7.6278	2.56	-4.304	2.104	1.923	2.252
80	70.30	15.81	6.6073	2.770	-1.549	3.970	5.906	2.546
135	123.99	11.60	7.4967	-6.586	8.604	-3.344	2.488	2.021
170	141.17	12.14	7.3704	-1.016	1.216	-4.316	2.674	3.033

VI. CONCLUSION

From this research the following conclusions can be drawn:

1- The principle distance for case I of the case study having a value differ significantly from that of case II.

2- With reference to fig. (2) its found the radial lens distortion curve and tangential lens distortion curve having similar forms, from which can be concluded that the radial and tangential lens distortion can be represented by 1 mathematical equation.

3- Comparing the result we found that there is a high correlation between the principle distance and the additional parameters (lens distortion coefficient.

4- The calibration with the target forms can be applied for the cases at which the object distance is closed to that of the calibration distance.

Real time calibration with very well distributed control points on the field can be recommended for any photographing case regardless the focal length.

REFERENCES

[1] *Sanjib, K. G.*: Fundamentals of computational photogrammctry, Ashok Kumar Mittal, New Delhi, 2005.

[2] *Farah, S.*: Accuracy Assessment Of Data Processing In Analytical Digital Photogrammetry Using Relative & Absolute Orientation Mathmatical Model. M.sC Thesis, University of Technology, 2015.

[3] *Mourtadha, S.*: Positioning by Analytical Photogrammetry with unknown camera parameters. M.sC Thesis, University of Baghdad, 2004.

[4] *Sanjib, K. G.*: Fundamentals of computational pbotogrammctry, Ashok Kumar Mittal, New Delhi, 2005.

[5] *Sanjib, K. G.*, Analytical Photogrammetry, Pergamon Press, New York, 1979.

[6] *Moffitt, F.H. and Mikhail, E.M.*, Photogrammetry, 3rd edition, Harper and Row Publishers, New York, 1980.

[7] *Wolf, P.R.*, Elements of Photogrammetry, 2nd edition, McGraw-Hill International Book Company, 1983.

[8] *Wolf, R. P., Dewitt, A. B. And Wilkinson, E. B.* Elements of Photogrammetry. 3rd edition, McGraw- Hill, New York, 2000.

Abbas Zedan Khalaf, Assistant Prof at Building and Construction Engineering Department, University of Technology. Ph.D. Civil Engineering (Photogrammetry), Civil Engineering Department, University of Washington, USA. Specialization: Application of Photogrammetry, Surveying Engineering, Digital Image Processing, Graduation Date: 1984. M.Sc. Civil Engineering (Photogrammetry), Civil Engineering Department, University of Washington, USA. Specialization: Application of Photogrammetry, Surveying Engineering, Digital Image Processing, Graduation Date: 1980. B.Sc. Civil Engineering, , University of Basrah, Iraq. Specialization: Building and Construction Engineering, Graduation Date: 1976. Research Interests, Digital Image Processing, Photogrammetry.
E-mail address: khalaf1955@yahoo.com

Israa H. Mohammed, Assistant Lecturer at Building and Construction Engineering Department, University of Technology. M.Sc. In Geomatic Engineering, Building and Construction Engineering Department, University of Technology, Iraq. Specialization: Application of Geomatics Engineering, Environmental Remote Sensing, Digital Image Processing, Graduation Date: 2012. B.Sc. In Building and Construction Engineering Management, Building and Construction Engineering Department, University of Technology, Iraq. Specialization: Building and Construction Engineering, Graduation Date: 2002. Research Interests, Environmental Remote Sensing, Digital Image Processing, Photogrammetry.
E-mail address: israa_hatem@yahoo.com

Tariq N. Otaiwi, Lecturer at Building and Construction Engineering Department, University of Technology. M.Sc. In Remote Sensing Engineering, Building and Construction Engineering Department, University of Technology, Iraq. Specialization: Application of Geomatics Engineering, Remote Sensing, Digital Image Processing, GPS Graduation Date: 2008. B.Sc. In Surveying Engineering, Technical College , Iraq. Specialization: Surveying Engineering, Graduation Date: 2001. Research Interests, Remote Sensing, Digital Image Processing, Photogrammetry.
E-mail address: tariqnaji@yahoo.com

Evaluation of Tigris river pollution using GIS techniques

Dr.Athraa H. Al-Habesh, Dr.Nawar O.A. Al-Musawi

Civil Engineering Department, University of Baghdad, Baghdad, Iraq

***Abstract*-Tigris river nowadays suffering from pollution because of heavy population and increasing water demands in the region. Also, there are many sources of pollution discharge their wastes into the river from both sides, like industrial waste water, sewage waste water and hazardous waste water. The heavy pollution and the deterioration of water quality are becoming big threats to Iraq. Therefore, the Iraqis are facing a serious problem, which is Tigris river pollution which has bad effects on increasing the possibility of diseases breakout and lack of suitable water for drinking and other uses.**

This research included evaluation of Tigris River pollution using GIS techniques, through collecting the data of ten pollutants parameters which are pH, Biochemical Oxygen Demand, Chemical Oxygen Demand, Sulfate, Phosphate, Nitrate, Total Dissolved Solids. Total Suspended Solids, Chlorides, and Oil, from eleven stations along Tigris River for the year 2013. The results are compared with the maximum permissible limits of Iraqi Specifications. The results indicated that most of these parameters are above the maximum permissible limits except pH , Nitrate, Chlorides and Oil where they are within the permissible limits of Iraqi Specifications, But the minimum values for most of the above parameters were at South Electrical Power Plant, because there is waste water treatment unit also their wastes are considered as thermal pollutants.

Key Words: Tigris River, GIS, Pollution, Iraqi Specifications

INTRODUCTION:

Tigris river nowadays suffering from pollution because of heavy population and increasing water demands in the region, also there are many sources of pollution discharge their wastes in to the river from both sides like sewage waste water, industrial waste water, and hazardous waste water, The heavy pollution and the deterioration of water quality are becoming serious threats to Iraq, therefore, the Iraqis facing a big problem, which is Tigris river pollution.

Pollution means increasing of elements concentrations than their natural back ground, this pollution of water causes many negative effects like increasing water salinity which is affecting the agricultural lands and decreasing crops that cannot survive in saline waters and the developed irrigation systems cannot be used, also the saline water cause the migration of fishes which are already live in fresh water. (1)

The few amounts of water reaching the southern part of Iraq affects the restoration of the marshlands due to Pollution and low chances for dilution (2)

Most fresh water pollution is caused by the addition of organic matter which is mainly sewage and can be food waste or farm effluent. Bacteria and other micro organisms feed on organic matter and large populations develop using much of the oxygen dissolved in the water. Normally oxygen is present in high quantities but even a small drop in the oxygen level can have a harmful effect on the river animals.(3)

During recent years there has been increasing awareness and concern about water pollution all over the world, and new approaches towards achieving sustainable exploitation of water resources have been developed. It is widely agreed that a properly developed policy framework is a key element in the sound management of water resources. A number of possible elements for such policies have been identified. (4). In this research we use the GIS technique in order to visualize the Tigris river pollution.-

Geographic information system (GIS):

Geographic information system (GIS) integrates hardware, software, and data for capturing, managing, analyzing, and displaying all forms of geographically referenced information.

GIS allows engineers to view, understand, question, interpret, and visualize data in many ways that reveal relationships, patterns, and trends in the form of maps, globes, reports, and

charts. Also GIS helps the engineers to answer questions and solve problems by looking at data in a way that is quickly understood and easily shared.GIS technology can be integrated into any enterprise information system framework, (5)

A GIS stores information about the world as a collection of thematic layers that can be linked together by geography. This simple but extremely powerful and versatile concept has proven invaluable for solving many real-world problems from tracking delivery vehicles, recording details of planning applications, to modeling global atmospheric circulation.(6)

The working of a GIS can be summarized as:

1. The Database View.

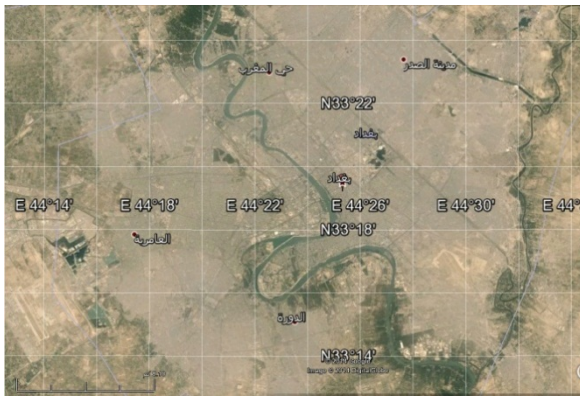

Figure 1 Geographic database

2. The Map View.

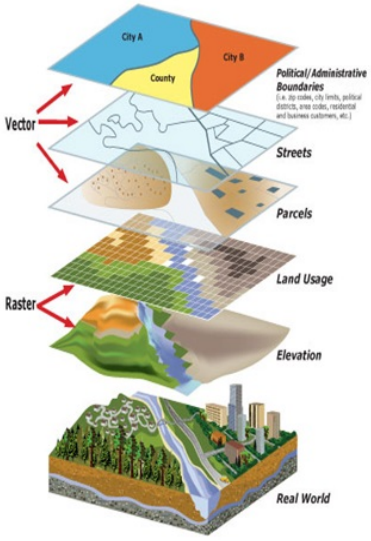

Figure 2 maps and layers

3. The Model View.

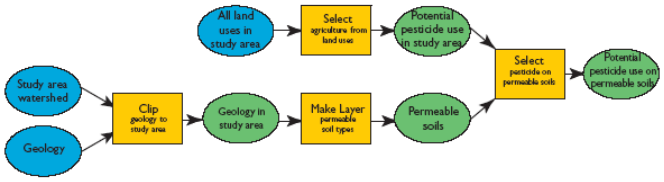

Figure 3 The reprocessing functions

METHODOLOGY:

In order to evaluate Tigris River pollution using GIS techniques, ten different pollutants parameters are selected during the year 2013 to be presented by GIS which are: pH, Biochemical Oxygen Demand(BOD), Chemical Oxygen Demand(COD), Sulfate(So_4)., Phosphate(PO_4), Nitrate(NO_3), Total Dissolved Solids(TDS). Total Suspended Solids(TSS), Chlorides(Cl), and Oil, from eleven stations along Tigris River from north to south, which are: Al-Saifia Pump Station , T1 Pump Station , Suspension Bridge Rain Station, PN Pump Station, , Al-Dora power Plant, Ali Baba Rain Station, South Electric Power Plant ,Dora Refinery, Al-Karkh Sewage Treatment Plant, North Rustmya Sewage Treatment Plant, South Rustmya Sewage Treatment Plant , the results are compared with the maximum permissible limits of Iraqi Specifications for the selected parameters as shown in table 1.

Table 1 The Maximum Permissible Limits according to Iraqi Specifications.(7)

Parameter	Maximum Permissible Limit(ppm)
Oil	10
Cl	600
TSS	60
TDS	1500
NO_3	50
PO_4	0.3
SO_4	400
COD	100
BOD	40
PH	9.5

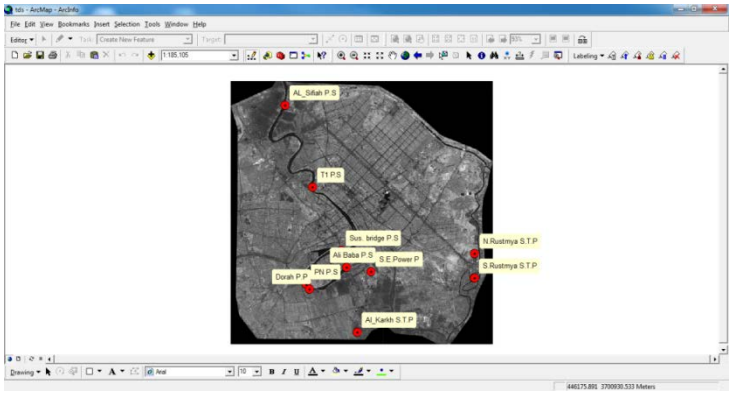

Figure 4 the selected station along Tigris River

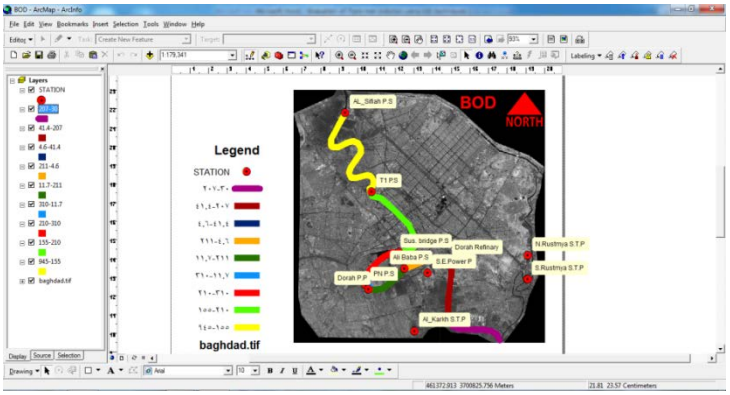

Figure 6 the variation of BOD concentration along Tigris River

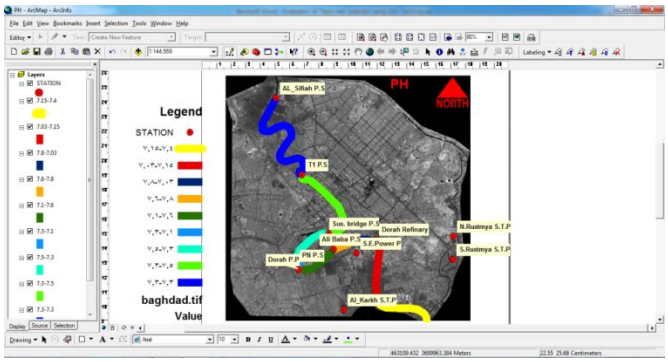

Figure 5 the variation of pH concentration along Tigris River

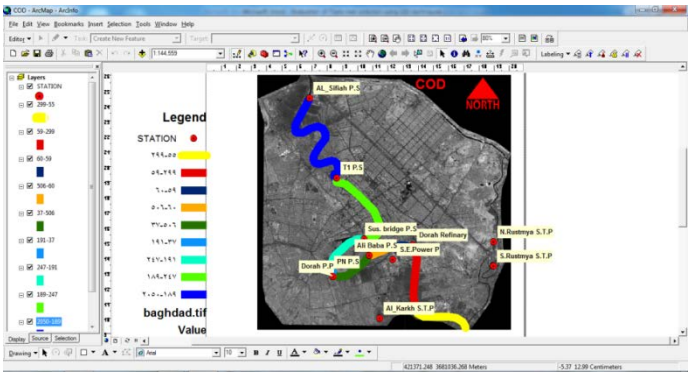

Figure7 the variation of COD concentration along Tigris River

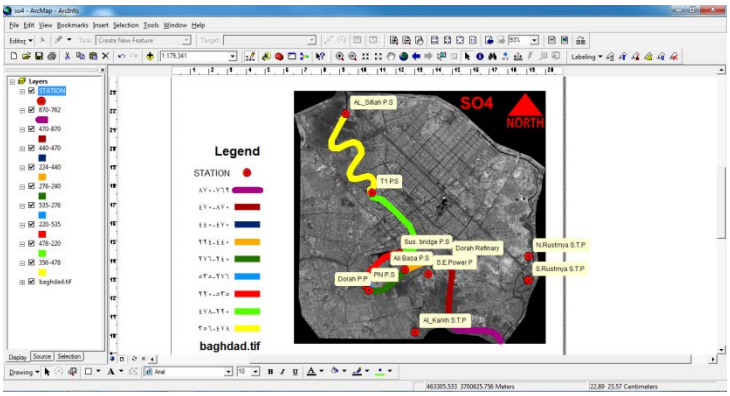

Figure8 the variation of So4 concentration along Tigris River

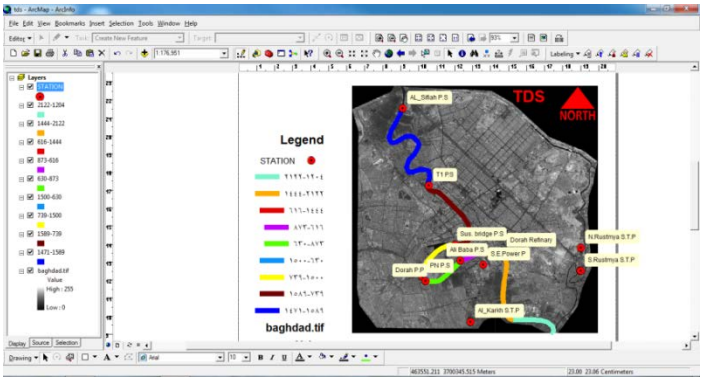

Figure 10 the variation of TDS concentration along Tigris River

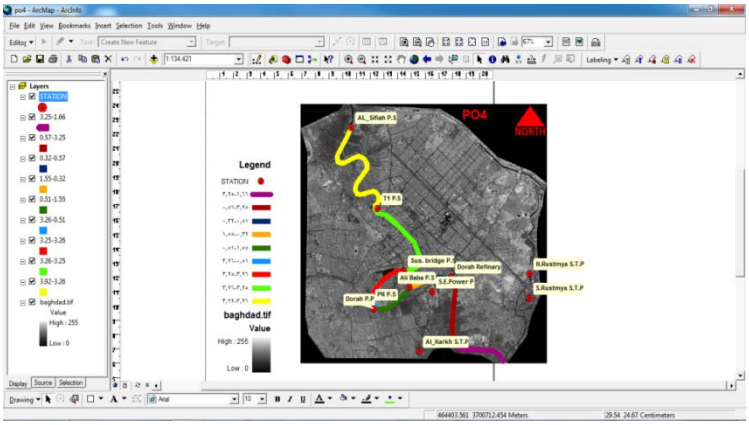

Figure 9 the variation of Po4 concentration along Tigris River

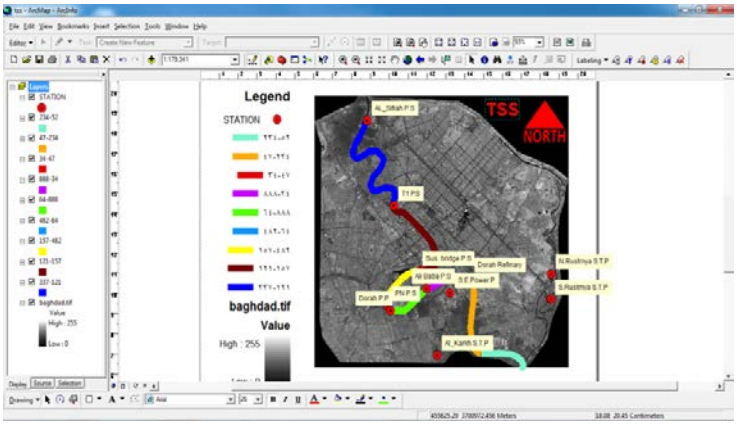

Figure 11 the variation of TSS concentration along Tigris River

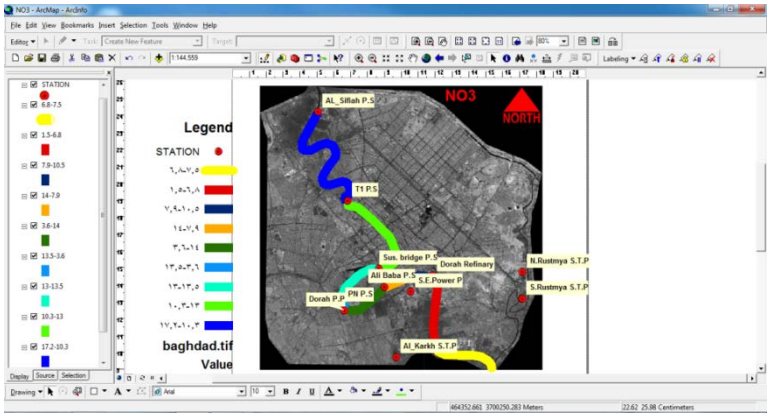

Figure 12 the variation of NO_3 concentration along Tigris River

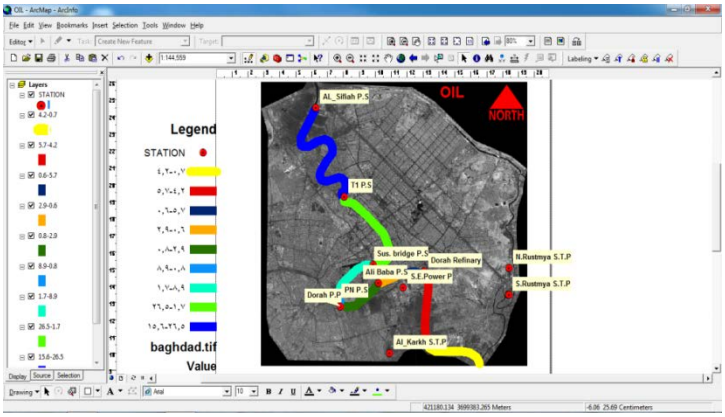

Figure 14 the variation of Oil concentration along Tigris River

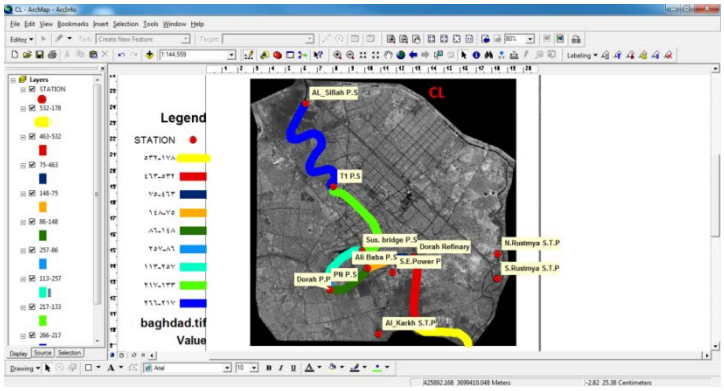

Figure 13 the variation of CL concentration along Tigris River

Discussion:

For the parameters BOD, COD, and PO_4 that are shown in figures 6,7, and 9 respectively. Their concentrations were reached the maximum values at Al-Saifiah Pump Station at the north of BaghdadAl –Karkh Waste Water Treatment Plant has the maximum values in both So_4 and TDS parameters that shown in figures 8,11 respectively that is due to the waste water that is discharged to Tigris river from both sides which are untreated or improperly treated causing the deterioration of Tigris river water quality. while the maximum value for the TSS parameter that shown in the figure 12 were at Ali Baba Rain Station in the middle of Baghdad. But, the minimum values for most of the above parameters were at South Electrical Power Plant, because there is waste water treatment unit also their wastes are considered as thermal pollutants. The waste water that are discharged from both North Rustmiya and South Rustmiya waste water treatment plants are discharged to DiyalaRiver in the south of Baghdad then DiyalaRiver discharged its water to Tigris River as shown in figure 4.Therefore, their effects are less than the other direct inputs. From GIS presentation the PO_4 concentrations were with high value north of Baghdad and decreases south of Baghdad as shown in the figure 9, it may consider that the PO_4 parameter as nutrients for water plants.Therefore, it isconsumed along the river flow. While the parameters Ph, NO_3, Cl, Oil parameters have been indicated by their low concentrations and less than the maximum permissible limits of of Iraqi Specifications as

shown in figures 5 10,13,14. From the GIS presentation it's clear that most of the pollutants parameters under study were exceeded the maximum permissible limits of Iraqi Specification that is applying by the Department to protect and improve the Environment in the Central Region, Ministry of Environment in Iraq

Conclusions and Recommendations:

The present results are considered as a threat to Baghdad City and the provinces south of Baghdad because of poor water quality that reached them, and that is why the river is unsuitable for drinking and other uses because of the high salinity and the poor dilution, also the difficulties in water treatment plants in the south region provinces. On the other hand the dangerous of diseases break down.

In order to improve Tigris River water quality, we recommend the plants on both sides of the river to develop their treatment procedures and be aware with the Iraqi Specifications in order to save the Iraqis life's from such catastrophe.

References:

1-Ofori,2004, Abigail Ofori-Amoahoforiaa@uwec.edu, Water Wars and International Conflict,Part of Water is Life, a class web site on water privatization and comodification, produced by students of Geography 378 (International Environmental Problems & Policy) at the University of Wisconsin-Eau Claire, USA, Spring 2004

2-UNEP,2005, www.unep.org/cpi/briefs/2005Aug24.doc

3-River Pollution,2008,Investigating River Pollution | Young ...vpte.org.uk/…heets/river-pollution/investigating...

4-WHO/UNEP ,1997, Water Pollution Control - A Guide to the Use of Water Quality Management, Principles, o Hespanhol
Published on behalf of the United Nations Environment Programme, the Water Supply & Sanitation Collaborative Council and the World Health Organization by E. & F. Spon
© 1997 WHO/UNEP ISBN 0 419 22910 8
5-ASCE, 1998," Basic of Geographic Information System", Journal of Computing in Civil Engineering, ASCE, January, pp 1-4.

6-ESRI,2011 "Geographical information systems as an integrating technology ,context ,concepts and definition", retrieved 9 June 2011

7-DPCR,2013, Department to protect and improve the Environment in the Central Region, Ministry of Environment, Republic of Iraq, 2013

Product Three Dimensional Model by Using Close Range Photogrammetry and Plane Surveying

Mr. Yousif Husain khalaf
Engineering College,University of Baghdad,Dep. surveying
yousif_husain@yahoo.com

***Abstrac*-In this study, a combination of close range photogrammetry techniques and plan surveying techniques are used to produce the three dimensional model, which is one of the important topics at the present time because it is used in many engineering applications, industrial, medical and other applications. The study area was in the University of Baghdad, specifically for the building of the university tower this research has been produced the three dimensional model of the tower depending on the overlapping ground images captured by digital camera and the distance between the exposure stations was 10 m and then the total stations device was used for measuring the coordinates of ground points distributed on the University of Baghdad Tower .The mathematical model used in this study is the direct linear transformation method to intensify ground points which are used to produce the three-dimensional model of the University Tower.**

Keywords: close range Photogrammetry-plan surveying -DLT-Matlab-RMSE

Introduction

Photogrammetry is a technology of measurement based on photographic images, which has long been used to map the surface of the earth usually from aircraft and recently from satellites Digital close range photogrammetry is a branch of photogrammetry which has been widely used for non-topographic applications in industrial and engineering areas with the digital technology and corresponding algorithms [1].

The term of close range photogrammetry is defined as the art , science and technology of extracting information of an object's geometry and position from photographic images . this information may be used to recreate an accurate representation of an object in three-dimensional space , alternatively it may be used to measure the change of an object position or shape [2].

This technique is used when an object to camera distance is not more than 300 meter as a maximum and a fraction of millimeters as a minimum . these limitations are assumed in order to distinguish between terrestrial , and close range photogrammetry [3].

The close range photogrammetry have a wide range of use and its applications are in many disciplines . such applications are different in terms of its importance some needs high measurement accuracy and other don't , the accuracy of these applications is a function of the elements of photogrammetric system . these elements are ,the camera used , the accuracy achieved by any camera is a function

of , the principal distance , the format size , the error of image points , and the resolution of image ,the layout of the two camera stations , the layout of the two camera stations relative to the object is a function of the external orientation parameters .These parameters determine the distribution , transformation , and magnification of the image error to the corresponding object points [4]. The techniques of three dimensional (3D) modeling have been advancing over the past few years. One of the main task of photogrammetry is to find the precise 3D coordinates of an object, this coordinates must be obtained from a stereopair images. Features in the image can be observed and 3D coordinates are determined in a given coordinates system, under a mathematical model Direct Linear Transformation (DLT).

Digital Close Range

Digital close-range Photogrammetry is a measurement technology which is used to acquire 3Dspatial information about an object that is captured on the images. By this means, this technology derives measurements from digital images, rather than measuring the object straight. Photogrammetry offers several advantages over the conventional and well-known land surveying methods. First, it is possible to map objects that are unreachable or too dangerous to reach on foot. Second, Photogrammetry provides a flexible framework in that all data needed to perform the mapping can be achieved almost immediately, enduringly and at a permanent cost with one photographic acquisition[5]. Mapping process can then be implemented at any time thereafter. Cost effectiveness may refer as a third advantage of Photogrammetry in contrast to conventional surveying or geodetic techniques. Finally, Photogrammetry provides several kinds of digital products such as maps, digital elevation models and ortho images. Due to this capability, digital close-range Photogrammetry is appropriate for a variety of applications, ranging from industry to archaeology, monitoring issues etc[6].

Mathematical Models

The used mathematical model is the (DLT) model which rely on the concept of direct transformation from comparator coordinates of image points to object space coordinates, thus by passing the intermediate step of transforming image coordinates from a comparator system to photo coordinates system.[7]. The concept is particularly useful for imaging with non-metric cameras which have no fiducial marks in the focal plane to define the axes of the photo coordinate system.[8]. The minimum number of points required to solve these equations using the least squares method are six points. Each point provides two equations one in *x* image coordinate and the other in *y* image coordinate. The standard (DLT) equations are:

$$x = \frac{L_1X + L_2Y + L_3Z + L_4}{L_9X + L_{10}Y + L_{11}Z + 1} \quad \text{……..(1)}$$

$$y = \frac{L_5X + L_6Y + L_7Z + L_8}{L_9X + L_{10}Y + L_{11}Z + 1} \quad \text{…….. (2)}$$

Where:

x, y: the measured coordinates of an image point.

X, Y, Z: the object space coordinates system.

L_1, L_2, …, L_{11}: the eleven transformation coefficients ((DLT) parameters).

The two equations (1) and (2) can be reduced to the following form:

$L_1X + L_2Y + L_3Z + L_4 - xL_9X - xL_{10}Y - xL_{11}Z = x$……(3)

$L_5X + L_6Y + L_7Z + L_8 - yL_9X - yL_{10}Y - yL_{11}Z = y$……..(4)

In matrix form

$$\begin{bmatrix} X_1 & Y_1 & Z_1 & 1 & 0 & 0 & 0 & 0 & -x_1X_1 & -x_1Y_1 & -x_1Z_1 \\ 0 & 0 & 0 & 0 & X_1 & Y_1 & Z_1 & 1 & -y_1X_1 & -y_1Y_1 & -y_1Z_1 \\ X_2 & Y_2 & Z_2 & 1 & 0 & 0 & 0 & 0 & -x_2X_2 & -x_2Y_2 & -x_2Z_2 \\ 0 & 0 & 0 & 0 & X_2 & Y_2 & Z_2 & 1 & -y_2X_2 & -y_2Y_2 & -y_2Z_2 \\ \vdots & & & & & & & & & & \\ X_n & Y_n & Z_n & 1 & 0 & 0 & 0 & 0 & -x_nX_n & -x_nX_n & -x_nZ_n \\ 0 & 0 & 0 & 0 & X_n & Y_n & Z_n & 1 & -y_nX_n & -y_nY_n & -y_nZ_n \end{bmatrix} \begin{bmatrix} L_1 \\ L_2 \\ L_3 \\ L_4 \\ L_5 \\ L_6 \\ L_7 \\ L_8 \\ L_9 \\ L_{10} \\ L_{11} \end{bmatrix} = \begin{bmatrix} x_1 \\ y_1 \\ x_2 \\ y_2 \\ \vdots \\ x_n \\ y_n \end{bmatrix} \quad \text{……(5)}$$

To obtain the (DLT) parameters using the least square method, we should consider solving the normal equation that can be derived from the observation, which can be expressed as [9].

B. X = f……(6)

Where

X: is the vector of (DLT) parameters.

The normal equation of previous observation equation can be written as follows:

$(B^tB)X = (B^tf)$… ……..(7)

By multiplying both sides of equation (7) by $(B^tB)^{-1}$ and reducing we obtain:

$X = (B^tB)^{-1} B^tf$……...……..(8)

After computing the DLT coefficients for all photos, the object space coordinate of any object point are computed. The formulas for computing object space coordinate from (DLT) coefficients is as follows [10]:

$(L_1 - xL_9)X + (L_2 - xL_{10})Y + (L_3 - xL_{11})Z = x - L_4$……..…(9)

$(L_5 - yL_9)X + (L_6 - yL_{10})Y + (L_7 - yL_{11})Z = y - L_8$ ……..……(10)

If the solution done by using Matrix (which mean measuring the ground coordinates for one point in two photos) the equations will be as the follow :-

$$\begin{bmatrix} L_1^{(1)} - xL_9^{(1)} & L_2^{(1)} - xL_{10}^{(1)} & L_3^{(1)} - xL_{11}^{(1)} \\ L_5^{(1)} - yL_9^{(1)} & L_6^{(1)} - yL_{10}^{(1)} & L_7^{(1)} - yL_{11}^{(1)} \\ L_1^{(2)} - xL_9^{(2)} & L_2^{(2)} - xL_{10}^{(2)} & L_3^{(2)} - xL_{11}^{(2)} \\ L_5^{(2)} - yL_9^{(2)} & L_6^{(2)} - yL_{10}^{(2)} & L_7^{(2)} - yL_{11}^{(2)} \end{bmatrix} \begin{bmatrix} X \\ Y \\ Z \end{bmatrix} = \begin{bmatrix} x^{(1)} - L_4^{(1)} \\ y^{(1)} - L_8^{(1)} \\ x^{(2)} - L_4^{(2)} \\ y^{(2)} - L_8^{(2)} \end{bmatrix} \quad \text{…….……(11)}$$

Experimental work:-

This research aims to compute the 3D coordinates the are used to produced three model according to the following steps

1. Selecting a base line with a length of 10 m.
2. Measuring the local 3D coordinates of 178 control points and check points on the University of Baghdad tower with the aid of Topcon total station ES 105.
3. Using Nikon D5200 camera to take a stereopair for the tower with overlap equal to 100% .
4. Measuring the digital photo coordinates to compute DLT parameters.
5. Using DLT program (MATLAB language) to intensify points, 250 points has been intensified points that are inaccessible .
6. The property of symmetric in the shape of Baghdad university tower has been used to compute the coordinates of the other side and then get 3D drawing of the tower.
7. The 3D design has been produced by using AutoCAD and QT Modeler programs .

The control points were precisely measured by using Topcon total station ES 105. A base line of ten meters has been chosen with two end stations A and B. The 3D coordinates of station A assumed locally to be (5000, 5000, 40) meter, then the total station has been mounted on A and back sight on B, the 3D coordinates of the control points have been measured directly by the total station.

The control points and check points have been distributed on the tower same of these points are shown in figure (1)

Figure 1. Stereopair of photos for the Baghdad University Tower

In order to establish the DLT, at least six control points are required. If more than six points be used, so that and improved solution can be arrived at by using least square. In this research 23 points are used to compute DLT parameter the measured ground coordinates of this points are listed in table (1).

Table 1. The measured object coordinates of the control points

Point	Northing	Easting	Elevation
Occ	500.0000	500.0000	40.0000
B.S	508.6860	499.9978	39.9550
63	538.4229	595.4597	35.1676
67	537.6394	595.1849	35.1799
68	537.3381	595.9473	35.1938
69	532.2048	593.0862	35.1875
73	531.4138	592.7802	35.1900
74	531.1309	593.6083	35.2160
75	524.2462	590.0477	35.1813
51	523.4825	589.7672	35.1773
52	523.1548	590.5008	35.1870
57	517.9772	587.6124	35.1812
58	517.1893	587.3590	35.1902
147	516.8882	58.1155	35.1881
175	515.8454	593.2299	35.1866
93	515.0512	592.9373	35.1752
117	514.7514	593.7130	35.1773
127	513.6983	598.8347	35.1839
131	512.9127	598.5543	35.1790
60	512.5939	599.2462	35.1811
72	511.5658	604.4550	35.1982
84	510.7608	604.1059	35.1823
96	510.4714	604.9048	35.1902
108	509.4389	610.0368	35.1944
163	508.6574	609.7711	35.1878

23control points distributed on the University of Baghdad tower are chosen for computing the (11 DLT) parameters . The photo coordinates were measured in the stereopair which is illustrated in figure (1). The results of image measurements have been listed in Table (2)

Table 2. The measured photo coordinates of the control points

Point No.	Left image		Right image	
	x_1 (mm)	y_1 (mm)	x_2 (mm)	y_2 (mm)
63	166	321.9	167.3	328.7
67	112.6	310.5	118.2	318.7
68	135.5	309.2	139.1	316.8
69	166.3	307.3	167.4	314.2
73	113.4	297.1	118.7	305.6
74	136.1	295.4	139.4	303.1
75	166.6	292.8	167.6	299.8

51	165.3	352.3	167.1	358.8
52	193.1	352.3	193.1	358.2
57	165.6	337	167.2	343.5
58	193.2	336.3	192.9	342.3
147	170.3	131.7	168.7	140.9
175	143.6	104.4	143.8	115.8
93	167.6	242.2	167.7	249.7
117	168.9	190.4	168.2	198.8
127	120.4	178.9	123.6	189.9
131	200.7	160.2	197.8	167.2
60	242.9	342.8	251.5	347.6
72	242.3	318.1	250.3	322.7
84	241.7	294	249.1	298.5
96	241	263.3	247.7	267.5
108	240.3	240.8	246.5	244.9
163	238.3	150.2	242.7	154.4

The DLT equations (1) and (2) were applied to compute the 11 DLT parameters and this process has been done by preparing a program in matlab language as in figure (2).

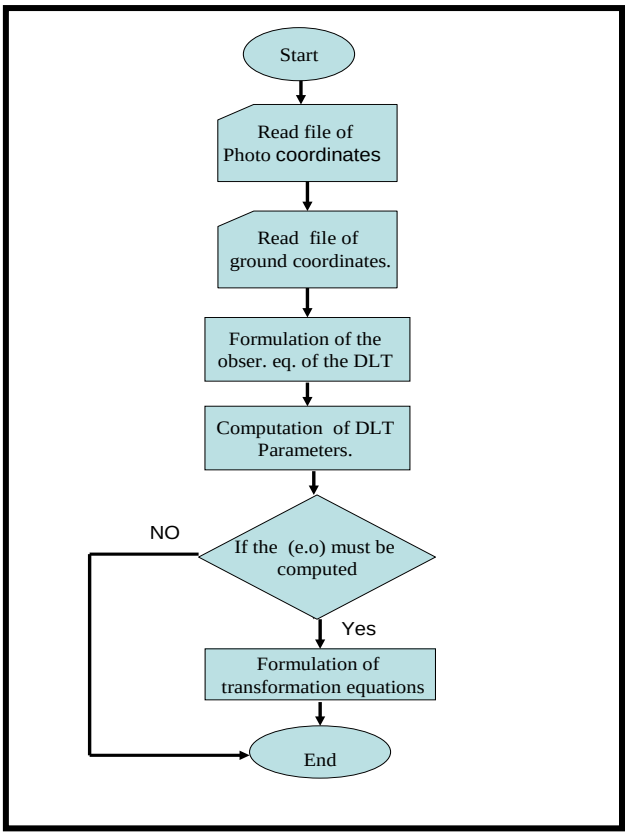

Figure 2. flow chart of the computation of DLT parameters

The results of the matlab program is listed in table(3).

Table 3. DLT parameters of the left and right photos

Par.	Left photo	Right photo
L_1	-0.40018	-0.43797

L_2	0.65625	0.58083
L_3	-0.09993	-0.08759
L_4	-129.80528	-67.63666
L_5	-0.61599	-0.57830
L_6	-0.08596	-0.14603
L_7	0.55700	0.51761
L_8	328.66370	341.26267
L_9	-0.00168	-0.00156
L_{10}	-0.00026	-0.00039
L_{11}	-0.00050	-0.00049

The three dimensional coordinates of any point appear in overlapped photos can be computed by using equation (11) after computing the 11 DLT parameters of and the photo coordinates in a stereopair.

23 check points were selected to validate the resulted accuracy of the 3D coordinates by determining the Root Mean Square Error (RMSE) which was found to be about RMSE = 2.2 cm as shown in Table (4).

Table 4. The coordinates of check points and their RMSE

Point No.	X (m)	Y (m)	Z (m)	Δ X (m)	ΔY (m)	Δ Z (m)
63	588.620	524.357	50.328	0.091	-0.027	0.025
67	594.238	538.601	53.646	-0.955	-0.050	-0.012
68	591.872	532.284	53.625	-0.119	0.032	0.009
69	588.683	524.374	53.585	0.034	-0.046	0.050
73	594.076	538.551	56.897	0.076	-0.010	0.025
74	591.701	532.551	56.883	0.055	0.070	0.034
75	588.955	524.431	56.934	-0.271	-0.104	-0.011
51	588.685	524.374	43.787	0.017	-0.040	-0.057
52	586.383	518.041	43.801	-0.075	0.040	-0.054
57	588.773	524.398	47.068	-0.068	0.055	-0.017
58	586.252	518.017	47.079	0.055	0.069	-0.021
147	588.786	524.365	98.723	-0.031	-0.037	-0.073
175	591.989	532.573	110.016	-0.075	0.082	0.026
93	588.712	524.414	68.945	0.011	-0.066	0.007
117	588.721	524.378	82.232	0.016	-0.038	-0.068
127	594.206	538.624	88.837	-0.039	-0.101	-0.074
131	586.688	516.367	88.870	-0.056	-0.022	-0.108
60	610.747	507.304	47.109	-0.163	-0.098	-0.062
72	610.634	507.259	53.611	-0.054	-0.044	0.0005
84	610.458	507.219	60.145	0.101	-0.001	0.050
96	610.464	507.143	68.858	0.090	0.055	0.071
108	610.505	507.138	75.5002	0.053	0.055	0.038
163	610.410	506.855	105.077	-0.035	0.033	-0.064
R.M.S.E				**0.025±**	**±0.024**	**±0.019**
Total R.M.S.E				**±0.022**		

After applying the DLT equations , the 3D coordinates of the intensified points were computed and then these coordinates could be used to product the 3D model of the Baghdad University tower this model is produced in this research by using two programs Auto CAD and QT modeler this drawing could be illustrated in figure (3).

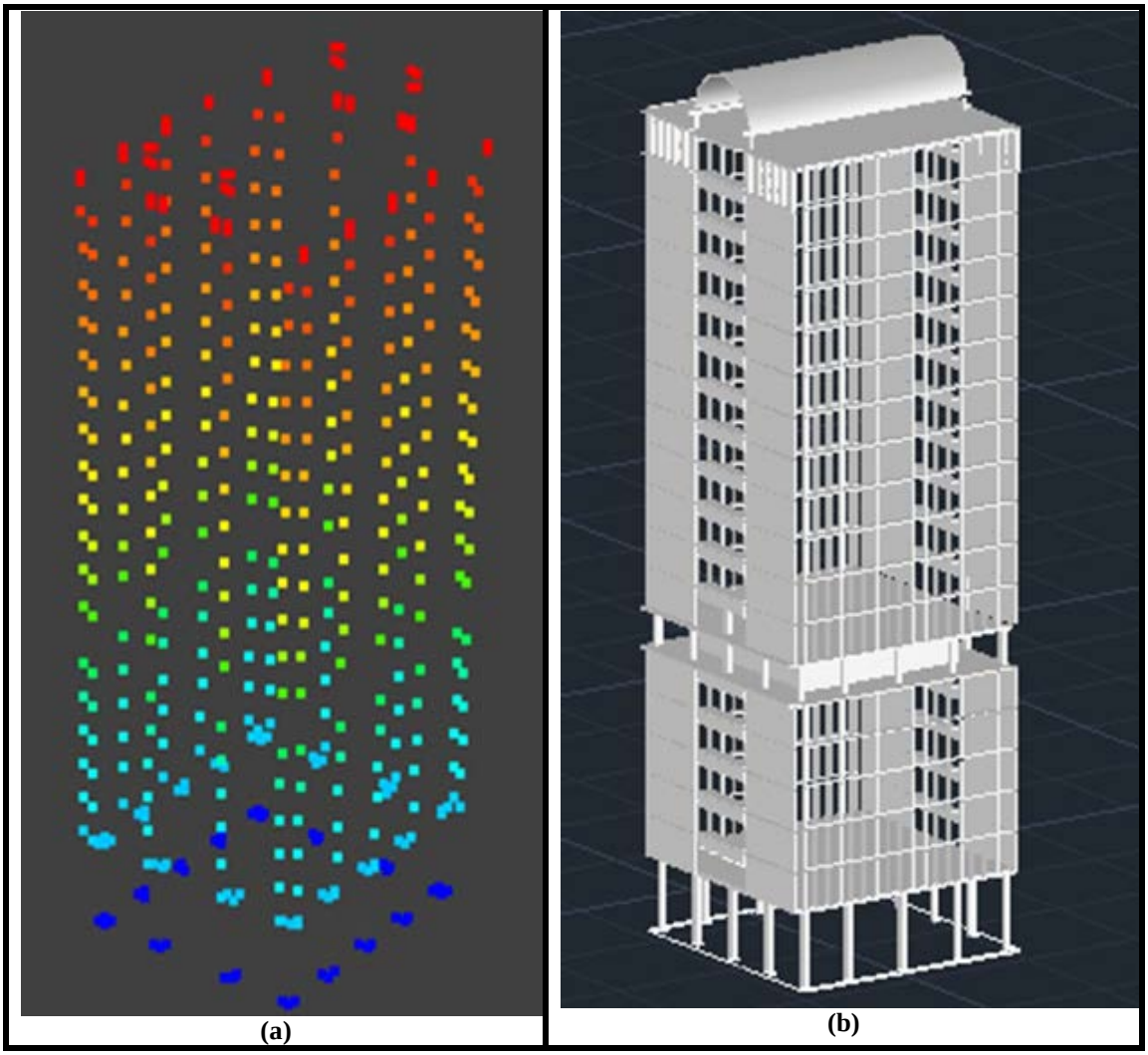

(a) (b)

Figure3. (a) 3D model for the University tower by using (QT Modeler) (b) 3D Model by using (Auto CAD) .

Conclusion

From the results obtained by this research it is concluded that the presented technique of DLT gives a good accuracy which is suitable for many engineering application, like architectural engineering and industrial engineering. The DLT could be used to recreate the 3D model of an object which is one of the important applications in close range photogrammetry specially when the objects are inaccessible. The presented technique in this research can save time and efforts because of the use of DLT equation which was easier than the other mathematical model in programming, the use of laser total station (without reflector) and digital camera.

REFERENCES

1- Li, X., (1999). Photogrammetric Investigation into Low- Resolution Digital Camera Systems, Doctoral Thesis, University of New Brunswich, Canada, 1999.

2- Mikhail, E., M., Bethel, J. S, Glone, J. C, Wiley, J. and Inc, S. (2000). Introduction to Modern Photogrammetry

3- Parmehr E., G., and Azizi A., (2004). A Comparative Evaluation of the Potential of Close Range Photogrammetric Technique for the 3D Measurements of the Body of a Nissan Patrol Car, ISPRS-Helsinki.

4- Remondino, F., (2006). Image-Based Modeling or Object and Human Reconstruction, Doctoral Thesis , Aristoteles University, Thessaloniki, Greece, Zurich.

5- Wolf, R., and Dewitt A., (2000). Elements of Photogrammetry with Application in GIS, 3rd edition.

6- Wong, X., and Clarke T.A, (1998). Separate Adjustment of Close Rang Photogrammetric Measurements, city University, London.

7- Parmehr E., G., and Azizi A., (2004). *A Comparative Evaluation of the Potential of Close Range Photogrammetric Technique for the 3D Measurements of the Body of a Nissan Patrol Car*, ISPRS-Helsinki.

8- Satchet, M., S., (2004). *Positioning by Analytical Photogrammetry with Unknown Camera Parameters*, MSc. Thesis, College of Engineering, Baghdad University

9- Sharqi, M., M., (2002). *Accuracy Assessment of Digital & Analytical Close Range Photogrammetric Techniques*, MSc. Thesis, College of Engineering, Baghdad University.

10- Abulateef, N., A., (2009). Accuracy Evaluation of Digital Close Range Photogrammetry by Free Adjustment Method, MSc. Thesis, College of Engineering, Baghdad University.

Evolution the Transportation Mode from Private Cars to Publics by Logit Method: A case Study in Baghdad

Lecturer Ali Ahmed Mohammed, Dr Hasan Hamodi Joni

Abstract— **This paper is an attempt to understand people's behavior and modal choice and try to shift them to means of public transportation. A survey of mode choice between cars users in a neighborhood in Baghdad was conducted. This paper is highlighted two models to improve the travel time reduction and travel cost reduction. The sensitivity analysis result showed that the main some attraction that might converse private car users is travel cost and travel time which they would lead to less traffic jam on the roads contributing to less pollution and greater safety.**

***Index Terms*— Baghdad, Mode of Transport, Reduction, Sensitivity Analysis, Switch, Travel Time.**

I. Introduction

The history of the Iraqi transportation evolved with the development of the modern state. In 1920s, Iraq's transportation system, like many systems in the Middle East region, encompassed traditional kinds of transport. The inhabitants relied on horse coaches and boats for commuting inside and outside the cities. Ships were used for travelling abroad and fishing off the Basra coast [1].

Since 1950s, the transportation has been markedly improved by using modern machinery. A large part of the road mileage is paved. Private cars and public service became a common scene in urban centers. There also good road links with Jordan and Syria. Steamboats navigating Tigris and Euphrates, Iraqi main two rivers, stepped up the export and import of commodities. Railway locomotives carried both cargo and passengers across Iraqi cities. Although it ran in a limited scale, the country's transportation systems are, by the standards of the region, were reasonably high [2].

This paper is highlighted two models to improve the travel time reduction and travel cost reduction. The sensitivity analysis result showed that the main some attraction that might converse private car users is travel cost and travel time which they would lead to less traffic jam on the roads contributing to less pollution and greater safety .

Ali Ahmed Mohammed. Lecturer in Ministry of Higher Education and Scientific Research, Department, IRAQ phone: +964-771-3091730 (e-mail: aliahmed@rpd-mohesr.edu.iq).

Dr Hasan Hamodi Joni Assistant prof in civil and structural Engineering, Department of Building and Construction, University of Technology, IRAQ; e-mail: hassan_jony@yahoo.com).

Iraq allocated a large share of the development domestic budget to upgrade and extend road, rail, air and river transport simultaneously. Highways were erected linking Baghdad to Mosul via Kirkuk, and then south to Basra in order to promote regional integration and expedite the pace of industrial progress. Modern ships and air jet have been brought into service to connect the country with a wide range of countries over the globe and create a vital hub for commercial trade [2].

After recuperating from years of wars and violence, Iraq has embarked on an ambitious plan to rehabilitate and enhance the performance of the existing transport networks by fielding new hi-tech equipment and starting cooperation in a broad range of transportation fields It should be noted that the development of transportation corridors within and across Iraq creates additional prerequisites for maintaining security in the country. For Iraqi society modernization of the transportation infrastructure would mean new jobs, industrial growth and electrification of the country. The construction of railways and highways and pipelines will assist in establishing a transportation and industrial infrastructure in Iraq that will ultimately raise living standards by creating favorable conditions for the development of domestic business and for attracting investors [2].

II. Methodology

Data collection in this study was done by questionnaire that involved different attributes including travel cost, age, race, and number of members of households and level of education in order to illustrate their socioeconomic and demographic profiles. Moreover, travel time, travel cost, number of trips and the preferred mean of transportation were taken in the consideration [3]. A total of 50 questionnaires were distributed and collected throughout the process of data collection. The data was collected by personal interview with car users since they are the influential factor of this study.

SPSS Statistical package for the social sciences is an analytical system used to analyze the questionnaire. The procedure used for the variables assesses the number of commonly used measures providing information on the relationships between the individual items in the scale such as gender, nationality,

age, household size and mode of transportation and the walking ability [4].

A modal shift was performed in this study to illustrate the shift ability for car users to be conversed from private modes to publics. A model shift occurs when one mode (A) has a comparative advantage in a similar market over another (B) a modal shift will occur only if the new mode offers time improvements, while for others it is mostly a matter of costs. The outcome is a series of decision was made by firms (for freight) or individuals (for passengers) to shift to a more convenient mode if comparative advantages are significant enough [5].

III. MODEL STRUCTURE

The logit model was used a final model to investigate mode choice behavior of travelers of modes of transport and to determine the tradeoffs travelers make when considering their mode of transport[6],[7]and[8]. The proposed model that contained all was used to determine the dependent variables. The logistic functional form is commonly identified as a single-layer "perception" or single-layer artificial neural network. A single-layer neural network computes a continuous output instead of a step function. The derivative of pi with respect to X is computed from the general form [8] the proposed model used to determine the dependent variables is evaluated based on the following equation.

$$y = \frac{1}{1+ e^{-f(X)}} \tag{1}$$

Where f (X) is an analytic function in X. With this choice, the single-layer network is identical to the logistic regression model. This function has a continuous derivative, which allows it to be used in back-propagation. [9]

$$P = \frac{1}{1+D\,e^{\alpha(\mathrm{variable})}} \tag{2}$$

$$P(t,a,m,n,\tau) = a\frac{1+m\,e^{-t/\tau}}{1+n\,e^{-t/\tau}} \tag{3}$$

The special case of the logistic function with a = 1, m = 0, n = 1, τ = 1, namely

$$P(t) = \frac{1}{1+ e^{-t}} \tag{4}$$

For real parameters a, m, n, and τ. These functions find applications in a range of fields, including economics [10].

A logistic function or logistic curve is the most common sigmoid curve. It models the "S-shaped" curve (abbreviated S-curve) of growth of some set: P denotes a set. P will be used to denote a function which varies over time. Normally such a function is written P (t). However, such a function may also be read as a set of ordered pairs of the form <t, P (t)>. The initial stage of growth is approximately exponential; then, as saturation begins, the growth slows, and at maturity, growth stops [20]

$$P(t) = \frac{1}{1+e^{(-t)}} = \frac{1}{1+exp^{(-t)}} = (1+exp(-t))^{-1} \tag{5}$$

$$P` = p(1-p) \tag{6}$$

The function P has the intuitively appealing quality that

$$1-P(\mathrm{t}) = p(-t) \tag{7}$$

Pilot survey data obtained from question related to proportion of people board on minibus with respective to a series of proposed travel time reduction has been used to calibrate the logit model with variable = time factor [21].

$$P = \frac{1}{1+D\,e^{\alpha(\mathrm{var})}} \tag{8}$$

P(t) is the probability of success when the value of the predictor variable is t.

$$P = \frac{1}{1+D\,e^{\alpha(r)}} \tag{9}$$

Algebraic manipulation shows that

$$\frac{1-P}{P} = D\,e^{(\alpha\cdot r)} \tag{10}$$

$$\ln\left[\frac{1-P}{P}\right] = \ln D + \alpha^{(r)} \tag{11}$$

The above equation investigates the calibration process based on the values of D and α values which were extracted from ANOVA Table using Microsoft Excel. These results applied to the final equation shown below and then the results were used for model validation according to the following equation [9],[10] and you should write reference.

$$P = \frac{1}{1+D\,e^{\alpha(\mathrm{variable})}} \tag{12}$$

IV. RESEARCH METHODOLOGY

Many reasons are standing behind making the privet cars most popular mode of travel Such as; travel time, economic factors, reliability and being comfortable [10]. The most acceptable reason for why people prefer privet transport rather than other is car offer opportunities not available by any other means of transport. The previous studies showing us there is minimization in the cost and travel time for the privet cars users, so our challenge is to develop balanced model to reduce the gap between the privet means of transport and the other models. To get a complete transportation planning us should concern about the most prevalent of the road users and how to design convenient and safe ways according to the main factors that affecting the level of service of people; design, location and the users[10].

A. Research Design

Research strategy being used is quantitative in character. Basically, this research is based on the primary and secondary data. Following that, the study revolves around the existing Method being used in Baghdad, to gauge uses public transport facilities. After that, case study and analytical Model choice behavior and the shift from private to public transportation mode were analyzed using through data collection being interpreted using SPSS and logit model choice model that approach is mainly used on a local level. The survey information included socio-economic characteristics of individuals, trip information of individuals, and attitudes and perceptions on travel and policy measures [10]. Socio-economic information included household income, individual's income, age, gender, vehicle ownership, and total number of members in household, occupation and education level [10]. Trip information of individuals included the purpose of the trip, mode of travel, total travel time and travel cost ,Improving the Frequency ,Suitable Waiting Time at the Minibus Stops ,Distance for the Residential Located etc. A logic model was developed alternatives namely, bus, train and car, with the aim of comparing the utility of these travel modes and to identify the factors that would influence car users to move from travelling by car to choosing the public transport alternative [10]. The explanatory variables were: age, gender, income, and travel time, travel cost and car ownership.

In several counties surveys are carried out concerning the mobility behavior of the population. In such contexts the willingness to undertake a modal shift was rarely surveyed [11]. It is very likely that the train companies, national and public transport companies have such data for analysis, but the competitive aspects of the situation make it difficult to obtain these data [11]. The details of the road user's behavior that we got from the data collection and the procedure of the data analysis to establish the model the determinant variables that were used [11].

V.EXPERMENTAL RESULTS AND ANALYSIS

Results for questionnaire analysis by SPSS are indicated in table I which illustrate the response of the car users to shift from private cars to public modes by improving the travel cost. It is clear to observe the percent of car users how aimed to shift from private mode to public was increased from around 15 % to 100% when the travel cost is improved by 75%.

TABLE I
RESULTS FOR QUESTIONNAIRE ANALYSIS BY SPSS]

Improving travel cost	Frequency	Percent	Valid Percent	Cumulative Percent
15%	35	15.3	15.3	15.3
30%	43	18.6	18.6	33.9
45%	75	33.1	33.1	67
60%	40	17.3	17.3	84.3
75%	35	15.5	15.5	100
Total	40	100	100	

Relationship between reduction travel time and the share percentage is illustrated in Fig.1. It is demonstrated that the sharing percentage was directly proportional with reduction of travel time. Travel time consider one of the important factors in mode choice. According to our survey 54% of the participant discouraged to use public transport cause it takes long time. Figure I showed that time reduction for the current service by 30% percent will attract 36% of car users to use the service and time reduction by 60% percent will attract 76% of car users.

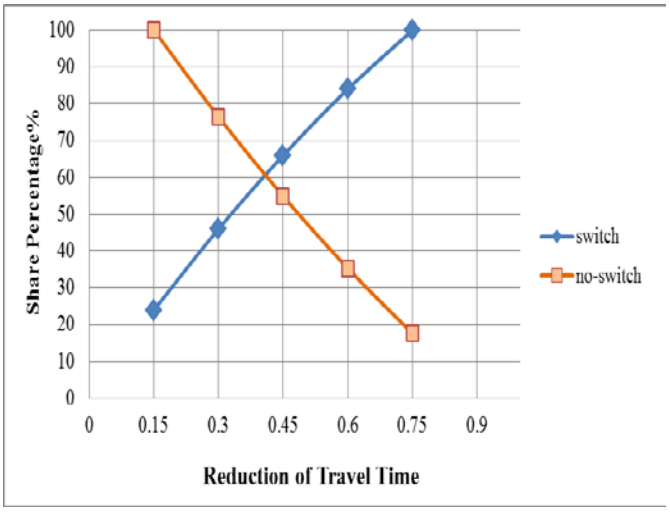

Figure. I: Relationship between sharing percentage and travel time reduction

Results for data calibration by regression statistics are given in table II and results for survey illustration is indicated in table III

TABLE .II
AN ILLUSTRATION SURVEY RESULTS AND DATA CALIBRATION

Improving Travel Cost	Survey results (P)	(1-P)/P	ln (1-P)/P
15%	0.22	3.2	1.1
30%	0.21	3.6	1.2
45%	0.19	4.1	1.4
60%	0.17	4.5	1.5
75%	0.15	5.3	1.6

TABLE .III
AN ILLUSTRATION SURVEY RESULTS AND LOGIT MODEL RESULT

Improving Travel Cost	Survey results (P)	Results from logit model
15%	0.22	3.2
30%	0.21	3.6
45%	0.19	4.1
60%	0.17	4.5
75%	0.15	5.3

Based on results indicated table II and table III which were used to model the survey results, it was found that survey results that were collected by Questionnaires and results were modeled by SPSS and the aforementioned equations were as approximated as it is shown in Figure II. Therefore, it is demonstrated that the reduction in travel time will be the key factor in shifting the people from private cars to public modes

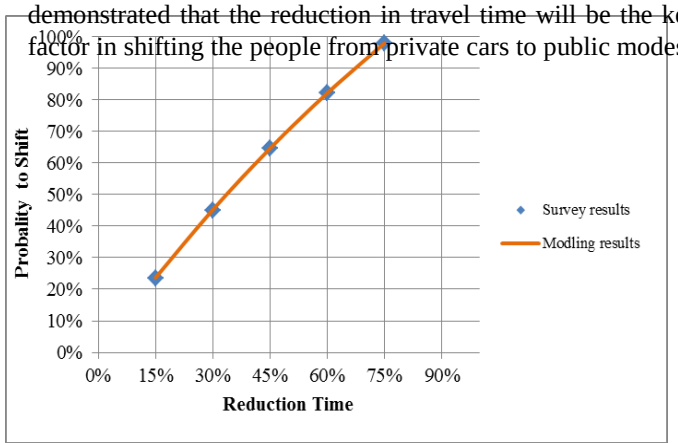

Figure. II: Relationship between reduction time and the probability shift

Relationship between reduction travel cost and the share percentage is illustrated in Figure. III it is it is demonstrated that the sharing percentage was directly proportional with reduction of travel cost. This may be attributed to the fact that money is an important issue. Improving the travel cost for the minibus by reduction the travel cost increase utilizations of the public transportation bus use 72% of the participants consider the public transport fares are affordable, that's mean we can convince them to use the public transport by developing cheaper service.

So when we reduce the travel coat by 30% percent we will increase the service users by 34.3% and if we reduce the travel cost by 60% percent we will increase the service users by 89%.

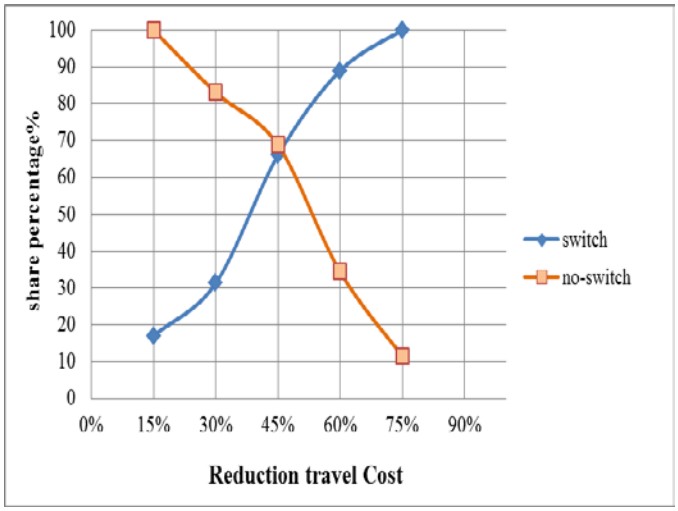

Figure.III: Relationship between sharing percentage and travel cost reduction

Questionnaires and results were modeled by SPSS and the aforementioned equations were as approximated as it is shown in Figure. IV. Therefore, it is demonstrated that the reduction in travel time will be the key factor in shifting the people from private cars to public modes

Figure. IV: Relationship between reduction time and the probability shift

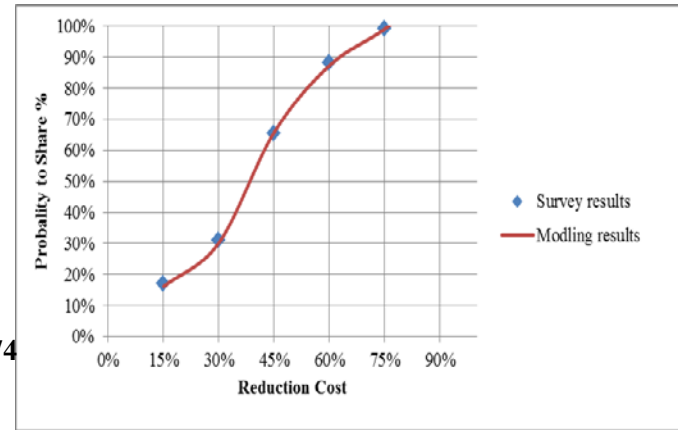

VI. CONCLUSION

TABLE .IV
AN ILLUSTRATION SURVEY RESULTS AND LOGIT MODEL RESULT

Changes in independent variable	Changes in dependent variable	Sensitivity Ratio
60% travel time reduction	21% model shift	0.35
60% travel cost reduction	18% model shift	0.3

Conclusions and future work can be drawn based on the investigation done in this study:

1. A private car shifting to public modes is highly influenced by the reduction of the travel cost.
2. The use of modern, air-conditioned buses and cheap for people of the most important means for switching to public
3. Sensitivity ratio between dependent and independent variables is (0.35-0.3) indicated low level of results.
4. Increase in petrol prices, which help to use public transport instead of private cars to create free of contaminants clean environment
5. One of future recommendation is improving the walking facility which may help to shift private modes to publics by providing pedestrians with comfortable facility protect them from rain and sun light. The pedestrians should be separated from the motorized mean of transport by using sign boards, crossing bridges and zebra lines to ensure the pedestrian safety. A good lighting system is needed to sway the darkness and protection and covered drains to ensure the protection from the wild animals.

ACKNOWLEDGMENT

I expressions Special thanks to Assist. Prof. Dr.Hasan Hamodi Joni for guidance in the research.

REFERENCES

[1] J.Garvill and A.Marell, "Effects of increased awareness on choice of travel mode", Transportation, 2003 pp. 63-79.

[2] S. Krygsman and D.M, "Multimodal trips in the Netherlands: Microlevel individual attributes and residential context", Transportation Research Record, 2001. Pp. 11-19.

[3] A. A.Mohammed, A Ahmed, "Conversion the Transportation Mode from Private Cars to Publics by Reduction the Travel Cost: A case Study in Kuala Lumpur". Proceedings National Graduate Conference 2012 (NatGrad2012), University Tenaga Nasional, Putrajaya Campus, 2012,8-10 Nov .

[4] A. A.Mohammed, A.Ahmed, "Curb parking in Campus and Stimulating Students to use Public Bus within Universiti Kebangsaan Malaysia (UKM) Campus" International Journal of Advances in Applied Sciences (IJAAS), September 2013, pp. 105~112.

[5] A.Mohammed, A.Ahmed, " factors that affect transport mode preference For graduate students in the national university Of Malaysia by logit method" Journal of Engineering Science and Technology, School of Engineering, Taylor's University,(2013, 351 – 363.

[6] A. Mohammed, Riza Atiq O.K.Rahmat, " An Optimization Solution for Utilization minibuses Service as an alternative of Utilize Private Cars: A Case Study around Hentian Kajang in Malaysia" , IOSR Journal of Engineering Apr. 2012, pp: 1032-1039.

[7] A. Hull," Policy integration: What will it take to achieve more sustainable transport solutions in cities?" School of the Built Environment, Heriot-Watt University. London, 2007, pp. 390-394.

[8] A. Mohammed and O. A. Alelweet, " An optimization solution by service science management and engineering (SSME) for using minibuses service as an alternative for private cars around Hentian Kajang in Malaysia, Journal of Civil Engineering and Construction Technology ,2012, pp. 25-41.

[9] A. Mohammed, "An Optimization Solution for Using Minibuses Service as an alternative of using Private Cars Around Hentian Kajang in Malaysia",master Dissertation,Dept .of civil .Eng., National University ., Malaysia, 2010.

[10] A.Mohammed, *An Optimization Solution for Using Minibuses Service in Malaysia.* Lambert Academic Publishing GmbH & Co. KG, Germany,2012,pp.7-88.

[11] N.Abdullah, and RAtiq, "Effect of transportation policies on modal shift from private car to public transport in Malaysia", Journal of applied Sciences,2007, pp.1013-1018.

Lecturer.Ali Ahmed Mohammed BSc. in Civil and Structural Engineering from University of Technology, IRAQ (1st Class Honours), hold M.Sc. in Civil and Structural Engineering, The National University of Malaysia (UKM) (Graduated with Honours) in transportation engineering .Currently He is Lecturer in Ministry of Higher Education and Scientific Research- Office Reconstruction and Projects Department, IRAQ. Became a Member (M) of IEEE in 2010, and Membership in Institution of Civil Engineers (ICE), England, London, Membership (M) of Board of Singapore international computer Science and information Technology (IACSIT), also Membership of Iraqi Engineers Union, Civil and Structural Engineering 2007 (IEU, Iraq), Membership in IAENG International Association Engineers,2010 USA .

He is a member in the American Association for Engineers; He had many papers published in various National and International Journals in USA, Canada, Malaysia, Indonesia, India, Iraq, Singapore, Germany and Australian. And published two books title is (An Optimization Solution for Using Minibuses Service in Malaysia) in "publisher in Lambert Academic Publishing GmbH & Co. KG, Germany, 2012"and title of book is (Development Of Bricks From Industrial Waste) publisher in Lambert Academic Publishing GmbH & Co. KG, Germany, 2013", One of my activities is to Review articles sent to me by various International journals and the articles that I reviewed are addressed accordingly.

Prospect Of Using RCA in Hot Mix Asphalt within Flexible Highway Pavement

Ali A. Alwash and Fatimah Fahem Al-Khafaji, Babylon University

***Abstract*—** Since the last decide, Iraq various economic and environmental campaign especially in the construction field , witnessed wide development industry to reduce costs and improve the quality of our environment . For achieving that both goals at the same time , this research focused on utilization of recycled concrete aggregate (RCA) in hot mix asphalt (HMA) for base layer .

RCA is aggregate resulting from the processing inorganic material previously used in construction and properly comprising crushed concrete . Also, concrete pavement can be broken in place and used either as base layer for HMA by process called rubblization , or as previously replacement of aggregate in HMA. But reinforcing steel and other embedded items , if any , must be removed and care must be taken to prevent contamination by other materials that can be trouble same.

The use of (RCA) in (HMA) is a sustainable construction proactive , provided that the addition of (RCA) does not adversely affect the (HMA) characteristics .

However, for this research Four percentages (0,10,20,30)% of free manually crushed concrete obtained from the control test specimen in the central laboratory , are used as replacer of virgin aggregate in HMA base coarse . The results confirm that the Marshall stiffness and indirect tensile strength as an indication for rutting and cracking problems respectively are largely perform well and agree with local specification with replacement rate reach to 30% of RCA .

Keywords : Recycled Concrete Aggregate , Hot Mix Asphalt , Marshall Stiffness , Indirect Tensile Strength .

Notation :

RCA : Recycled concrete aggregate .
RA : Recycled aggregate .
HMA : Hot Mix Asphalt .

I. INTRODUCTION

Recycled aggregate **(RA)** is highly recommended to be researched in a recent atmosphere in which the environmental protection rises as a matter of national concern.

It was estimated that some 80 million tons of demolition wastes arise from reconstruction in the European Economic Communities each year and in the United States ,it has been estimated that approximately 60 million tons of concrete are demolished each year.

Approximately 70% of it is recycled and reused in new construction work . These quantities would be double by the year 2000 and tripled by the year 2020 **.** Also ,in Iraq ; after the last war , a large amount of waste concrete is generated , resulting in a difficult environmental problem in acquiring disposal sites.

Concrete aggregate collected from demolition sites is put through a crushing machine. Crushing facilities accept only uncontaminated concrete, which must be free of trash, wood, paper and other such materials. Metals such as rebar are accepted, since they can be removed with magnets and other sorting devices and melted down for recycling elsewhere. The remaining aggregate chunks are sorted by size. Larger chunks may go through the crusher again. After crushing has taken place, other particulates are filtered out through a variety of methods including hand-picking and water flotation .

Crushing at the actual construction site using portable crushers reduces construction costs and the pollution generated when compared with transporting material to and from a quarry.

Smaller pieces of concrete are used as gravel for new construction projects. Sub-base gravel is laid down as the lowest layer in a road, with fresh concrete or asphalt poured over it .

With proper quality control at the crushing facility, well graded and aesthetically pleasing materials can be provided as a substitute for landscaping stone or mulch.

Wire gabions (cages), can be filled with crushed concrete and stacked together to provide economical retaining walls. Stacked gabions are also used to build privacy screen walls (in lieu of fencing) .

There are a variety of benefits in recycling concrete rather than dumping it or burying it in a landfill. Keeping concrete debris out of landfills saves landfill space. Using recycled material as gravel reduces the need for gravel mining. Using recycled concrete as the base material for roadways reduces the pollution involved in trucking material .

In general, applications without any processing include :

- Many types of general bulk fills
- Bank protection
- Base or fill for drainage structures
- Road construction
- Noise barriers and embankments

Most of the unprocessed crushed concrete aggregate is sold as 1½ inches or 2 inches fraction for pavementt Subbases .

After removal of contaminants through selective demolition, screening, and /or air separation and size reduction in a crusher to aggregate sizes, crushed concrete can be used as: new concrete for pavements, shoulders, median barriers, sidewalks, curbs and gutters, and bridge foundations structural grade concrete soil-cement pavement bases lean-concrete or concrete bases and bituminous concrete.

The crushing characteristics of hardened concrete are similar to those of natural rock and are not significantly affected by the grade or quality of the original concrete. Recycled concrete aggregates produced from all but the poorest quality original concrete can be expected to pass the same tests required of conventional aggregates .

Recycled concrete aggregates contain not only the original aggregates, but also hydrated cement paste. This paste reduces the specific gravity and increases the porosity compared to similar virgin aggregates. Higher porosity of RCA leads to a higher absorption.

Experimental Work

Materials :-

The materials provided in this research are widely used in asphalt paving works in middle and south of Iraq.

- Asphalt Cement :-

One type of asphalt cement is used with (40-50) penetration grad brought from AL-Daurah refinery. The physical properties and tests of the asphalt cement used are shown in table (1).

Table (1)Physical properties and tests of asphalt cement

Property	ASTM designation	Test result	SCRB specification
Penetration (25c,100gm,5sec),0.1mm	D-5	46	(40-50)
KINEMATIC viscosity at 135C ,(CST)	D-2170	385	-
DUCTILITY (25C,5CM/min).(cm)	D-113	109	>100
Flash point (Cleveland open cup),(^{o}c)	D-92	399	Min.232
Softening point (^{o}c)	D-36	54	-
Specific gravity at 25 ^{o}c	D-70	1.04	(1.01-1.05)

* These of tests were accomplished in the transportation engineering of civil department engineering in the Babylon University and laboratory of AL of Daurah refinery south-west of Baghdad.

- **Aggregate**

The coarse aggregate used in this study is crushed aggregate from Al- Najaf quarry. This aggregate is widely used in the middle and south areas of Iraq for asphalt pavement The particles tend to off white in color with angular surfaces. The fine aggregate obtained from Karbala quarry. The coarse and fine aggregates used in this work are sieved and recombined in the proper proportions to meet the base course gradation as required by SCRB specification.

Routine tests are performed on the aggregate to evaluate their physical properties. The results together with the specification limits as set by the SCRB are summarized in table (2). The specification gradation with specification limits are presented in table (3).

Table(2)Physical properties of aggregate

PROPERTY	ASTM DESIGNATION	COARSE AGGREGATE	FINE AGGREGATE	SCRB APECIFICATION
BULK specific gravity	C-127 C-1	2.54	2.66	-
Apparent specific gravity	C-127 C-128	2.67	2.68	-
absorption% water	C-127 C-128	0.86	0.63	-
Abrasion (lose angles)	C-131	25%	-	MAX 30%
Fractured pieces %	D-5821	96%	-	MIN 95%

* These tests were accomplished in the transportation and material laboratories of civil engineering in the Babylon University.

Table (3) Gradation of used aggregate

Standard Sieves size (mm)	Specification limit	GRADATION
37	100	100
25	90-100	95
19	76-90	83
12.5	56-80	68
9.5	48-74	61
NO.4	29-59	44
NO.8	19-45	32
NO.50	5-17	11
NO.200	2-8	5

- **FILLER:**

In this study one type of mineral fillers is u ordinary Portland cement (Tasluja).The physical properties of filler are presented in table (4):

Table (4) Properties of used filler

Property	Cement filler
Specific gravity	3.13
Passing sieve no.200 (0.075mm)	96

* These tests were accomplished in the transportation and material laboratories of civil engineering in the Babylon University.

Test Methods

The experimental work for this research is made in the laboratories of the engineering college, Babylon university and in the construction laboratory in Babylon city .

- **Marshall Mix Design for optimum Asphalt Content**

In order to complete the requirements of the experiment design work , specimens are tested by Marshall apparatus test . Four different percentage of asphalt contents (3.8, 4.2, 4.6 and 5)% are used Marshall mix design for optimum asphalt content and it is found (4.6%) as in average content for the replacement percentage. The mixtures properties at optimum asphalt contents must become with table that meet the Iraqi specification requirements SCRB, R/9 2004) for base layer of pavement .

- **Marshall Test for Specimens :-**

standard method of Marshall as in (ASTM D-1559), specifications is used to find Marshall properties (volumetric properties) for compacted asphalt concrete specimens.

- **Indirect Tensile Strength Test :-**

The tensile strength of compacted asphalt specimens is typically determined by the indirect tensile strength test , which is determined according to the method described in ASTM D4123 (1989) . The mechanics of the test place a nearly uniform state of tensile stress across the diametral plane. At road laboratory of civil engineering , Babylon University by converting Marshall test to measure indirect tensile test.

Indirect tensile test is used to develop tensile stresses along the diametric axis of the test specimen. The horizontal tensile stress at the center of the test specimen is calculated to determine the indirect tensile strength by doubling the peak load (P) and then dividing it by the diameter (D) and the thickness (t) of the sample using the following equation (1).

$$ITS = (2*p)/(3.14 *t*D) \quad \text{…….(1)}$$

Where :- ITS= Indirect Tensile Strength (Mpa)
P= peak load (N)
t= thickness of specimen (mm)
D= diameter of specimen (mm)

Results and Discussion

Results of Marshall Test:

The first test method for characterizing performance is Marshall test. The properties of asphalt concrete mixtures, such as (stability, stiffness ,flow, bulk density, and air void) The has been of investigated this to evaluate their effect on the performance of mixtures. The results of this test are shown in table (5) three samples are used to obtain the average value.

Table (5) : Marshall test results for control mixture& asphalt mixtures with different RCA contents

Sample	Marshall stability (kN)	Marshall Flow (mm)	Bulk Density gm/cm^3	Av%	Marshall Stiffness kN/mm
Control 0% replacement	9.4	3	2.23	4.05 %	3.13
Agg. Replaced with 10% RCA	7.7	3.5	2.229	4.16 %	2.20
Agg. Replaced with 20% RCA	7.75	4.0	2.225	4.7%	1.94
Agg. Replaced with 30% RCA	8.3	3.75	2.2 13	4%	2.21

Results or Indirect Tensile Strength (ITS)Test:-

The indirect tensile test, ASTM D4123 is used to evaluate the tensile strength of asphaltic mixtures, where the test is completed by applied load at rate(50.8mm/ min) on the Marshall specimen The tensile strength corresponding to maximum load occurs to failure of sample at intermediate to low temperatures (20^{o}c). It is indicated to evaluate the strength of Flexible pavement to strength for fatigue cracking resistance. Three samples are used to obtain the average value. Indirect strength test results for control mixture & asphalt mixtures with different RCA content as shown in table (6).

Table(6) indirect Tensile strength (ITS)Test for control mixture& asphalt mixtures with different RCA contents

Sample	ITS=(2P/(3.14DT)) MPa
CONTROL 0% replacement	1.91
Agg. Replaced with 10% RCA	2.087
Agg. Replaced with 20% RCA	2.303
Agg. Replaced with 30% RCA	2.599

DISCUSSION

The use of recycled concrete aggregate(RCA) in asphalt mix is a sustainable construction practice, provided that the addition of RCA does not adversely affect the performance of the asphalt mix. In this research, the effects of RCA on the performance behavior of hot mix asphalt(HMA) were examined. The mixes produced by blending RCA with virgin aggregate at four different percentages (0%, 10%, 20% ,30%). The mix design results indicate that the RCA is highly absorptive, and that as the percentage of RCA in the mix increases, the optimum asphalt content increases significantly. In terms of performance behavior, the addition of RCA to the HMA mix affect, resistance to rutting, fatigue and thermal cracking of the asphalt mix. Considering the performance behavior and the need for a higher asphalt content, the use of RCA as HMA aggregate is not recommended, for high percentage of replacement, even though all the RCA mixes met the volumetric requirements. More important, the findings in this research indicate that the absorbed asphalt might plays significant role at high temperatures, likely because of expansion of the asphalt.

CONCLUSIONS

On the basis of the materials used and laboratory tests performed in this study the following conclusion can be stated .

1. The Marshall stability for the mix containing RCA decrease about 20% than control for percentages (10%, 20%) & 11% for percentage (30%) but still agree with the Iraqi specifications (5kN) due to increase the asphalt content cause decrease of inter partical friction .
2. The Marshall flow increase about (16,33,25%) for percentage (10%, 20%, 30%) respectively and still within specification limiting (2- 4mm)
3. Bulk density decrease due to replacement of RCA (less specific gravity than vigin aggregate) the decrement reach to 5% than control mix.
4. A.V% for mixes containing RCA increase slightly about 10% than control mix & still with specifications (3-6%)
5. The cracking performance is improved for mix containing RCA by increase the ITS of mixes about (9%, 21%, 36%) than control mix . for RCA replacement percentage (10%, 20%, 30%) respectively due to increase of crushed faces of aggregate particles by using (crushed RCA) .

REFERENCES

[1] *M. Cupo-Paguno. A. DAndrea. c. Giavarini and C. Marro 1994.* **"Use of building demolished wastes for asphalt mixes: first results"**. Energy environment and technological innovation- proceedings of 111 international congress Caracas-Venezuela, 5-11/11/1994, pp. 203.208, Congress.

[2] *The recdemo website LIFE00 ENVD000319, 2004.* **"Complete utilization of the sand fraction from demolished wastes recycling"**. Available: http://www.recdemo.bamde, pp. 12.

[3] *Farias A. , Facale S . , Gusmao A. , Maia, 2013.* **"Technical and Economic analysis of construction and demolished waster used in paving project ",** proceedings of the 18 th international conference on soil mechanics and geotechnical Engineering , Paris. Modeling Study on the Suitability of Demolishing Waste .

[4] *I. Vegas: J. A. lbaficz: A. Lisbona: A. Siez de Cortazar: M. Frias, 2011.* **"Pre- normative research on the use of mixed recycled aggregates in unbound road"**. Construction and Building Materials- CONSTR BUILD MATER vol. 25, no. 5, pp. 2674-2682.

[5] *Shen, D. H. and Du, J. C. 2004.* **"Evaluation of building materials recycling on HMA permanent deformation**". Construction and Building Materials. Vol 18, 391-397.

[6] *Perez, A R Pasandnot and J Gallego, 2012*, **Stripping in hot mix asphalt produced by aggregates from construction and demolished wastes".** Waste Management and Research. vol. 30. pp. (3-11).

[7] *American Society for Testing Materials, 1989.* **ASTM. section 4. Vol.04. 08**.

[8] *ACI Committee 555*, Removal and Reuse of Hardened Concrete, ACI 555R-01 .

[9] *ACI Committee 555* Report, American Concrete Institute, Farmington Hills, Michigan, 2001, 26 pages .

[10] *FHWA,* Transportation Applications of Recycled Concrete Aggregate, Federal Highway .

[11] *SCRB,* 2004. Iraq specification of Roads & Bridge (R9).

Estimated Convergence of Quantitative Methods in Estimating Land Use Transport An Empirical Study in the City of Fallujah

Dr. Mohammed Al ani
Center of Urban & Regional Planning
for Postgraduate Studies
University of Baghdad
Email: mohalani @yahoo.com

Dr. Nada Mohammed Alhayani
Center of Urban & Regional Planning
for Postgraduate Studies
University of Baghdad
Email: nanmoon00@yahoo.com

Abstract- **Transport is one of the important infrastructure services in the city, which shares its land uses several different and sizes and often the use of transport have a significant impact on the formation of these uses that save time, effort and be the cause of accessibility to achieve efficiency in the functional interdependence connection toward the desired formation for the installation of the city.**

With the increase in population numbers in the cities and the emergence of social and economic developments produced a dramatic increase in the number of cars that came require additional network be able to accommodate these changes and organization as required, which gives the city the possibility of urban growth in the right direction processions of the evolution of population sizes and uses of the land. So now it requires techniques and methods which have the ability to determine the size of these developments, if correct and revised estimates adopted where possible that the results of the style of the other estimates differ to varying degrees, which requires the adoption of a style results closest to the real application.

Perhaps the typical use of linear regression and time series may lead to the first glance that the alleged disparity if adopted these models in urban land uses estimates for the purposes of transport, especially since the first model belongs to the static models static while the second model belongs to the dynamic models dynamic.

Therefore comes this research in order to detect the extent of convergence estimated these two models when calculating the size of land use for transportation in the city of Fallujah, which was waiting required for the transport network in which expansion in line with population growth and the expansion of residential neighborhoods that spanned the edges over last few years and to improve the almost equality between the estimations of the two models ; static and dynamic .

The goal and the importance of search

This research aim to provide a picture record of rapprochement between linear regression which involves the case of abstraction dwells in the diagnosis of the factors affecting the estimate of the need of the uses of urban land transport in the city of Fallujah model and the time-series model, which represents the dynamic state of the influence of factors when estimating that need and acceding here under the effect of the time factor so as to lay the intellectual stability to the user quantitative methods that the adoption of any of these methods will not expand the appreciation gap and thus spreading confidence when adopting alternative quantitative methods in accordance with the state of use of the methods, whether static or dynamic at a time when different applications for one model seeks to detect the change and the difference in the same phenomenon from time to time, or between a worker and another by virtue of the inevitability of stability and convergence in the estimates in the application of some of the models in the same direction and the necessity of difference in the case of one model to measure the change towards the studied case.

Research problem

The problem research think that the different mechanism of some models between the estimation model linear regression and time series deliberate here for the purposes of transport in Fallujah may lead to differences in results by virtue of static and the first dynamic second and therefore any of them will be relying especially since the logical abstraction and dynamic working together in determining the direction of the magnitude of the phenomenon .

Research Hypothesis

Released research hypothesis that the size of the uses of urban land for transport depends on the size of the population in the city through morphological stages (time) and therefore can exit appreciated tight for those uses, whether taking the population factor is just across the simple linear regression model, or if taken time through chains model where in both models there is a tendency for one year and that the change differed influential personnel transactions.

Research Methodology

The use of descriptive and analytical style, quantitative methods represented by linear regression manner and style of the time series and the adoption of a previous data to assess the results the authors get from two modes and the adoption of a style of the closest results in the application of land use to evaluate future forecast .

The first topic - Uses of land transport

Introduction

The early planning studies which meant planning the city focused on the reality of planning and transport networks within the city, and this prompted researchers and specialists to address this issue both the competence angle in order to reach results and solutions to the problems that are plaguing cities (1). With the increase in urban population and the consequent of a growing increase in the uses and means of private transport and the public led to the increased allocation of land for this use, whether in developed or developing

countries, which requires guess the future need for such use, which became a rate ranging between 19% - 36%. If the modern technology for transportation proportion of land use have kept to this sector not exceeding 24% and became the increase in Arab cities, including Iraq has become up to 36% (2). It's a second rate after residential uses in the city. Perhaps the Orbiter morphological stages of the evolution of Iraqi cities (including the city of Fallujah which is under study) notes the continuation of works land use for the purposes of transport to this place. Than it always pays to his pasture basic sectoral and detailed plans for the quality and patterns of streets and roads network in the city to meet the accessibility and efficient connectivity to parts of the city property.

Uses the concept of urban land use and transport planning

Since the inception of the city and the evolution of forms and functional configuration and the representation of competition between the various functions in the seizure of the land became the town planning and the organization uses its territory, the best way to achieve balance and control of that competition, prompting experts to organize optimal use of the land which serves the city's community according to various purpose (3) .

Since the land use represent distributions spatial functions multi-city provided by the city for its residents and residents of the surrounding areas and are therefore the engine of the overall events and activities practiced or carried out by the man on the ground was the phenomenon of land use remained of spatial phenomena that ran a lot of researchers as representing the events and activities of man and interactions with human nature changes and organize resources and land use within the city for the purpose of their study and employment possibilities available best use (2). Therefore, the process of using the land is considered complex compared to other planning processes . Because it related to the overall social, economic and natural events in the process of use and the extent of integration (1).

The scientists knew a lot of the concept of land use planning, each according to what he saw fit for his region and its population and their need to use (2).

In the area of regulating land use for the purposes of transport is determined land use for the city and the calculation of the space required for each of them, then comes the step distribution to the available land (4).

Hence, the use of urban land in the city as a whole and land use for the purposes of transport are linked with each other and can not be separated as transport contributes to the distribution of urban land uses and helps economic activities in a balanced distribution within the city.

Also his key role in giving the city its final form and is no doubt heavily influenced by the volume of traffic and use space as traffic volume increases generated by increasing the intensity of use varies depending on the size of the traffic generated by land use (5).

Evolution of the use of land transport across the morphological stages of the city

It has become recognized that the city growth and development of land use which affects the road and street network growth through the space occupied by such use. Where land use contribute to the identification of streets and roads that have a role in shaping the structure of the type and form of the city as the road and street network based on urban uses and characteristics of the position type, and this makes coherent city between uses of space and function, as well as expansions which are linked simultaneously with the growth stages and morphological changes of cities (6). Therefore urban land uses for each stage of the growth of cities have to give expressions morphology of road and street network specific forms and patterns by which uses phase synchronization and interaction dwell and dealing with those uses. And thus a function of traffic uses the land has become, for the existence of reciprocal functional relationship between the movement factor of transport and between other land of different activities in the city uses and this easy the planner to move and link land use with the population ,economic ,social ,physical and service characteristics within the required planning and estimating variables size of the urban area conditions affecting the spatial relationship between land use and varieties of roads and streets (7).

Transportation land use models

Transport models are a source of assistance and guidance when making predictions about the impact of transport schemes implemented on decision-making and help to predict the impact of these decisions on congestion and overpopulation and manpower. And developed many models use land transport since 1960 to evaluate the interaction of transport and spatial patterns and changes, and some of them finally focus on the modeling techniques and theories underlying the type of policies that can be analyzed (8). The building transport models to find mathematical relationships adoption of the base year for the use of existing land transport is used to predict the evolution expected a certain area in the coming years, or when the target year, also use the form differs depending on the purpose of the data to be unpredictable and depending on the available data when using the model (9).

These models have evolved a lot in recent years, especially after the use of computer techniques. It is worth mentioning that there are 20 model is currently being used to transport the land uses in the world classified as Wegener, and most of these models will usually be carried uses the land transport representation in the urban area and some of the other static and dynamic (10).

The second topic - An Empirical Study for transportation area in the city of Fallujah

Introduction to the emergence of the city of Fallujah: -

Dating originated the city of Fallujah to the last of the nineteenth century quarter when making the subject of the city of Fallujah current farming village characterized by the fertility of its soil and the quality of the agricultural product where making it attracts a lot of farmers led to the development and then it expands, until it became experienced by most of the roads through which place it linked the upper Euphrates cities in the Levant on the one hand and the city of Baghdad, the capital, on the other hand. It was then for the passage of the highway after 1923 the main factor in the promotion and its urban economic status to become after the 1920 city central province of secondary track him Saqlawiyah

and karma and the rest of its sides to the west and south and to expand the city by providing the services and functions of regional dimension and make it a central city in the territory and led to an increase in population and thus the city as a center of urban growth to meet these services and functions of human settlements in its territory (11). Also the city of Fallujah, passed after the first creation multiple developmental stages for each stage of which was a private features both in terms of land use and functions or forms of architecture and buildings or streets systems (12).

Evolution of transportation for the city of Fallujah through morphological stages

Through the development of the city of Fallujah possible discrimination five morphological stages of the city of Fallujah contributed to each of them to draw a picture of uses of urban land as shown in the map (1), by which they can distinguish uses for the purposes of transport being a trace of successive changes of basic designs and accompanied by a distinctive and clear the road network and the streets where that displays the image of the map (2) can be described as follows: -

1. Phase I: as a result of expansion accelerated in the city and the absence of orientations land and urban planning administration impact on irregular pieces of land and the mixing of uses of the land, as there was traditional compact urban tissue fabric in line with the membership of the street network which continued during this stage and adopted in the streets of the city planning on the web style .
2. Phase II: characterized by a marked expansion of the network of local streets in new neighborhoods, according to the networking system where straight streets appeared, as well as maintaining the organic style is straight and is in force.
3. Phase III: I saw prepare a comprehensive basic design of the city focused on the concepts in the streets and roads network planning two Functionality within the residential neighborhood and the link between sectors through a network of roads and streets where the distinction between the two is clearly afternoon.
4. Phase IV: the preparation of the design basis for the year 1981 was completed to develop and expand the streets of the inner city network within the main streets linking the city's neighborhoods, with the central business district in which the traditional region.

   So marked streets in the city network during this phase style while the organic system prevails in the traditional segment, there is a network system in modern neighborhoods . Design basis at this stage has sowed a new type of straight streets has given the city a new cultural dimension commensurate with the increasing number of automobiles but did not take into account the future increase in the number of cars has not been the capacity for current and future expansion of the streets of the city .
5. Phase V: as the fourth stage continued expansion streets, according to the network system in the new neighborhoods of the cities with the ever-increasing number of vehicles and the emergence of traffic congestion in the central business districts.
6. Phase VI: This stage also was complementary to the fifth stage with the very large increase in the number of vehicles, especially private cars so the city suffers from big traffic jams began to increase the pressure on the infrastructure of roads and streets, where he became the actual power is much greater than the capacity and the design capacity of the roads, which unless it is taking it into consideration (13).

By represented urban land and transportation land for the city of Fallujah area through the stages of development and urban land to transportation land area ratio in the table (1). Through analysis the table (1) we find that the ratio of transportation area to the urban area for the city of Falluja is approximately equal across the stages of development of the city and as shown in Figure (1).

Table (1) Urban land area and transportation land area for the city of Fallujah through the stages of its development

No.	Year	Urban land area of the city (Hector)	Transportation land area (Hector)	Ratio (%)
1	1925	74	16	21.62
2	1959	495	117	23.64
3	1971	978	234	23.93
4	1990	1539	374	24.30
5	2000	2123	511	24.07
6	2010	2470	598	24.21

Source: Researcher action based on basic designs for the city of Fallujah, according to transportation land use through the stages as recorded in the city's urban planning directorate

Map (1) use of urban land in the city of Fallujah until 2012

Source: Researcher action based on the urban planning directorate in Anbar Governorate

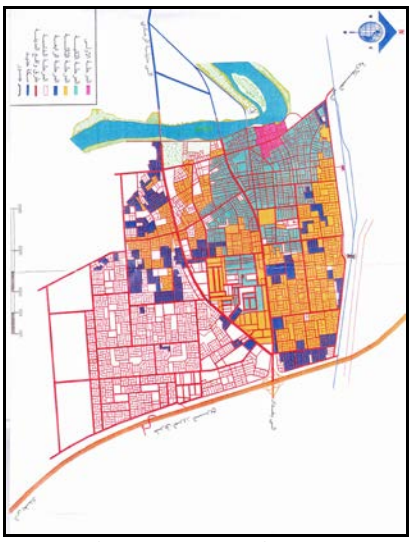

Map (2) land use for the purposes of transport in the city of Fallujah until 2012

Source: Researcher action based on the urban planning directorate in Anbar Governorate

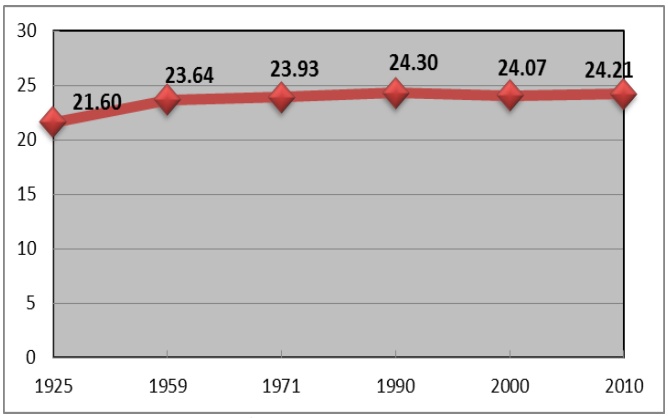

Figure(1) The ratio of transportation land area to urban land area for the city of Fallujah through the stages of its development

Source: Researcher action based on the table (1)

Need of urban land in the city of Fallujah, using time-series model account

By reference to the table (1) which displays the urban land area in the city of Fallujah and the percentage of land use for the purposes of transportation of them, it can be applied to the style of the time series to assess the need for the overall land use in the city of Fallujah, as well as uses of land transport. Applying the time-series model and the use of Minitab software Computerized predicted the value of urban land area and the area of land transport to the city of Fallujah, as shown in Figures (2) and (3) and it is clear that the urban land area transportation land area for the city of Fallujah are increasing towards the year and there was no effect of seasonal changes in the data series, as shown in Table 2 (below): -

Table (2) urban land area and transportation land area for the city of Fallujah through the stages of its development and estimation for years 2015, and 2020

Year	1925	1959	1971	1990	2000	2010	2015	2020
Urban land area (Hector)	74	495	978	1539	2123	2470	3022	3520
Transportation land area (Hector)	16	117	234	374	511	598	731	852

Source: Researcher action based on table (1) and figures (2),(3)

Evolution of transportation land use and increasing numbers of the population

The number of the population for the city of Fallujah was increased in a large percent according to the general census of the population for the years since 1947 until the year 2010, where the population has grown to more than 23 times in 2010 for numbering in 1947, and the 2020 population estimates indicate the possibility of increasing the number of population to more than 31 times than its number in 1947 .

This increase in population also accompanied by an increase in the use of urban land for the city, including the use of land transport, this indication to the existence of unexpected relationship between land use and transport of the population as shown in table (3)

Need of urban land in the city of Fallujah by using the linear regression model account

By reference to the population of the city of Fallujah by years of general census of population and area of urban land and land use for the purposes of transportation of the city for some years the census, and estimating the numbers of the population for the years 2015 and 2020, it can be applied to the style of simple linear regression to estimate the need for overall land use in the city of Fallujah as well as the use of land transport. Applying the simple linear regression model, using Minitab software Computerized predicted the value of urban land area and the area of land transport to the city of Fallujah, as shown in figures (4) and (5).

Thus the authors complete the estimation for urban and area and transportation land area for the city of Falluja in years 2015 , 2020 as shown in table (4) .

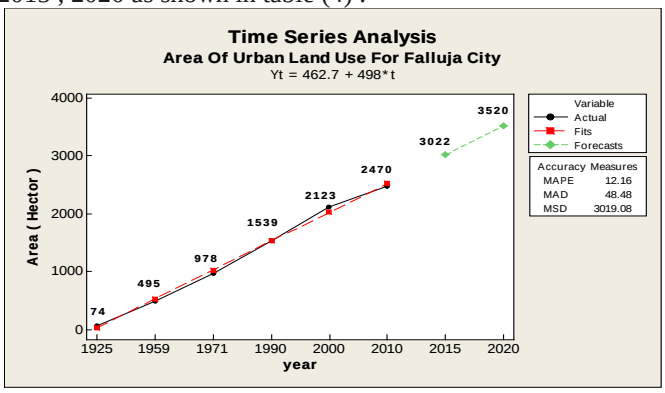

(Figure 2) The expected urban land area for the city of Fallujah

Source: Researcher action based on applying Minitab program

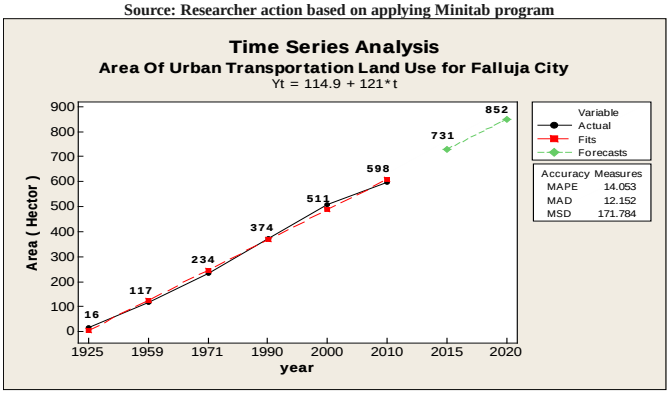

(Figure 3) The expected transportation land area for the city of Fallujah

Source: Researcher action based on applying Minitab report program

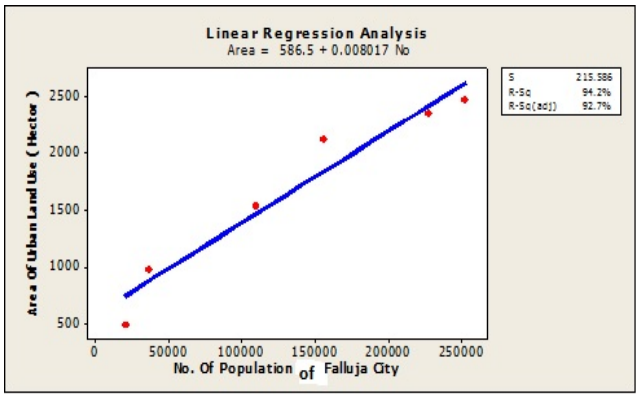

Figure (4) Simple linear regression model of urban land area for the city of Fallujah

Source: Researcher action based on applying Minitab report program

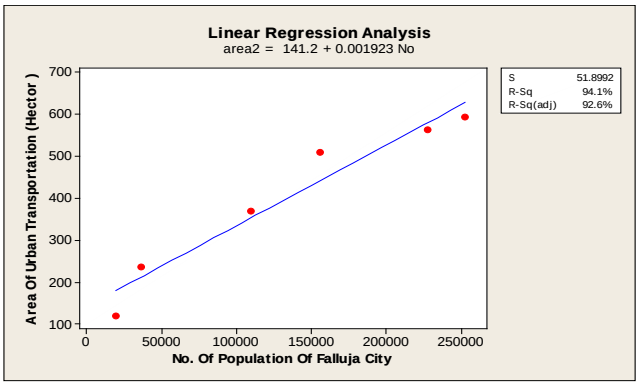

Figure (5) Simple linear regression model of Transportation land area for Fallujah

Source: Researcher action based on applying Minitab report program

Table (3) No of population for census years , urban land area , transportation land area and the estimations of population urban land area , transportation land area in 2015 & 2020 for the city of Fallujah

No.	Year	Population No. (capita)	Urban land area (Hector)	Transportation land area (Hector)
1	1947	10947	----	----
2	1957	19844	495	119
3	1965	36330	978	235
4	1977	63050	----	----
5	1987	109731	1539	370
6	1997	155806	2123	510
7	2007	227675	2346	563
8	2010	252946	2470	593
9	2015	293417	2940	706
10	2020	339006	3304	794

Source: Researcher action based on table (4) for the city of Fallujah using simple linear regression model and by apply Minitab program

Table (4) The estimations of urban land area and transportation land area for the city of Fallujah for years 2015,2020 using the time-series and simple linear regression

Model / Area (Hector)	Time-series model		simple linear regression model	
	2015	2020	2015	2020
Urban land area	3022	3520	2940	3304
Transportation land area	731	852	706	794

Source: Researcher action based on tables (2) , (3)

The third topic

Analysis of the results

The use of the style of the time series and that was a dynamic nature depends on the time all the givens, but the general trend of the development of phenomena remains a case of the link between this model and the model of linear regression, which is basically a static model has one direction depends regression coefficient (marginal propensity to change) mainly in this trend, which shares as this with time-series model, which makes for a time transactions to move towards the general direction that differed over the chain and its developments, and this is what made estimates take-oriented general trend static for the linear regression corresponding to the direction the time series, where the time evolution relatively close no significant changes affect the overall trend. Therefore, the estimated urban land area for the years 2015, 2020 to the city of Fallujah by using the time-series model is an approach almost to the estimated area of urban land for the same two years, the city using simple linear regression model. The two models share a single equation can be described as the following: -

$Y = a + bX$ in the regression model

$Y = a + bT$ in time-series model

Both models start with a minimum estimate of the level of an average change in variable b and in one direction, (if this neglected seasonal and periodic and episodic changes in the time series represented by time). On this basis it assumes that estimates be linear regression user model to predict the uses of urban land in the city of Fallujah and uses for the purposes of converged transport that were not identical and this sought to in such a models require estimates of conformity unlike other models that need to be the difference in the estimates according to case required of change model user product or gravity models .

So as far as the authors aim to estimate both its urban land use and transportation, the state of congruence in the estimates remain desirable in this regard .

Today, in light of the expansion of the city three cases crawling or jumping or filled out the neighborhoods have become spread over a wide swath of the land also the need to link the process with each other by linked cities and its back and therefore the city needs to expansion in light of the continuing evolution of the city . It displays the traditional city expansion to the natural and human determinants, which became surrounded the city from four sides (of the Euphrates to the west and the railroad north rapid line east industrial district south) make the city expands as planned in a manner to jump to cross these determinants which necessitated a review of the road and street network to link neighborhoods new among themselves and within the old city, This came to the use of this model is consistent and dynamic estimate to assess the need to use transport, taking into account the stomach designs for these neighborhoods that did not stray from the previous time and the typical situation that called for the use of the dynamic model. Therefore Find sought through a survey of the entire road network and streets in the city to urban land appreciation in general devoted to the uses of transport and land in particular, and found that the second relative to the first

is enough to extend the proposed network and remain on the same percentage and typical extensions of the network connection with impair uses diverse urban land ratio large enough from the ground to the expansion of commercial and industrial pattern and uses the rest of the sites as well as the presence of a rising network streets comes from specialty commercial area and industrial area stations for parking. It takes the use of land for transportation typical dual-use nature. Where occupancy rates firming uses transport within urban land through morphological stages in the two estimates static (linear regression) and dynamic (time series) goes back to the lack of diversity of needs for land use and the process of the formation of the city and one pattern is currently only needed residential and requirements, including the need to use transport Therefore, we find sufficient city the position of one transfer to the outside and like the inside through each morphological stages and the survival of the large market in the traditional center of the city, which leads all major business functions in the city, fruits and vegetables in the same place that created it (downtown now) to this day

Conclusions

1. The proportion allocated to the purposes of transportation area in the city of Fallujah is roughly equal across the stages of development of the city and it has increased at a fixed rate with the increase in the urban area of the city and the urban equivalent to a quarter of the land area of the city.
2. The urban area of the ground and land transport to the city of Fallujah area are increasing towards the year and there was no effect of seasonal changes in the data series.
3. The estimated urban land area for the years 2015, 2020 to the city of Fallujah by using the time-series model is almost equal to the estimated area of urban land for the city using simple linear regression model for the same two years.
4. The stability of occupancy rates for the use of transport within urban land through morphological stages in the two estimates static (linear regression) and dynamic (time series) goes back to the lack of diversity of needs for land use and the process of the formation of the city and one pattern is currently only needed residential and requirements, including the need to use transport.
5. To offer the city expands the traditional to the natural and human limitations make the city expands as planned in a manner to jump to cross these determinants with a review of road and street network to new neighborhoods connect with each other and within the old city, came the use of this model is consistent and dynamic estimation to estimate the need to use transport where not stray from the previous time and the typical situation that called for the use of the dynamic model.

Recommendations

Where was preparing a new detailed plans illustrate trends and alternatives to urban expansions to the city of Fallujah, indicating the road network and the streets in their four classifications , so the authors recommend: -

6. Formation algorithm for transfer with each alternative describes the tracks to generate trips shortest time and lower costs in accordance with the modes of transport available.
7. Adopt scientific studies on the formation of expansion alternatives in the city of Fallujah and the nomination of the best alternative to be elected algorithm for approval of the transfer of the most successful alternative.
8. Adopt the principle of convergence in the use of urban land use and transport as possible in the case to allow for diversity and the preservation of the estimates required for both land uses .

References

9. Raja khalil Ahmed al-Dulaimi , "The impact of motor transport in urban construction job for the city of Baquba", master submitted to the Center of Urban & Regional planning –university of Baghdad, 2001,p 24, unpublished.
10. Ibrahim, Abdul Baqi and Lami Salih, "Architectural design and urban planning in the foundations of the Islamic Ages - an analytical study on the city of Cairo", the issuance of Islamic Capitals and Cities Organization, 1990.
11. Abu Ismail, Ahmad, "Transport Industry", Arab Renaissance Publishing House, House authoring Printing, Cairo , 1960.
12. Kayed Abossbha, Geographical Cities, floor 1, Dar Wael, Oman ,2003.
13. Dr. Mohammad Ali Alanbari, "The role of the highway network in regional development" , master thesis submitted to the Center of Urban and Regional Planning -University of Baghdad, 1985, p15.
14. Dr. Mohammed Tawfiq Salim, "Transport and Traffic Engineering", Dar Alratib universal ,1985.
15. Taking the source of the book after Mohammed al-Ani, Page 24
16. Wegener, M., F. Furst (1999) Land-Use Transport Interaction: State of the Art. Deliverable, D2a of the project TRANSLAND (Integration of Transport and Land use Planning). Brecht as den Institute for Raumplanung 46, University of Dortmund, Institute for Raumplanung, Dortmund.
17. Dr. Musaid Mssenid , "Land use and transportation planning", University of Imam Muhammad bin Saud Islamic ,2002.
18. Michael Wegener & Spiekermann Urban Regional Research, "Overview of Land use Transport Models", University of Dortmund, D-44137, Dortmund, Germany, 2010 .
19. Jumaili, , Arak Mutlab, Historically and Socially of Fallujah, Baghdad , p 10 ,1971.
20. Jumaili, Mahmood Ismail, Phd submitted to the Center of Urban & Regional Planning, University of Baghdad, 2011,Unpublished .
21. Design basis reports through morphological stages of the city of Fallujah, the Urban Planning Directorate.

Map Georeferencing Using GIS (Arc Python) Program

Shaima kh. elias. Assit.Prof. Dr. Abbas Z. Khalaf , Assit. Prof. Dr. Imzahim A. Alwan

***Abstract*— according the importance of maps and images in this day, which considered a multipurpose database spatially and environmentally around us. there are many programs to rectify processing maps and images to utilize them for different purposes, GIS (Arc Python) is one of the map georeferencing program at the moment to, which contains the mathematical models designed to rectify processing the maps and images. ArcPython was done used it to provide plenty of effort and time in georeferencing process, suitable for large projects, can be convert the scripts language to tool and considered new georeferencing method of maps and images.**

The aim of this paper is map georeferencing using GIS (Arc Python) program. was done using three register points (points intersection of latitude and longitude for the same map) to map georeferencing process. The purpose assessment map resulting was done conformity with the Quickbird satellite image 60 cm spatial resolution and the results showed that the matching accuracy for all study area objects almost to 95%.

I. INTRODUCTION

Maps are fast information sources when people want to know, to study and to develop projects in any region. Users, when consulting a map, expect information to be found. Sometimes, information cannot appear due to scale or to the not updating of the map. It is necessary to adapt the scale and content to the desired objective of the map [1].

Geometry correction is the process of digitally manipulating image data such that the image's projection precisely matches a specific projection surface or shape [2].

Traditional geometric correction model of remote sensing images or maps is based on ground control points (GCPs). When accurate ground control points are available, the point-based geometric correction model can improve the positioning accuracy of the image [3], thus it is possible to generate maps on various scales keeping in view the end users requirement.

Manuscript received August 23, 2015.

Shaima kh. elias is with the Ministry of Oil; e-mail: shaima.elias232@ yahoo.com).

Abbas Z. Khalaf is with the Department of Building and Construction Engineering, University of Technology- Baghdad- Iraq (e-mail: khalaf1955@yahoo.com).

Imzahim A. Alwan is with the Department of Building and Construction Engineering, University of Technology- Baghdad- Iraq (mzahim74@gmail.com).

II. RESEARCH OBJECTIVE

The following objectives were assigned for this paper:

1- Map georeferencing using GIS Program (Arc Python).

2- Using register points (Latitude and Longitude intersection points for the same map) as Ground Control Points.

III. THE STUDY AREA

kirkuk is one of the most important and the largest governorates of Iraq. It lies between (44.41°E) longitude and (35.47°N) latitude. We focus exclusively on the province of Kirkuk center city (Figure1) due to the availability of Quickbird satellite image 60 cm spatial resolution for the conformity. The following sources of information have been used in the study area:

1- The Quickbird satellite image 60 cm spatial resolution [4].

2- The data register point supplied from longitude and latitude of the NIMA map scale 1:100,000 [5] as shown in Figure (1-b).

3- Iraq Landsat Image 14m Resolution [5] as shown in Figure (1-a).

Fig. 1. kirkuk city

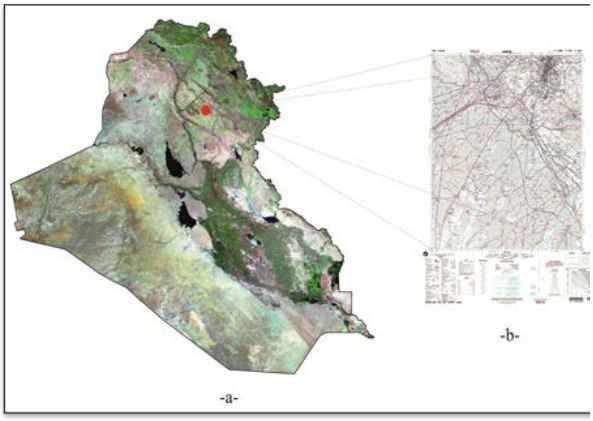

IV. RESEARCH METHODOLOGY

To achieve the research objectives, a general flowchart to cover the requirements of map correction was planned as illustrated in Figure (2).

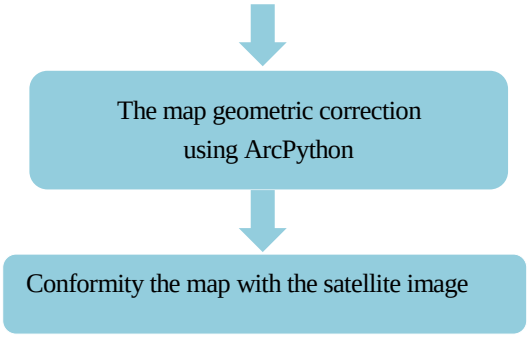

Fig. 2. work plan flow chart

V. MAP GEOREFERENCING BY GIS (ARC PYTHON) SOFTWARE 10.2.1

A simple geometric model usually involves mathematical functions, which are easier to understand, The mathematical function parameters are solved with the help of the GCPs collected throughout the image by using the least squares adjustment process. Once the mathematical function parameters are determined, the correct positions of each pixel in the image can be estimated by these functions.The mathematical models used in this research is 2D Polynomial Model . Polynomial equations are used to convert source file coordinates to rectified map coordinates. rectification is the process of transforming the data from one grid system into another grid system using a geometric transformation. From above, the rectification or registration involves the following general steps, regardless of the application [6].

1. Locating ground control points (GCPs).
2. Computing and testing a transformation between the original and corrected coordinate system.
3. Creating an output image with the new coordinate. The pixels must be resampled to conform to the new grid.

The order of transformation is the order of the polynomial used in the transformation. Usually, 1st order or 2nd order transformations are used. The needed transformation can be expressed in different orders of the polynomials based on the distortion of the image, the number of GCPs and terrain type. The order of the transformation is simply the highest exponent used in the polynomial.

The *2D polynomial* functions do not take into account the elevations of the GCPs, these models can be efficiently used when the imaged area is relatively flat. Their usage is generally limited to images which have few or small distortions. The following equations are used to express the general form of the polynomial models in 2D case [9]:

$$E = f_1(r,c) = a_0 + a_1 r + a_2 c + a_3 r^2 + a_4 rc + a_5 c^2 + \cdots \quad (1)$$

$$N = f_2(r,c) = b_0 + b_1 r + b_2 c + b_3 r^2 + b_4 rc + b_5 c^2 + \cdots \quad (2)$$

Where a_i and b_i (i = 0, 1, 2, ...) are the transformation coefficients. Polynomial equations as shown above do not recognize the internal relationship between (r, c) of a pixel and its (E, N).

VI. SELECTION AND NUMER OF GCPS

The quality of ground control points (GCPs) directly affects the accuracy of mathematical model, and that, in turn, determines the outcome of the project. The typical GCPs are highway intersections, airport runways, and towers that can be clearly identified, accurately located on the image or the map. However care must also be given to the locations of the points. A general rule is that there should be a distribution of control points around the edges of the image to be corrected with a scattering of points over the body of the image [10].

The relationship between the minimum number of GCPs required N_{min} and the order of polynomial equations t is generally expressed as [9]:

$$N_{min} = (t+1) \times \frac{(t+2)}{2} \quad (3)$$

Where t is the order of polynomial model.

For example table (1) shows the minimum number of ground control points required to perform a transformation for (1st) through (4th) order transformation after applying above equation.

TABLE (1)
MINIMUM NUMBER OF GCPS PER ORDER OF TRANSFORMATION [9]

Order of Transformation	Minimum No. of GCPs Required
1	3
2	6
3	10
4	15
5	21
6	28

VII. THE MAP RESAMPLING

The location of output pixels derived from the ground control points (GCPs) is used to establish the geometry of the output image and its relationship to the input image. Difference between actual GCPs location and their position in the image are used to determine the geometric transformation required to restore the image. This transformation can be done by different resampling methods where original pixels are resampled to match the geometric coordinates. Each resampling method employs a different strategy to estimate values at output grid for given known values for the input grid [12].

Resampling techniques are used during geometric projection, correction, and co-registration.it is the final step in the rectification/registration process. In general there are three methods for resampling [13].

1. Nearest Neighbor.

2. Bilinear Interpolation.
3. Cubic Convolution.

VIII. PYTHON

Python is a free; object oriented programming language used across multiple computer platforms. Its initial development began in the late 1980s by Guido van Rossum, a computer programmer at the National Research Institute for Mathematics and Computer Science in the Netherlands. The programming language is open source. Since its inception, Python has become a popular choice among programmers for both its powerful tools and the easy-to-use syntax. Special implementations of the original Python language has allowed users to write programs and call up methods of many other common programming languages such as Java and Microsoft's .NET architecture. With these advantages, Python has earned an audience that employs its flexibility in many different applications. Python is used as an academic research tool in many fields. O'Boyle and Hutchison (2008) report that they have developed a Python-based set of tools called Cinfony which incorporates three popular but incompatible open source cheminformatics toolkits in one interface. Decision support system (DSS) research has also benefited from the use of Python. Python has been used to model a DSS by calculating multi objective mathematical functions and using artificial intelligence. The biosciences also benefit from Python by using its graphical toolset to create three dimensional representations of plant structures and even entire plant communities. These recreations allow researchers to model spatial interactions between competing plant species [14].

Importing modules: a module is a Python file that generally includes functions and classes. ArcPy is supported by a series of modules, including a data access module (arcpy.da), mapping module (arcpy.mapping), an ArcGIS Spatial Analyst extension module (arcpy.sa), and an ArcGIS Network Analyst extension module (arcpy.na). The Network Analyst module arcpy.na is a Python module for working with network analysis functionality provided with the ArcGIS Network Analyst extension. It provides access to all the geoprocessing tools available in the Network Analyst toolbox as well as other helper functions and classes that allow you to automate Network Analyst workflow through Python. ESRI has fully embraced Python for ArcGIS and sees Python as the language that fulfills the needs of our user community. Here are just some of the advantages of Python:

- Easy to learn and excellent for beginners, yet superb for experts
- Highly scalable, suitable for large projects or small one-off programs known as scripts
- Portable, cross-platform
- Embeddable (making ArcGIS scriptable)
- Stable and mature
- A large user community

Python extends across ArcGIS and becomes the language for data analysis, data conversion, data management, and map automation, helping increase productivity [15].

IX. IMAGE GEOPROCESSING

- warp

Performs a transformation on the raster based on the source and target control points using a polynomial transformation [15].

Syntax:

Warp_management(in_raster,source_control_ points, target_control_points, out_raster, {transformation_type}, {resampling_type})

in_raster: The input raster dataset.
source_control_points: The source points are the "from" coordinates of the links.
target_control_points: The target points are the "to" coordinates of the links
out_raster: Output raster dataset. When storing the raster dataset in a file format, you need to specify the file extension:

- bil—Esri BIL
- bip—Esri BIP
- bmp—BMP
- bsq—Esri BSQ
- dat—ENVI DAT
- gif—GIF
- img—ERDAS IMAGINE
- jpg—JPEG
- jp2—JPEG 2000
- png—PNG
- tif—TIFF

transformation_type (Optional): The geometric transformation type.

- POLYORDER0
- POLYORDER1
- POLYORDER2
- POLYORDER3
- ADJUST
- SPLINE
- PROJECTIVE

resampling_type (Optional): The resampling algorithm to be used.

- NEAREST —Nearest neighbor assignment
- BILINEAR —Bilinear interpolation
- CUBIC —Cubic convolution
- MAJORITY —Majority resampling

- Define Projection

This tool overwrites the coordinate system information (map projection and datum) stored with a dataset. The only use for this tool is for datsets that have an unknown or incorrect coordinate system defined.

Syntax

DefineProjection_management (in_dataset, coor_system)

in_dataset: Dataset or feature class whose projection is to be defined.
coor_system: Valid values are a Spatial Reference object, a file with a .prj extension, or a string representation of a coordinate system.

X. ANALYSIS AND RESULT

After getting the NIMA map with scale 1/100,000 was been determined the register points (three points) on the map which are the same intersection points of latitude and longitude and distributed regularly on the map to cover the entire area.

The geometric correction has been done by using 1st order polynomial, and then selecting the projection system which complies with the map projection system. As shown code below, the resulting of geometric correction illustrated in figure (3).

```
import arcpy
from arcpy import env
env.workspace =
"E:\MapsStudyArea\MapsWarp1"
#Map Name  KARKUK, ZONE 38
source_pnt = "'1046.989 -
765.012';'2464.993 -
812.984';'1708.984 -  2354.986'"
target_pnt = "'421000
3918000';'445000 3917000';'432000
3891000'"
arcpy.Warp_management("K643X4860_
geo.jpg", source_pnt, target_pnt,
"K643X4860.tif",
"POLYORDER1",\"BILINEAR")
sr = arcpy.SpatialReference("WGS
1984 UTM Zone 38N")
arcpy.DefineProjection_management
("K643X4860.tif", sr)
```

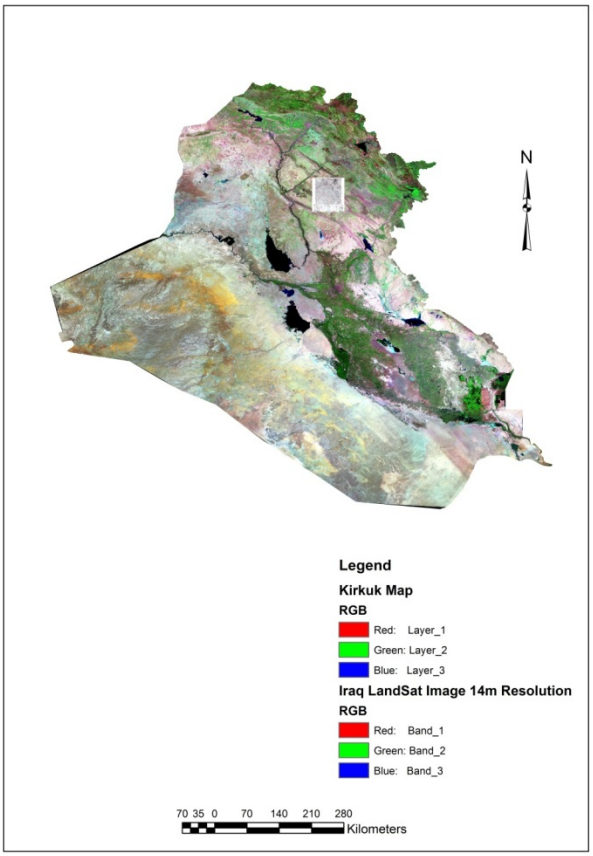

Fig. 3. Map Georeferencing Spatial Location

XI. ASSESSMENT GEOREFERENCING MAP

For the purpose of assessing the georeferencing by using Arc Python, was done conformity the map resulting from the georeferencing process with the Quickbird satellite image 60 cm spatial resolution. The results showed that most of the objects were conformity with the satellite image, and that the proportion of matching almost equal 95% with Total RMS error equal 0.0001, as illustrates in the figures below (4, 5, 6 and 7).

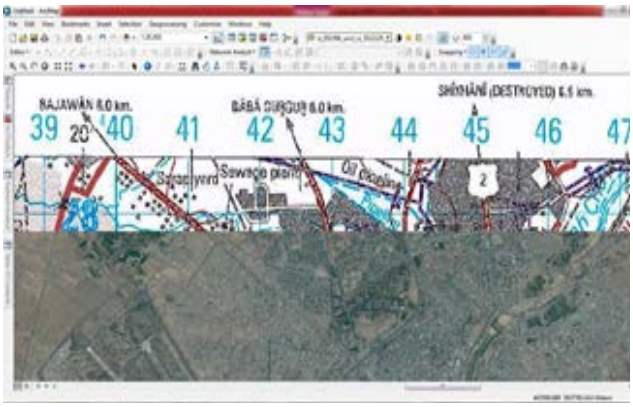

Fig.4. Conformity accuracy

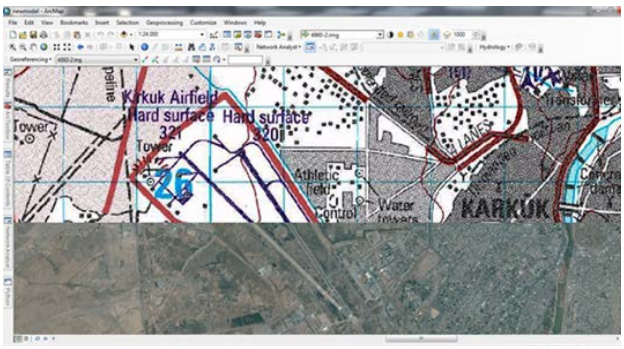

Fig.5. Conformity accuracy

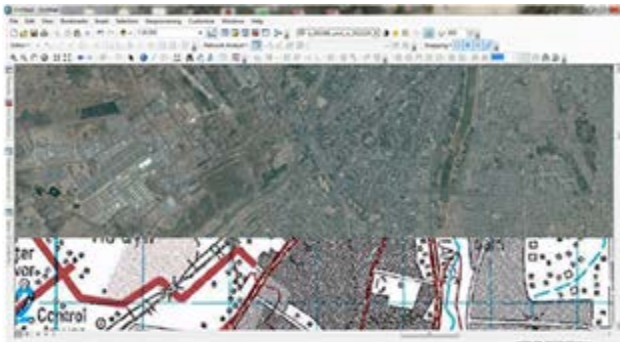

Fig.6. Conformity accuracy

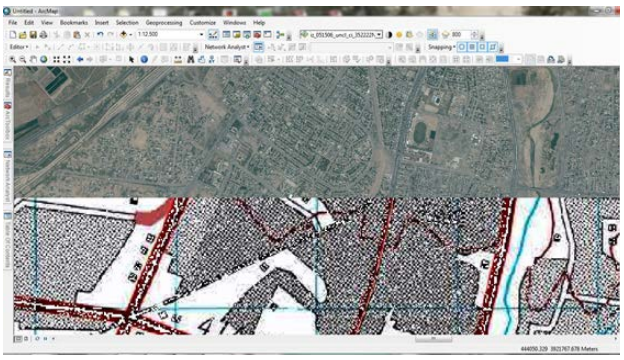

Fig.7. Conformity accuracy

XII. CONCLUSION

The results above showed that:

1. Latitude and Longitude intersection are highly accurate spatially and can be used as GCPs to correct the related maps.

2. Use of three register point are enough to achieve the required accuracy because of intersection points of latitude longitude it is very clear and that high accuracy. Accuracy resulting from the georeferencing process do not changed with increase number points, therefore; were used less number of points (three points) for georeferencing leading to provide plenty of time and effort.

3. Use Arc Python in the map georeferencing instead of traditionally program for maps georeferencing because it is the faster, less effort and more accurate. As well as that does not need additional point (check point).

REFRENCE

[1] Li R., Zhou G., Yang S., Tuell G., Schmidt N. J. and Flower C, (2003)," Astudy of the Potential Attainable Geometric Accuracy of IKONOS Satellite Images", IAPRS, 33(B4), 587-595.

[2] Wood S., (2014),"Technology-Image Geometry Correction", spreading on en.wikipedia.org/wiki/ Image Geometry Correction .

[3] Tengfei LONG, Weili JIAO, (2012)," The Geometric Correction Model Based On Areal Features For Multisource Images Rectification", International Archives of the Photogrammetry, Remote Sensing and Spatial Information Sciences, Volume XXXIX-B1, 2012XXII ISPRS Congress, 25 August – 01 September 2012, Melbourne, Australia.

[4] Kirkuk satellite image, (2010)," Ministry of Sciences and Technology"

[5] NIMA map, (1997)," Wasit Provincial Council ".

[6] Nawal Muhsen Abd Ali, 2013, " Accuracy Assessment of Photo Maps Producing From Satellite Images",Msc, University of Technology, Building and Construction Engineering Department..

[8] Hosseini M. and Amini J., (2005), "Comparison Between 2-D and 3-D Transformations for Geometric Correction of IKONOS images", Department of Geomatics Engineering, Faculty of Engineering, University of Tehran.

[9] Jay Gao, (2009), ″ Digital Analysis of Remotely Sensed Imagery″ , Ph.D., attended Wuhan Technical University of Surveying and Mapping in China.

[10] Richards, J. A. and Xiuping, J., (2006), " Remote Sensing Digital Image Analysis ", 4th Edition, Springer-Verlag Berlin Heidelberg, Germany.

[11] Sharpe .B, Wiebe .K., " Planimetric Accuracy in Satellite Mapping", Canada V6X 2Z9 .

[12] Leica Geosystems, (2008), " ERDAS Field Guide™ " , Volume One,Leica Geosystems Geospatial Imaging, LLC, USA.

[13] Behdinian, B. , (2002), " Generating Orthoimage from IKONOS Data", Asian Conference on Remote Sensing(ACRS), Taiwan.

[14] Chauvin, D. P. (2013) Advanced Techniques in Emergency Preparedness and Geoprocessing. MSc. Thesis, University of Connecticut, United States.

[15] Arc GIS, (2013) Arc GIS Desktop Help.

Lane Changing and Lane Utilisation Behaviour: Empirical Study

Dr Hamid Athab Al-Jameel /University of Kufa

Abstract— **Discernment of driver behaviour is the key to understanding dynamic driver behaviour for lane changing (LC) and lane utilization (LU). The LC and LU parameters are critically important for the calibration and validation of a traffic simulation model and therefore, this study focuses on LC and LU behaviour. Field data has been collected from examples of three typical motorway cross-sections types: two-lane (M602), three-lane (M60) and four lanes (M60). All are located in the City of Manchester in the UK. Video cameras have been installed at suitable vantage points in order to observe traffic in these sections. The data analysis for these locations indicated that there is a relationship between volume of flow and the frequency of LC. As the flow increases, the number of instances of LC increases up to a certain flow but then declines if the traffic flow increases further. The value of flow for maximum LC depends on the section, whether two lane, three lane or four lane. The LU behaviour has also been investigated for each type of cross-sections under study. A number of empirical equations have been derived from this study which will be used in the calibration and validation of a simulation model for subsequent stage of this project.**

Index Terms— **Driver behaviour, lane changing, lane utilisation and loop detector.**

I. INTRODUCTION

A lane change (LC) can be defined as the transition of a vehicle from one traffic lane to another. The behaviour of drivers during the LC process is complex because the driver has several decisions to make [1]. Studying LC behaviour is an essential factor for the interpretation of a number of traffic characteristics such as a merge bottleneck when this is due to systemic lane changing activities thereby creating a bottleneck with a consequential decreases capacity and the formation and escalation of stop-and-go conditions [2], [3] and [4].

Different methodologies have been proposed by different researchers to represent driver lane changing behaviour, such as Sparman[5], Gipps[6], Yousif[7], Ahmed[8], Hidas [9] and [10], Toledo[11], and Choudhoury[12]. Generally, Sultan and McDonald [13] classified these models into three groups as shown in Table 1.

Depending on the motivation of the driver, a lane change can be classified as either mandatory (MLC)when a driver needs to change lane to reach his/her destination or discretionary (DLC) when a driver looks for better traffic conditions such as to increase his/her speed[8], [11] and [10]. Another type of lane change is called anticipated. This type refers to a lane change that a driver willingly makes to avoid potential congestion in a downstream location [14]. Ahmed [8] stated that the process of LC consists of three main steps: the decision to consider lane change (DLC or MLC), the selection of the target lane and the perception of gap acceptance in the target lane.

II. DATA COLLECTION

A range of methods and equipment was used to capture traffic data for different traffic studies. The nature of the study and the availability of equipment determined the method that should be used. There are two types of measuring data: single point data, such as spot speed, flow, headway, and occupancy, and data measured along segments of highway such as the moving car observer method to estimate speed and flow of traffic [15].

Recently, several methods have been introduced and developed to collect data. However the traditional manual and video recording methods are still the dominant methods used in the UK for the purpose of academic research because of the high cost of more advanced methods compared with the relatively reasonable cost of manual and video methods [7]. Furthermore, videotape-recording systems are ubiquitous tools for investigating some traffic characteristics such as Frequency of lane changing FLC [13], and Gap acceptance [16] and [17].

In addition, the link to the Motorway Incident Detection and Automated Signalling (or MIDAS) data was obtained from the Highway Agency through the initiative of the Civil Engineering Group at Salford University. Two programs have been used to manage the MIDAS data. First is the MIDAS Traffic Data Analysis System (TDAS), which is a Microsoft Access application. It allows the user to record data in the form of tables showing flow, headway and speed for each lane in each minute. The configuration of loop detectors is as shown in Fig. 1.

Manuscript received May 30, 2015.

Dr Hamid Athab Eedan Al-Jameel. University of Kufa, Civil Engineering Department.

Fig. 1 Loop detector configurations in the UK[18].

Secondly, the MIDAS Map Setup gives the locations of loop detectors for the whole of the UK and the name for each detector. Therefore this helps the user to select the location of the appropriate loop detector for various sectors, roads, junctions as well as providing the number the loop. After extracting this information, the TDAS is used to determine the speed, flow, and headway and lane occupancy.

A. FLC

Investigation of the FLC is based on the essential characteristics that determine driver behaviour within traffic streams. There is a need for video recording of real time data to track the movement of vehicles within a certain length of a normal section of a motorway or carriageway. In this study, two sections have been investigated as shown in Table 2.

To ensure normal behaviour for the tested sections, the sections under study have been selected to be free from the influence of areas of turbulence such as merge, diverge and weaving sections. Therefore, the sections, M602 J2-3 and M60 J22-23, have been selected as each is 500m or more in either direction from areas of turbulence.

B. Two lane section

To investigate the FLC behaviour of a normal section with two lanes, the M602 within Manchester has been selected. This section is at the location where Derby road crosses over the two-lane M602 motorway between J 2 and J3.

Two hours 30 minutes of data were collected for a 200m length for each direction by using two video cameras installed on the Derby Road Bridge covering both directions: one orientated towards Manchester and the other away from the city. Data periods of 10-minutes were used for the analysis to reduce the error that would otherwise result from the relatively short distance and time. The behaviour exhibited within this data is similar to the field data observed by Yousif [7] that were obtained from different testing periods; 5-minute periods were adopted by Yousif [7] as shown in Fig. 2. However, there are some differences in the number of FLC instances observed because the percentage of heavy goods vehicles (HGVs) is markedly different: around 5% for this data and some 15% in Yousif's data.

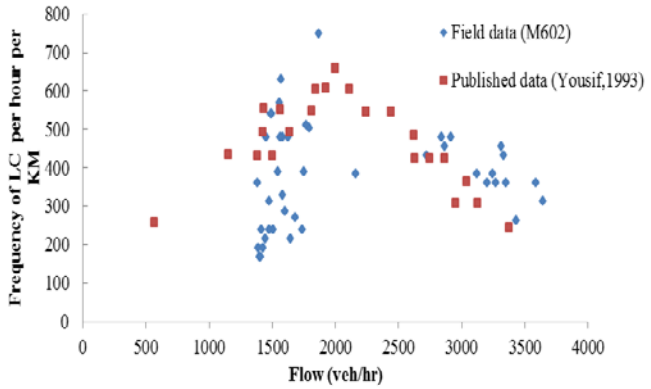

Fig. 2 Frequency of LC with flow within two-lane normal section M602.

It was noted that within the current field data there was a lack of FLC occurrences in the moderate flow range; there being only a single data point within the range 1800 - 2800 vehicles/ hour.

Finally, by comparing the field data with published data for varying percentages of HGVs, it could be concluded that the occurrence and the percentage of HGVs in the traffic flow had a noticeable effect on the FLC but that the actual behaviour of driver was nonetheless approximately the same, with the observance that as flow increases, the FLC increases.

C. Four lane section

Because there is limited data within the literature about FLC behaviour, especially for four lane sections, a four lane normal section within the Greater Manchester city which satisfied normality behaviour as described above has been selected. This section is located on the M60 between J24 and J25.

Two video cameras were installed on the foot bridge above the section of this motorway between J23 and J24. For this site, a length of 250m was covered in both directions.

Fig. 3 shows the relationship between flow and the FLC as observed for each 5 minute period. In this survey, 4 lane flow ranges from 2200 to 4800 vehicles per hour were covered, limited range which is purposely constrained to the low to moderate flow range, with heavy flow conditions being excluded from the data. However, it is may reasonably be postulated that the behaviour of FLC, as observed within the reported flow ranges, increases slightly as flow increases, up to a maximum of 1800 LC per hour per km at a flow of 4200 veh/hr. From that maximum, the FLC decreases slightly to a value of approximately 1600 LC per hour per km. However, there is insufficient data to provide a robust case for how vehicles will behave under heavy flow conditions.

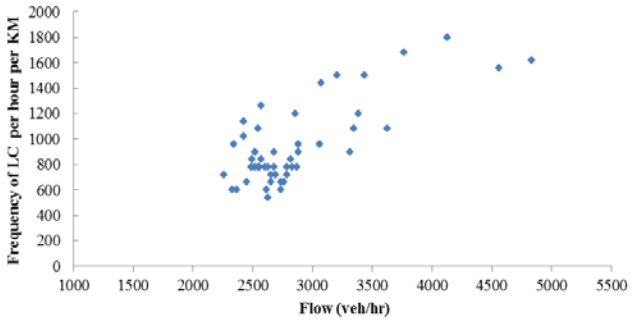

Fig. 3 Frequency of LC for four-lane normal section M60 J23and J22).

Finally, even using the limited range of flow as investigated by this study is sufficient for the derived relationship to be used as a benchmark. The results could be used in the calibration process for the particular range of flow when developing a micro-simulation model.

D. Lane utilization

In theory, and ideally, the LU factor could allow the representation of a sequence of lane change frequency, but because this factor is not widely covered by the existing literature, there has hitherto been insufficient data to allow this. Therefore, in this study a very great quantity of data was obtained and used for three types of normal section: two, three and four lanes. The Highways Agency's MIDAS data was the data source for this analysis. This data has extended over different days, months, and years as shown in Table 3 for the sections under investigation, which as stated, lie outside the influence of "interrupted" sections such as at intersections, and merging, diverging and weaving areas.

The specific reason for studying the lane utilisation factor under a number of different normal sections is to gain understanding of how vehicles behave and are distributed under regimes of different numbers of lanes. In addition, the data allowed the effects of different levels of flow and of types of vehicle (either passenger car or HGV) to be considered. The resulting relationships as described through this section and the following sections will then be used in the simulation model that is being developed by the current study.

For the purpose of this study, lane utilisation under both non-congested and congested conditions was considered since it is known that driver behaviour changes in response to levels of congestion. Lacking data for a range of these conditions could affect negatively the resulting description of traffic behaviour. To differentiate congested from non-congested behaviour, speed has been used as a determining measure. The particular value of 50km/hr has been assumed as a critical value because traffic moving at less than this value correlates with the observance of a breakdown of free flow conditions [19] and [20]. This value was also adopted by Wang[21] as a critical threshold between congested and non-congested conditions in her car-following model.

Information for the selected days was sorted into categories of congested and non-congested conditions. The 24 hour data obtained during the day under different traffic flow provided a robust data base to understand how traffic is distributed amongst the available lanes. The data was aggregated for each five minutes and was then transcribed to obtain the equivalent flow for each hour. Three locations along the motorway were selected. These locations were M602 as a two-lane section, M60 J3 as a three-lane section, and M60 J23 as a four-lane section. Further details about each section are provided in the following sub-sections.

a.Two Lane section

As indicated in Table 4, this section is located on the M602 remote from any merging and diverging regions. Data was obtained from MIDAS data (Loop M602/6056B) for 16 days. Then relevant data was extracted and analysed into five minute segments and separated into two groups: congested and non-congested flow regimes, as shown in Fig. 4.

Fig.s 4-A and B show the lane utilisation under non-congested flow behaviour. Lane utilisation for congested flow behaviour is shown in Fig. 4-C and D. These Fig.s show that drivers distribute themselves equally among lanes. Then further investigation was carried out for lane utilisation under conditions of congestion notwithstanding that these are unusual events, rarely occurring according to the evidence of the MIDAS data. It was found that this occurred on only three out of sixteen days of observations, and that in total there were only two hours of such congestion.

Focusing on the behaviour shown in Fig. 4-A and B, further evidence of atypical behaviour was noted. Such behaviour included making use of only the first lane with no vehicles travelling in the second lane. This behaviour may be acceptable under very low flow conditions. but this behaviour was observed in flow ranges up to 1000 veh/hr. On closer examination, it was found that the period when this behaviour was occurring extended to more than 80 minutes, which indicates that at a point downstream, there was a high probability that the second lane of the M602 may have been closed or closing. Therefore, this period has been excluded from the analysis, and the data was re-analysed as shown in Fig. 5.

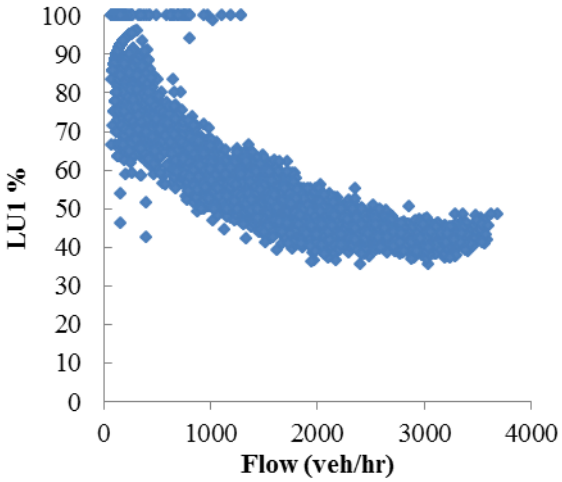

A. 1st lane for non-congested case.

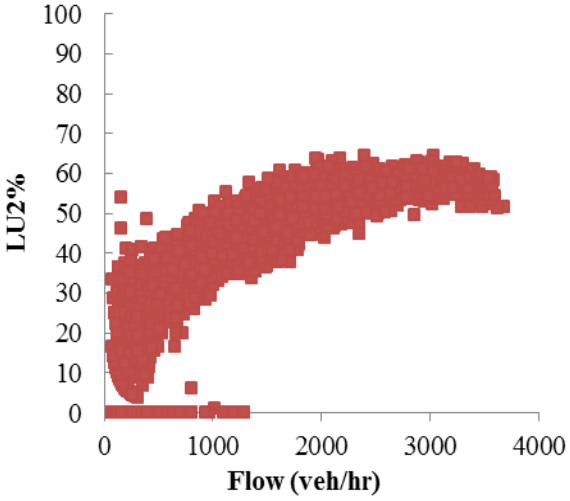

B. 2nd lane for non-congested case.

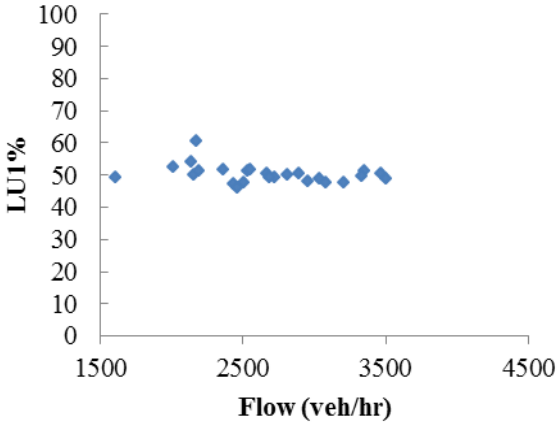

C.1st lane for congested case.

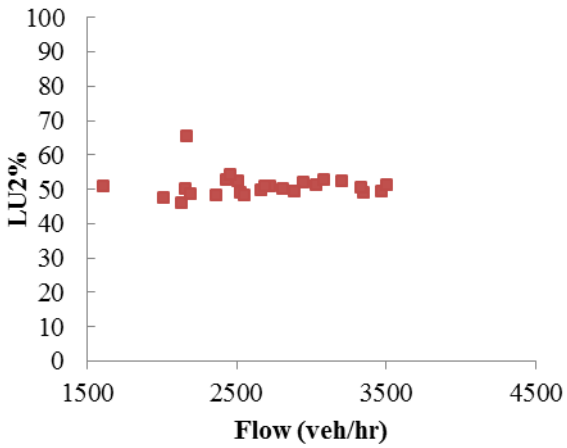

D. 2nd lane for congested case.

Fig. 4 Lane utilisation for two-lane normal section (M602).

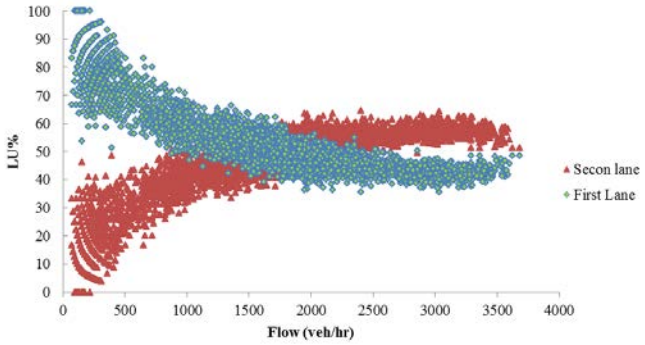

Fig. 5 Filtered lane utilisation for two-lane normal section (M602)

The re-analysis showed a relationship with higher correlation, as indicated in the following equations. The relationship for the second lane has been determined from the following equations:-

$$LU_2 = \begin{cases} 14.716*\ln(Q) - 60.255 & For\ Q > 60 \\ 0.0 & For\ Q < 60 \end{cases} \quad (1)$$

$R^2 = 0.87$

$$LU_1 = 100 - LU_2 \quad (2)$$

Where;
Q is the flow entering the section (veh/hr).
LU_1 is the lane utilisation for the first lane.
LU_2 is the lane utilisation for the second lane.

It can be concluded that these equations can reliably represent lane utilisation when used in a simulation model, because they were obtained from a significantly large amount of data, which included observations of a range of different levels of flow and conditions. To confirm, the details of the data that was collected consist of four days in March (1st,3rd, 5th and 16th in 2010), five days in May (3rd, 4th, 5th, 6th and 7th in 2010) and seven days in

October (1st, 8th, 15th, 22th and 29th in 2010 and 1st and 8th in 2009).

b. Three normal section

The same procedure as described for investigation of the two-lane section has been used for the three-lane normal section. The relevant data has been downloaded from the MIDAS data files (Loop M60 9013B). This section is located on the M60 between J1 and J2 as indicated in Table 4. The data was collected over 21 days divided into 5 days in April (1st, 2nd, 3rd, 4th, and 7th in 2010), 4 days in March (1st, 3rd, 5th and 15th in 2010), 5 days in October (1st, 8th, 15th, 22th and 29th in 2010) and 2 days in October (1st and 8th in 2009). Different days of the week, and different months and years, were used so that different traffic conditions could be included in the analysis.

As carried out for the two lane sections, data from unusual events such blocking a lane or accidents was filtered out, with this being implemented for the sets of data before carrying out any analysis of raw data. Following that, one-minute MIDAS data has been analysed into 5-minute time periods from which the averages of speed and flow from this data were obtained to be used in the further analysis (as was carried out for the previous 2 lane sections and the following for four lanes). Fig. 6 shows the relationships between percentage of lane utilisation and flow for non-congested conditions for the first, second and third lanes, respectively.

These relationships could also be represented by the following equations:

$$LU1 = 446.94(Q) - 0.319 \quad For\ Q \geq 150 \qquad (3)$$

$$R^2 = 0.91$$

$$LU_3 = \begin{cases} -4*10^{-8}(Q)^2 + 0.0096(Q) - 2.2136 & For\ Q \geq 150 \\ 0.0 & For\ Q < 150 \end{cases} \qquad (4)$$

Where;

LU3 is the lane utilisation for the third lane (%).

The relationships for the first and third lanes are more robust than that for the second lane (R^2 = 0.5245). Therefore the lane utilisation (LU2) of the second lane has instead been extracted from the following equation:

$$LU2 = 100 - LU1 - LU3 \qquad (5)$$

Fig. 7 shows the relationships between lane utilisation and flow under congested conditions. In these conditions, the lane utilisation for the first lane is higher at the point of flow breakdown as shown in Fig. 7, because the third lane is the first to suffer from a marked decrease in flow under such conditions, and significantly before any such affect upon the other lanes. However, the observed range of flow among the three lanes is approximately equal.

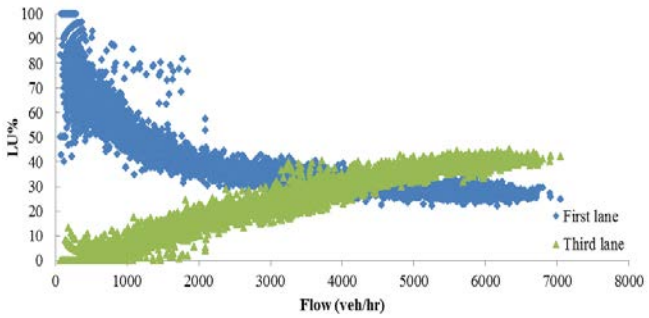

A. Lane utilisation for the first and third lane.

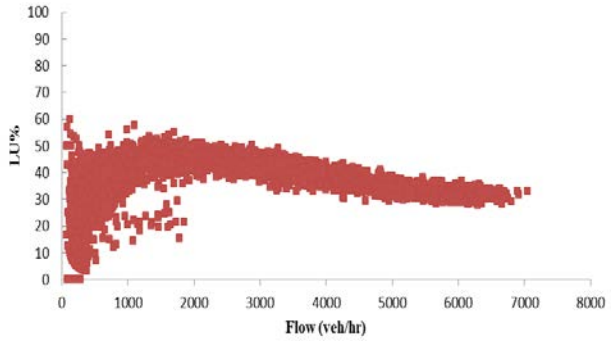

B. Lane utilisation for the second lane.

Fig. 6 Lane utilisation for three-lane normal section (M60).

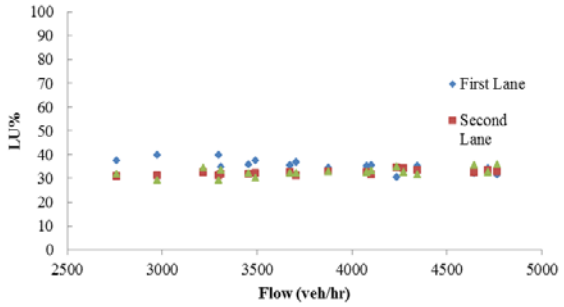

Fig. 7 Lane utilisation for three-lane normal section (M60).

c. Four normal section

The section between J22 and J23 on the M60 was used to investigate the lane utilisation for a four-lane section. The MIDAS loop detector used as a source for this data is (M60/9035B). The days data was collected were 5 days in April (1st, 2nd, 3rd, 4th, and 7th in 2010), 3days in March (1st, 3rd and 5th in 2010), 5 days in October (1st, 8th, 15th, 22th and 29th in 2010) and 2 days in October (1st and 8th in 2009). The 20 days of data collected for this section of the motorway did not include any days or times of congested conditions

Fig. 8-A shows relationships for lane utilisation for the first and third lanes, with Fig. 8-B representing lane utilisation for the second and fourth lanes. These relationships for lane utilisations are also represented by the following equations:

$$LU_1 = 306.56(Q)^{-0.337} \quad For \quad Q \geq 28 \qquad (6)$$
$$R^2 = 0.81$$
$$LU_3 = 4(10^{-10})(Q)^3 - 5(10^{-6})(Q)^2 + 0.0224(Q) + 4.688 \quad For Q \geq 400 \qquad (7)$$
$$R^2 = 0.85$$
$$LU_4 = 5(10^{-7})(Q)^2 + 0.0028(Q) - 0.7871 \quad For\ Q \geq 281 \qquad (8)$$
$$R^2 = 0.93$$

The weakest relationship among the lanes is that of the second lane as shown in Fig. 8-B. Consequently, the LU2 can be extracted from the following equation:

$$LU_2 = 100 - LU_1 - LU_3 - LU_4 \qquad (9)$$

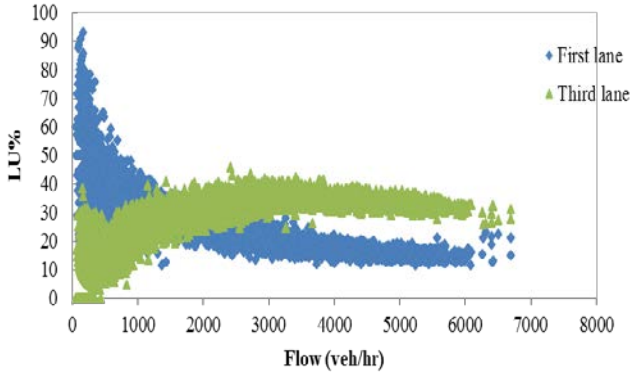

A. Lane utilisation for the first and third lanes.

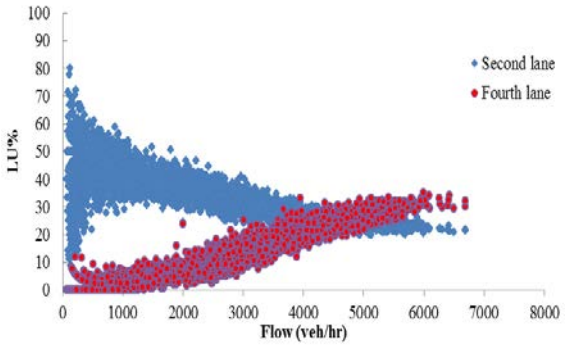

B. Lane utilisation for the second and fourth lanes.

Fig. 8 Lane utilisation for four-lane normal section (M60).

Fig. 8 shows that at low levels below 2000 veh/hr, flow concentrates, in the second lane, and that above this level, drivers tended to transfer to the third and fourth lanes to seek greater speed advantage. An interpretation of this phenomenon is that when flow is low, the third and fourth lanes serve as passing zones only. However, as the flow increases, overtaking drivers in the third and fourth lanes will not accept returning to the slower lanes because they consider that they would have to reduce their speed and accept greater delay.

III. Conclusions and Recommendations

The main points of this study can be summarised as:

1. It was found from field data that relationships can be established between the FLC and the flow rate for two and four lane sections. These relationships will be used for calibration and validation for any simulation model.
2. Various lane utilisation relationships were investigated for different types of normal sections (two, three, and four) under varying levels of flow and other conditions. These relations will be used as initial inputs to distribute traffic across different lanes in any simulation model.
3. The LU has also been investigated for HGVs. This is also an important factor to allow accurate calibration or validation for a simulated model.
4. Using the MIDAS data has provided sufficient information about the flow regime on normal section which will be used in investigating the LU factor.
5. The next step of this study is to use this data in the calibration and validation of a simulation model that has already been developed by the author.

IV. References

1. Taylor, M., Bonsall, P., and Young, W.: Understanding Traffic Systems: Data, Analysis and Presentation. Aldershot, Ashgate, (2000), UK.

2. Cassidy, M., and Rudjanakand, J.: Increasing the Capacity of an Isolated Merge by Metering its on-ramp. *Transportation Research B: Methodological*, 39(10), (2005), pp.896-913.

3. Bertini, R., and Leal, M.: Empirical Study of Traffic Features at a Freeway Lane Drop. *Journal of Transportation Engineering*, 131 (6), (2005), pp.397-407.

4. Ahn, S., and Cassidy, M.: Freeway Traffic Oscillations and Vehicle Lane-changing Manoeuvres. In: *Proceedings of 17th International Transportation and Traffic Theory*, London, UK, (2007), pp.691-710.

5. Sparmann, I.: The Importance of Lane-changing on Motorway. *Traffic Engineering+ Control*, (20), (1979), pp.320-323.

6. Gipps, P.: A Behavioural Car-Following Model for Computer Simulation. *Transportation Research Part B*, (15), (1981), pp.105-111.

7. Yousif, S.: *Effect of Lane Changing on Traffic Operation for Dual Carriageway Roads with Roadworks*. (PhD Thesis), University of Wales, (1993), Cardiff.

8. Ahmed, K.: *Modelling Drivers' Acceleration and Lane Changing Behaviour*. (PhD Thesis), Massachusetts Institute of Technology, (1999), USA.

9. Hidas, P.: Modelling Lane Changing and Merging in Microscopic Traffic Simulation. *Transportation Research Part C*, (2002), pp.351-371.
10. Hidas, P.: Modelling Vehicle Interactions in Microscopic Simulation of Merging and Weaving. *Transportation Research Part C*, (13), (2005), pp.37-62.
11. Toledo, T.: *Integrated Driving Behaviour Modelling.* (PhD Thesis), Massachusetts Institute of Technology, (2003), USA.
12. Choudhury, C.: *Modelling Driving Decision with Latent Plans.* (PhD Thesis), Massachusetts Institute of Technology, (2007), USA.
13. Sultan B., and McDonald, M.: The lane changing process: Data analysis and modelling behaviour. *Traffic Engineering + Control*, 43(5), (2001), pp.202- 207.
14. Kim, J., Kim, J., and Chang, M.: Lane Changing Gap Acceptance Model For Freeway Merging in Simulation. *Journal of Civil Engineering*, Canada, (2008), pp. 301-311.
15. Pakshir, A., and Farajollahzadeh, R.: Traffic Characteristics and Moving Car Observer. The proceeding of the 1st Iranian Students Scientific Conference in Malaysia, (2010).
16. Zheng, P.: *A Microscopic Simulation Model of Merging Operation at Motorway On-ramps.* (PhD Thesis), University of Southampton, Southampton, (2003), UK.
17. Kusuma, A., and Koutsopoulos, H.: Critical Gap Analysis of Dual Lane Roundabouts. In: 6thInternational Symposium on Highway Capacity and Quality of Service, Stockholm, Sweden, Procedia Social and Behavioral Sciences, (16), (2011), pp.709-717.
18. ***www.google.com/earth/download-earth.html*** *(Showing a map of the sites used for the survey-Accessed 01/08/2010).*
19. Hounsell, N., and McDonald, M.: An investigation of flow breakdown and merge capacity on motorways. Contractor Report 338, (1992), UK: Transport Research Laboratory.
20. Dijker, T, Bovy,P.,and Vermijs, R.: Car-Following Under Congested Conditions: Empirical Findings. *Transportation Research Record*, (1644), (1998), pp.20-28.
21. Wang, J.: *A Merging Model for Motorway.* (PhD Thesis), University of Leeds, (2006), Leeds.

TABLE I
CLASSIFICATION OF LC MODELS.

The model	The assumption	Limitations
Safety Based Model such as Gipp's model.	LC depends mainly on the deceleration of the new follower in the target lane	This model does not consider the desire to change lane due to being delayed behind slower vehicle.
Threshold model such SISTM model.	LC depends mainly on thresholds such as speed advantage and the relative distance	These factors are difficult to calibrate.
Action point model developed by Sparman[5].	LC based mainly on capturing the behavior of drivers in estimating the relative speed and distance.	This model suffers from uncertain assumed values.

TABLE 2
NORMAL SECTION OF FIELD DATA.

Section	Location	Direction	Date, day and Time	Description
M602	At crossing of Derby Road with M602 between J2 and J3.	Both directions	16/03/2010, Tuesday, evening peak for 145 minutes.	Two-lane normal section more than 600m away from merging or any traffic interruptions in both directions.
M60	Between J23 and J22.	Both directions.	11/03/2010, Thursday, morning peak.	Four lane section.

TABLE 3
DETAILS OF LOCATIONS FOR LANE UTILIZATION.

Site	Type of section	Location	Direction	Days of investigations
M602	Two lane	At crossing of Derby Road with M602	Toward north direction (out of Manchester).	16 days (24 hours in each day).
M60 J1 and J2	Three lane	At crossing with Healthside Road.	Toward East direction.	21 days (24 hours in each day).
M60 J22 and J23	Four lane	Between J22 and J23.	Toward East direction.	20 days (24 hours in each day).

3D Preliminary Survey Planning and Design Route Road Using Geomatic Technical and Data

Wafaa Kh. Leabi, Abdulrazzak T. Ziboon, Khaled I. Hasoon

***Abstract*—The problem of determining the route between two locations is one of the important application in highway engineering to determine the purpose like topography and land use. utilizing geomatics engineering, includes field survey remote sensing and GIS techniques to prepare the digital details map to study and evaluate the route location. The presented work includes different stages: the first one required image processed at high resolution satellite (quick bird) for the region under study (Karbala province). The image processing includes geometric correction using (18) selected ground control point GCPs from field survey. The next stage using DEM for Karbala of the export point (x, y, z) to AutoCAD for drawing the alignment of road and building the profile with cross section. Finally, calculating the volume (cut& fill) for determining the best economic rout and export route to GIS to determine the land use from cadastral map and producing the digital map of study area.**

***Index Terms*— satellite image, preliminary survey, design road**

I. Introduction

Geomatics engineering has applications in many field such as agriculture, industry and urban development. One of these applications is highway engineering. and mapping ….etc [1]. Many reasons have been taken to utilize digital requirements geometric correction for highway application. First the road alignment has been made a very large area secondly terrain (slope, geology, surface, materials and water conditions) and its influence on location and design of road. Remote sensing contributes most significantly to highway engineering during reconnaissance of rout planning when general information is needed for large area of terrain rather than specific information for small area as would be required for the final alignment. Highway survey usually involve measuring and computing horizontal and vertical curve in geometric design of road [2].

Manuscript received May 20, 2015. Revised August 6, 2015, Accepted August 16, 2015.

W. Kh. Leabi is with the University of Mustansiriya, College of engineering, Department of Transportation and High Way.
(email: wleabi@gmail.com).
Prof. Dr. A. T. Ziboon, is with University of Technology, Department of Civil (e-mail: razzak1956@yahoo.com).
Dr Kh. I. Hasoon is with the Ministry of Science and Technology.
(e-mail: dr.khalid68@yahoo.com).

II. The Proposed Design

A. Data Analysis and Computation

Highway survey techniques have been applied during the past to rapid development of electronic equipment and computer programming. These technique includes three general conventional ground survey, remote sensing and GIS based on information technology and graphic techniques [3]. The work in this research can be summarized in to following stages.

a- Use the satellite image (quick bird) with 0.6m resolution have been selection region of study (Karbala province) due to preparation the land-use layer and its corresponding spatial Data of this study.

b- Field survey includes measuring ground control points (GCPs) (18) using differential GPS, (15) GCPs measured in Trimble (5700) and (3) GCPs using Topcon (GR3) these point taken from many different location in Karbala province, as shown in figure 1.

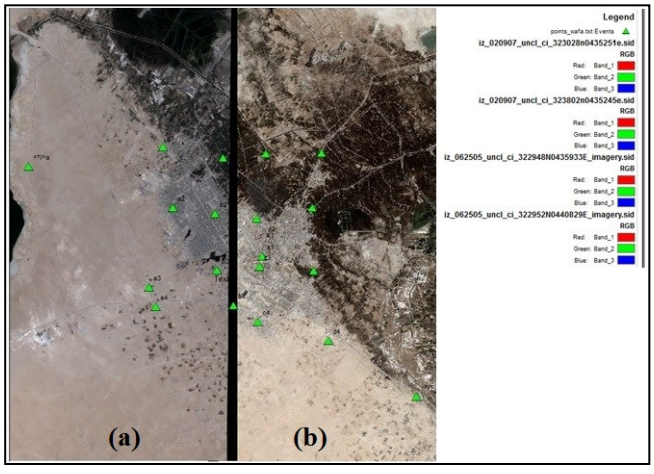

Fig. 1: (a) Q.B, Digital Globe comp. (0.6m) Satellite Image and (b) High Resolution Digital Aerial Image (0.1m) for Karbala Province

B. Measuring GCPS

The measured points by GPS r1(cement factory),r2(gas

station),r3(company canning poultry) have sent to Global Navigation Satellite System (GNSS) NET for correction process of GCPs as shown in table 1 and are demonstrated in the GNSS figure 2. The following is the received report from GNSS that gave the details about the three measured GPS points r1,r2,r3.

Report from GNSS
Project
Project name: wafaa.ttp
Project folder: C:\Users\kasim\Desktop\bgh\wafaa-4
Creation time: 3/23/2014 9:12:23 PM
Created by:
Comment:
Linear unit: Meters
Angular unit: DMS
Projection: UTMNorth-Zone_38 : 42E to 48E
Datum: WGS84
Geoids': EGM2008

TABLE 1
POINT SUMMARY

Point Summary						
Name	Longitude	Latitude	Ell.Height (m)	Grid Easting (m)	Grid Northing (m)	Elevation (m)
Base irrigation directing	44°02'01.73100"E	32°36'15.54086"N	25.835	409340.413	3607834.778	26.978
r1 cement factory	44°04'02.19792"E	32°33'40.09091"N	26.869	412438.482	3603019.789	28.157
r2 gas station	43°58'06.20067"E	32°38'57.15485"N	28.932	403249.463	3612869.317	29.807
r3 company canning poultry	44°06'18.88044"E	32°35'59.22945"N	25.418	416038.915	3607273.825	26.852

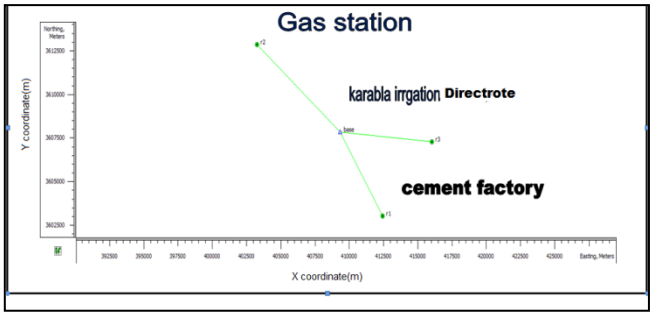

Fig. 2.A: GCPs Distribution

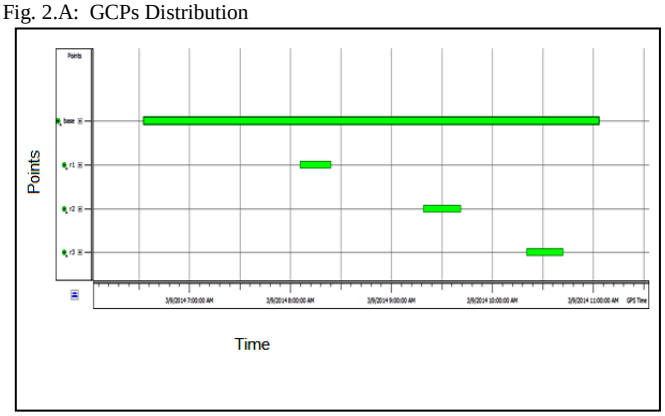

Fig. 2.B: Time Scheme of GCPs Measured

C. Satellite Image Processing

The procedure of satellite image processing includes geometric correction using ground control points (GCPs) taken from field survey after correction and corresponding to the same point found in satellite image coverage distribution GCP. Also, This step includes georeference to compute the rectified root mean Square RMS of GCPs and its residuals by using GIS VERSION 9.3 soft ware which contains georeference tools, columns for the X and Y residuals. Residuals are the distances between the source and retransformed coordinates in one direction. The Y residual is the distance between the source Y coordinate and the retransformed Y coordinate. If the GCPs are consistently off in either the X or the Y direction, more points should be added in that direction, as shown in table (2).

This is a common problem in off-nadir data. The RMS error of each point is reported to evaluate the GCPs [4]. RMS is calculated by using equation (1).

$$R_i = \sqrt{XR_i^2 + YR_i^2} \quad (1)$$

Where:

Ri = the RMS error for GCP*i*

XRi = the X residual for GCP*i*

YRi = the Y residual for GCP*i*

C.1 Total RMS Error

From the residuals, the following calculations are made to determine the total RMS error, the X RMS and the Y RMS errors, as the following equations (2), (3) and (4).

$$R_x = \sqrt{\frac{1}{n}\sum_{i=1}^{n} \mathrm{XR}_i^2} \quad (2)$$

$$R_y = \sqrt{\frac{1}{n}\sum_{i=1}^{n} \mathrm{YR}_i^2} \quad (3)$$

$$T = \sqrt{R_x^2 + R_y^2} \quad (4)$$

where,

R_x = *X RMS error*
R_y = *Y RMS error*
T = total RMS error
n = the number of GCPs
i = GCP number
XR_i = *the X residual for* GCP_i
YR_i = *the Y residual for* GCP_i

The (15) GCPs cover the case study and their geometric corrections operation are shown in table 2. While, the georeference implementation results on satellite image are shown in figure 3.

TABLE 2
GCPS GEOMETRIC CORRECTION

POINT	X	Y
A1	403137.511	3612851.506
A2	403624.221	3609840.121
A3	402463.310	3605884.603
A4	402789.991	3604913.0434
B1	406136.908	3612186.501
B2	405725.486	3609521.645
B3	405793.113	3606717.572
B4	406609.792	3604959.765
C1	408230.267	3612467.108
C2	407754.855	3609277.368
C3	407909.125	3606904.42
C4	407827.007	3604165.158
D1	410969.328	3612548.637
D2	410514.263	3609832.561
D3	410581.004	3606703.283

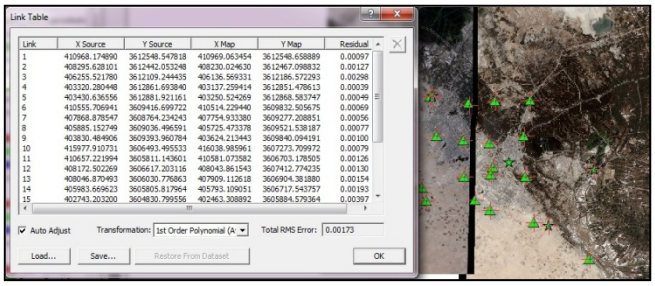

Fig. 3: Georeference on Satellite Image

D. Preliminary Survey

The preliminary survey involve digital elevation model (DEM) and Global Mapper software. The terms digital elevation model (DEM), digital terrain model (DTM) and digital surface model (DSM) are commonly used in scientific literatures. In most cases the term digital surface model represents the earth's surface and includes all objects on it. In contrast to a DSM, the digital terrain model represents the bare ground surface without any objects like plants and buildings [5]**.** Construction of digital elevation model(DEM), for the region study and exported to the Global Mapper software, after then the DEM for region study has been subsetting for later processing.

Global Mapper's 3D modeling and analysis functionality has made a major development focus over recent years and for many users. The utilization of the Z-value is the most important facet of the application.

E. Autocad Civil 3D Software

The exported data of the DEM are set region of (x, y, z) points, these data have been processed using AutoCAD Civil 3D, the functions of the Civil 3D ware is to design the final route of the suggested road. As a result, a change to one part of the design propagates throughout the entire project, greatly reducing drafting errors as well as the time it takes to implement design changes and evaluate multiple design scenarios. For example, if you adjust the vertical design alignment, Civil 3D automatically updates the road model, redisplays proposed contours, recalculates volumes, updates profile labels, and corrects section plots for the road [6].

F. Design Road

The civil 3D AutoCAD software can automatically design the road by drawing surface from the imported coordinate points (x, y, z) by using software terrain command, next step is the alignment drawing of route road by using software alignment command. Hence, the drawing profile is prepared along with its design finished line. Then, the vertical curve (crest and sag) is designed with minimum radius (R), as shown in equation (5) [7].

$$R_{min} = V2/127\,(e + f) \tag{5}$$

F.1 Design Crest Vertical Curves

Minimum lengths of crest vertical curves based on sight distance criteria generally are satisfactory from the standpoint of safety, comfort, and appearance. An exception may be at decision areas, such as sight distance to ramp exit gores, where longer lengths are needed; for further information, refer to the section of this chapter concerning decision sight distance.

The parameters used in determining the length of a parabolic crest vertical curve needed to provide any specified value of sight distance. The vertical curve is shown in figure 4.

The basic equations for length of a crest vertical curve in terms of algebraic difference in grade and sight distance are as follows.

When S is less than L, (m)

$$L = \frac{AS^2}{100(\sqrt{2h1}+\sqrt{2h2})^2} \tag{6}$$

when S is greater than L

$$L = \frac{2S - 200\sqrt{(\sqrt{h1}+\sqrt{h2})^2}}{A} \tag{7}$$

where,

L = length of vertical curve, m;
S = sight distance, m;
A = algebraic difference in grades, percent;
h1 = height of eye above roadway surface, m;
h2 = height of object above roadway surface, m

F.2 Design Sag Vertical Curves

At least four different criteria for establishing lengths of sag vertical curves are recognized to some extent. These are (1) headlight sight distance, (2) passenger comfort, (3) drainage control, and (4) general appearance [8].

Headlight sight distance has been used directly by some agencies and for the most part is the basis for determining the length of sag vertical curves recommended here. When a vehicle traverses a sag vertical curve at night, the portion of highway lighted ahead is dependent on the position of the headlights and the direction of the light beam. A headlight

height of 600 mm [2 ft] and a degree upward divergence of the light beam from the longitudinal axis of the vehicle is commonly assumed. The upward spread of the light beam above the 1-degree divergence angle provides some additional visible length of roadway, but is not generally considered in design. The following equations show the relationships between S, L, and A, using S as the distance between [7]. Design sag curve is depended on the following equation.

When S is less than L(m)

$$L = \frac{AS^2}{200[0.6(tan10)]} \quad (8)$$

Or

$$L = \frac{AS^2}{120+3.55} \quad (9)$$

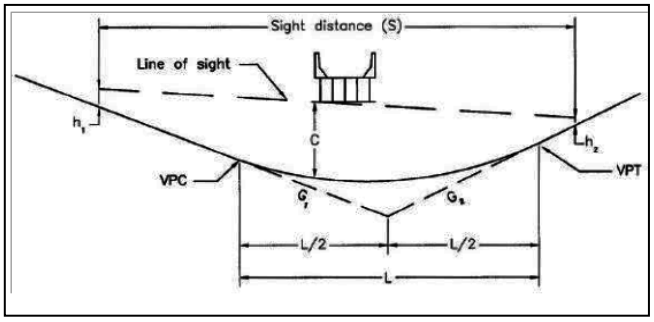

Fig. 4: Vertical Curve

III. Results and Discussion

A. Cadastral Map

The word Cadastral refers to land ownership information. This information has references to location of the parcels. In Sweden, the word has a more general meaning. It includes a lot of other information connected to the land parcel, like ownership and rights to land, taxation information, buildings and real property information, mortgages, plans, regulations etc [9].

The final tuning for the route road has been performed by using the available cadastral map with large scale between (1:2.5 to 1:10000), this process is implemented by avoiding the private parcels from the suggested route road as shown in figure 5.

B. Volume Cut and Fill

The quantities volume details a small part of the route road within 60 km length have been contain in design on (604+00 stations), the small part beginning from station(0+00) to station(20+00) have been illustrate in table (3).

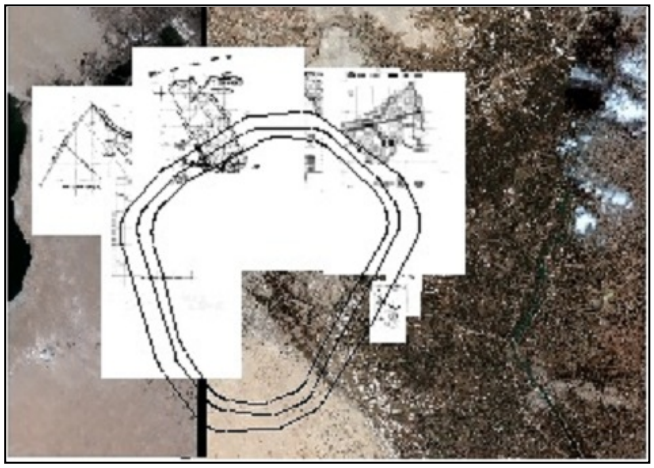
Fig. 5: Cadastral Map on Satellite Image

TABLE 3
QUANTITIES VOLUME CUT AND FILL

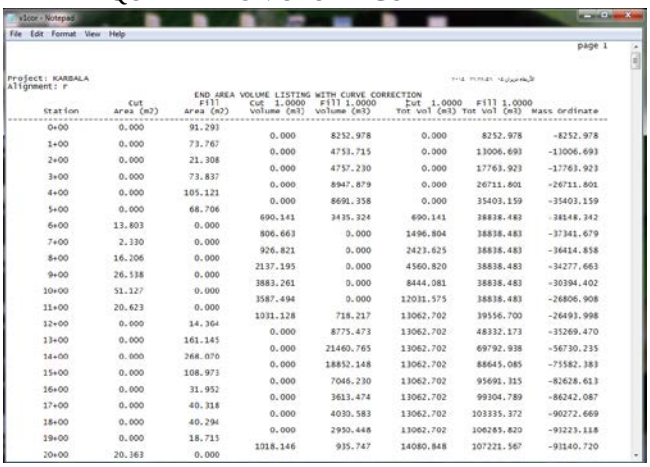

Project: KARBALA
Alignment: r

END AREA VOLUME LISTING WITH CURVE CORRECTION

Station	Cut Area (m2)	Fill Area (m2)	Cut 1.0000 Volume (m3)	Fill 1.0000 Volume (m3)	Cut 1.0000 Tot vol (m3)	Fill 1.0000 Tot vol (m3)	Mass Ordinate
0+00	0.000	91.293					
			0.000	8252.978	0.000	8252.978	-8252.978
1+00	0.000	73.767					
			0.000	4753.715	0.000	13006.693	-13006.693
2+00	0.000	21.308					
			0.000	4757.230	0.000	17763.923	-17763.923
3+00	0.000	73.837					
			0.000	8947.879	0.000	26711.801	-26711.801
4+00	0.000	105.121					
			0.000	8691.358	0.000	35403.159	-35403.159
5+00	0.000	68.706					
			690.141	3435.324	690.141	38838.483	-38148.342
6+00	13.803	0.000					
			806.663	0.000	1496.804	38838.483	-37341.679
7+00	2.330	0.000					
			926.821	0.000	2423.625	38838.483	-36414.858
8+00	16.206	0.000					
			2137.195	0.000	4560.820	38838.483	-34277.663
9+00	26.538	0.000					
			3883.261	0.000	8444.081	38838.483	-30394.402
10+00	51.127	0.000					
			3587.494	0.000	12031.575	38838.483	-26806.908
11+00	20.623	0.000					
			1031.128	718.217	13062.702	39556.700	-26493.998
12+00	0.000	14.364					
			0.000	8775.473	13062.702	48332.173	-35269.470
13+00	0.000	161.145					
			0.000	21460.765	13062.702	69792.938	-56730.235
14+00	0.000	268.070					
			0.000	18852.148	13062.702	88645.085	-75582.383
15+00	0.000	108.973					
			0.000	7046.230	13062.702	95691.315	-82628.613
16+00	0.000	31.952					
			0.000	3613.474	13062.702	99304.789	-86242.087
17+00	0.000	40.318					
			0.000	4030.583	13062.702	103335.372	-90272.669
18+00	0.000	40.294					
			0.000	2950.448	13062.702	106285.820	-93223.118
19+00	0.000	18.713					
			1018.146	935.747	14080.848	107221.567	-93140.720
20+00	20.363	0.000					

IV. Conclusion

By using geomatics techniques, the following points may be drawn.

1) It is concluded that is not necessary to cover all region study with the high resolution image (0.1m) because of the existents of blank (not used area) special for that region with slow variation in terrain.
2) Throughout the geometric correction processing, it is that the used GPS device type (Topcon with accuracy (3mm+5mm) is slightly better than GPS device type (Trimble 5700 with accuracy (5mm+5mm).
3) It is concluded that there is integrated relationship between these stages.
4) Using AutoCAD Civil 3D software yields high accuracy results and decreasing the time required and effort.
5) The cadastral map with its updated land-use maps are very important in final drawing for the route road.

REFERENCES

[1] Omer Ali Alahbaby, "The Use of Remote Sensing And GIS Techniques In Selecting The Best Highway Location for Mosul City", University Of Technology, Bagdad, 2005, pp.2-30.

[2] Elsayed Hermas and Islam Abo El-Magd, "Land Use Mapping For Path Selection of Strategic Road Using Egypt Sat-1 Imagery", ENGINEERING@UNSW UNS, 2005, pp. 2-13.

[3] Bedru Sherefa Muzein, "Remote Sensing & GIS for Land Cover/ Land Use Change Detection and Analysis In The Semi-Natural Ecosystems and Agriculture Landscapes of The Central Ethiopian Rift Valley" Dresden, Germany, 2006.

[4] Field Guide, Fifth Edition Erdas, Inc. Atlanta, Georgia, 1999.

[5] Li, Z., Zhu, Q. and Gold, C., "Digital Terrain Modeling: Principle and Methodology, CRC Press, Boca Raton, 2005.

[6] Eric Colburn, PLS, To Civil 3D 237A1-050000-PM02A, June 2013.

[7] Nicholas J.Garber, Lester A. Hoel, "Traffic and Highway Engineering", Second Edition, Department of Civil Engineering University of Virginia, 1997.

[8] Policy, "Geometric Design of Highways and Streets" Fourth Edition, 2004.

[9] Carmen Conjeo. F, "Spanish Cadastral Information System" Deputy for the G. Sub. for Studies and Information System, 2003.

Influence of Selected Additives on Warm Asphalt Mixtures Performance

Asst. Prof. Dr. Mohammed Abbas Hasan Al-Jumaili
Dept. of Civil Engineering, Faculty of Engineering – University of Kufa
E-mail: mohammedah.aljumaili @uokufa.edu.iq

Abstract— **Warm Mix Asphalt (WMA) is a technology that allows significant lowering of the mixing and compaction temperature of conventional Hot Mix Asphalt (HMA). This research presents the results of laboratory tests conducted to evaluate the properties and performance of warm mix asphalt. The WMA has been prepared from two asphalt grades and one aggregate source with two additives (Aspha-min® and Sasobit®). The crumb rubber is also added to WMA which is prepared with Aspha-min® and Sasobit® to evaluate effect of crumb rubber on WMA properties. The results of the study indicated that the two additives to the warm asphalt affected the mixture properties differently. When the mixture properties were compared, it was observed that Aspha-min® reduced the indirect tensile strength and resilient modulus values of the mixes, the two WMA additives increased the rut depths of the mixes, and both the additives reduced the tensile strength ratio of the mixes. The crumb rubber improved the properties of WMA by increasing the tensile strength , fatigue life and tensile strength ratio and relatively decreasing rut depth as compared with WMA without crumb rubber.**

Key words: Aspha-min®, indirect tensile strength, indirect tensile resilient modulus, indirect tensile fatigue, rut depth, Sasobit®, and warm mix asphalt (WMA).

I. INTRODUCTION

Asphalt mixtures could be classified into different categories such as hot mix asphalt (HMA), cold mix asphalt and warm mix, which is less common than the others. The author reported that hot mix asphalt properties are much better than cold mix asphalt. Therefore, HMA is mainly used for a pavement with high volume traffic [1]. Moreover, the temperature of the mix depends mainly on the type of mix and grade of binder. In general hot mix asphalt properties are much better than cold mix asphalt so HMA is being used for the higher volume traffic. The type of mix and grade of any binder largely governs the temperature of the mix [1]. To overcome some of these problems, a study conducted by Kolo Veidekke suggested the asphalt mix at somewhat lower temperatures than conventional HMA that was called as warm asphalt [2]. The warm mix asphalt (WMA) is an asphalt mixture which is mixed at temperatures lower than conventional hot mix asphalt. Typically, the mixing temperatures of warm mix asphalt range from 100 to 140 °C compared to the mixing temperatures of 150 to 180 °C for hot mix asphalt [3], [4].

Probably due to their relatively higher prices of fossil fuels and asphalt, Europe [2], South Africa [5], and Australia [3] began early to examine the benefits and performance of WMA. Although WMAs have been used in the USA in 2002, they are being evaluated at a rapidly increasing rate.

There is no need for a major plant modification to the existing HMA plant system in order to obtain WMA. The WMA technologies are original and the manufacturing processes are various from the others (*NCAT, FHWA*). Aspha-min® could be defined as a fine powder. This powder releases its hydration bound water and creates foaming to asphalt binder, the lubricating action keeps the mix workable at a temperature range between 130-140 ^{0}C [6]. Sasobit® contains the organic additives which are mixed with asphalt binder, which melts at about 100 ^{0}C and these chemically change the temperature -viscosity behavior of the asphalt binder. So the workability of the mix is acceptable at a low temperature of 90 ^{0}C [6].

The rutting resistance of HMA and WMA mixtures (as measured using the Asphalt Pavement Analyzer, APA) was more linked to the aggregate type than to the WMA technology [7]. The Sasobit® additive yielded the lowest rut depths, whereas the mixes containing Aspha-min® and Evotherm have APA rutting characteristics similar to the control HMA mixtures. On the other hand, reference [8] reported that the use of WMA technologists will not significantly influence rutting and fatigue performance. However, authors found no significant difference in the level of moisture sensitivity between the control HMA and the WMA mixtures.

In general, there are two categories of crumb rubber mix asphalt: the wet process and the dry process. The wet process is the most efficient in improving properties of an asphalt mixture [9]. Crumb rubber is known to absorb liquids and swell, depends on the temperature and viscosity of the liquids it is absorbing [10]. The interaction of the rubber particles with the asphalt can be affected by several factors such as temperature and type of mix, rubber size and texture, and chemical composition of the asphalt [11].

II. AIM OF THE STUDY

In light of the above, various binder properties and warm asphalt additive type affect the performance of the warm mix such as the moisture susceptibility, rutting potential and fatigue life. So a thorough understanding of the properties and performance of the warm mixture technologies is necessary in order to be able to implement WMA safely, especially since WMA is a relatively new topic in Iraq, and no thorough research has been conducted to investigate many aspects of warm asphalt. The current study aims to evaluate the influence of selected two additives (Aspha-min® and Sasobit®) on the warm mix asphalt properties and performance (the indirect tensile strength, rutting, potential fatigue life and moisture susceptibility).

III. EXPERIMENTAL WORK

A. Materials

The experimental part of this study has been conducted using control mixture (without any WMA additives) and two commercially available WMA additives (Aspha-min® and Sasobit®).The materials used in this work, namely asphalt , aggregate , fillers were characterized using conventional tests and results were compared with State Corporation for Roads and Bridges specifications (SCRB, R/9,2003) [12].

Asphalt cements 40/50 and 60/70 brought from Daurah refinery with the physical properties given in Table I were used within this research. The aggregate used in this work was crushed quartz obtained from Al-Nibaie quarry .The coarse and fine aggregates used in this work were sieved and recombined in the proper proportions to meet the type IIIA mixes of wearing course gradation as required by SCRB specifications (SCRB, R/9,2003) [12]. The gradation for the aggregate is shown in Table II . Routine tests were performed on the aggregate to evaluate their physical properties. The results together with the specification limits as set by the SCRB are summarized in Table III. Test results show that the chosen aggregate met the SCRB specifications.

TABLE I

PROPERTIES OF USED ASPHALT CEMENT

Property	ASTM Designation	Test Results		Requirements Penetration –Graded Asphalt Cement	
				(40/50)	(60/70)
1.Penetration at 25 ^{o}C , (0.10mm)	D5	48	66	40-50	60-70
2. Ductility at 25 ^{o}C , (cm)	D113	110	120	>100	>100
3.Specific gravity at 25 ^{o}C	D70	1.03	1.01	------	-----
4.Flash point ,(^{o}C)	D92	275	249	>232	>232
5.Solubility in trichloroethylene, (%wt)	D2042	99.37	99.26	>99	>99
6.Residue from thin –film oven test - Retained penetration , % of original -Ductility at 25 ^{o}C, (cm)	D1754 D5 D113	 68 57	 61 73	 >55 >25	 >52 >50

TABLE II

SELECTED MIX GRADATION FOR THE TYPE IIIA MIXES OF WEARING COURSE

Sieve	19 mm	12.5 mm	9.5 mm	No.4	No.8	No.50	No.200
% Passing	100	95	83	59	43	13	7

The filler is a non- plastic material that passing sieve No.200 (0.075 mm). In this work, the asphalt mixes were prepared using limestone dust as mineral filler at a content of 7 percent; this content represents the mid-range set by the SCRB specifications for the type III A mixes of wearing course. The limestone dust was obtained from lime factory in Karbala governorate, south east of Baghdad. The physical properties of the fillers are presented in Table IV below.

TABLE IV

PROPERTIES OF LIMESTONE DUST FILLER

Physical Properties		
Specific gravity	Surface area (m^2/kg)	% Passing sieve No.200(0.075mm)
2.41	244	94

Aspha-min® and Sasobit® were utilized as WMA additives in this work. Aspha-min® powder is a sodium–aluminum–silicate crystal, which is hydrothermally crystallized into fine powder. The addition of Aspha-min® (containing 21% water by weight) into the warm mix causes the release of all the crystalline water and forming a very fine water spray and a volumetric expansion of bitumen. This volume expansion will increase the workability and the compatibility of the mixture at lower temperatures [13].

Sasobit® is a Sasol Wax company production and is a fine crystalline, long-chain aliphatic polyethylene hydrocarbon extracted from coal gasification using the Fischer–Tropsch (F–T) process. Sasobit® forms a homogenous solution with the base bitumen when mixed at a rate of 1.5% by weight of the bitumen, and reduces the bitumen viscosity. It is completely soluble in asphalt at temperature higher than 98 and it has ability to reduce the viscosity of asphalt .This can reduce the workability temperature by 15 – 55 ^{o}C [14].

TABLE III

PHYSICAL PROPERTIES OF AGGREGATES

Property	ASTM Designation	Test results	SCRB specifications
Coarse aggregate			
• Bulk specific gravity	C 127	2.614	….
• Apparent specific gravity	C 127	2.686	….
• Percent wear by Los Angeles abrasion , %	C131 C88	22.7 3.4	30 Max. 12 Max.
• Soundness loss by sodium sulfate solution,%	C 4791 D5821	5 96	10 Max. 90 Min.
• Flat and elongated particles ,%			
• Degree of crushing, %			
Fine aggregate			
• Bulk specific gravity	C127	2.664	….
• Apparent specific gravity	C127	2.696	….
• Sand equivalent, %	D2419	57	45 Min.
• Angularity ,%	C1252	54	….
• Clay lumps and friable particles, %	C142	1.85	3 Max.

Crumb rubber (CR) was brought from tires factory in Al-Najaf governorate, which is a black, large size pieces casting to a small size in the laboratory with specific gravity (1.16). Crumb rubber that has been subjected to treatment by heat, pressure or by addition of softening agents after grinding to alter physical and chemical properties of the recycled material. In this study single particle size of crumb rubber retained on mesh the No.50 (0.300 mm). The process of mixing crumb rubber with asphalt used in this study is the wet process, in which crumb rubber is added to the asphalt before introducing it in the warm mix asphalt. CR will be directly blended with asphalt in blending machine for 60 minutes at 150 ^{o}C temperature. After mixing, the asphalt with CR was allowed to cool to room temperature for 24 hours before being reheated for testing. The warm asphalt mix was prepared with the concentrations of 15 and 20% by the weight of asphalt cement for 66 and 48 penetration grade respectively.

B. Asphalt Mixtures Code

Six asphalt mixture types of different combinations of asphalt type and additive type are coded as shown in Table V.

TABLE V

THE CODE FOR THE SIX ASPHALT MIXTURE TYPES

Asphalt mixture code	Description
HMA48	Control mix 48 penetration grade asphalt
HMA66	Control mix 66 penetration grade asphalt
WMA48AS	Warm mix asphalt 48 penetration grade asphalt , Aspha-min® additive
WMA66AS	Warm mix asphalt 66 penetration grade asphalt , Aspha-min® additive
WMA48SS	Warm mix asphalt 48 penetration grade asphalt , Sasobit aditive
WMA66SS	Warm mix asphalt 66 penetration grade asphalt , Sasobit addive
CWMA48 AS	Warm mix asphalt 48 penetration grade asphalt , Aspha-min® additive and crumb rubber
CWMA66 AS	Warm mix asphalt 66 penetration grade asphalt , Aspha-min® additive and crumb rubber
CWMA48 SS	Warm mix asphalt 48 penetration grade asphalt , Sasobit aditive and crumb rubber
CWMA66 SS	Warm mix asphalt 66 penetration grade asphalt , Sasobit additive and crumb rubber

C. Sample Preparation

Following the aggregate gradation, they have been stored in different buckets. Aggregates were heated at the temperature of 125 ^{o}C for 6 hours in the oven prior to mixing process. The asphalt grade 40/50 or 60/70 was selected as the binder for this study. The binder was kept in the oven for 2 hours at 150 ^{o}C prior to mixing process. To produce WMA mixtures by the dry process, WMA additive was added to the heated aggregate and manually stirred in bucket mixer and then asphalt was added. All examined asphalt concrete mixtures were prepared in accordance to (ASTM Designation: D 1559-89) [15] with the standard 75-blow Marshall design method for designing hot asphalt concrete mixtures, designated as using automatic compaction.

There is no standard specifications available for WMA mixing and compaction temperature in Iraq, the values were obtained from making trial mixes to get required properties such as 125-135 °C mixing temperature and 120-125 °C compaction temperature. The manufacturer of Aspha-min recommends 30 °C reduction in mixing and compaction temperature and Sasobit allows working temperatures to be decreased by 18–54 °C [13],[14], [16], [17] and [18].

D. Marshall and Volumetric Properties

The Marshall test was performed during the mix design according to the (ASTM Designation: D 1559-89) [15]. This test is performed at a deformation rate of 51 mm/min (2 inch/min) and a temperature of 60 ºC. The properties obtained from this test are the Marshall stability and flow. The Marshall stability of an asphalt mixture is the maximum load the material can carry when tested in the Marshall apparatus. The Marshall flow is the deformation of the specimen when the load starts to decrease. Stability is reported in (KN) and flow is reported in (mm) of deformation. Three specimens were tested and an average is reported and used in the analysis.

Marshall Properties at optimum asphalt content by weight of total mix and SCRB [12] specifications for asphalt mixes used as a surface course are presented in Table VI.

As reported in Table VI that all properties of asphalt paving mixture are within SCRB specification [12] requirements for surface course asphalt mixtures.

TABLE VI

MARSHALL AND VOLUMETRIC PROPERTIES OF DIFFERENT MIXTURE TYPES

Mix type	*Asphalt paving properties*					
	Optimum Asphalt Content (%)	*Marshall Stability (KN)*	Marshall flow (mm)	*Voids in total mix (%)*	*Voids in mineral aggregate (%)*	*Voids filled with asphalt (%)*
HMA48	4.9	13.6	2.8	4.2	16.2	74.07
HMA66	4.7	10.3	3.1	4.1	15.9	74.21
WMA48AS	5.3	11.9	3.0	4.3	16.0	73.13
WMA66AS	5.2	9.8	3.2	4.0	14.9	73.15
WMA48SS	5.6	11.3	3.1	3.9	14.9	73.83
WMA66SS	5.5	*9.2*	*3.4*	*3.8*	*15.2*	*75.0*
CWMA48 AS	5.1	*12.0*	*2.9*	*3.7*	*15.4*	*75.97*
CWMA66 AS	5.0	*10.4*	*3.1*	*3.6*	*15.6*	*76.92*
CWMA48 SS	5.3	*11.6*	*3.2*	*3.7*	*15.0*	*75.33*
CWMA66 SS	5.2	*9.7*	*3.3*	*4.1*	*15.7*	*73.88*
SCRB specifications	(4-6)%	*Min. 8 KN*	*(2-4) mm*	*(3-5) %*	*Min. 14*	*(65-85)%*

IV. MECHANICAL BEHAVIOR TESTS

The mechanical behaviors of the polymer-modified and unmodified mixtures were evaluated based on the indirect tensile strength, indirect tensile resilient modulus, flexural beam fatigue and Hamburg Wheel-Tracking tests.

A. Indirect Tensile Strength Test

The indirect tensile strength tests were conducted using the standard method designated by ASTM D 4123 [15]. The experimental procedure used to determine the tensile, or splitting, strength of a cylindrical specimen is based on loading it diametrically in compression to create a tension zone along the specimen's loaded diameter. The expression for the maximum tensile strength generated can be stated as:

$$\sigma_t = \frac{2P_{\max}}{\pi.H.D} \qquad (1)$$

Where σ_t is the indirect tensile strength(kPa) , P_{max} is the maximum applied load(kN) , and H, D are the height and the diameter of the specimen(m) , respectively.

B. Indirect Tensile Resilient Modulus Test

The indirect tensile resilient modulus test is conducted at temperatures of 25ºC according to the modified ASTM D4123 [19].It is a repeated load indirect tension test for determining the resilient modulus of the asphalt mixtures. The recoverable horizontal deformation, ΔH was used to calculate the indirect tensile resilient modulus, MR in (2).

$$M_R = \frac{P.(0.27+\mu)}{t.\Delta H} \qquad (2)$$

Where:

M_R = Resilient Modulus, MPa
P = Applied vertical load, N
t = Sample thickness, mm
μ =Poisson's ratio (assumed 0.35 for asphalt concrete mixtures) , and
ΔH = Horizontal deformation, mm.

C. Flexural Beam Fatigue Tests

The purpose of the flexural beam fatigue tests is to measure the fatigue behavior of the mixture. Pavements that are experiencing fatigue failure will suffer cracking caused by repeated traffic loading. These cracks occur in the wheel paths, initiating as longitudinal cracks and progressing to an alligator crack pattern. The results from a beam fatigue test can be used to provide an estimation of the number of wheel loads that can be carried by a pavement before fatigue cracking appears. In this study, the fatigue properties of the modified and unmodified asphalt mixtures were measured and compared.

Flexural fatigue testing was performed in accordance with AASHTO T 321-07 [20]. Three specimens were tested for each mix at 300 micro-strains and at a temperature of 20 ± 0.5°C. The specimens were compacted in a kneading beam compactor, and then trimmed to the dimensions of 380 ± 6 mm in length, 63 ± 2 mm in width, and50 ± 2 mm in height. The target void content was 7 ± 1 percent. Data acquisition software was used to record load cycles, applied loads, strain levels and beam deflection. The software calculates the beam stiffness in each a loading iteration. At the beginning of each test, the initial beam

stiffness was calculated by the data acquisition software after 50 conditioning cycles. AASHTO T 321-07 [20] was used to define beam failure as a 50% reduction in beam stiffness in terms of number of cycles until failure. Fatigue life relationship (power model) result in log strain applied (ε_t) versus N_f relationship plotted. This results in a relationship for fatigue tests of the form [21].

$$N_f = K_1 \varepsilon_t^{-k2} \quad \textbf{(3)}$$

K_1= Fatigue constant value of N_f when ε_t=1

K_2= Inverse slope of the straight line the logarithmic fatigue relationship.

N_f= Number of repetition to fracture.

D. Hamburg wheel-tracking test

The Hamburg wheel tracking test was conducted using the latest version of APA in accordance with the testing procedures specified in AASHTO T324[20]. Samples were submerged in the water bath controlled at 50±0.5 ^{o}C for a minimum of 30 min. A data acquisition system records rutting out to 20,000 wheel passes at 25 Hz and plots rut depth versus number of passes for each sample automatically. The target air-void content was 7 ± 0.5%.The WMA rut depth was slightly greater than the HMA rut depth; however, both were less than the commonly used criterion of 10mm at 20,000 passes.

E. Moisture sensitivity

To evaluate the moisture sensitivity of WMA mixtures, the modified Lottman test following AASHTO T283 [20]was performed. Six specimens (three for dry condition and three for wet condition) for each WMA mixtures, and the control HMA mixture were prepared. For dry conditioning, three specimens in a sealed pack were placed in the water bath at 25 ^{o}C for 2 hours and , for wet conditioning three specimens saturated between 70 % and 80% were placed in a freezer at -18 ^{o}C for 16 hours and in water bath at 60 ^{o}C for 24 hours followed by conditioning in water bath at 25^{o}C for 2 hours. The moisture damage in asphalt mixtures is determined as a loss of strength due to the presence of moisture in terms of a tensile strength ratio (TSR) that is defined as a ratio of the indirect tensile strength of a wet specimen over that of a dry specimen.

V. DISCUSSION OF RESULTS

After implementing the above experimental works, five results have been obtained from the conduction of these experimental works. Firstly, Fig. 1 indicates the average results of the indirect tensile strength (ITS) test for the surface course mixtures with different types of mix. In general, the two control HMA demonstrates higher values for ITS than WMA mixtures. WMA66AS mixtures have lower strengths than the other mixture types wearing course mixes. However, this figure reveals all WMA mixtures give low tensile strength which shows lower resistance under tension stresses.

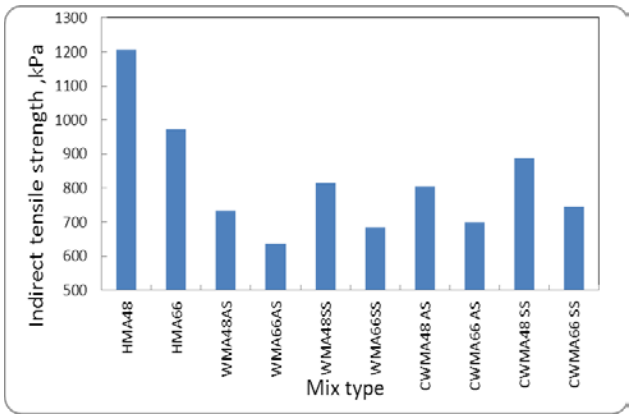

Fig. 1. Effect of mix type on indirect tensile strength values.

Fig. 2 represents the relationship between the indirect tensile resilient modulus (MR) of the surface course mixtures at 20 ^{o}C test temperature with different type of mixtures. The results show minor differences among other mixtures. The HMA48 is the highest in the indirect tensile resilient modulus among other types. Whereas, the second level of difference which less in the tensile than the HMA48 comes with the WMA48SS and WMA48AS mixtures. The third level is WMA66SS and WMA66AS. On the hand , the addition of crumb rubber causes the relative increase in indirect tensile strength and resilient modulus of WMA .

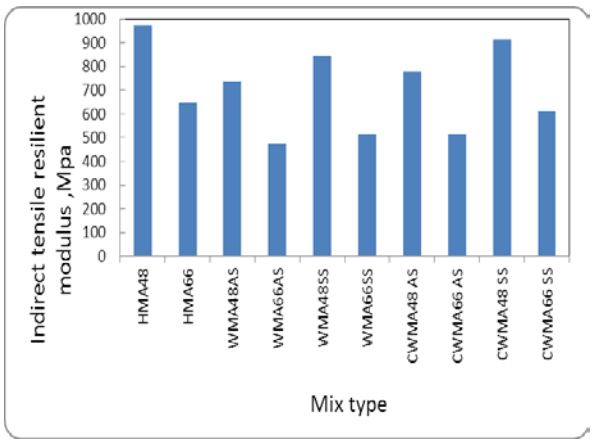

Fig. 2. Effect of mix type on indirect tensile resilient modulus values

The results of the flexural beam fatigue test for various mix types are presented in Fig. 3. While evaluating the fatigue resistance of asphalt concrete mixes, the numbers of cycles to failure are used as performance indicators. A high number of cycles to failure are the desired properties to resist fatigue cracking. From this figure, it is clearly shown

there is no significant influence of additive types on fatigue life of WMA. However, fatigue life for two control HMA mixtures is more that of various WMA by about 50 % this conclusion contrasts with [8]. The difference between the current study and the other reported by [8]could be resulted from the aggregate, asphalt and additive properties that have been used in preparing of WMA. On other hand, it was found that the asphalt grade has effect on fatigue life

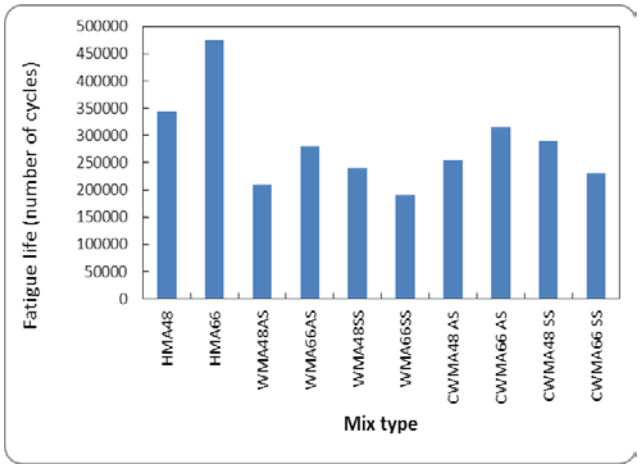

Fig. 3. Effect of mix type on indirect fatigue life values

Fig. 4 illustrates the influence of the selected additives on rut depth. As it is clear from Fig. 4 the average rut depth of the WMA was higher than that of the HMA by about 75%**.** It can be concluded that the using of WMA in the construction of surface course for the pavement structure increases the rutting in comparison with using HMA. In addition, it can be observed for same asphalt type that there is no significance influence of additive types on rut depth values of WMA.

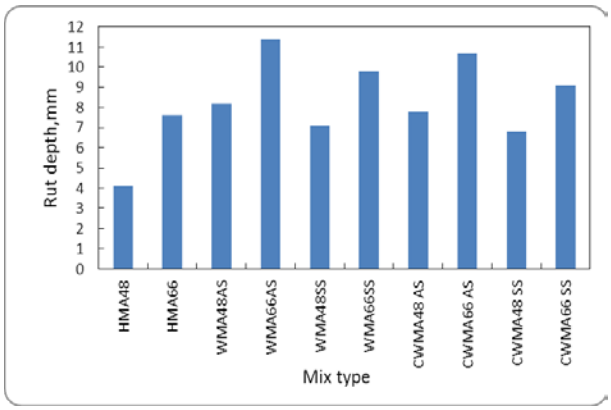

Fig. 4. Effect of mix type on rut depth values

Fig. 5 shows the tensile strength ratio (TSR) values in HMA and WMA, TSR gives an idea of moisture sensitivity of various mixtures. Almost control HMA and warm asphalt mixes got TSR higher than acceptable value of 80% except WMA66AS and WMASS exhibited TSR values of 67% and 74%, respectively. The WMA66SS mixture showed higher TSR among other warm asphalt mixtures. Lower temperatures used for preparing WMA can result in incomplete drying of the aggregates. The resulting trapped water in the coated aggregates may cause moisture damage. Care must be taken to monitor this. This could be attributed that the WMA mixes gives lower TSR values than for the HMA.

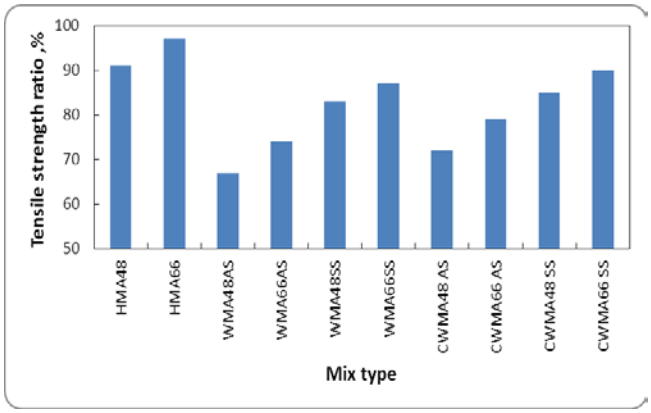

Fig. 5. Effect of mix type on tensile strength ratio

VI. CONCLUSIONS

According to the above study, the main conclusions can be drawn as:

1. The values of indirect tensile strength (ITS) obtained from various WMA mixtures were lower than those of control mixtures, but in WMA prepared from Sasobit(WMA48SS,WMA66SS, CWMA48 SS and CWMA48 SS) ITS values were higher than those of the others. This means that the WMA appears low resistance to tensile stresses.

2. Laboratory measurements of indirect tensile resilient modulus (M_R) values indicated the various WMA exhibited lower values than those of control HMA.

3. The incorporation of WMA additives in warm asphalt mixes lead to reduction in the fatigue life as compared with the response of HMA.

4. The performance of warm mixture that contained Sasobit is better than that contained Aspha-min but the performance of HMA is relatively better than that of WMA.

5. Alternatively, introducing warm mix asphalt (WMA) is known to provide decreased optimum mixing and compaction temperatures of the rubberized mixes and expected to be comparable to those of conventional mixes. Also, the crumb rubber improved the properties of WMA by increasing the tensile strength , fatigue life and tensile strength ratio and decreasing rut depth as compared with WMA without crumb rubber.

VII. REFERENCES

[1] **Larsen, O., Moen, Ø., Robertus, C., and Koenders, B.(2004),** ***WAM Foam Asphalt Production at Lower Operating Temperatures as an Environmental Friendly Alternative to HMA.*** **In Proceedings of the 3rd Eurasphalt and Eurobitume Conference, Book 1, Foundation Eurasphalt, Breukelen, The Neterhlands, , pp 641-650.**

[2] **Koenders, B.G., D.A. Stoker, C. Bowen, P. de Groot, O. Larsen, D. Hardy, and K.P. Wilms (2000) ,*Innovative Processes in Asphalt Production and Application to Obtain Lower Operating Temperatures*. 2nd Eurasphalt & Eurobitume Congress, Barcelona, Spain.**

[3] **AAPA (2001) ,*Warm Mix Asphalt–A-State-of-the-Art Review*. Advisory Note 17, Australian Asphalt Pavement Association, Kew, Victoria, Australia,(http://www.aapa.asn.au/content/aapa/download/AdvisoryNote17.pdf).**

[4] **Prowell, B., Hurley, G., and Crews, E. (2007) ,*Field Performance of Warm-Mix Asphalt at National Center for Asphalt Center for Asphalt Technology Test Track.* Transportation Research Record: Journal of the Transportation Research Board, No. 1998, pp. 96-102.**

[5] **Jenkins, K.J., A.A.A. Molenaar, J.L.A. de Groot, and M.F.C. van de Ven (2002), *Foamed Asphalt Produced Using Warmed Aggregates.* Journal of the Association of Asphalt Paving Technologists. Volume 71, Colorado Springs, Colorado.**

[6] **Jones, W. (2004) ,*Warm Mix Asphalt Pavements: Technology of the Future*. http://www.asphaltinstitute.org/Upload/_Fall_Mag_Warm_Mix_Asphalt_Pavements.pdf.**

[7] **Xiao , F., S.N. Amirkhanian , and B.J.Putman (2010), *Evaluation of Rutting Resistance in Warm Mix Asphalts Containing Moist Aggregate.* Proceedings (CD), 89th Annual Meeting of the Transportation Research Board, The National Academies, Washington D.C.**

[8] **Jones, D., C. Barros, J.T. Harvey , B.W.Tsai, and R.Wu. (2010), *Preliminary Results from the California Warm Mix Asphalt Study*. Proceedings (CD), 89th Annual Meeting of the Transportation Research Board, the National Academies, Washington D.C.**

[9] **Takallou H.B., Takallou M.B. (1991) , *Recycling Tires in Rubber Asphalt Paving Yields Cost, Disposal Benefits.* Elastomeric, Vol.123, pp.19-24.**

[10] **Gawel , Irena, Stepkowski, Robert and Czechowski, Franciszek (2006), *Molecular Interactions between Rubber and Asphalt.* Industrial and Engineering Chemistry Research, Vol.45, pp.3044-3049.**

[11] **Mathias Leite L .F., Almeida da Silva , P. , Edel G., Goretti da Motta L. , and Herrmann do Nascimento L.A. (2003) ,*Asphalt Rubber in Brazil : Pavement Performance and Laboratory Study.* Proceedings of the Asphalt Rubber 2003 Conference , Brasilia , Brazil, pp.229-245.**

[12] **State Commission of Roads and Bridges (SCRB/R9), (2003) ,*General Specification for Roads and Bridges.* Republic of Iraq, Ministry of Housing and Construction, Department of Planning and Studies, Baghdad, Revised Edition, Addendum No.3.**

[13] **Hurley G and Prowell B. (2005a), *Evaluation of Aspha-Min for use in warm mix asphalt.* NCAT report 05-04. Auburn.**

[14] **Hurley G, Prowell B. (2005b) ,*Evaluation of Sasobit for use in warm mix asphalt.* NCAT report 05-06. Auburn.**

[15] **ASTM Standards, (2004), *Roads and Paving Materials.* Annual Book of the American Society for Testing and Materials Standards, Section 4, Vol. 04-03.**

[16] **Gandhi T, Xiao F,and Amirkhanian SN (2009), *Estimating indirect tensile strength of mixtures containing anti-Stripping agents using an artificial neural network approach.* Int J Pavement Res Technol; 2(1):1–12.**

[17] **Kristjansdottir O, Muench S, Michael L, Burke G. (2007) ,*Assessing potential for warm-mix asphalt technology adoption*. J Transport Res Board, vol (2040): 91–9.**

[18] **Xiao F, Zhao W, Gandhi T, Amirkhanian SN. (2010) , *Influence of Anti-stripping Additives on Moisture Susceptibility of Warm Mix Asphalt Mixtures.* J Mater Civil Eng. 2010; 22(10):1047–55.**

[19] **Mohammad, L.N. and Paul, H. (1993) ,*Evaluation of the Indirect Tensile Test for Determining the Structural Properties of Asphalt Mix.* Transportation Research Record, No. 1417, TRB, National Academy of Science, Washington, D.C.**

[20] **AASHTO, (2007), *Standard Specifications for Transportation Materials and Methods of Sampling and Testing.* 5 th edition , American Association of State Highway and Transportation Officials, Washington, D.C., USA.**

[21] **Monismith C.L., Epps, J. E., Kasianchuk , D., A.,McLean, D., B. (1971) , *Asphalt mixture behavior in repeated flexure.* Report TE 70-5, University of California, Berkeley.**

Using Remote Sensing to Hindcast Water Quality in a Semi-Arid Reservoir

Eliza Sarah Deutsch and Ibrahim Alamaddine

***Abstract*—Landsat 7 ETM+ images were used to predict and hindcast the summer trophic status and peak surface area of Qaraoun Reservoir in Lebanon between 1999 and 2012. Trophic status was determined using an empirical algorithm developed for detecting chlorophyll-a content in the reservoir using near-infrared, red, blue, and green bands. The results show that over the study period, the reservoir has oscillated between mesotrophic and eutrophic states, with indications of a slight shift towards a more eutrophic status over time. Peak reservoir surface area was found to vary inter-annually, a typical feature of semi-arid reservoirs. The maximum annual surface area ranged between 6.7 and 10.2 km2. No consistent and statistically significant area changes were found over time.**

***Index Terms*—Landsat 7, ETM+, Trophic Status, Chlorophyll-a, Eutrophication, Qaraoun Reservoir.**

I. Introduction

IN SITU water quality monitoring programs are necessary for developing management programs for inland water bodies that are often subject to major pollution and eutrophication problems. Nonetheless, monitoring programs can be cost prohibitive, and are lacking in many parts of the globe, particularly in developing countries. Over the past two decades, there has been an increase interest in finding non-traditional and low-cost data-generation method that can be used to assess and monitor changes in water quality and quantity. The use of remote sensing is one of these methods.

Eutrophication of freshwater sources describes the condition in which the aquatic environment becomes enriched with nutrients, resulting in cascading impacts on algae growth and higher order foodweb dynamics [1]–[3]. Eutrophication is on the rise worldwide [4]–[7] due to mounting anthropogenic stressors; as such the need to better understand the temporal patterns in algae growth in inland water bodies is imperative. This paper uses radiometric data from the Landsat 7 ETM+ satellite sensor to reconstruct a historical time series of eutrophication and surface area changes for a typical semi-arid reservoir in Lebanon, namely the Qaraoun Reservoir.

Manuscript received September 20, 2015. This work was supported in part by a US Agency for International Development (USAID) PEER Grant, the American University of Beirut, and the Natural Sciences and Engineering Research Council of Canada (NSERC).

E.S. Deutsch is with the Department of Civil and Environmental Engineering, American University of Beirut, Riad El Solh, Beirut, Lebanon (e-mail: esd02@mail.aub.edu).

I. Alamaddine is with the Department of Civil and Environmental Engineering, American University of Beirut, Riad El Solh, Beirut, Lebanon (e-mail: ia04@aub.edu.lb).

II. Methods

Landsat 7 images were obtained from the U.S. Geological Survey (USGS) for the period stretching between 1999 and 2012. Images were initially corrected for the failure of the Scan Line Corrector. A land mask was then developed using histogram splicing applied on the mid-infrared band to trace the outline of the reservoir and remove contamination of land pixels [8]. Reservoir surface area was then calculated by multiplying the number of pixels in the reservoir image by the satellite's spatial resolution (30 m*30 m). For Chlorophyll-a (chl-a) level estimation, Landsat 7 digital numbers were converted to radiance and top-of-atmosphere reflectance using typical NASA derived conversions. No atmospheric correction was attempted due to the lack of data on the atmospheric column during satellite overpass. The generated reflectance values were then used to predict chl-a concentration, using the following equation from Landsat 7 bands [9]:

$$ln(Chl-a) = 3.9 + 1.5 * ln\left(\frac{NIR\ Band}{Red\ Band}\right) - 1.5 * \ln\left(\frac{Blue\ Band - Red\ Band}{Green\ Band}\right) \quad (1)$$

Lake averaged chl-a values for each image were converted to the Carlson Trophic State Index (TSI) using the following equation [10]:

$$TSI = 10 * \left[6 - \left(\frac{2.04 - 0.68 * ln(Chl-a)}{ln(2)}\right)\right] \quad (2)$$

TSI values between 40-50 indicate mesotrophy, 50-70 specifies eutrophy, and values above 70 specifies hypereutrophy [11]. Changes in TSI were assessed for the summer months (averaged extracted values from July 1-September 10) over the entire dataset (1999-2012), while changes in reservoir area were assessed for spring months (April or May) when lake area was at its peak following snow-melt.

III. Results and Discussion

For the 13 years of the study, Qaraoun Reservoir mostly exists either in a mesotrophic or a eutrophic state (Figure 1a). Yet, there was a slight statistically significant increase in Trophic Status with time (TSI = -3700 + 1.8*Year, P=0.0673, R^2=0.2724). This increase is likely due to increased development in the watershed, resulting in increased nutrient loading to the reservoir. Changes in peak reservoir area did not show a consistent patter with time, with large fluctuations from year to year (Figure 1b). These fluctuations are likely due to the combination of changes climatic forcings and dam operations.

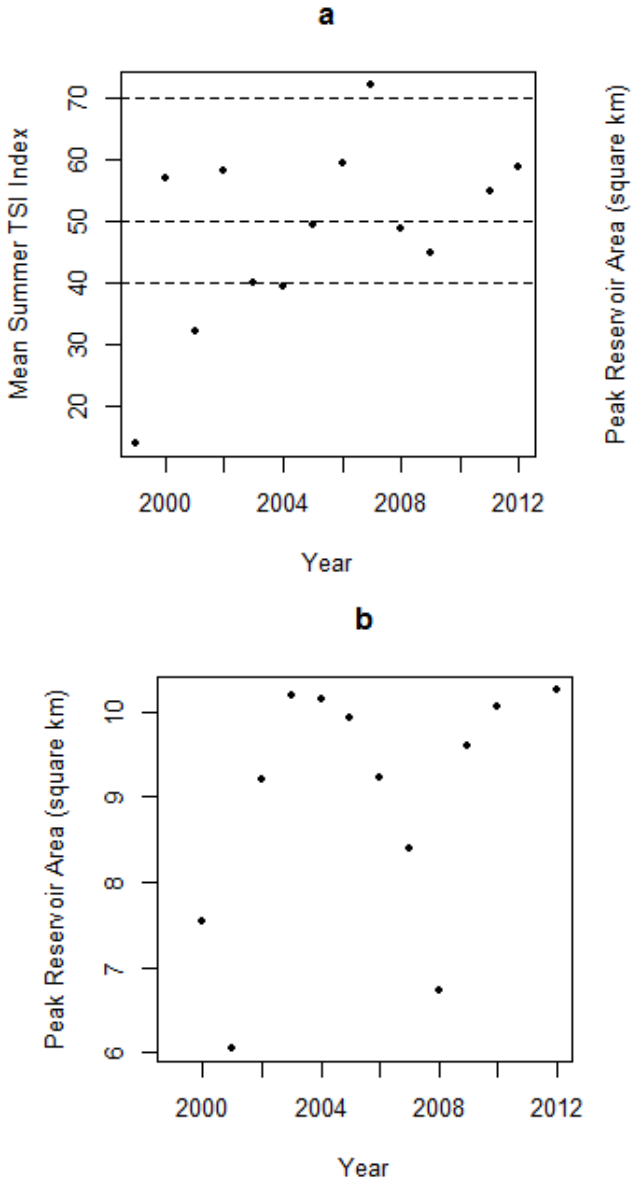

Fig. 1. Changes in mean summer TSI Index (a) and peak spring reservoir area (b) throughout the study. For figure 1(a), TSI values between 40-50 indicate mesotrophy, 50-70 specifies eutrophy, and values above 70 specifies hypereutrophy.

Conclusions

This study shows the usefulness of using the Landsat 7 image record for assessing changes in water quality and quantity through time, which can have important implications for tracking changing environmental conditions in lakes and reservoirs that lack *in situ* data records. This information can have important implications for tracking impacts of climate change on the water resource and for quantifying the impact of increased human development on pollution loads. Over the past 17 years, Qaraoun Reservoir is becoming more polluted and eutrophic, during a time where there was significant development in the contributing watershed. Although water surface area also fluctuates significantly, the water budget does not seem to show any trends towards increasing or decreasing area.

Acknowledgment

E.S. Deutsch and I. Alameddine thank Dr. Mutasem El Fadel for his assistance with funding and advice on the project. They would also like to thank Sara Dia, Abbass Baalbacki, Lea Korban, and Daniah Turjman for their field assistance.

References

[1] D. L. Correll, "The role of phosphorus in the eutrophication of receiving waters: A review," *J. Environ. Qual.*, vol. 27, no. 2, pp. 261–266, 1998.
[2] P. J. Dillon and F. H. Rigler, "The phosphorus-chlorophyll relationship in lakes," *Limnol. Oceanogr.*, vol. 19, no. 5, pp. 767–773, 1974.
[3] R. E. Hecky and P. Kilham, "Nutrient limitation of phytoplankton in freshwater and marine environments: a review of recent evidence on the effects of enrichment.," *Limnol. Oceanogr.*, vol. 33, no. 4, pp. 796–822, 1988.
[4] G. A. Codd, "Cyanobacterial toxins, the perception of water quality, and the prioritisation of eutrophication control," *Ecol. Eng.*, vol. 16, no. 1, pp. 51–60, 2000.
[5] I. A. S. Costa, S. M. F. O. Azevedo, P. A. C. Senna, R. R. Bernardo, S. M. Costa, and N. T. Chellappa, "Occurrence of toxin-producing cyanobacteria blooms in a Brazilian semiarid reservoir.," *Brazilian J. Biol.*, vol. 66, no. 1b, pp. 211–219, 2006.
[6] A. Fadel, B. J. Lemaire, A. Atoui, B. Vinc, N. Amacha, K. Slim, B. Tassin, and P. Paristech, "First assessment of the ecological status of Karaoun reservoir , Lebanon," *Lakes Reserv. Res. Manag.*, vol. 19, pp. 142–157, 2014.
[7] J. M. O'Neil, T. W. Davis, M. A. Burford, and C. J. Gobler, "The rise of harmful cyanobacteria blooms: The potential roles of eutrophication and climate change," *Harmful Algae*, vol. 14, pp. 313–334, 2012.
[8] P. S. Frazier and K. J. Page, "Water Body Detection and Delineation with Landsat TM Data," *Photogramm. Eng. Remote Sensing*, vol. 66, no. 12, pp. 1461–1467, 2000.
[9] E. S. Deutsch and I. Alameddine, "Unpublished Data."
[10] R. E. Carlson, "A trophic state index for lakes," *Limnol. Oceanogr.*, vol. 22, pp. 361–369, 1977.
[11] R. E. Carlson and J. Simpson, *A coordinator's guide to volunteer lake monitoring methods.* 1996.

Evaluation of Contaminated Soils in The Vicinity of Basrah Refinery by Using GIS Technical

Dr. Ali Sadiq Resheq, Pro. Dr. Abdul Razzak T. Ziboon, Jr., Asst. Pro. Dr. Basim Hasan Hashim and Dr. Zainab B. Mohammed, *University of Technology, Baghdad, Iraq*

***Abstract*— Basrah refinery is located 15 km west of Basrah governorate south of Iraq. The main structures in the refinery and the storage tanks were subjected to several air attacks during the first and second gulf wars causing many environmental problems. The problems were generated from the release of heavy metals due to oil industrial processes and spillage of oil waste in the vicinity of the complex, in addition to the widespread of uncontrolled emission of particulates and gases from stacks. The main concern in evaluation the degree of pollution in soils is the determination of the concentrations of heavy metals Cd , Pb , Ni , Cu , Cr and Zn as their higher values cause heavy metal poisoning. Soil samples were taken from the area (6km x 6km), keeping the source of contamination in the center using grid method (1km x 1km). 24 samples were collected from the ground surface, 100 mm and 500 mm below N.G.L. Concentrations of heavy metals Cd , Pb , Ni , Cu , Cr and Zn were determined in addition to soil constituents, soil pH and iron oxide Fe2O3. The results demonstrate that the range of concentrations of Cd is between 4 to 11.7 mg/kg, Pb between 8 to 54 mg/kg, Ni between 23 to 110 mg/kg, Cu between 6 to 35 mg/kg, Cr between 23 to 68 mg/kg and Zn between 8 to 49 mg/kg. Furthermore the results also exhibit a decreasing trend in metals concentration with increasing clay content. Higher adsorptions of heavy metals were noticed when pH values exceed 7.**

***Keywords* — soil pollution, heavy metal, contaminated soil, Polyaromatics, soil adsorptions**

Manuscript received October 9, 2001. (Write the date on which you submitted your paper for review.) This work was supported in part by the U.S. Department of Commerce under Grant BS123456 (sponsor and financial support acknowledgment goes here). Paper titles should be written in uppercase and lowercase letters, not all uppercase. Avoid writing long formulas with subscripts in the title; short formulas that identify the elements are fine (e.g., "Nd–Fe–B"). Do not write "(Invited)" in the title. Full names of authors are preferred in the author field, but are not required. Put a space between authors' initials.

F. A. Author is with the National Institute of Standards and Technology, Boulder, CO 80305 USA (corresponding author to provide phone: 303-555-5555; fax: 303-555-5555; e-mail: author@ boulder.nist.gov).

S. B. Author, Jr., was with Rice University, Houston, TX 77005 USA. He is now with the Department of Physics, Colorado State University, Fort Collins, CO 80523 USA (e-mail: author@lamar.colostate.edu).

T. C. Author is with the Electrical Engineering Department, University of Colorado, Boulder, CO 80309 USA, on leave from the National Research Institute for Metals, Tsukuba, Japan (e-mail: author@nrim.go.jp).

I. INTRODUCTION

Contaminated land is referred to land area that contains contaminants, the soil is a good indicator of pollutants and it is continuously subjected to pollutants because it is considered as an open system [1]. Iraq suffers from the destruction of military and industrial infrastructure during Iraqi wars especially the area located in the south.

Heavy metals (or trace metals) refers to the group of metals and semimetals (metalloids) that have been associated with contamination and potential toxicity or eco toxicity,[2].Heavy metals, such as cadmium, copper, lead; chromium, zinc, and nickel are important environmental pollutants, particularly in areas with high anthropogenic pressure [3].

Polyaromatics hydrocarbon (PAHs), defined as chemicals containing two or more fused benzene rings in a linear angular or cluster arrangement. (PAHs) contain only carbon and hydrogen [4]. The (PAHs) came to the environmental from anthropogenic sources such as burning of fossil fuels, petroleum refinery and industrial process.

II. STUDY AREA

Basrah governorate is located between (30˚ 22′ N 47˚ 22′ E) along Shatt al-Arab waterway, about 55 kilometers north of the Arabian Gulf and 545 kilometers south of the capital Baghdad. The total area of Basrah is 19070 km2, represents 4.4% of the total area of Iraq, with population of 3800200 inhabitants.

Basrah refinery began production on (1974) after establishing (Refining Unit No. 1). The tank of this unit was refining crude oil, manufacturing fat and recycling prior to placing in special plastic containers.

III. SOIL SAMPLING

For selected contaminated site, the samples were taken from the area (6km* 6km), keeping the source of contamination at the center. A grid (1km*1km) is identified and location of each point was fixed using (GPS) as shown in Figure (1). A total number of 72 samples were collected from each point of the grid, 24 samples were collected from the ground surface,

100mm and 500mm below N.G.L.

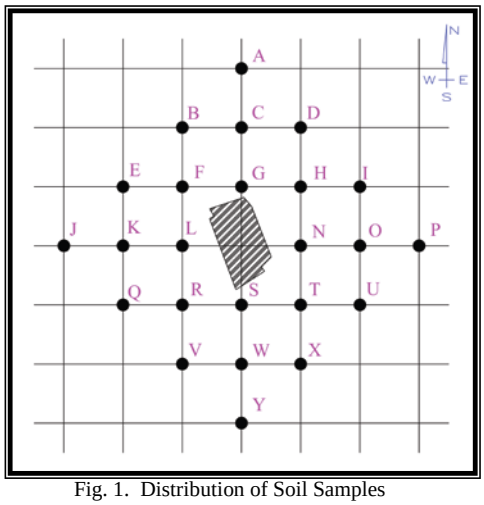

Fig. 1. Distribution of Soil Samples

IV. EXPERIMENTAL WORK

Series of tests were carried out for each soil sample and the outputs cover the determination of heavy metals (Zn, Ni, Cu, Cd, Cr, Pb). Other chemical compounds (Fe2O3, MgO, MnO and PAH). pH values and soil constituents were also determined.

The tests performed on each soil sample are illustrated in Table (1).

Chemical Test :		
parameter	Method	Reference
PAH	Soxhlet or simple Extraction by using hexane	EPA, 2007.
heavy metals		
Fe2O3 ,MgO, MnO	Acid digestion	EPA , 1988.
Organic matter	Walkley–Black titration method.	Brian , 2002.
Physical Tests:		
specific gravity of soil solids	using a water pycnometer	(ASTMD 854) , Krishna,2002
(particle – size analysis of soil)	Unified Soil Classification System	(particle – size analysis of soil)
plastic limit , liquid limit	Unified Soil Classification System	(ASTMD 4318), Krishna,2002

* Group A include metals (Cd, Pb, Ni)

** Group B include metals (Cu, Cr, Zn)

V. RESULTS AND DISCUSSION

Series of tests were carried out for each soil sample and the outputs cover the determination of heavy metals (Zn, Ni, Cu, Cd, Cr, Pb). Other chemical compounds (Fe2O3, MgO, MnO and PAH). pH values and soil constituents were also determined.

A. Group (A) results

• The outputs indicate minimum values of (Cd) of (4, 5 and 4 mg/kg) and maximum values of (10, 11.7 and 10.3 mg/kg) at depths (0, 100, and 500 mm) below N.G.L respectively. Comparing these results with maximum international limit, (0.06 mg/kg) [5] demonstrate that the obtained values of (Cd) highly exceed the allowable recommend value.

• Minimum values of (Pb) were (8, 20 and 21 mg/kg) and maximum values of (36, 48 and 54 mg/kg) at depths (0, 100, and 500 mm) below N.G.L respectively. Comparing these results with allowable international limit, (10 mg/kg) [5] demonstrate that the obtained values of (Pb) exceed the recommend value.

• The minimum values of (Ni) of (23, 29 and 43 mg/kg) and maximum values of (90, 110 and 104 mg/kg) at depths (0, 100, and 500 mm) below N.G.L respectively. Comparing these results with allowable international limit, (40 mg/kg) [5] demonstrate that the values of (Ni) exceed the recommend value.

After thorough investigation along the history of the refinery and the industrial processes and products, it was noticed that the presence of high values of metals (Cd, Pb, Ni) in the soil in the vicinity of the refinery is due to mechanical defects in the treatment unit generated by the action of wars. Oil was spilled and percolated into the ground, in the nearby area. Plate (1), shows the accumulation of spilled oil in the south east zone of the refinery.

Figures (2, 3, and 4) show the distribution of metals (Cd, Pb, Ni) using Arc GIS maps (version 10) at depths (0,100 and 500mm) respectively. Considering the distribution of (Cd, Pb, Ni) at ground surface, Figures (2a, 3a and 4a) demonstrate that high concentrations of (Cd, Pb, Ni) are located mainly on the east area of the refinery, and lower concentrations exist on west zone of the refinery. Since the wind in general is directed from the north west down word to the south east, there is great evidence that the wind has participated in transporting the contaminated top soil from the north west direction and precipitated on the south east zone.

In Figurers (2b, 3b, and 4b) at depth 100 mm, the area of higher concentration of (Cd, Pb, Ni) is extended largely towards the east. This may particularly due to the percolation and seepage of oil, accumulated on the surface and moved gradually downward in the direction of gravity. The movement or mobility of (Cd, Pb, Ni) through soil skeleton is encouraged by the granular constituents of the soil.

At depth 500 mm Figurers (2c and 3c), the zone of higher concentration of Cd and Pb is reduced and narrowed in a zone located south of the refinery while for Ni, Figure (4c) the higher concentration is located in the south east. As an overall

look on the three figures it may be stated that the mobility of (Cd, Pb, Ni) in the soil occurs substantially in the top 100mm below N.G.L and gradually decreases with depth.

As a support to this argument the overall classification of the soil in these zones are silt loams as indicated in Figure (5).According to this type of soil. The silt content ranges from (26.02 % - 68.9 %) with average value (54.93 %). The expected coefficient of permeability for such soil is expected be in the range (10-4 - 10-7 m/s).Such values indicate restricted mobility of fluids between particles.

The variation of pH with depth for the zones (N, NE ,E, and SE) are shown in Figure (6a) is about 7.2 indicating slight alkalinity , under such circumstance the soil becomes good storage for (Cd, Pb, Ni) metals and limited their mobility between the particles .

On the contrary the general texture of soil in the (S, SW, W, NW) is sandy loam as shown in Figure (5). The sand content ranges from (41.24 % - 75.08%) with average value (57.7%). Thus the expected coefficient of permeability for this soil will be in the rang (10-1 - 0-4 m/s), encouraging metals to penetrate deeper in the soil. Another support for this argument is the slight acidic environment, pH ≈ 6.6, as shown in Figure (6b). [6] reported that high mobility of (Cd, Pb, Ni) occurs in acidic soil rather than alkaline soil.

Plate. 1. Accumulation of Oil in the South East Zone of the Refinery

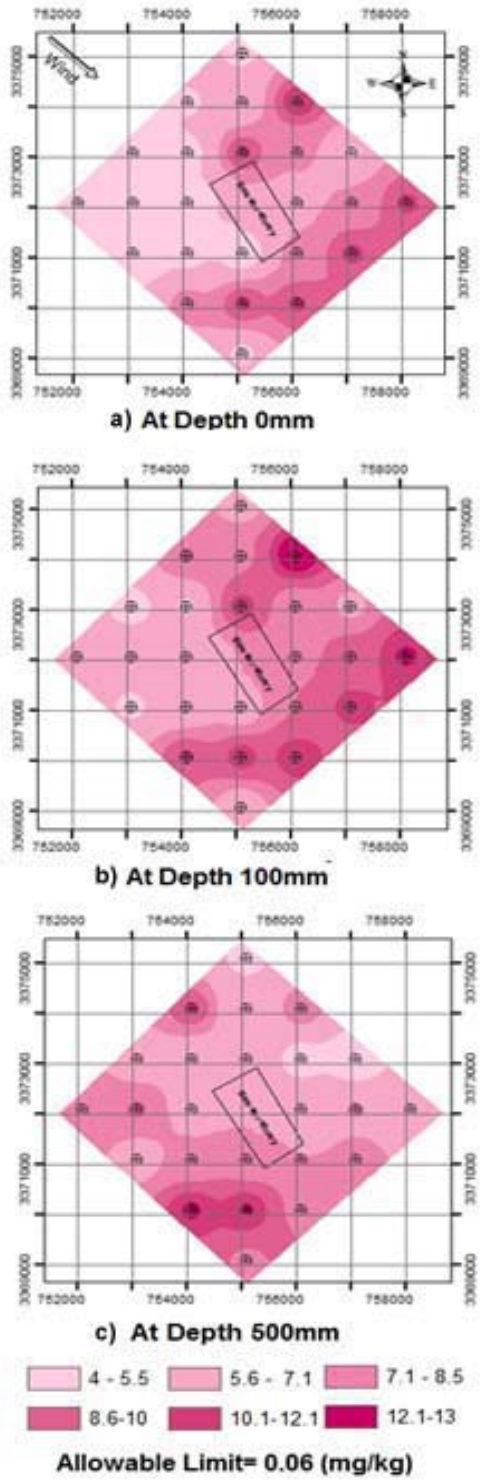

Fig. 2. Concentration of Cd

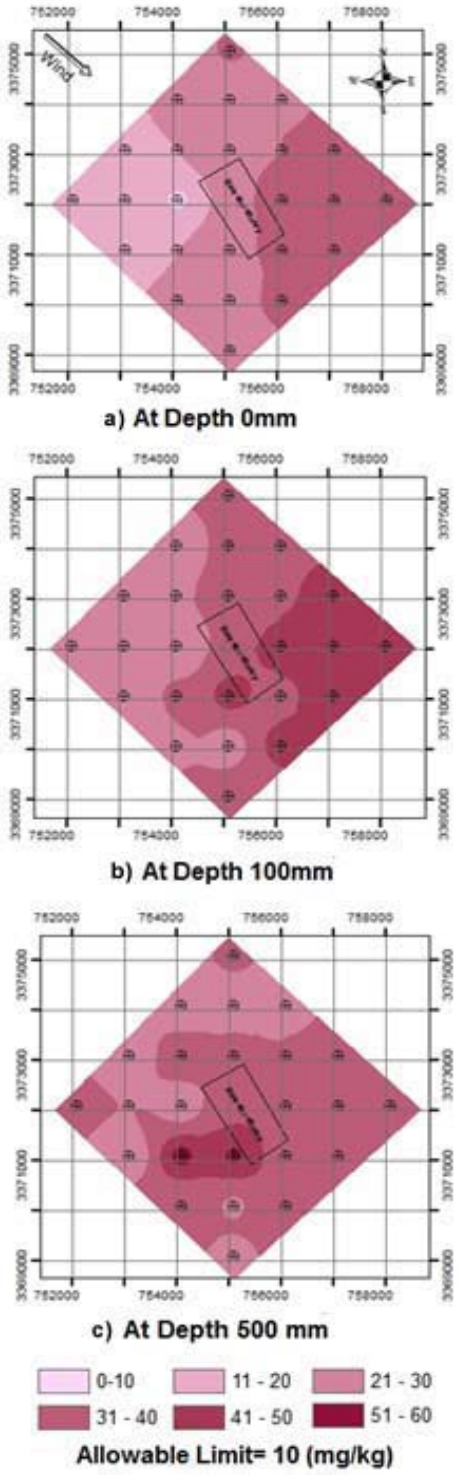

Fig. 3. Concentration of Pb

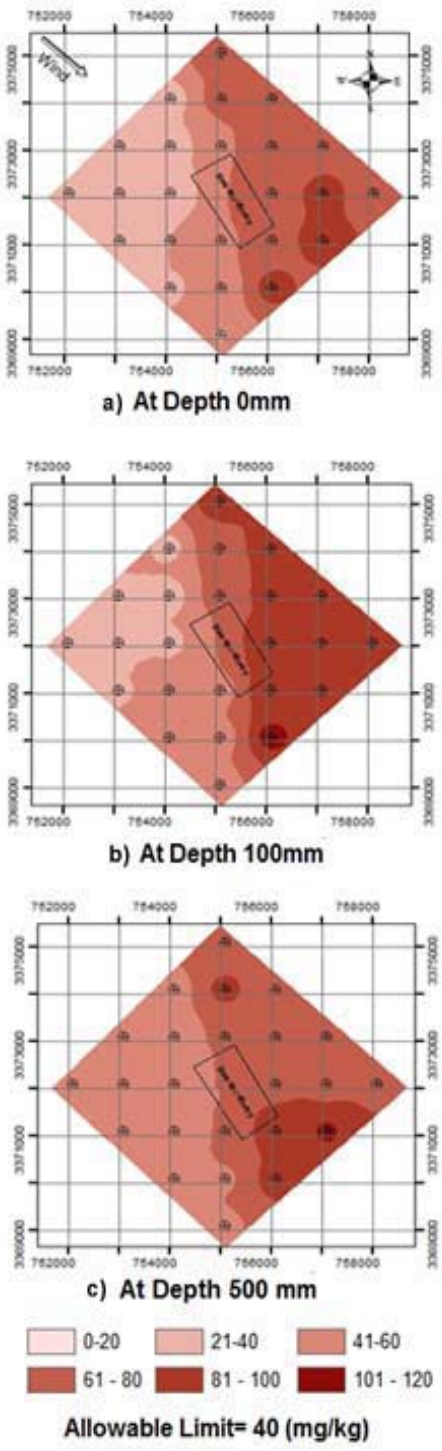

Fig. 4. Concentration of Ni

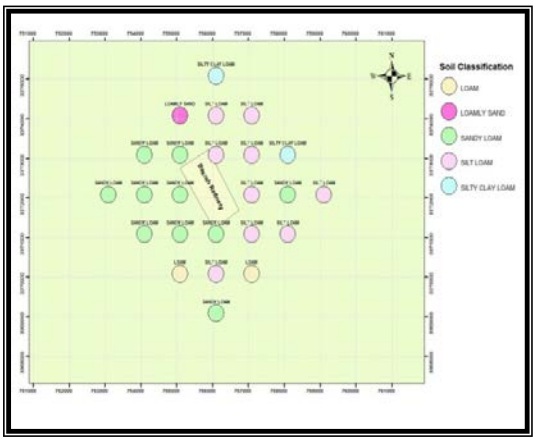

Fig. 5. Soil Classification

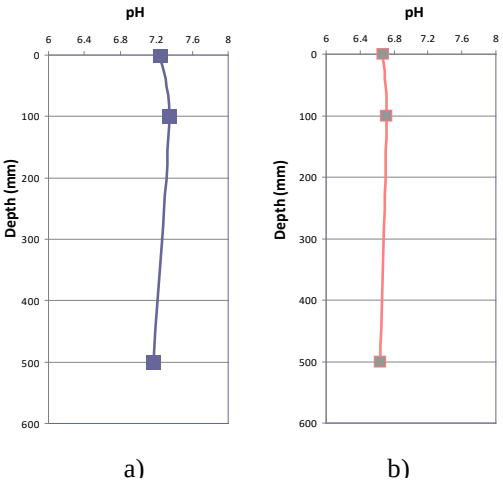

Fig. 6. Value of pH with soil depth

B. Group (B) results

Group (B) includes Cu, Cr, and Zn metals where their existing values did not exceed the allowable limits.

Copper (Cu)

Minimum values of (Cu) were (6, 8 and 9 mg/kg) while maximum values were (27, 35 and 28 mg/kg) at depths (0, 100, and 500 mm) below N.G.L respectively. Comparing these results with allowable international limit, (30 mg/kg) [5] demonstrate that the obtained values of (Cu) did not exceed the recommend value.

Figure (9a) demonstrates that the high concentration of (Cu) is allocated in the east area where, the existence of organic matter and Fe2O3 as shown in Figures (7 and 8) more than west area. The greatest amounts of Cu have been always found adsorbed by organic soil constituents, Fe and Mn oxides [7].

The top soil is exposed to wind movements directed towards the south east as shown in Figure (9) .The distribution of Cu in the study area around the refinery indicates accumulation of moderate concentration between (21-25mg/kg) along the east direction at ground level.

The concentration increase to the range between (26-30mg/kg) at depth 100mm below N.G.L. As the depth increases to 500mm below N.G.L the concentration decrease again to (21-25mg/kg).

Adsorption is the most important process affecting the bioavailability of (Cu) in soils. The mobility of copper was associated with the transport of organic material since the copper was highly adsorbed by them [8]. The organic substances in the soil make major contribution to the cation exchange capacity of soil due to their high surface area [9]. Colloidal soil organic matter works as surfaces on which cation exchange capacity takes place, most colloids are smaller than 2 µm and have large external surface area per unit mass.

Lieve et al [10] reported that sandy soil usually contains less organic matter rather than fine soil, due to lower moisture content and greater aeration expected in sandy soils causes more rapid oxidation of organic matter .This argument supports the above discussion in regarding the distribution of copper in the study area.

Further support to the previous discussion is the variation of pH values verses depth for zones (NW, W, SW, S) where highest copper concentration exists. The average pH value is found to be around (6.6). Indicating an acidic environment which increases the copper mobility as reported by Brog and Johansson,[11].

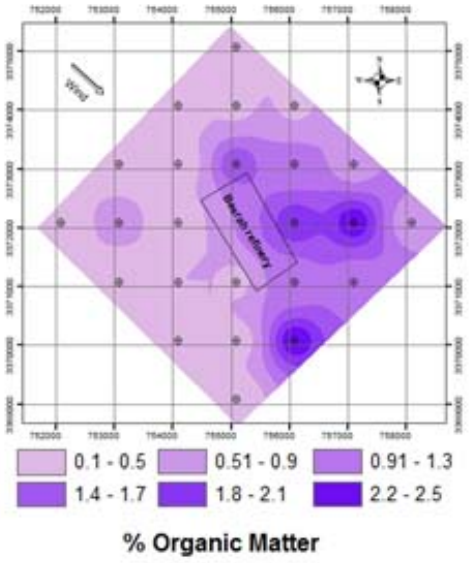

Fig. 7. Percentage of Organic Matter in Soil

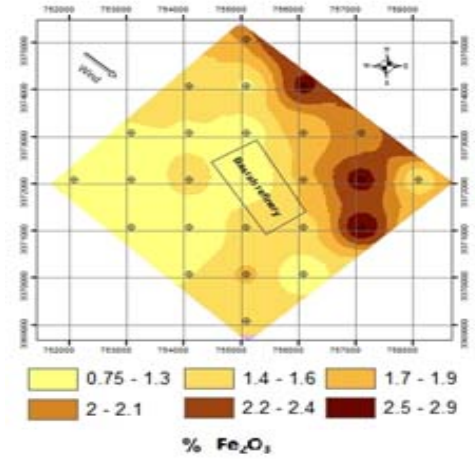

Fig. 8. Percentage of Fe2O3 in Soil

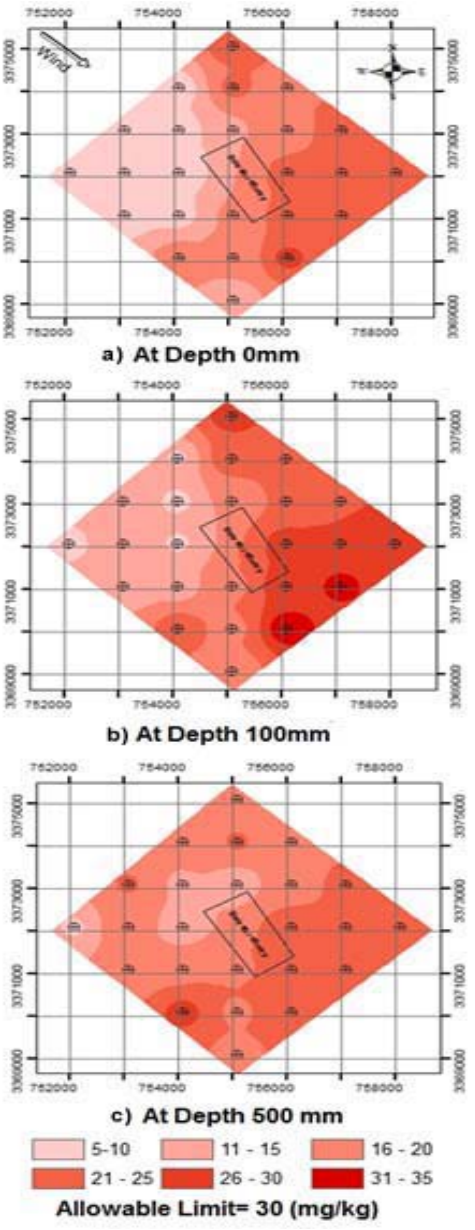

Fig. 9. Concentration of Cu

Chromium (Cr)

Chromium is the second metal that its percentage does not exceed the international limits.

Minimum values of (Cr) (23, 27and 30 mg/kg) and maximum values (58, 68 and 58 mg/kg) were obtained at depths (0, 100, and 500 mm) below N.G.L respectively. Comparing these results with allowable international limit, (100 mg/kg) (EPA, 2002) demonstrate that the values of (Cr) are below the recommend value as shown in Figure (10).

At the ground surface the majority of the east side has a concentration of (Cr) ranging between (41-50mg/kg). Few spots indicate higher concentration between (51-60 mg/kg).

At 100mm depth below N.G.L, the results demonstrate a zone of high concentration, (51-60mg/kg) located in east side of the refinery and directed towards the south.

At 500mm depth there is a wide spread of chromium covering approximately half the lower study area. The concentration in this specific area ranging between (41-50mg/kg). Higher concentration spots were noticed on the boundaries of the study area.

Zinc (Zn)

Zinc is the third metal that its percentage does not exceed the international limits.

Minimum values of (Zn) (8, 10 and 13 mg/kg) and maximum values (40, 49 and 42 mg/kg) were obtained at depths (0, 100, and 500 mm) below N.G.L respectively. Comparing these results with allowable international limit, (50 mg/kg) [5] demonstrate that the values of (Zn) were below the recommend value as shown in Figure (11).

Chukwuma et al. 2010[12] reported that soils with excess amounts of clay or organic matter and iron oxides had higher adsorption capacity for Zn than sandy soils of low in organic matter. Kabata-Pendias and Pendiass,[7] stated that surface area of silt loam is (120-200 m2/g) and sandy loam is (10-40 m2/g). In the present study silt loam is spread in the east zone with substantial amounts of organic matter and Fe2O3 thus encouraging the accumulation of (Zn) as compared to the west side of the site where sand loam exists.

At ground surface the majority of the east side has a concentration of (Zn) ranging between

(21-30mg/kg) with highest concentration ranging between (31-40 mg/kg) as shown Figure (11a).

At depth 100mm below N.G.L, the results demonstrate a zone of high concentration, (41-50mg/kg) located in the east side of the refinery and directed towards the south as shown Figure (11b).

At depth 500mm there is a wide spread of zinc covering approximately south east of study area. The concentration in this specific area ranges between (31-40mg/kg), with high concentration spot observed on the study area as shown Figure (11c).

The average value of pH in the east direction is within (7.2)

indicating slight alkaline media, under such circumstances the soil becomes good storage for zinc and restricts it is mobility. pH is another factor affecting on the mobility of (Zn) in soil where the adsorption mechanisms increase with increasing pH that encourages to excess the cation exchange capacity (CEC) [13].

On the contrary the pH ≈ 6.6 in the west direction is slight acidic media. It has been reported, [6], that high mobility of zinc occurs in acidic soil rather than alkaline soil.

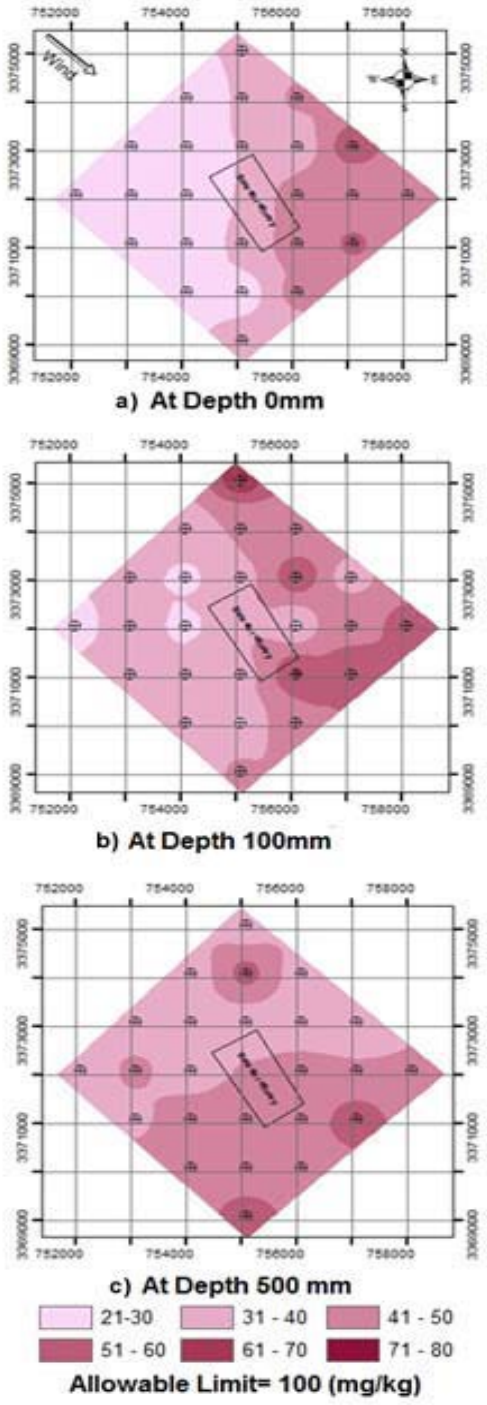

Fig. 10. Concentration of Cr

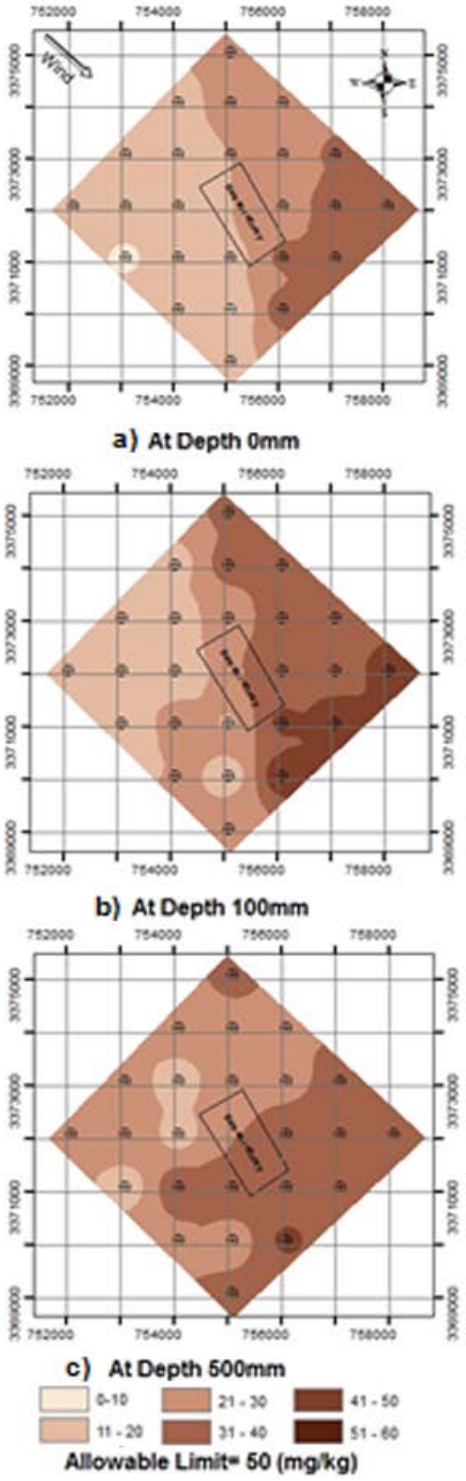

Fig. 11. Concentration of Zn

Anthracene Results

Polyaromatic hydrocarbon PAH is a class of persistent organic pollutants made up of multiple carbon ring structures. These compounds have become a global concern due to their persistence in the environment and their carcinogenic effects [14]. PAHs occur in oil, coal, and tar deposits, and are produced as byproducts of fuel burning. The outputs indicate minimum values of (Anth.) Of (0, 0 and 0 µg/kg) and maximum values of (39, 30 and 25 µg/kg) at depths (0, 100, and 500 mm) below N.G.L respectively. Comparing these results with maximum international limit, (13 µg/kg) [6] demonstrate that the values of (Anth.) were above the recommend values.

higher concentration of (Anth.) located on the east side of refinery. At ground surface the majority of the east side has (Anth) concentration ranging between (24-29 µg/kg).Large spot indicates higher concentration between (30-39 µg/kg).

At 100mm depth below N.G.L, the results demonstrate a zone of concentration, (12-17 µg/kg) located in east side of the refinery with highest spot concentration between (18-23 µg/kg).

At 500mm depth the concentration in the east side area ranges between (5.1-11 µg/kg) with few spots concentration between (12-17 µg/kg).

CONCLUTIONS

The concentrations of six heavy metals indicate high concentration of Cd ranging between 4 to 11.7 mg/kg , Pb between 8 to 54 mg/kg and Ni between 23 to 110mg/kg . The other three metals Cu , Cr and Zn ,revealed concentrations ranging between 6 to 35 mg/kg , 23 to 68 mg/kg and 8 to 49 mg/kg respectively .The concentrations of these three metals did not exceed the allowable limits recommended by EPA.

The concentration of the polyaromatic hydrocarbon (PAH) ranges between 0 to 39 µg/kg. This value also exceeds the allowable limit. For this site it is advisable to use biological treatment technology such as phytoremediation.

When alkaline environment exists in soil i.e. pH > 7, high adsorption of the heavy metals ability exists by Iron Oxide Fe2O3. Lower adsorption ability was noticed by organic matter and clay content.

Although the concentrations of heavy metals depend primarily on the source of pollution and time of contamination .The type of soil may also play a major part on the mobility of the contaminates. Higher concentrations of heavy metals were observed at higher sand percent or lower silt /sand ratio.

The GIS Technique is considered as a powerful tool for representing the distribution of heavy metals in the vicinity of any contaminated source. Results indicated in all figures provide comprehensive view about the distribute of any pollutant in both vertical and horizontal directions.

REFERENCES

[1] Mirsal, I. A., (2008), "Soil Pollution Origin, Monitoring & Remediation ", Second edition, Springer-Verlag Berlin Heidelberg.

[2] Duffus, J.H., (2002),"Heavy Metals", Pure and Applied Chemistry, Volume: 74, Pages: 793-807.

[3] United States Environmental Protection Agency (USEPA) (1997), "Cleaning up the Nation's Waste Sites: Markets and Technology Trends", EPA/542/R-96/005, Office of Solid Waste and Emergency Response, Washington, DC.

[4] Nam, J.J, Song, B.H., Eom, K.C., Lee, S.H. and Smith, A., (2003), "Distribution of Polycyclic Aromatic Hydrocarbons (PAHs) in Agricultural Soils in South Korea", Environmental sciences Volume: 50, Issue: 10, Pages: 1281-1289.

[5] EPA, Environmental Protection Agency, (2002)," Behavior of Metals in Soils", Ground Water Issue, EPA/540/S-92/018.

[6] CCME , Canadian Council of Ministers of the Environment , (1999), "Total Canadian Soil Quality Guidelines For The Protection Of Environmental And Human Health: Cadmium , Lead ,Nickel , Copper , Chromium and Zinc" , Excerpt from Publication No. 1299; ISBN 1-896997-34-1.

[7] Kabata – Pendias, A., and Pendias (2001), "Trace Element in Soil and Plant", 3rd edition. CRC Press LLC C. J. Kaufman, Rocky Mountain Research Lab., Boulder, CO, private communication, May 1995.

[8] Ramos, L., Hernandez ,L.M. and Gonzalez, M.J., (1994)," Sequential Fractionation Of Copper, Lead, Cadmium And Zinc In Soils From or Near Donana National Park", Journal of Environmental Quality ,Volume: 23, Pages: 50-57.

[9] Alloway, B.J., (1995), "Heavy Metals in Soil", Published by Blackie Academic & Professional, London.

[10] Lieve , C., Benilde , B., Anna , R. G., Robert, J. , Luca , M. and Claudia ,O., (2004), "Reports Of The Technical Working Groups Established Under The Thematic Strategy for Soil Protection", Publications of the European Communities, Luxembourg.

[11] Borg, H. and Johansson, K., (1989), "Metal Fluxes to Swedish Forest Lakes", Journal of Water, Air and Soil Pollution, Volume: 47, Pages: 427-440.

[12] Chukwuma ,M. C., Eshett, E. T., Onweremadu, E. U. and Okon ,M. A. , (2010) , "Zinc Availability In Relation to Selected Soil Properties in A Crude Oil Polluted Eutric Tropofluvent" , Journal of Environmental Sciences and Technology , Volume: 7 ,Number :2, Pages: 261-270.

[13] Singer, M. J. and Munns, D. N., (1999), "Soils, an Introduction", 4th. Ed. Rentice-Hall, Inc. New Jersey.

[14] Tang, L., Tang, X., Zhu, Y., Zheng, M.H., and Miao, Q. , (2005), "Contamination of Polycyclic Aromatic Hydrocarbons (PAHs) In Urban Soils In Beijing, China", Journal of Environment International, Volume: 31, Pages: 822 – 828.

Ali Sadiq Resheq holding B.Sc. degree in Civil Engineering, Building and Construction Engineering Department, University of Technology Baghdad, Iraq, June 1999. In October 1999, he studied MSc. Degree in Structural Engineering, Building and Construction Engineering Department, University of Technology, Baghdad, Iraq and hold the degree in Jan 2003. He joined University of Technology as assistant lecturer in Building and Construction Engineering Department. In 2013, he completed Ph.D. Degree in Structual Engineering, Building and Construction Engineering Department, University of Technology, Baghdad, Iraq. During 2010 till now he continues working in Building and Construction Engineering Department as lecturer. .

رقم الايداع في دار الكتب والوثائق 160 لسنة 2016

المؤتمر الدولي الثاني لهندسة البناء والإنشاءات والبيئة

17-18 تشرين الأول 2015

بيروت - لبنان

الجزء 4: محور هندسة الطرق وهندسة الجيوماتيك